

## TABLE OF CONTENTS

	Page
<b>1 Introduction</b>	<b>1</b>
1.1 Prefix . . . . .	1
1.2 Introduction . . . . .	1
1.2.1 Habitat loss . . . . .	4
1.2.2 Communities of single and multiple interaction types . . . . .	4
1.2.3 Spatially explicit model and metrics . . . . .	7
1.2.4 Modelling Habitat Loss . . . . .	7
1.2.5 The effects of habitat loss . . . . .	7
<b>2 Habitat loss: Modelling approach</b>	<b>9</b>
2.1 Context (temp) . . . . .	9
2.2 Agent based simulation . . . . .	9
2.2.1 The interaction network . . . . .	10
2.2.1.1 The niche model . . . . .	10
2.2.1.2 Link Replacement . . . . .	12
2.2.2 Model specification . . . . .	13
2.2.2.1 Celluar-automata rules . . . . .	14
2.2.2.2 Model Parameters . . . . .	16
2.2.3 Modelling habitat loss . . . . .	16
2.2.3.1 Random Habitat Loss . . . . .	16
2.2.3.2 Contiguous Habitat Loss . . . . .	18
2.2.4 Implementation . . . . .	18
2.3 Dynamics of the model . . . . .	19
2.3.1 Transience . . . . .	19
2.3.2 Long term distribution . . . . .	19
2.3.3 Diffusion behaviour . . . . .	19
2.4 Ecological metrics and analysis methods . . . . .	19
2.4.1 Biodiversity metrics . . . . .	19
2.4.2 Stability metrics . . . . .	19

---

**TABLE OF CONTENTS**

---

2.4.3	Network metrics . . . . .	19
2.4.4	Spatial metrics . . . . .	21
2.4.5	Interaction strength metrics . . . . .	21
<b>3</b>	<b>Habitat loss with high immigration</b>	<b>23</b>
3.1	Introduction . . . . .	23
3.2	Methods . . . . .	24
3.2.1	Simulation procedure . . . . .	24
3.2.2	Rank abundance distributions . . . . .	25
3.2.3	Sampling and analysis . . . . .	26
3.2.4	Invariability . . . . .	26
3.3	Results . . . . .	26
3.3.1	Diversity . . . . .	27
3.3.2	Network properties . . . . .	34
3.3.3	Stability and spatial metrics . . . . .	39
3.3.4	Invariability . . . . .	44
3.3.5	Synthesis . . . . .	46
3.4	Discussion (or conclusion?) . . . . .	53
<b>4</b>	<b>Persistence and Stationarity</b>	<b>55</b>
4.1	Introduction . . . . .	55
4.2	Persistence in closed communities . . . . .	56
4.2.1	Mutualistic to antagonistic interaction (MAI) ratio . . . . .	57
4.2.2	Reproduction rate (RR) . . . . .	59
4.2.3	Landscape size . . . . .	63
4.2.4	Number of initial species . . . . .	64
4.2.5	Network structure . . . . .	66
4.2.6	Discussion . . . . .	66
4.3	Problems with temporal variability . . . . .	69
4.3.1	Second-order stationarity . . . . .	70
4.3.1.1	Tests for stationarity . . . . .	71
4.3.1.2	Characterising the tests . . . . .	71
4.3.1.3	Stationarity results . . . . .	79
4.3.2	Determinism tests . . . . .	83
4.3.2.1	Recurrence quantification analysis . . . . .	83
4.3.2.2	Results . . . . .	84
4.3.3	Accuracy and repeatability . . . . .	85
4.3.3.1	Accuracy . . . . .	87
4.3.3.2	Repeatability . . . . .	87

---

## TABLE OF CONTENTS

---

4.3.4	Discussion	89
4.4	Conclusion	93
<b>5</b>	<b>Varying Immigration rate</b>	<b>95</b>
5.1	New predictions (Temp)	95
5.2	Assumptions of what has gone before	96
5.3	Literature review for immigration	97
5.4	Motivation	99
5.5	Exploration of parameter space: habitat loss and immigration	101
5.5.1	Summary heat-maps	105
5.5.2	Example dynamics	109
5.5.3	Relative abundances and abundance distributions	112
5.5.4	Rank abundance distributions	112
5.6	Points for discussion (Rough Notes)	116
5.7	Habitat loss with low immigration	117
5.8	Questions for Alan or Daniel	117
5.9	RADS with averaging	120
5.10	New results: without vegetarian predators	122
<b>6</b>	<b>Inferring species interactions</b>	<b>125</b>
6.1	Motivation	125
6.2	Methodology	126
6.2.1	Interaction strength	127
6.2.2	Population models	128
6.2.3	Simulation procedure	131
6.2.4	Numerical estimation method	132
6.2.5	Examples	135
6.3	Results	138
6.3.1	Linear model	138
6.3.2	Holling model	141
6.3.3	Range sampling	141
6.4	TEMP : other results	141
6.5	Application to IBM (optional)	142
6.5.1	Testing functional response (and intrinsic growth functions)	144
6.5.2	2 Species IBM model	145
6.5.3	Extend methodology (3, 4 and 5 species)	147
6.5.4	Results	147
6.5.5	2 species	149
6.5.6	3 species	156

## TABLE OF CONTENTS

---

6.5.7 5 species . . . . .	164
6.6 Discussion . . . . .	173
<b>Bibliography</b>	<b>175</b>

## INTRODUCTION

### 1.1 Prefix

It is a prevalent stance, in our society, to consider oneself separate from Nature. Somehow the natural world gives rise to a consciousness that is above and distinct from that of all other organisms - the human consciousness. And this particular consciousness is able to bend Nature to its will. At least that is the premise of the modern, secular society. Prior, and concurrent, to these societies, are those that

Our relationship with Nature has been one of asking what

The human relationship with Nature is purely extractive..

Indeed this has been the story of

The history of modern civilisation has been a tale of removing ourselves from the natural world

Here we study nature in a very separate way, from behind the computer screen..

Ecosystems are the foundation on which human society

This thesis explores the effects of habitat loss, and the role of species interactions in mediating these effects, on ecological communities. In the introduction we address, in turn,

### 1.2 Motivation

An ecosystem is a subset of the *biosphere* - the entirety of the living systems on this planet. These biological systems are closely coupled, in a two way relationship, to the abiotic systems of the planet to such an extent that Lovelock, and other proponents of the *Gaia theory*, suggest that the biotic and abiotic components together form a single homeostatic system which maintains conditions that are harmonious to life. In the strongest version of the theory the planet itself is a

living system. This is not the place to argue for or against the theory, but regardless of its validity it remains undeniable that living systems generate significant effects at a planetary scale[REFS]. Humans, as one component of the biosphere, are fairly unique not only in the extent of their impact on planetary systems, but also their *potential ability* to make reasoned decisions about collective actions based on knowledge of their impact. Given that the rate of species extinctions in the last century has been conservatively estimated at between 8 and 100 times the background extinction rate [? ], and that the major drivers for these extinctions are anthropogenic [REF], it is abundantly clear that humans are failing to realise the aforementioned potential. Arguably the main reason for this failure is the systems of organisation..hard to make reasoned decisions when don't have sound theory!..but also lack of understanding about how ecosystems function..Second paragraph on stewardship, conservation and restoration.. This is my reason for studying the field of ecology....

Habitat loss/alteration and climate change as the main anthropogenic drivers..Focus here on habitat loss. Community ecology - tools for the study of localised groups of species. Computational approach - hypothesis generation - defend bottom-up modelling of complex systems - make clear what it can and cannot do..

## 1.3 Community ecology

An ecological community may be broadly defined as a collection of species that coexist in time and space. The study of these collections - *community ecology* - attempts to understand their structure, dynamics and function, following the tenet that these three properties are related.

### 1.3.1 Species interactions

### 1.3.2 The role of structure

### 1.3.3 Network generation

Possible section: how are networks created - refers to the problem of estimating species interaction strengths and relating these to dynamics and function.

## 1.4 Habitat loss

This project focuses on the impact of habitat destruction on communities of species. A habitat may be defined as the environment containing an organism, or collection of organisms. It has both biotic and abiotic components. Therefore habitats are constantly changing due to ongoing environmental processes. These changes may make the habitat more or less hospitable to different organisms, generating emergent effects at the species and community levels. Human activity in particular creates pronounced and significant changes in habitat. There is good evidence [58]

that anthropogenic climate change has affected living systems by changing regional habitat suitability. An example of this is the northward shift in butterfly species ranges attributed to rising temperatures [57]. Other activities such as agriculture, deforestation and urbanisation interfere directly with physical habitat components and with local flora. This alters the type of species and the community that can be supported [8, 39]. Globally the scale of these man-made effects is huge. Various studies have suggested that habitat modification is the leading cause of global species extinctions [19, 74]. Therefore an understanding of how ecological communities respond to changes in habitat is essential in order to mediate the destructive effects of human activity, and to create beneficial conservation, land management and restoration strategies. The subject has received much attention in the ecological literature, and this project is a continuation of that dialogue.

The destruction of habitats due to human activity has also received much attention in the media. This has done a lot to raise public awareness, and to fuel a growing number of campaign groups, charities and conservation organisations. In most cases the focus is on *single species effects*, especially on those threatened with extinction. The most notorious example of this may be the polar bear as the media face of global warming (see figure 1.1). Similarly the habitat loss literature has largely focused on the loss of species [19, 73], and has reinforced the notion of *species richness*<sup>1</sup> as a measure of biodiversity and ecosystem health. This is perhaps because species level effects are the most visible results of ecosystem damage, and the easiest to study empirically. However they are symptomatic of underlying system processes. At least since Darwin's marvel at the complexity of the "Tangled Bank" [12] ecologists have understood that species exist in highly interdependent communities. Therefore the ecological impacts of habitat destruction, and other human activities, must be approached from a systems perspective.

In community ecology the system of study is the ecological community - a local collection of co-existing species. The focus is on the structure, patterns and processes within the community. A key aspect of this is the pattern of *interactions between species*, which underlies many of the processes that shape the community (for more detail refer Chapter 2). Recently the habitat loss literature has begun to move away from species level effects, towards community wide effects and especially inter-specific interactions [75]. This has been facilitated by the wider availability of ecological network data, improved methods for data collection, and the ability to simulate large ecological networks and communities. Advances in ecological network theory have also provided many new metrics for community stability, biodiversity and for analysis of network structure (section 2.4). Our approach to the study of habitat loss is situated in this context.

There is now a growing consensus that ecological interactions are the key to understanding the effects of habitat loss on ecological communities [25, 27, 48]. In addition to the loss species, it has long been known that habitat loss also leads to the important loss of inter-specific interactions. As Janzen remarked [32] in 1974: "what escapes the eye, however, is a much more insidious

---

<sup>1</sup>Simply defined as the number of different species present in a community.



Figure 1.1: Stranded polar bears on Cross Island outside Prudhoe Bay, Alaska. The plight of the polar bear has received much attention in the media. The habitat loss it suffers from is very visible. However the focus of conservation strategies must be on the ecological communities, of which it is one member species. (Source: [www.greenpeace.org.uk](http://www.greenpeace.org.uk))

kind of extinction: the extinction of ecological interactions". It has since been demonstrated that ecosystems experiencing habitat alteration often suffer loss of interactions *before* loss of species [2, 22, 75]. This can result in detectable changes in community structure, without any detectable change in species richness [74]. These structural changes have consequences for community stability, robustness and population dynamics. A significant part of the ongoing challenge is to identify meaningful measures for the structural (network) changes, and to generalise the ways in which they impact on the community. The bulk of the recent literature supports the belief of Valiente et al. [75] in "the importance of focusing on species interactions as the major biodiversity component on which the 'health' of ecosystems depends."

#### 1.4.1 Habitat loss

#### 1.4.2 Communities of single and multiple interaction types

In the habitat loss literature most studies have looked at communities with a single type of interaction. The same has been true for network ecology in general, with the bulk of the literature

focused on either antagonistic or mutualistic networks. In these networks a node represents a species, and a directed link represents a certain type of interaction (for example predation). Such networks represent the interaction structure of an idealised and closed community. For example it is common to study mutualistic communities, such as plants and their pollinators, in isolation. This is represented as a bipartite network of plant and pollinator species, with mutualistic interactions between them. Both empirical and *in silico* studies have derived some apparently general results on the response of such single-interaction communities to habitat loss. We discuss some of these findings here. However in nature a single-interaction community is a subset of a larger group of species with multiple types of interaction (predation, mutualism, competition, parasitism). There has been a recent move towards studies of communities with multiple types of interaction [34], which are less simplistic models of natural systems. These hybrid communities are represented as networks with more than one type of link. We also discuss this body of work, some of which challenges previous finding based on single-interaction communities.

Perhaps most the general result, already discussed, is that habitat destruction leads to a loss of inter-specific interactions. This may be accompanied by lower interaction frequencies, changes in interaction strength, reduced connectivity, or other structural changes in the network due to rewiring. Tylianakis et al. [74] showed that empirical antagonistic communities (host-parasitoid) responded to habitat degradation with reduced evenness in interaction frequencies. This means that certain interactions became relatively more frequent, so that energy flow through the community became concentrated along certain pathways. Also, importantly, the quantitative changes in network structure that they observed were not detectable by equivalent qualitative metrics. Neither were conventional diversity metrics, based on species abundance or richness, able to distinguish between habitats at different levels of degradation. Similarly Albrecht et al. [2] showed that insect food webs in a grassland system lost interaction diversity faster than species diversity, when subjected to habitat alteration. This suggests a biodiversity reduction in the interaction structure that is not measurable by metrics based on species abundance. Both of these examples highlight the sensitivity of results to the metrics used, when studying community response to habitat loss. Hence the large suite of metrics introduced and discussed in section 2.4.

An issue of particular interest is community stability, its response to habitat loss and its relationship to network structure. Mutualistic networks tend to have a highly nested structure and low modularity [5]. These properties are believed to improve the stability of the community [72]. It has been shown that habitat destruction can push mutualistic networks towards higher modularity, higher connectivity, and lower nestedness, thereby reducing stability [27, 69]. Conversely antagonistic networks tend to be modular in structure, which is believed to promote stability and robustness in these communities [72]. Habitat loss has been shown to destabilise antagonistic communities by lowering modularity and increasing interaction strengths [27]. Generally the literature suggests, as expected, that habitat loss reduces community stability, irrespective of the interaction type. However the underlying changes driving this loss in stability

appears to differ between mutualistic and antagonistic communities. It should also be noted here that the definition and measurement of stability is non-trivial. Lurgi et al. [42] have shown that certain stability metrics may respond differently to a changing control variable, meaning that a combined, or multi-stability approach is required.

The above examples represent attempts to understand the structural changes that occur due to habitat loss, prior to the occurrence of species extinctions. From a conservation perspective this highlights the importance of targeting inter-specific interactions and the maintenance of network structure and function, rather than focusing on species level effects [48]. Fortuna and Bascompte [21] have demonstrated that real-world networks have better persistence against habitat loss than random networks assembled using null-models. This suggests that artificially managed ecosystems may be more vulnerable to perturbations than their ‘wild-type’ equivalents, unless careful attention is paid to those properties that promote stability and robustness. In food webs there appear to be certain simple properties that mediate the impacts of habitat destruction [47]. For example omnivory is shown to increase extinction thresholds, as is a reduction in top-down control by predators. However these numerical results are for small model networks and remain to be demonstrated empirically.

Recently ecologists have realised the importance of studying ecological networks that contain multiple types of inter-specific interaction [20, 34, 49]. It is known that mutualistic communities have knock on effects on food webs, and vice versa. Indeed certain species are simultaneously involved in more than one type of network or community. A powerful example of this phenomenon was demonstrated empirically by Knight et al. [36]. They showed the presence of a trophic cascade, crossing ecosystem and habitat boundaries, by which freshwater fish were able to facilitate terrestrial plant reproduction. The inclusion of such indirect and cascading effects is one of the many strengths of the network paradigm in ecology. However this study highlights the limitations of focusing on localised community subsets and single-interaction types.

A large scale study by Pocock et al. [59] was one of the first to combine networks of different types into a network of ecological networks. They used empirical networks constructed over different habitats on a farm, to construct a whole farm network. This included host-parasitoid, seed-dispersal, plant-pollinator and predator-prey networks. Using quantitative robustness analysis (section 2.4), they were able to identify keystone plant species which generated significant cascading effects across networks, and also determined the most fragile components of the meta-network. This type of integrated analysis has different implications for conservation and restoration than an approach which looks at the individual networks in isolation.

The integration of multiple interaction types has begun to shed new light on the stability of ecological communities. This is because the conventional understanding is based on studies of communities with single-interaction types. In general complex antagonistic networks with strong interactions are thought to be unstable [54]. This presents a problem for ecological theory since natural food webs, which are inherently complex, appear to be stable. The problem may lie in the

fact that antagonistic networks have been studied in isolation. It has been shown theoretically that introducing mutualistic interactions into the network can be stabilising [42, 51]. Specifically Lurgi et al. [42] propose that increasing the proportion of mutualistic interactions at the base of a food web reduces the overall strength of species interactions. They found that this improved the stability of their model communities, according to a spatial aggregation metric (section 2.4).

Recently Sauve et al. [66] have brought into question the established wisdom on the relationship between network structure and stability. As discussed previously, the structural properties believed to promote stability differ between antagonistic and mutualistic communities. High modularity and high nestedness are thought to promote stability in antagonistic and mutualistic networks respectively. However Sauve's work suggests that, for a combined network of mutualisms and antagonisms, modularity and nestedness do not strongly affect stability. The results of Lurgi et al. also support this finding [42]. Therefore new metrics, accounting for diversity in interaction type, may be required in order to understand community structure and stability in hybrid networks<sup>2</sup>.

Since hybrid networks of multiple interaction type are relatively new, there are few studies relating them to habitat loss. One study, by Evans et al. [16], uses the same empirical network of networks as [59]. They employed a robustness algorithm to determine how vulnerable the hybrid network is to the loss of different habitats from the farm<sup>3</sup>. Aside from this study there is a lack of empirical and theoretical results on the response of hybrid networks to habitat loss. This project aims to make a contribution towards this area. We will extend on the work of Lurgi et al. [42] to simulate multi-trophic communities with mutualistic and antagonistic interactions. By investigating the response of these communities to simulated habitat destruction we will be generating novel results and predictions which can be tested empirically in the future. To do this we will employ a range of metrics to quantify structural changes and community stability. We will focus on the regime before species are lost from the community, with an interest in the underlying changes that occur as a result of habitat destruction.

#### 1.4.3 Spatially explicit model and metrics

Another novel aspect of this work is the spatially explicit modelling approach... And some of the spatial analysis employed...

[68] - spatially explicit analysis.

[22] mutualistic interactions decrease non-linearly. Connectance increases? Abrupt change in number of interactions, spatial skewness in number of interactions.

[33] - quantitative food web metrics did not vary between fragmented habitat patches in different landscape contexts.

---

<sup>2</sup>See suggestions in the text of [66] and talk to Alix about possibly including these in our analysis?

<sup>3</sup>Interestingly they reported that two of the most important habitats, relative to their sizes, were hedgerow and wasteland.

[54] - interaction strengths is focus, but also spatial stability. c.f. a,b,g stability and Lurgi et al.

#### 1.4.4 Modelling Habitat Loss

The importance of the spatial pattern of HL! - "As we saw in section 1.2.4 numerous studies have found that the spatial pattern of habitat destruction plays an important role in mediating the effect on the community or meta-community (for example [31, 56? ])"

Habitat loss has been modelled in various ways..Spatial auto-correlation..how does our approach fit in with the literature..

[18] - controlled habitat destruction, large empirical project

#### 1.4.5 The effects of habitat loss

Tylianakis - go into detail of the changes and why this is important (see intro of chapter 3)

## HABITAT LOSS: MODELLING APPROACH

### 2.1 Context (temp)

- Make sure introduce realised network.

### 2.2 Agent based simulation

We study the effects of habitat loss on ecological communities using a spatially explicit agent-based model. This simulation model was first published by Lurgi et al in [42] (section 2.2.2). The landscape consists of a homogeneous 2-dimensional grid ( $200 \times 200$  cells) on which individuals of 60 species move around and interact subject to bio-energetic constraints. Local rules define dispersal, demographic processes and interaction behaviour of the individuals. The potential for interaction between two individuals is governed by an underlying species interaction network, which is generated using the niche model [78] (section 2.2.1.1. (GIVE A BIT MORE ABOUT NICHE HERE))

Unlike most previous *in silico* studies, the model includes both trophic and mutualistic interactions. Species belong to four trophic levels. The niche model generates a trophic interaction network. Then a fraction of the links between species in the first two trophic levels are changed to define mutualisms ( $-+ \rightarrow ++$ ). The fraction of links switched is called the mutualistic vs. antagonistic interaction (MAI) ratio.

To simulate habitat loss, a fraction of the grid cells are made inhospitable to all species. We compare two algorithms for choosing which cells to destroy: 1) random destruction and 2) contiguous destruction. For random destruction grid cells are destroyed uniformly at random, up to the desired fraction of the total landscape. For contiguous destruction a seed cell is chosen uniformly at random, then destruction spreads radially in all directions from this point.

We simulated communities with MAI values of 0, 0.1, 0.2, ..., 1.0, with habitat loss (HL) percentages of 0, 10, 20, ..., 90. For each combination of MAI and HL values, 25 replicates were simulated with different interaction networks (same species richness, same connectance).

### 2.2.1 The interaction network

An underlying interaction network defines which direct interactions between species are allowed. This network contains two types of link: *antagonistic* (predator-prey) and *mutualistic* (plant-pollinator). To construct this network a food web, containing only antagonistic links, is generated using the niche model (section 2.2.1.1). This network consists of 60 species belonging to 4 trophic levels, with links that define the feeding relationships between them. Species in the basal trophic level represent plants and those in the trophic level above represent herbivores. To introduce mutualism a fraction of the herbivorous links are replaced by mutualistic links (section 2.2.1.2).

#### 2.2.1.1 The niche model

We use the niche model (NM) of Williams & Martinez [78] is used to generate food webs. This simple model has been shown to produce network structures that closely resemble empirically derived food webs<sup>1</sup>, and has become a standard tool for creation of model food webs [15, 70, 78]. The model has two parameters: the number of species  $S$ , and the desired connectance  $C$ . The model output is an adjacency matrix  $\mathbf{a}$  for which the element  $a_{ij} = 1$  implies that species  $i$  consumes species  $j$ , and  $a_{ij} = 0$  implies the absence of an interaction. Connectance is defined as the proportion of the maximum possible number of links that are realised i.e.  $C = L/S^2$ , where  $L$  is the number of links in the network.

Figure 2.1 illustrates the ideas of niche space, niche value  $n_i$  for a particular species  $i$ , its feeding range  $r_i$ . Niche space is the 1-dimensional range of real numbers  $[0, 1]$ . Each of the  $S$  species is assigned a niche value  $n_i$ , drawn uniformly at random from the niche space. It is then assigned a feeding range with a central value  $c_i$  and a width  $r_i$ . Species  $i$  consumes all species, including itself, whose niche values fall within its feeding range.

To determine the width of the feeding range, a beta function with expectation  $2C$  is used to draw a number from the range  $[0, 1]$ . This number is then multiplied by  $n_i$  to give the chosen value of  $r_i$ . Since  $n_i \sim U(0, 1)$ , we know that the expectation value  $E(n_i) = 0.5$ , and so  $E(r_i) = C$ . Therefore on average a species consumes a fraction  $C$  of the total number of species, resulting in a network with close to the desired connectance.

A beta function has two parameters:  $\alpha, \beta \in \mathbb{R}^+$  [REF]. The choice of  $\alpha = 1$  simplifies the probability density function to

---

<sup>1</sup>FIND MORE REFS HERE.

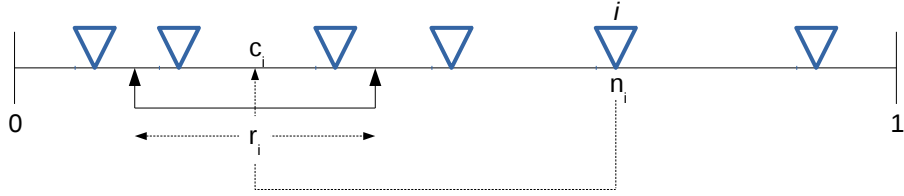


Figure 2.1: A representation of 1-dimensional *niche space* as visualised in the original publication [78], for number of species  $S = 6$ . The blue triangles represent the placement of species in niche space. The niche value of species  $i$  is given by  $n_i$ . The width and centre of the feeding range for species  $i$  are denoted by  $r_i$  and  $c_i$  respectively. Species  $i$  consumes all species whose niche values fall within the feeding range.

$$f(x; 1, \beta) = \begin{cases} \beta(1-x)^{\beta-1} & \text{if } 0 < x < 1, \\ 0 & \text{otherwise.} \end{cases}$$

The cumulative distribution function is derived by:

$$\begin{aligned} P(x) &= \int_0^x \beta(1-x')^{\beta-1} dx' \\ &= 1 - (1-x)^\beta. \end{aligned}$$

Therefore, by choosing a probability value  $y$  uniformly at random from the interval  $[0, 1]$ , we can draw an  $x$  value from our beta distribution:

$$\begin{aligned} y &= 1 - (1-x)^\beta, \quad \text{such that} \\ x &= 1 - (1-y)^{1/\beta}. \end{aligned}$$

The expectation value of this beta distribution is given by  $E(x) = \frac{1}{1+\beta}$ , therefore we choose

$$\beta = \frac{1}{2C} - 1$$

to give the desired expectation of  $E(x) = 2C$ .

Once the width  $r_i$  has been chosen, the feeding range is placed in niche space by randomly drawing the range centre  $c_i$  from the interval  $[r_i/2, n_i]$ . Therefore cannibalism and looping are

possible because up to half of the feeding range may contain niche values  $\geq n_i$ . In some cases the generated network may not be connected (i.e. contains one or more disconnected components), or two species may be trophically identical. In these cases the guilty species are deleted and replaced until the network is connected and without identical species. Also the species with the smallest niche value is give  $r_i = 0$ , such that there is at least one basal species (i.e. species with no prey).

INSERT NICE PICTURE OF A NETWORK!

### 2.2.1.2 Link Replacement

Having generated a food web with only antagonistic links, we now introduce mutualism. The mutualistic interactions are trophic, as with antagonisms, since there is an energy flow from resource to consumer. For example pollinators receive nectar from flowering plants. However in a mutualistic interaction there is a benefit for both parties. In this example flowering plants are pollinated and can reproduce. In the simulation model the plants receive better dispersion abilities as a result of mutualisms (section 2.2.2.1). We impose the constraint that mutualisms can only exist between species of the first two trophic levels: plants and herbivores. Some of the antagonistic links between the first two trophic levels are replaced by mutualistic links. This changes the rules of interaction between individuals of these species in the cellular automata model (section 2.2.2.1). The fraction of these links switched is defined as the mutualistic vs. antagonistic interaction (MAI) ratio. Figure 2.2 is a schematic of a possible interaction network generated by this procedure, for a nineteen species community. In this case there are twelve links between the first two trophic levels, and six of these have been replaced by mutualistic links. The other six links remain antagonistic. Since half of the basal links have been replaced, the MAI ratio for this community is 0.5.

The result of link replacement is a hybrid network that defines two types of interaction between species. We can define two functional groups in each of the first two trophic levels. In the first trophic level *non-mutualistic plants* are basal species which do not have any mutualistic links. This group represents wind-dispersed plants which only have antagonistic interactions with the trophic level above. *Mutualistic plants* are any basal species with at least one mutualistic link. This group are dispersed by species from the second trophic level via their mutualistic interactions and can no longer be wind dispersed. They may also be predated upon by herbivores, if they have such links. Similarly *herbivores* are members of the second trophic level which only predate on basal species, whereas *animal mutualists* may either predate or engage in mutualisms. See figure 2.2 for a visualisation of these groups.

For the simulations we generated networks with eleven different MAI ratios ( $[0, 0.1, 0.2, \dots, 1.0]$ ). This is in accordance with the previous study [42], and allows us to look at how communities with different MAI ratios respond to habitat loss.

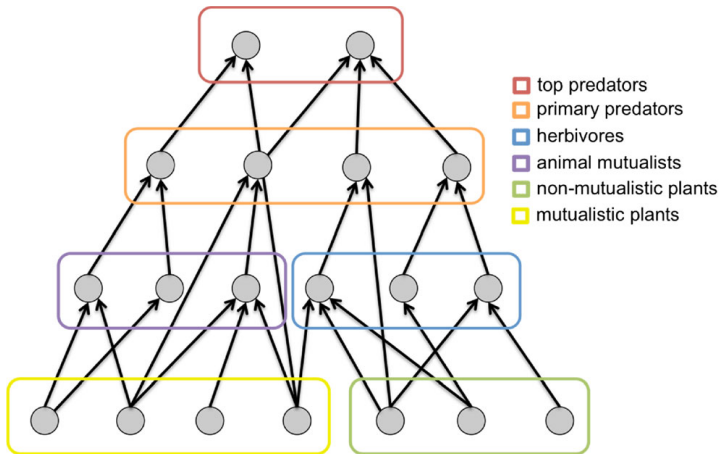


Figure 2.2: Schematic of an underlying interaction network (reproduced from [42]). Nodes correspond to species, and arrows to trophic links (antagonistic or mutualistic), from resource to consumer. The six functional groups of species are colour coded, and named in the legend. In this case there are twelve links between the first two trophic levels, six of these have been replaced by mutualistic links giving a MAI ratio of 0.5. Mutualistic plants and animal mutualists are defined by any species that has at least one mutualistic links. However both these groups of species may also have antagonistic links.

### 2.2.2 Model specification

We use the model of Lurgi, Montoya & Montoya [42] as the basis of our simulation model. It is a cellular automaton (CA) in which individuals belonging to different species move around, reproduce, die and interact. These actions are subject to bioenergetic constraint and the rules governing them are detailed in section 2.2.2.1 below. The CA landscape is a homogeneous 2D square lattice with toroidal boundaries. Each cell can contain up to two individuals: at most one animal and one plant individual. It may not contain more than one individual of either type. Types of individual are defined by its trophic position in the underlying interaction network (section 2.2.1). All basal species are plants, all other species are animals.

Distance on the lattice is defined as follows. The immediate neighbours of any given cells are the eight adjacent cells including diagonals (i.e. a Moore neighbourhood). These eight neighbours have distance-1 from the central cell. This distance metric is used in the rules for movement and reproduction (SEE BELOW NUM?), and also in the calculation of various spatial metrics (section SECTIONNUM).

Initial conditions are defined randomly by the following setup procedure. A species is selected uniformly at random from the sixty species in the underlying network. A cell from the landscape is selected uniformly at random. If there is space in the cell, an individual belonging to the selected species is placed in the selected cell. This is repeated until the value of parameter *occupied cells* is reached.

Table 2.1 shows all the model parameters, their values and definitions. Where possible the

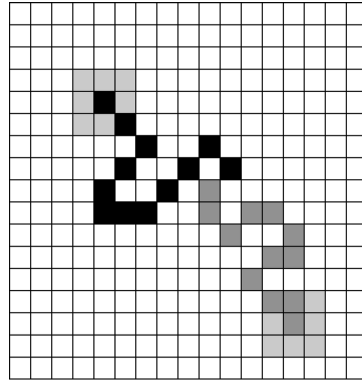


Figure 2.3: Example trajectories and neighbourhoods of two individuals.

parameters values are chosen to be biologically realistic. A discussion of values chosen for these parameters can be found in section 2.2.2.2.

#### 2.2.2.1 Celluar-automata rules

In the following description italicised words refer to model parameters, which are defined in table 2.1. Each individual stores energy (or resource), which it expends to perform actions. If the energy of an individual drops below *min\_resource* it dies and is removed from the landscape. On each iteration the basic demographic processes occur in the following order (FOR EACH SPECIES?):

1. Death
2. Movement
3. Reproduction
4. Feeding
5. Immigration

##### 1) Death

As stated, if an individual's energy drops below *min\_resource*, it is removed from the simulation.

##### 2) Movement

For each individual, a neighbouring cell (distance 1) is selected uniformly at random. If the cell is available the individual moves there. Otherwise it remains stationary.

### 3) Reproduction

All species may only reproduce if their stored energy is greater than *mating\_resource*. Animals reproduce sexually, plants reproduce asexually.

- **Sexual reproduction:** This occurs between two members of the same animal species if:  
1) There is a member of the same species in the immediate neighbourhood of the subject species; and 2) there is an available cell for the offspring in the distance 4 neighbourhood of the subject individual. When these two conditions are met both parents give a fraction of their stored energy (*mating\_energy*) to the offspring. The offspring is placed in a cell chosen uniformly at random from the available cells within distance 4 of the subject individual.
- **Asexual reproduction:** This occurs for plants via two possible mechanisms.
  1. Wind dispersal occurs for non-mutualistic plants, on each iteration with a probability equal to *reproduction\_rate*. If reproduction occurs the offspring is placed in a randomly selected available cell in the distance 4 neighbourhood. For plants, available means empty or only occupied by an animal individual. If no cells are available the plant cannot reproduce. Again a fraction of the parent plant's stored energy (*mating\_energy*) is given to the offspring to the offspring.
  2. Mutualistic dispersal occurs for mutualistic plants. This action is carried out by the animal partner, and is done in the 'feeding' phase (see below), since it is also a trophic interaction. The 'seed' of the parent plant is carried by the animal partner, so it may be placed beyond the distance 4 neighbourhood.

### 3) Feeding

For a trophic (feeding) interaction to occur, two individuals must belong to species that are connected in the interaction network. Also the individuals must explicitly find each other in space - in the 'movement' phase one must choose the cell occupied by the other. If this happens there are three possibilities:

1. **Predation:** If neither individual belongs to a basal species a predation event occurs with probability *capture\_probability*. The prey species dies and a fraction of its energy *efficiency\_transfer* is given to the predator.
2. **Herbivory:** If one individual is a non-mutualistic animal and the other is a plant, they interact. A fraction of the plant's energy *herb\_fraction* is lost, and a fraction (*herb\_efficiency*) of this energy is given to the herbivore. Both individuals continue living. If the animal is an omnivore and additional trade-off (*omni\_tradeoff*) is applied to its energy gained, since omnivores are less efficient at digesting plant matter than straight herbivores.

3. **Mutualism:** If the individuals share a mutualistic interaction they interact. A fraction of the plant's energy (*mut\_fraction*) is transferred to the animal. The animal also keeps track of which plant it interacted with. If it reaches an available cell in the landscape it creates an offspring of this plant with probability *mut\_efficiency*. On each iteration that an offspring is not produced, the mutualistic efficiency is reduced by a fraction *mut\_cooling*.

#### 4) Immigration

At each iteration there is a probability (*immigration*) with which each empty cell may be colonised by an individual selected at random from the original species pool.

#### 5) Energy update

On each iteration all animal individuals' energy stores are reduced by a fraction *living\_expend*, to account for metabolic losses. Also all plant individuals autotrophically increase their energy stores by a fraction *synthesis\_ability*. This is the only energy input to the system.

##### 2.2.2.2 Model Parameters

The model parameters were chosen blablabla... reference Ings et al. Which parameters are most interesting, why? Also discuss sensitivity analysis from previous publications, findings. We I conduct my own version? With regard to which parameters? (Maybe discuss this lat bit somewhere else).

##### 2.2.3 Modelling habitat loss

The current project extends the above defined model of Lurgi, Montoya and Montoya [42] by implementing habitat loss algorithms. The algorithms are simple. A fraction of the cells in the landscape are made uninhabitable to all species. We denote the fraction of destroyed cells by HL. The simulations are set up and run as detailed above (section 2.2.2), after 1000 iterations one of two habitat loss algorithms is applied to the landscape. The species inhabiting the destroyed cells are deleted. Species attempting to move into destroyed cell are unable to and remain stationary. Destroyed cells are counted as unavailable for the placement of offspring. We choose the cells to destroy using one of two habitat loss algorithms: 1) Random and 2) Contiguous.

###### 2.2.3.1 Random Habitat Loss

Cells in the landscape may contain habitats in two states: pristine or destroyed. Pristine corresponds to the cells in the original model. To destroy habitat randomly, cells are selected and destroyed uniformly at random from the set of cells containing pristine landscape. This is repeated until the desired fraction of HL is achieved.

## 2.2. AGENT BASED SIMULATION

---

Parameter name	Value	Description
OCCUPIED_CELLS	0.4	Fraction of the grid initially occupied by individuals randomly placed on it.
MAX_RESOURCE	20	Maximum amount of resource an individual may possess at any given time.
MIN_RESOURCE	3	Death threshold: minimum amount of resource an individual may possess. Any individual possessing less than this amount at any given iteration will die (see text).
LIVING_EXPEND	0.01	Fraction of resource an individual spends in living every iteration of the model. Metabolic rate.
MATING_RESOURCE	0.5	Fraction of MAX_RESOURCE that is required for an individual to be able to reproduce.
MATING_ENERGY	0.2	Fraction of resource given to the offspring by the parent during reproduction. Each parent gives the same fraction. The total amount depends on how much resource the parent possesses at the time of reproduction.
IMMIGRATION	0.005	Probability that a new individual will appear in a cell of the grid each iteration. The species this individual belongs to is randomly chosen from the original species pool.
SYNTHESIS_ABILITY	0.1	Fraction of resource that is autotrophically created by each individual from the basal species every iteration. This is the only energy input to the system.
HERB_FRACTION	0.7	Fraction of resource lost to herbivores by individuals belonging to a basal species during a trophic event, i.e. a species in the first trophic level feeding on a species in the basal level.
OMNI_TRADEOFF	0.4	Fraction of resource that omnivores are effectively able to gather when feeding on a species from the basal level (a plant).
MUT_FRACTION	0.25	Fraction of resource of a primary producer (basal species individual) that a mutualistic partner obtains when an interaction of this type occurs.
CAPTURE_PROB	0.4	Probability that a predator individual embark upon a trophic relationship with one of its prey individuals when it encounters it.
EFFICIENCY_TRANS_F	0.2	Fraction of the resource the prey that is assimilated by the predator in a carnivorous interaction, i.e. trophic interaction not involving individuals from the basal species.
HERB EFFICIENCY	0.8	Fraction of the resource of the prey assimilated by the herbivore in an herbivorous interaction.
MUT_EFFICIENCY	0.8	Efficiency of an individual mutualist when dispersing a plant partner. In other words, the probability with which a mutualistic individual will facilitate the creation of a new individual of the last species of plant it visited when it is positioned on an empty cell immediately after it interacted with a mutualistic plant partner.
MUT_COOLING	0.9	Cooling factor for the mutualistic efficiency of plant dispersers (mutualists). This is the fraction of mutualistic efficiency that remains after each iteration.
REPROD_RATE	0.01	Reproduction rate of non-mutualistic plant species. Probability with which an individual belonging to a plant species that does not possess mutualistic partners for dispersal will create an offspring in any given iteration of the simulation run.

Table 2.1: The parameters of the model and what they mean.

### 2.2.3.2 Contiguous Habitat Loss

This algorithm results in a contiguous region of cells with destroyed habitat. A 'seed cell' is selected uniformly at random from the fully pristine landscape. The seed cell is destroyed, and destruction proceeds radially from the seed cell until the desired fraction of HL is achieved. This process follows the same toroidal boundary conditions as the CA.

### 2.2.4 Implementation

The code for the simulation model was originally written by Miguel Lurgi for research leading to the publication [42]. He and Daniel Montoya were responsible for the bulk of the model development, testing and parameter selection - a considerable task. My task was to take this legacy code and work with it to generate results that would allow us to study the effects of habitat loss.

The model is implemented in *Python*, with several switches that ensure portability between different versions of python. The programme makes extensive use of *numpy* and *networkx*, amongst other *Python* libraries. The original code was well written to allow for the easy implementation of new mechanisms. The intention was always to extend the model for further study. For example there is a parameter for *habitat type*, whereby the landscape would be heterogeneous with certain habitats best suited for different species. (In the current implementation this is not used and the landscape is homogeneous.) There was also a prototype algorithm for contiguous habitat loss.

Working with the legacy code I implemented the random habitat loss algorithm, and tested both the contiguous and random algorithms to ensure they were performing as desired. I also added methods to an already extensive library for saving simulation outputs, with a view to conducting more analysis on the spatial state of the system<sup>2</sup>. I then ran numerous simulations without habitat loss (HL=0) to ensure that the model reproduced the results presented in [42].

Simulation ensembles were run on Blue Crystal Phase 3 (BC3), Bristol's computer cluster. Compatibility issues arose because only *networkx* version 1.9 is available on this system, which has significant differences in the return

My contribution to the model was the implementation of the random habitat loss algorithm, and running all the simulations on Bristol's computer cluster Blue Crystal. The former was trivial but key to this project. The latter involved a considerable amount of debugging and scripting and testing. I also made

I conducted post-simulation analyses in the statistical package *R*, and in *Python*. Analyses in *R* used adapted legacy code from the previous project. Analysis and plotting methods implemented in *Python* were written by myself.

---

<sup>2</sup>IMPORTANT: don't write about this if you are not going to do the analysis properly.

Write here about code, my contributions, Blue Crystal. Repeats runs, result format, run times etc.

## 2.3 Dynamics of the model

Display and discuss several example full runs. Also with varied parameters?

Well mixed approximation?

### 2.3.1 Transience

Discuss and analyse transience. How long is it? Are the general relationships? Perhaps use simplified modelling (ODEs) to try and predict the length of transience.

### 2.3.2 Long term distribution

Is the final dynamics (after transience) steady state? What can we say about this?

### 2.3.3 Diffusion behaviour

How is species movement/dispersion affected by habitat loss? Can we derive a diffusion coefficient?

## 2.4 Ecological metrics and analysis methods

Introduce, define and discuss each metric.

Stability - Jacobian, dynamic stability, multi-stability, CoV, reproductive stability.

Robustness - secondary extinctions, cascading effects [16]. Re-wiring algorithms?

### 2.4.1 Biodiversity metrics

Richness, Simplicons, Shannon Entropy.

### 2.4.2 Stability metrics

Coefficient of Variation, May Stability

### 2.4.3 Network metrics

We use a number of *qualitative* and *quantitative* descriptors to characterise the realised interaction networks. Good definitions of the suite of network metrics available to community ecologists, including quantitative metrics for network with links weights, can be found in []. Our choice of metrics is the same as in [42].

Various quantitative network metrics are based on the *Shannon entropy* of link weights - analogous to the way it is used to measure diversity of species abundances. It is common practice to use interaction frequency to define link weights, in part because this is easier to measure empirically than, for example, biomass flow<sup>3</sup>. We present here the standard definitions of the Shannon network metrics,

using the notation of Bluthgen et al [7]. The base of the logarithm used varies between the studies cited, here we use the natural logarithm (base  $e$ ) for all metrics. Interaction frequency  $a_{ij}$  is the number of interaction events recorded between species  $i$  and  $j$ .

It is necessary in what follows to define  $\log(0) = 0$ , which is equivalent to excluding zero elements in the interaction matrix from the calculations. Rows or columns with sum equal to zero are removed, to avoid division by zero.

As discussed we use interaction frequency instead of biomass, giving us an asymmetric weighted matrix of interaction frequencies  $\mathbb{B}$ , where element  $b_{ij}$  is the number of individuals of species  $i$  consumed by species  $j$  during the sampling period. Therefore we can define interaction diversities for the links coming into a species  $k$  from its prey, and the links going out of  $k$  to its predators:

$$(2.1) \quad H_{N,k} = -\sum_{i=1}^s \left( \frac{b_{ik}}{b_{.k}} \log \left( \frac{b_{ik}}{b_{.k}} \right) \right)$$

$$(2.2) \quad H_{P,k} = -\sum_{j=1}^s \left( \frac{b_{kj}}{b_{k.}} \log \left( \frac{b_{kj}}{b_{k.}} \right) \right)$$

where  $H_{N,k}$  is the diversity of inflows from prey;  $H_{P,k}$  is the diversity of outflows to predators;  $s$  is the total number of species; and  $b_{.k}$ ,  $b_{k.}$  are column and row sums giving the total number of interactions that species  $k$  has with its prey and predators respectively. The interaction diversity metrics behave just as the Shannon entropy - the higher the number of interaction partners and the more even the interaction frequencies across these partners, the higher the interaction diversities. The exponents of (2.1) and (2.2) are used to calculate the *effective number* of prey and predators respectively:

$$(2.3) \quad n_{N,k} = \begin{cases} e^{H_{N,k}} \\ 0 \text{ if } b_{.k} = 0 \end{cases}$$

$$(2.4) \quad n_{P,k} = \begin{cases} e^{H_{P,k}} \\ 0 \text{ if } b_{k.} = 0 \end{cases}$$

where the symbols have the same meaning previously. These metrics have the property that if the interaction frequencies of species  $k$  are distributed equally amongst its interaction partners,

---

<sup>3</sup>Refer forwards to discussion on IS!

then the effective number of prey/predators is equal to the actual number. However, if the interaction frequencies are not equal between partners, the effective number of prey/predators is reduced, since there is some preferential interaction. These effective number of species are used to calculate *weighted quantitative generality and vulnerability*, which are defined as:

$$(2.5) \quad G_q = \sum_{k=1}^s \left( \frac{b_{..}}{b_{..}} n_{N,k} \right)$$

$$(2.6) \quad V_q = \sum_{k=1}^s \left( \frac{b_{..}}{b_{..}} n_{P,k} \right)$$

where  $b_{..}$  is the total number of interactions. So the metrics in (2.5) and (2.6) give a weighted average of the effective numbers of prey and predators respectively. They are weighted by the fraction of the total interactions the species  $k$  is involved, such that species with more interactions contribute most to the average.  $G_q$ ,  $V_q$ , MTP, H2'

We use the standard network metrics, such as connectance and number of links.

GenSd, VulSd, , Connectance, Nestedness, Compartmentalisation

#### 2.4.4 Spatial metrics

Moran's I, Geary's C. Spatial autocorrelation. Centroids.

#### 2.4.5 Interaction strength metrics

IS1, IS2, IS3 [6].



CHAPTER



## HABITAT LOSS WITH HIGH IMMIGRATION

### 3.1 Introduction

In this chapter we conduct a preliminary investigation of how simulated communities respond to habitat loss. Using the individual based model (IBM) defined in section 2.2 we study the response of communities with varying levels of mutualism (MAI ratio) to the destruction of different percentages of the landscape. As discussed in section 1.2.2, a solid theoretical understanding of communities comprising multiple types of interaction is lacking. Studies in this area are relatively recent [16, 20, 34, 51, 59, 66], and as a result are scarce compared studies of single interaction communities, which have been ongoing for several decades. Therefore the inclusion of mutualism in the model, in addition to antagonistic interactions, represents a key novel feature of this investigation.

To destroy habitat we use the two algorithms described in section 2.2.3. Therefore there are two habitat loss (HL) scenarios to study, which we refer to as the *random* and *contiguous* scenarios according the way in which habitat is destroyed. As we saw in section 1.2.4 numerous studies have found that the spatial pattern of habitat destruction plays an important role in mediating the effect on the community or meta-community (for example [31, 56?]). Therefore the inclusion two types of HL, which represent the extremes of the way in which a natural habitat may be destroyed, allows us to test for different community responses and draw comparisons with previous studies.

To determine the effect of HL on the simulated communities we employ the suite of metrics defined in section 2.4, and study how they change along a gradient of increasing destruction. These metrics capture aspects of diversity, stability, spatial organisation and properties of the network of interactions between species. We predict that both diversity and stability will be

negatively impacted by HL, and that beyond some threshold of destruction species will become extinct from the landscape. Based on the previous HL studies cited above we also expect that random HL will impact communities more than contiguous HL, at least in terms of number of extinctions. However, following the work of Tylianakis [74], we may also expect to see underlying changes in the community structure and network properties prior to the loss of any species from the landscape. This region of the HL gradient, prior to species extinctions, will be of particular interest since such underlying changes are not well understood, and may not be detected by conventional studies and metrics (see section 1.2.5 for more discussion on this). The role of MAI ratio in mediating the effects of HL is also of interest. Based on the findings in [42], which used the same IBM, we may expect communities with high MAI ratio to be more robust the HL.

More intro to come:

- Generate hypotheses to test and relate back to them at the end.
- Make sure to justify the use of all metrics we calculate, based on previous work, and predictions about how they will change, so as not to be accused of fishing.
- Discuss aggregate/community level response. Justify averaging (probably in section 3.2.3).

## 3.2 Methods

Here we outline the experimental procedure used to generate the results presented in section 6.3. The model used for simulation is the IBM defined in section 2.2, and the metrics used in the analysis are mostly defined in section 2.4. In addition to those metrics we employ *rank abundance distributions* (RADs), which are introduced in 3.2.2, and four *invariability* metrics, which are defined in section 3.2.4. We also discuss the relationship between the invariability metrics and community stability<sup>1</sup>.

### 3.2.1 Simulation procedure

For this chapter we ran two ensembles of simulations using the IBM model described in section 2.2. One ensemble employed the random habitat loss algorithm, and the other employed the contiguous algorithm, both of which were defined in section 2.2.3. In both ensembles the level of habitat loss (HL) is varied between 0% and 90% in steps of 10%. At each value of HL there are 25 repeat simulations at each of the 11 MAI ratios ( $MAI = [0.0, 0.1, \dots, 0.9, 1.0]$ ). Therefore there are a total of 2750 ( $= 25 \times 11 \times 10$ ) simulations in each ensemble. Each simulation uses a unique interaction network, generated using the method described in section 2.2.1. The ensembles use the same simulations at  $HL = 0\%$ , since no habitat is destroyed and all else is held constant. All model parameters use the *default values* as given in table 2.1 and published in [42]. The model,

---

<sup>1</sup>Move RADs and invariability to previous chapter, and change this sentence.

as stated previously, is implemented in the programming language *Python* [3]. Simulations were run on BlueCrystal, the university's high performance computer cluster<sup>2</sup>.

### 3.2.2 Rank abundance distributions

Rank abundance distributions (RADs) are used to study the pattern of abundances across numerous species. They are sometimes referred to as Whittaker plots, after his 1965 paper on species abundances in plant communities [77]. To construct the RAD, species are simply ranked from most to least abundant, such that the distribution is monotonically decreasing. It is typical to use the logarithm of the relative abundance of each species. In natural communities it has been observed that these distributions tend to be *long-tailed* - with relatively few species of high abundance, and relatively many species of low abundance. As such RADs have often been found to fit well to a *log-normal* distribution [42, 77]. However numerous alternative models have been proposed [79], and are implemented in the *vegan* package [55] of the programming language *R*. We use this package to fit models to RADs constructed from the simulated communities, with the particular goal of determining how the *evenness* of species abundances changes under HL (see predictions in section 3.1). Therefore we chose to use two models from those available in *vegan*: the *Zipf* and the *preemption* model, because both have a parameter which is easily interpreted as a measure of the evenness of the distribution. The Zipf model is given by the power law:

$$(3.1) \quad \hat{a}_r = N \hat{p}_1 r^\gamma$$

where  $\hat{a}_r$  is the predicted abundance of the species rank  $r$ ;  $N$  is the total number of individuals;  $\hat{p}_1$  is the estimated proportion of the most abundant species (rank 1); and  $\gamma \in \mathbf{R}^-$  is estimated exponent of the power law. So  $\gamma$  gives the gradient of the line defined by (3.1) in log-log space. Therefore a smaller value of  $|\gamma|$  indicates a shallower line and more even distribution of abundances (see for example figure 3.3). The preemption model is given by a geometric sequence:

$$(3.2) \quad \hat{a}_r = N \alpha (1 - \alpha)^{r-1}$$

where  $\alpha \in [0, 1]$  is the single model parameter, and other symbols have the same meaning as in (3.1). Therefore the estimated abundance decreases by a fraction  $(1 - \alpha)$  for each rank, and the choice of  $\alpha$  is constrained such that the estimated abundances sum to  $N$ . In semi-log space, as is used to plot the RADs, the preemption model gives a straight line, since (3.3) implies:

$$(3.3) \quad \log(\hat{a}_r) = \log(1 - \alpha)r + C,$$

where  $C$  is constant. Therefore the smaller the value of  $\alpha$ , the closer the gradient of the line is to zero, and the more even the distribution of abundances. In our case, as is common [55], we

---

<sup>2</sup>Transience, refer back? Habitat loss after 1000 time steps, already mentioned?

use relative abundances to allow comparison of the RADs between communities with a different total number of individuals. Therefore  $N = 1$  in (3.1) and (3.3). The models are fitted using  $R$ , and the parameters  $\gamma$  and  $\alpha$  used as complementary metrics for evenness - in both cases *the smaller the absolute value of the parameter, the more even the distribution of abundances is between the species in the community.*

### 3.2.3 Sampling and analysis

To calculate the analysis metrics from the simulation output we follow the precedent set in [42]. Metrics based only on species abundances are calculated from a ‘snapshot’ of the simulation state on the final time step. Other metrics (for example temporal variability and network metrics) are calculated from samples aggregated over the final 200 iterations of the simulation. For these metrics we use mean species abundances over the 200 time steps, where measures of abundance are required. The *realised network* of interactions is constructed by counting the total number of interactions between each pair of species during the 200 time steps. The assumptions behind this sampling methodology, and their validity, are investigated in chapter ??<sup>3</sup>.

Throughout the analysis we look for robust changes of the metrics evaluated in response to HL. Therefore, as in [42], we fit linear models to identify statistically significant trends, and where necessary we log-transform the data to attempt to linearise the response (see for example figure 3.15)<sup>4</sup>. The linear models are fitted using the *ordinary least squares* method of the *statsmodels* package in *Python*. The *p-value* of the fits are given as a measure for statistical significance<sup>5</sup>.

### 3.2.4 Invariability

Here we discuss stability and the interpretation the invariability metrics...or do this in the previous chapter?

## 3.3 Results

We find that simulated communities respond differently to the two HL scenarios. Therefore in this section we draw comparisons between the results for *random* and *contiguous* HL, and seek to understand the differences. In general we find that there is little qualitative difference in the results for communities with different MAI ratios. Certain quantitative differences, reported in [42], hold true across the HL gradients. For example high MAI communities are more aggregated in space, have more biomass in the lower trophic levels, and support a greater total number of individuals. Despite these quantitative differences, we find that communities with different MAI ratios respond in qualitatively the same way to both types of HL. Therefore, to simplify matters,

<sup>3</sup>Refer to plots in previous chapter, transience.

<sup>4</sup>Check this! And refer forwards to SEM modelling?

<sup>5</sup>More on this..

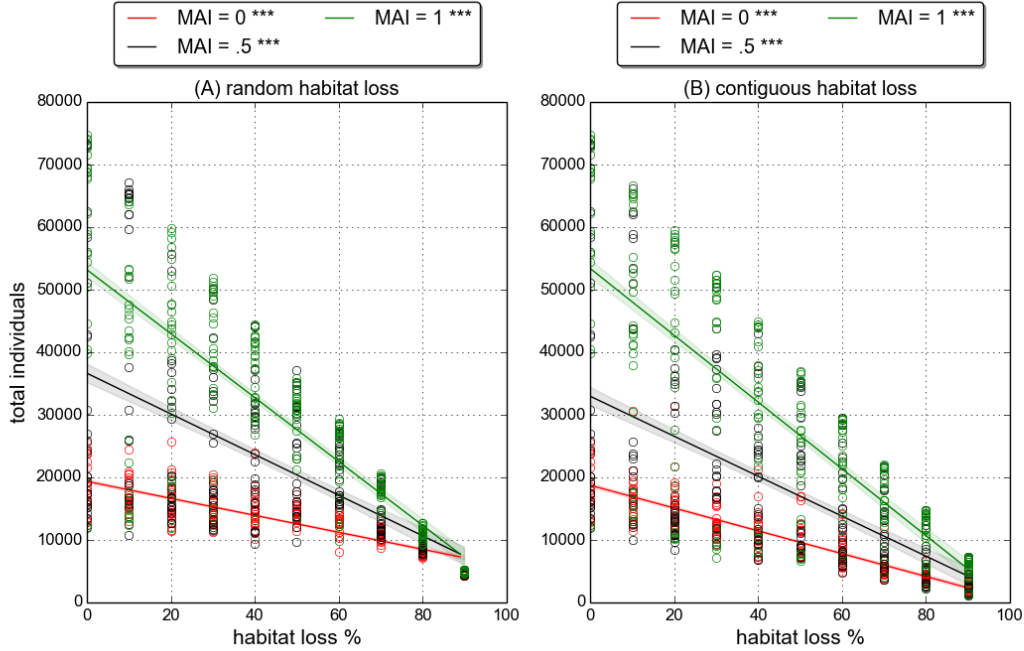


**Figure 3.1: Total number of individuals** against percentage habitat loss, for both scenarios: (A) Random HL, and (B) Contiguous HL. Circles represent the number of individuals for a single community; lines represent a linear fit to the data and the shaded regions indicate the standard error of the mean.  $p$ -value  $< 0.001$  for all linear model fits (indicated by \*\*\*).

we present results for three MAI ratios only ( $MAI = 0.0, 0.5, 1.0$ ). In general we refer only to qualitative trends in the response metrics which hold true across MAI ratios, but make it clear where this is not the case<sup>6</sup>.

For clarity we separate the results into subsections according the type of metric analysed: *Diversity* (section 3.3.1); *Network properties* (section 3.3.2); *Stability and space* (section 3.3.3); and *Invariability* (section 3.3.4). In general we find significant changes in metrics associated with diversity, stability and space. Whereas we find few significant changes in network properties. We address these areas in turn, before providing a summary and synthesis of the results in section 3.3.5.

### 3.3.1 Diversity

Figure 3.1 shows that the total number of individuals decreases in response to HL, in both the random and contiguous scenarios. This is expected - as the number of available cells becomes fewer the landscape is able to support fewer individuals. The linear fits to the data suggest that the average number of individuals is similar at each point in the HL gradient in the two HL

<sup>6</sup>Check this!

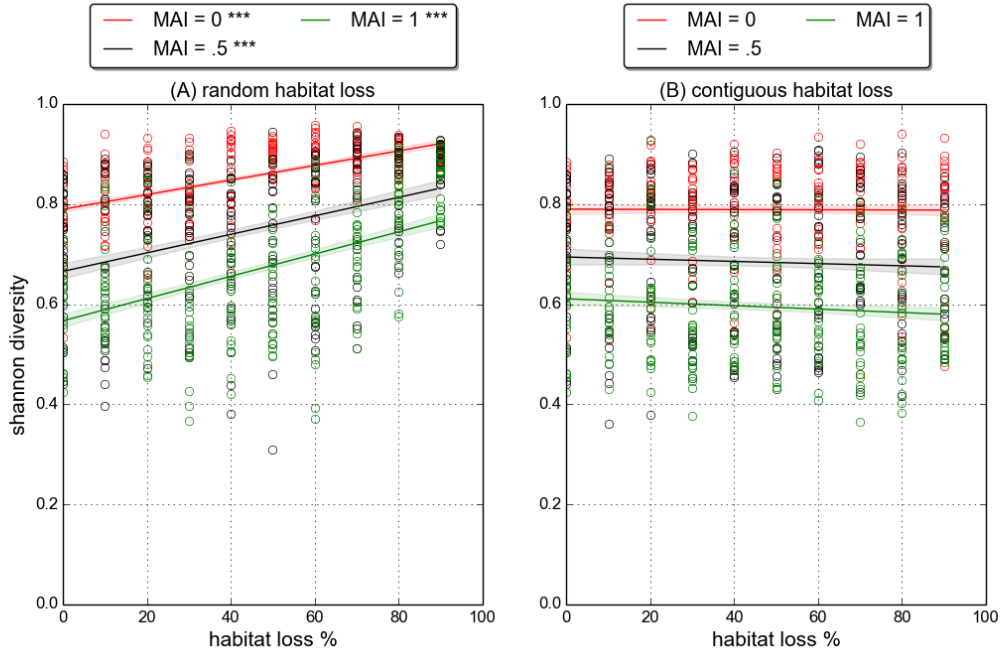


**Figure 3.2: Shannon diversity** against percentage habitat loss, for both scenarios: (A) Random HL, and (B) Contiguous HL. Circles represent the Shannon index value for a single community; lines represent a linear fit to the data and the shaded regions indicate the standard error of the mean. \*\*\* indicates  $p\text{-value} < 0.001$  for linear model fit, whilst no marker indicates  $p\text{-value} > 0.1$ .

scenarios. Therefore there is little to distinguish between the scenarios based on the number of individuals. The figure also shows that communities with higher MAI ratio support more individuals than those with lower MAI ratio, as previously reported [42].

Despite the decreases in the total number of individuals species do not go extinct (results not shown). At 90% HL, when averaged over all AMI ratios and replicates, we observed a mean of 0.0 and 0.23 species extinctions per community for random and contiguous HL respectively. Therefore we effectively see *no change in species richness* in response to habitat loss. The lack of extinctions is due to a relatively high immigration rate (IR). The default value of IR= 0.005 means that, if the landscape were empty, we expect on each time step an average of 200 ( $= 0.005 \times 200 \times 200$ ) immigrant individuals drawn uniformly at random from the pool of 60 species. Therefore species may recover from extinction via a *rescue effect* that is common to all species. The immigration mechanism also allows for the maintenance of very low species abundances, which are maintained by immigration rather than interactions. The absence of extinctions is an interesting feature of these results, since it allows us to focus on underlying structural changes that are not associated with the loss of species (see section 1.2.1 for literature relating to this issue, and section 6.6 for discussion relating to these results).

Although we do not observe changes in species richness under either HL scenario, we do

### 3.3. RESULTS

see changes in community structure. Figure 3.2 shows that the normalised *Shannon diversity* (equation ??) increases for random HL, but does not change significantly for contiguous HL. The same trends are observed when diversity is calculated for each functional group separately (results not shown). This tells us that communities, both at the community level and within functional groups, become more diverse under random HL, whereas under contiguous HL there are *no significant changes in diversity*. Since we know that there is no change in the number of species, any change in diversity must be driven by changes in *evenness* in the distribution of species abundances.

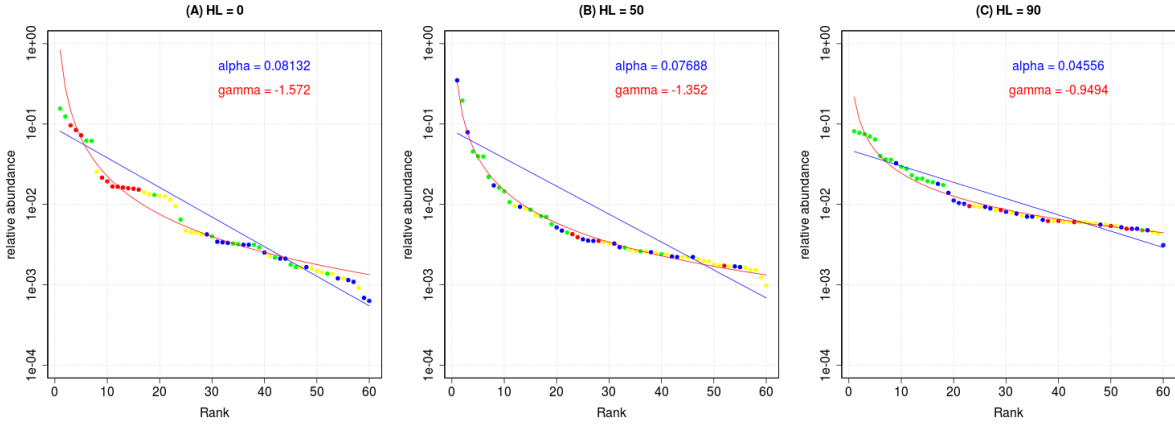


**Figure 3.3: Example rank abundance distributions (RADs)** for three communities with **MAI=0.5** at different levels of **random HL**: (A) HL=0%; (B) HL=50%; (C) 90%. Species abundances are relative to the total number of individuals in the community, and plotted on a logarithmic scale. Points represent species, coloured according to trophic level: green=basal; blue=herbivore/animal-mutualist; yellow=omnivore; red=top predator. Blue and red lines give the pre-emption and Zipf model fits respectively (see text in section 3.2.2 for definitions), best fit parameter value for each model given as annotations on plot.

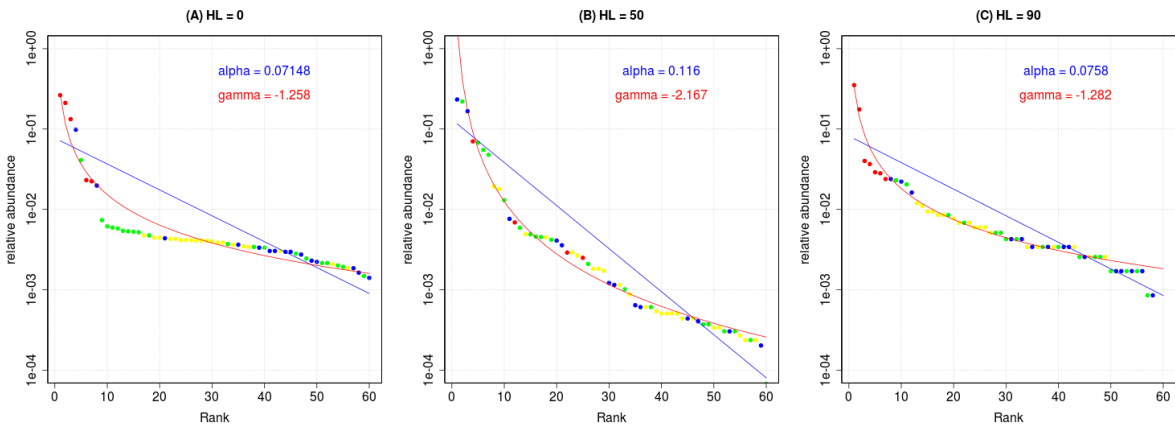


**Figure 3.4:** Similar to figure 3.3 but for **contiguous HL**.

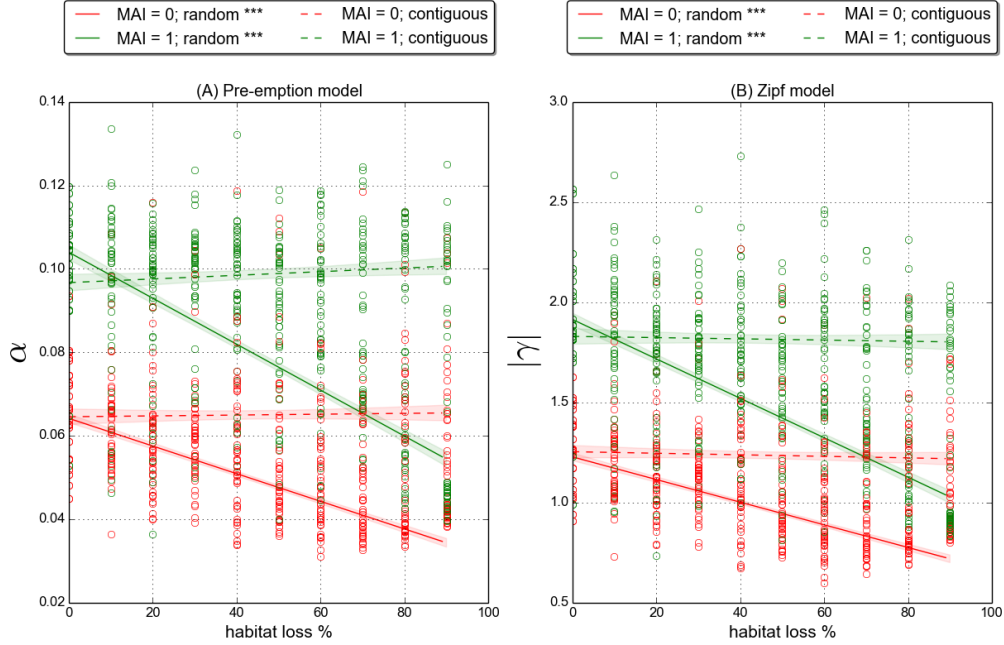


**Figure 3.5: Rank abundance model fit** parameters against HL. Panel A: Pre-emption model parameter  $\alpha$  is smaller for more even distributions. Panel B: Absolute value of Zipf model parameter  $|\gamma|$  is smaller for more even distributions. (See model definitions in section 3.2.2). Solid lines represent linear fits to the random HL data, dashed lines indicate linear fits to the contiguous HL data, and error bars give  $\pm 1$  standard-deviation. \*\*\* indicates  $p$ -value  $< 0.001$  for linear model fit, whilst no marker indicates  $p$ -value  $> 0.1$ .

To look explicitly at changes in evenness we construct *rank abundance distributions* (RADs) for each community, and fit standard models to these distributions (defined in section 3.2.2). Figures 3.3 and 3.4 show example RADs for three communities at different levels of HL, all with MAI= 0.5 (qualitatively the RADs and how they change under HL are similar across all MAI ratios). Since these plots are for single communities we cannot draw general conclusions from them. However, they serve to visualise the model fits and their interpretation. The solid blue and red lines in these plots show the *preemption* and *Zipf* model fits to the RADs, respectively. Each model has an evenness parameter and, as discussed in section 3.2.2, the lower the magnitude of the parameter the more even the distribution. From visual inspection panel C in figure 3.3 is the most even RAD of the six displayed. Correspondingly the model fits to this RADs have the lowest magnitude values for  $\alpha$  and  $\gamma$ . Although the Zipf model appears to give a qualitatively better fits to the data, we use both models the test for evenness in our simulated communities. In this way we can check for consistency in the conclusions.

Figure 3.5 uses all replicates at a given MAI ratio to show how the evenness parameters,  $\alpha$  and  $\gamma$ , change in response to HL. For clarity the results are shown for two MAI ratios only

### 3.3. RESULTS

---

(0.0, 1.0), but are consistent across all MAI ratios. The modelling suggests that under contiguous HL the RADS show no significant change in evenness. However both the preemption and Zipf models indicate that communities under random HL show a significant increase in evenness. These findings are consistent with the changes in Shannon diversity discussed above.

The RADs in figure 3.3 suggest another trend in response to random HL - there appears to be a systematic shift in the relative abundances according to trophic level. This is most visible for the basal and top trophic levels, shown in green and red respectively. For the example communities shown, the top predator species have high relative abundance in pristine landscape (HL= 0), but reduced abundances after habitat loss. At 90% HL all top predators in the community shown have a relative abundance less than 0.01. This is consistent with empirical observations, since species in higher trophic levels tend to be more sensitive to perturbations [13, 63]. On the other hand basal species have a wide range of relative abundances in pristine landscape, but come to dominate the community at 90% HL with all but one basal species in the top 18 ranks. To investigate this effect further we look at the relative abundances of all six functional groups in response to habitat loss. These are plotted in figures 3.6 and 3.7 for the random and contiguous scenarios respectively. For the contiguous scenario community structure, according to these relative abundances, is remarkably constant across the habitat loss gradient. The only statistically significant changes are in the non-mutualistic plant and top predator species at MAI= 0, where there is a slight decrease in top predator abundance relative to plant abundance. In the random scenario there are clear systematic shifts in the distribution of abundance across functional groups. In particular, and in agreement with the RADs in figure 3.3, there is a relative increase in plant abundance and decrease in top predator abundance, which is statistically significant across all MAI ratios. There is also a slight decrease in the relative abundance of species in the second trophic level (herbivores and mutualistic animals). Overall there is a shift in relative abundance towards the basal level, but interestingly there is no significant change in the abundance of omnivore species. This suggests that there is some benefit to being omnivorous in this context (see discussion in 3.3.5).

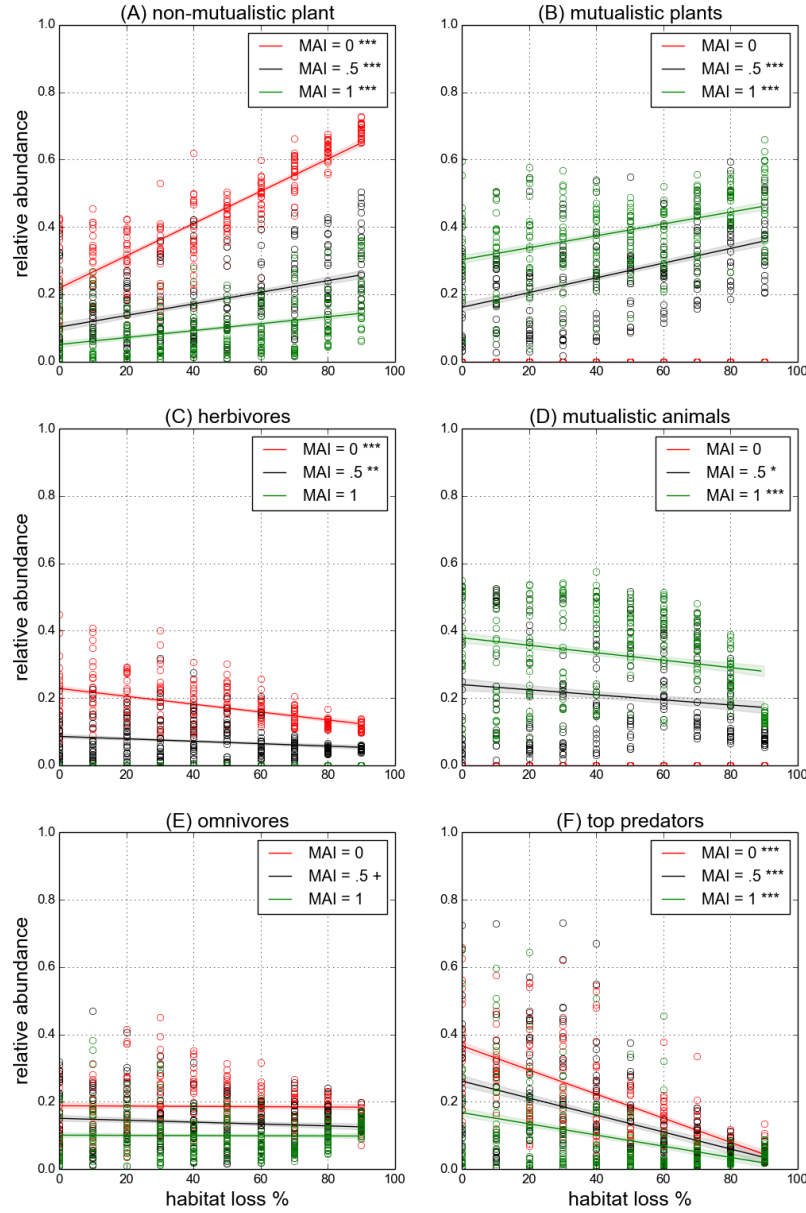


**Figure 3.6: Relative abundance by functional group for random HL.** Abundance relative to total number of individuals in the community. Circles represent the value for a single community; lines represent a linear fit to the data and the shaded regions indicate the standard error of the mean. The markers \*\*\*; \*\*; \* and + corresponds to linear model fit p-values of  $< 0.001$ ,  $< 0.01$ ,  $< 0.05$  and  $< 0.1$  (marginal significance) respectively.

### 3.3. RESULTS

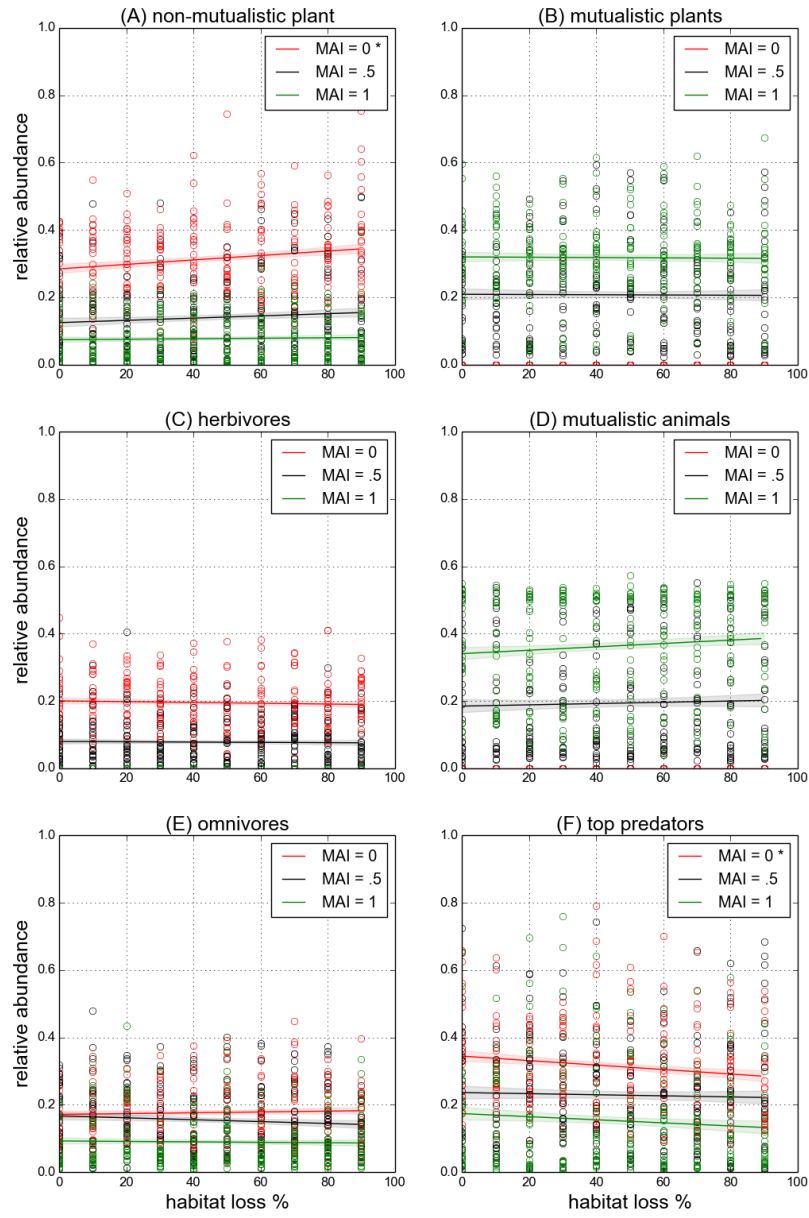


Figure 3.7: Similar to figure 3.6, but for **contiguous HL**.

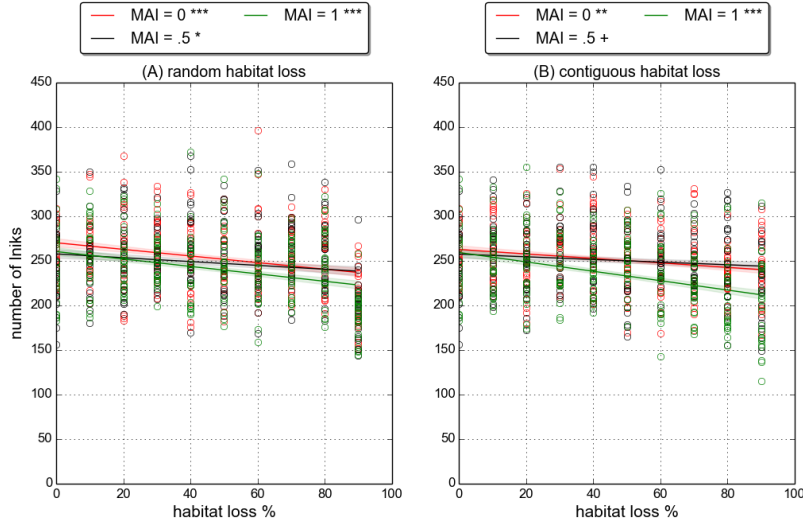


Figure 3.8: **Number of links** of links in the realised network (see text in section 3.2.3 for definition). Linear fits and p-value markers as in previous plots (see caption of figure 3.6).

### 3.3.2 Network properties

Figure 3.8 shows that, in both HL scenarios, there is a slight decrease in the number of links in the realised network. This result indicates that some species, which would be able to interact, do not encounter each other in space as a result of HL. The number of links lost, on average is few - the greatest loss according to the linear models is under contiguous HL for MAI= 1.0 where the number of links falls from  $\approx 250$  in pristine landscape to  $\approx 200$  at  $HL = 90\%$ <sup>7</sup>. However loosing any number of links may be enough to create detectable changes in network topology. In addition to the loss of links from the network we see a decrease in the total number of interactions in both scenarios, which is shown in figure 3.9. This is in agreement with the loss of individuals (figure 3.1), since if there are fewer individuals in the landscape we should expect fewer interactions. In general we expect the frequency on an interaction to be largely determined by the abundances of the interacting species. This effect was discussed in section ??, and is studied in more detail in chapter ???. However it appears from figure 3.9 that more interactions are lost due to random HL than contiguous, since the slopes of the linear fits are steeper<sup>8</sup>. This suggests a mechanism under random HL that results in fewer interactions than under contiguous HL, despite similar numbers of individuals. We propose such a mechanism in section 3.3.5.

Together the loss of links, and the change in interaction frequencies indicate changes in realised network of interactions. Therefore we seek to characterise these changes, using the network metrics defined in section 2.4.3. The nestedness and compartmentalisation of communities

<sup>7</sup>Why is the greatest change here?

<sup>8</sup>Also look at high HL values - it is clear.

### 3.3. RESULTS

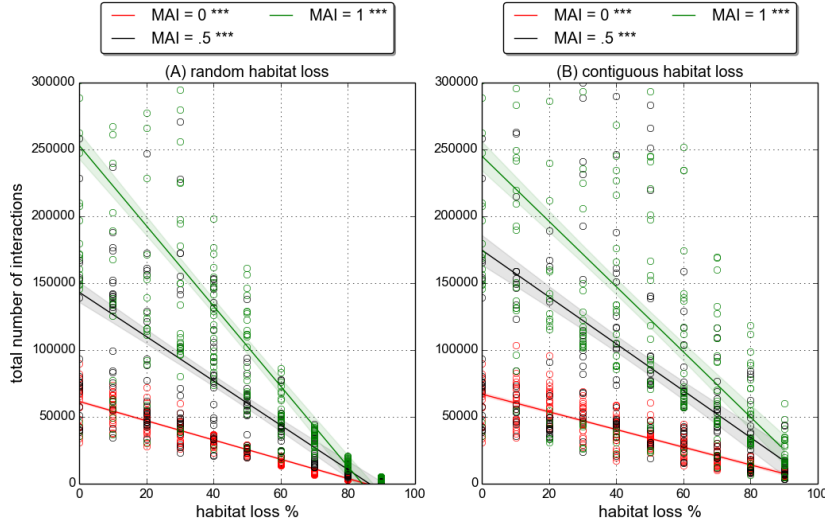


Figure 3.9: **Total number of interactions** between all species during final 200 iterations of a simulation. Linear fits and p-value markers as in previous plots (see caption of figure 3.6).

showed no significant change under either HL scenario. Therefore these plots are not shown. The response of the binary (non-quantitative) metrics follows directly from the loss of links, since there is no change in species richness. Therefore connectance, generality and vulnerability all decrease in both scenarios (results not shown), as a result of the loss of links shown in figure 3.8. The response of the quantitative network metrics is more interesting because these metrics are based not only on the presence/absence of links, but on the frequency of each interaction.

The results for the weighted quantitative generality and vulnerability metrics (hereafter generality and vulnerability) are shown in figures 3.10 and 3.11. For contiguous HL neither metric shows significant change. This tells us that the loss of links and decrease in interaction frequencies occur in a such a way that the average number of effective prey and predators per species is constant across the contiguous HL gradient. For this to occur the changes must be distributed homogeneously across the network such that there is no change, on average, in the number of interactions per species and the relative frequencies of those interactions. This finding is in agreement with the observed lack of change in diversity and rank-abundance patterns under contiguous HL (section 3.3.1) - if the relative abundance of all species is constant across the HL gradient, and interaction frequencies are mainly driven by species absolute abundances, then the lack of change in quantitative network metrics follows directly. This appears to be what is happening in the contiguous scenario.

In the random scenario quantitative generality and vulnerability decrease and increase respectively (figures 3.10 and 3.11). This represents ad asymmetry between the responses of predator interactions compared to prey interactions. The increase in vulnerability means that the average *effective* number of predators per prey increases. It is unlikely that the *actual* number of

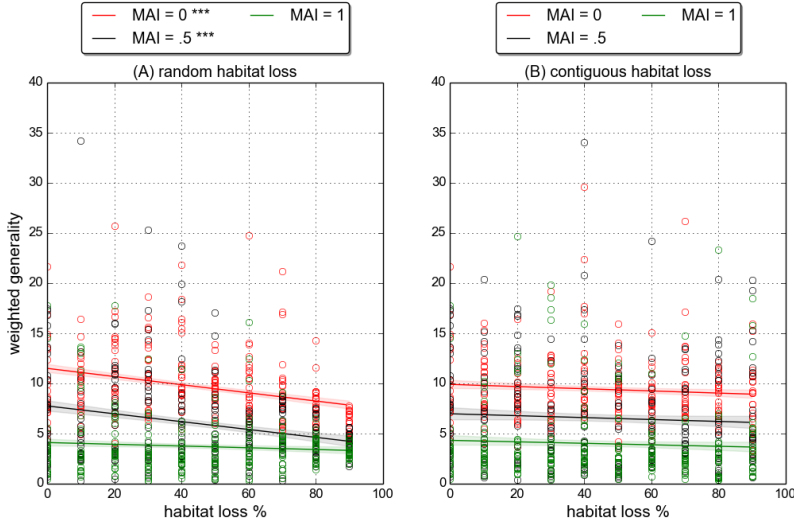


Figure 3.10: **Weighted quantitative generality**, of whole network (see section 2.4.3 for definition). Linear fits and p-value markers as in previous plots (see caption of figure 3.6).

predators per prey increases, since links are lost from the network. Therefore the only way that vulnerability could increase is if the interaction frequencies of prey with their predators became more even. We know from section 3.3.1 that species abundances become more even in response to random HL, and that diversity increases both at the community level and within functional groups. Therefore the change in vulnerability appears to be explained by the increased evenness of prey and predator species, leading to more evenness interaction frequencies between the two.

The drop in generality tells us that the average *effective* number of prey per predator decreases under random HL. Since we have just concluded that interaction frequencies become more even, we must attribute this to a decrease in the *actual number of prey* per predator. Since we know that the relative abundance of top predators is greatly reduced (figure 3.6), it is reasonable to conclude that some struggle to find prey. Interestingly the change in generality at MAI= 1.0 (figure 3.10A) is not significant (although it was significant at all other MAI ratios) suggesting that either prey are not lost, or more likely that the loss of prey to top predators is offset by the increased evenness of interactions. We know that high MAI communities have fewer individuals in the top trophic level (figures 3.6 and 3.7) and so the top predator contribution to generality is likely to be lower. Also high MAI communities contain more individuals than low MAI communities across the HL gradient, meaning a greater absolute number of prey. Together these two mechanisms may be enough to explain why generality does not change at MAI= 1.0.

The results for the bipartite network metrics, interaction diversity and H2', are shown in figures 3.12 and 3.13. They support the conclusion that the changes in quantitative network metrics are driven by changes in species relative abundances. In the contiguous scenario neither metric shows significant change, in agreement with the generality and vulnerability results.

### 3.3. RESULTS

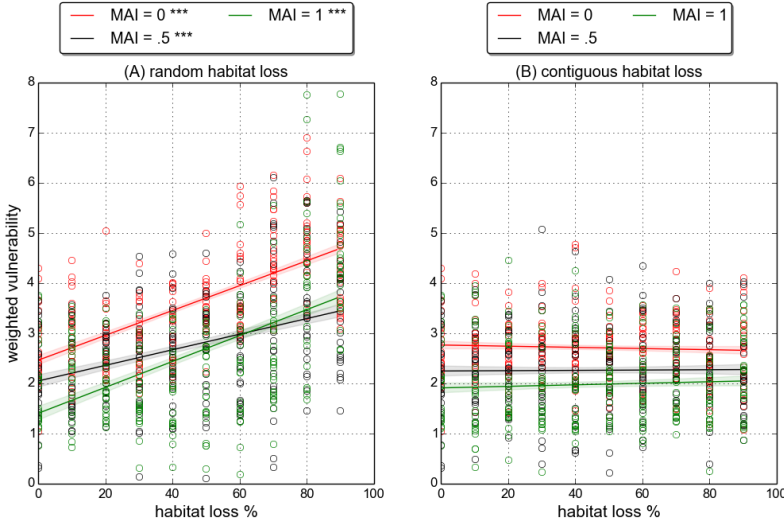


Figure 3.11: **Weighted quantitative vulnerability**, of the whole network (see section 2.4.3 for definition). Linear fits and p-value markers as in previous plots (see caption of figure 3.6).

In the random scenario interaction diversity increases, whereas the specialisation metric  $H2'$  shows no significant change. The increase in interaction diversity means that the interactions frequencies between plant and animal mutualists become more even. Again we assert that this is due to the observed increase in evenness of species relative abundances in these two groups<sup>9</sup>.

The fact that  $H2'$  does not change significantly means that interactions in the mutualistic sub-network do not become more even or less even relative to a null model. The null model (see definition in section 2.4.3) calculates the minimum and maximum interaction diversity,  $H2_{min}$  and  $H2_{max}$ , with the constraint that the total number of interactions of each species is held constant. If we assume, as we have argued, that the total number of interactions of a species is proportional to its abundance, then the constraint is equivalent to fixing the distribution of species abundances constant. The  $H2'$  result then implies that interactions do not become more diverse than expected, given the abundance of each species. In other words, the change in the diversity of interactions is due to changes in species relative abundances<sup>10</sup>.

<sup>9</sup>Refer to new figure!

<sup>10</sup>This is still not clear! Give example?

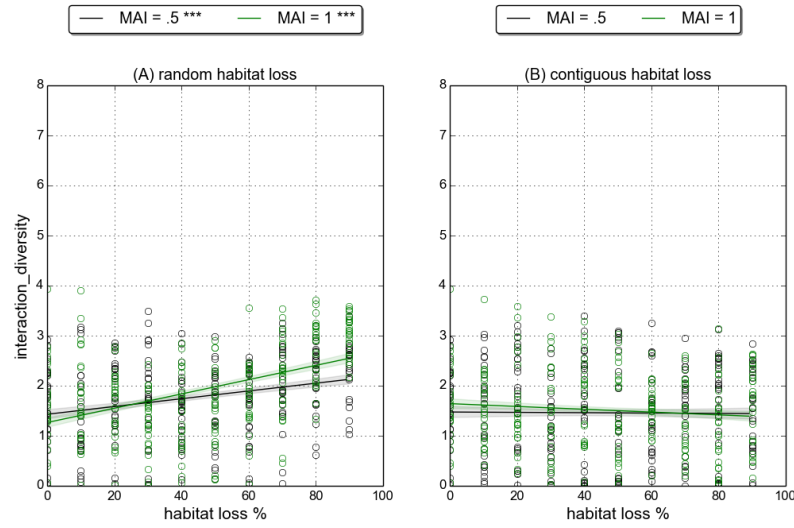


Figure 3.12: **Interaction diversity** in the mutualistic sub-network (see section 2.4.3 for definition). Linear fits and p-value markers as in previous plots (see caption of figure 3.6).

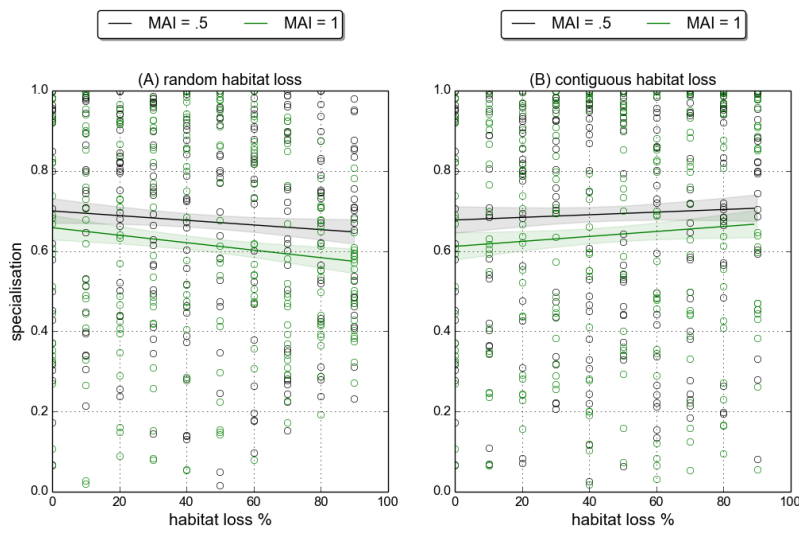
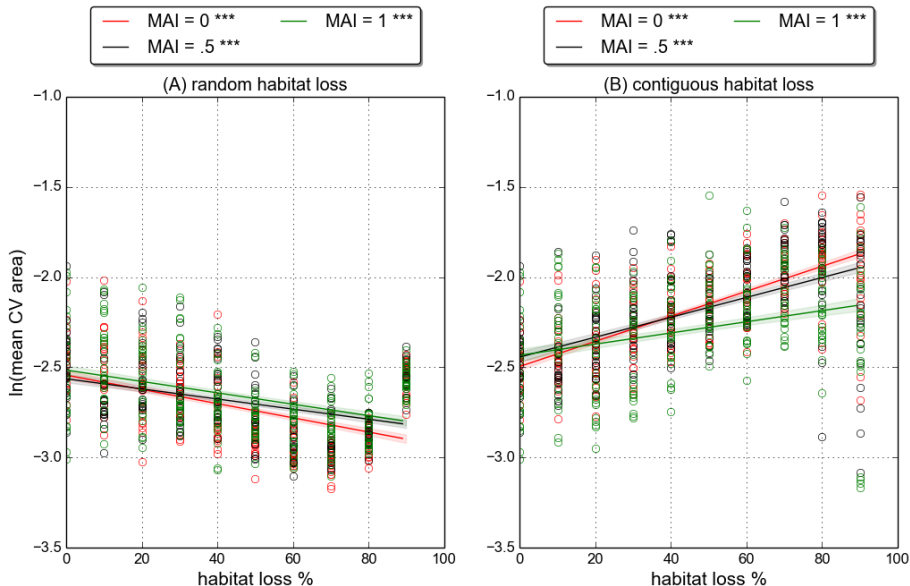


Figure 3.13: **Specialisation H2'** in the mutualistic sub-network (see section 2.4.3 for definition). Linear fits and p-value markers as in previous plots (see caption of figure 3.6).

### 3.3.3 Stability and spatial metrics

In this section we measure stability using the four variability metrics defined in section 2.4.2: the temporal coefficients of variation (CV) in species abundances (*mean CV*), species range area (*mean CV area*), species range centroid (*mean CV centroid*), and species spatial density (*mean CV density*). At the end of the section we also look at the spatial aggregation metrics, as defined in section 2.4.2. Although these are not directly related to stability, they are relevant to the spatial structure of the communities. All metrics are calculated at the species level, and then averaged over all species in the community. In the following section (3.3.4) we show that the stability results are consistent with the alternative *invariability* metrics, which are defined in section 3.2.4.

The stability results are consistent across the four variability metrics - *communities become more variable under random HL, and less variable under contiguous HL*. To analyse the metrics we take the natural logarithm of the variability metrics before fitting linear models. The raw data show trends that are clearly non-linear, and appear approximately exponential (responses change at an increasing rate). Therefore the log-transform serves to linearise the data and make a linear model fit more appropriate. The log-linear trends are illustrated for species area variability in figure 3.14, and for species abundance variability in the middle row of figure 3.15. The same trends are observed for the other variability metrics (results not shown), and they are statistically significant across all MAI ratios. Therefore we conclude that the variability response is robust.



**Figure 3.14: Species area variability:** coefficient of variation in area of species range, averaged over all species (definition in section 2.4.2). Linear fits and p-value markers as in previous plots (see caption of figure 3.6).

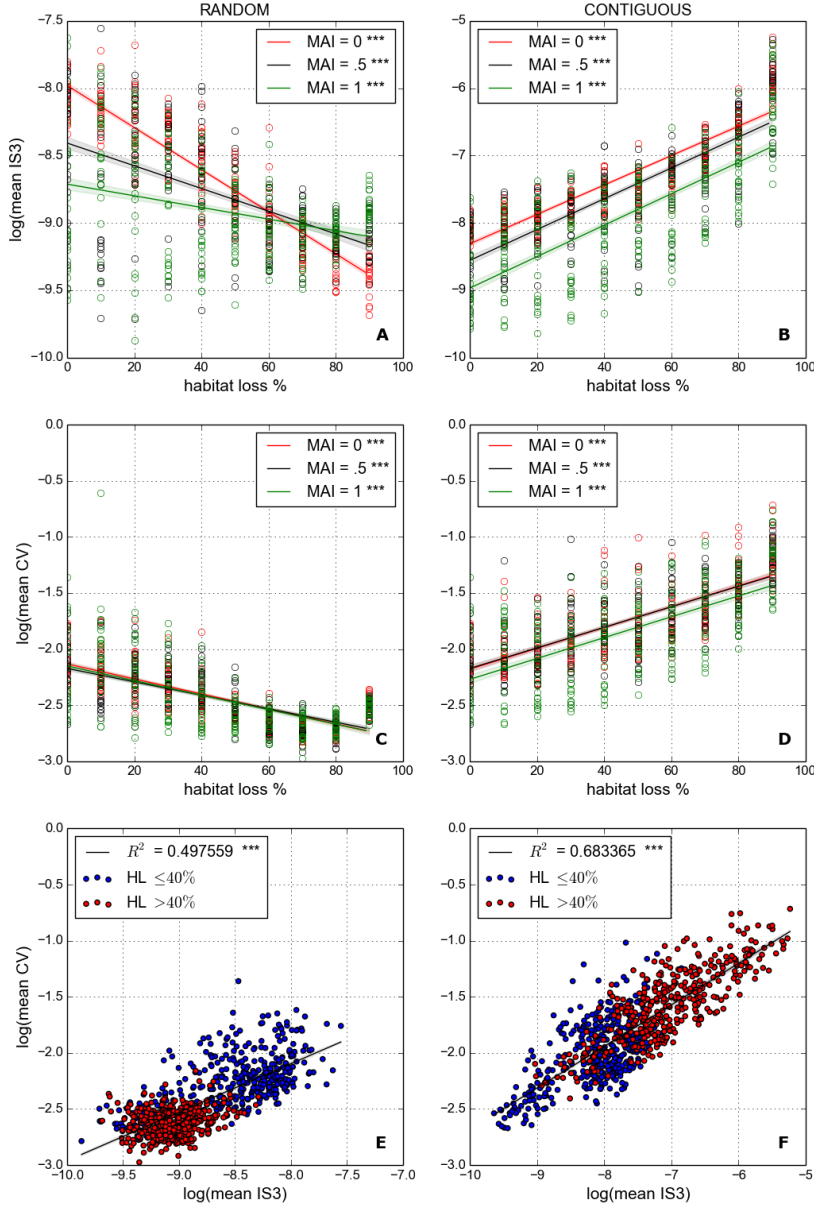


**Figure 3.15: Interaction strengths and temporal variability.** Both natural log-transformed to linearise trends. Panels A-B: Interaction strength metric IS3 (defined in section 2.4.2) averaged over all interactions in realised network. Panels C-D: mean CV, coefficient of variation in species abundances (defined in section 2.4.2) averaged over all species. Panels E-F: IS3 as a linear predictor for mean CV, with low and high HL communities indicated by blue and red circle respectively. All communities for MAI= 0.0, 0.5, 1.0 shown. Linear fits and p-value markers as in previous plots (see caption of figure 3.6).

The variability response also represents a striking difference between the two HL scenarios. In all other metrics presented communities either respond in the same way (e.g. number of individuals, number of links), or display significant changes under one scenario but not the other (for example population evenness). However the trends observed in variability are qualitatively opposite for the two HL scenarios. This leads us to question the mechanism behind the change in variability.

The only metric, aside from variability, which shows trends in opposite directions under different types of HL is *interaction strength* (IS3). These trends are illustrated in the top row of figure 3.15, where we again use the natural log-transform of the data. Under random HL the average interaction strength decreases, whereas under contiguous HL it increases. We also observe the dependence of interaction strength on MAI ratio, as reported in [42]. In pristine landscape higher MAI communities have weaker interaction strengths. Under contiguous HL this ordering of IS3 according to MAI is conserved across the HL gradient. However under random habitat loss communities with a high MAI ratio do not lose interaction strength as much as low MAI communities. The result is that beyond about 70% HL high MAI communities tend to have greater interaction strength than low MAI communities. Although only shown for three MAI ratios, the pattern described is consistent across all eleven MAI ratios. The possible explanations for the dependence of the IS3 response on MAI ratio are discussed in section 6.6.

The bottom row (panels E and F) of figure 3.15 shows the log-transformed values of IS3 plotted against the log-transformed abundance variability. These figures are an aggregate representation of all the simulation repeats with MAI= 0.0, 0.5, 1.0. In both the random and the contiguous scenario there is a significant linear trend between the log-transformed interaction strength and variability. The coefficient of determination  $R^2$  values of these linear models are, as given on the plot,  $\approx 0.5$  and  $\approx 0.7$  in the random and contiguous cases respectively. This means that, on aggregate, interaction strengths can explain at least half of the variance in temporal variability, and more than this in the contiguous case. The dependence on habitat loss is also striking. In the random case, high HL ( $> 40\%$ ) shifts communities towards lower IS3 and lower variability, whilst the converse is true for the contiguous case. In both cases the relationship between IS3 and variability is consistent at low and high HL. Therefore we conclude that there is a strong correlation between IS3 and temporal variability, which is mediated by habitat loss. In section 3.3.5 we present the evidence that this correlation represents a causal relationship, and that *interaction strengths are key to understanding how simulated communities respond to HL*.

We observe changes in spatial aggregation under random HL, but not under contiguous HL. Spatial aggregation is measured at the local and global scales using the metrics *Geary's C* and *Moran's I* respectively. Both metrics are bound between 0 and 1. A value of Geary's C close to 0 indicates high local aggregation, whereas a value of Moran's I close to 1 indicates high global aggregation. Figures 3.16 and 3.17 show that, across the board, species are not highly aggregated on average<sup>11</sup>. Also higher MAI communities are found to be more aggregated than

---

<sup>11</sup>What does a random distribution give?

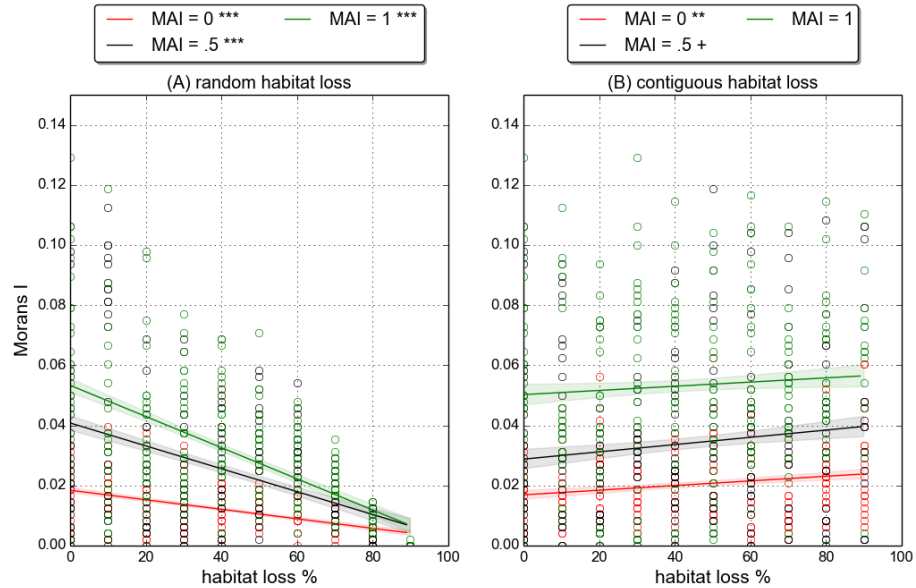


Figure 3.16: **Moran's I** metric for global aggregation (defined in section 2.4.4, averaged over all species. Linear fits and p-value markers as in previous plots (see caption of figure 3.6).

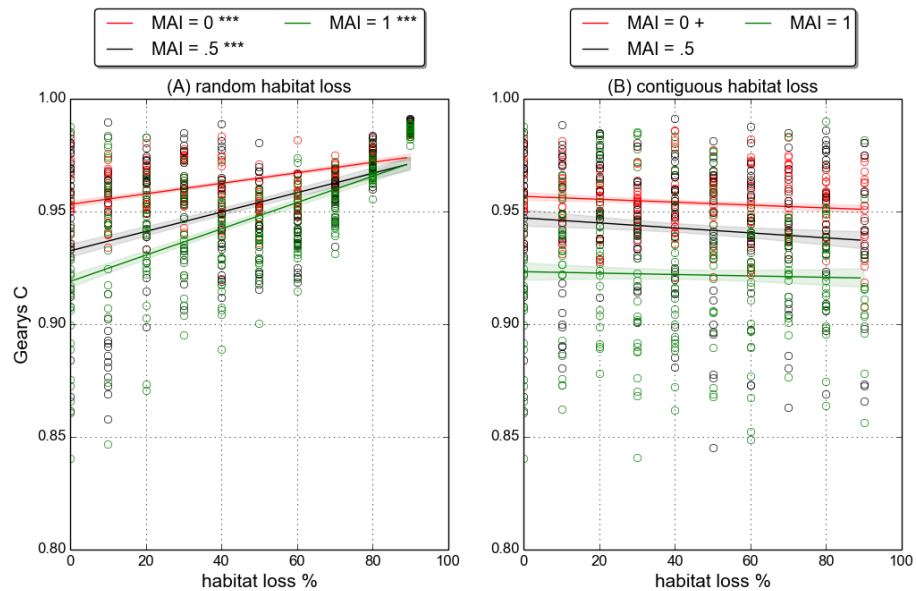


Figure 3.17: **Geary's C** metric for local aggregation (defined in section 2.4.4, averaged over all species. Linear fits and p-value markers as in previous plots (see caption of figure 3.6).

### 3.3. RESULTS

---

low MAI communities. As argued in [42], this is caused by an increase in the aggregation of plant species due to reduced herbivory pressure and increased local reproduction. The increase in plant aggregation cascades up to higher trophic levels since species thrive close to aggregations of food resource<sup>12</sup>. In response to random HL, species on average become less aggregated in space at both the local and global scales. This is expected because the way in which habitat is destroyed creates a patchy landscape which acts against aggregation. Conversely there is some evidence that contiguous HL leads to a slight increase in aggregation. However the only significant linear trend is in Moran's I at MAI= 0.0 (figure 3.16B). Therefore we conclude that contiguous HL does not create significant and robust changes in aggregation. This may be linked to the reduction in stability, since dynamics become more variable it may be harder for species to form local aggregations in space.

---

<sup>12</sup>Good place to refer to animation/spatial plot.

### 3.3.4 Invariability

The alternative stability metrics defined in section 2.4.2 are based on *invariability*. These include minimum invariability, population invariability, ecosystem invariability and ecosystem synchrony. Here we demonstrate that the first three of these metrics respond in the same way to HL as the *variability metrics*, giving more weight to the conclusions on stability. The fourth metric, ecosystem synchrony, gives us a new piece of evidence about how the dynamics of the communities change in response to HL.

Figure 3.18 shows the response of minimum invariability to HL. We use the natural log-transform of the data, as in section 3.2.4, because of the apparent exponential nature of the trends in the raw data. From the figure we see that minimum invariability increases in response to random HL, whereas it decreases in response to contiguous HL. The trends are the same for population and ecosystem invariability, and statistically significant at all MAI ratios (results not shown). These changes in invariability are in agreement with the results of the previous section - community dynamics becomes less variable under random HL, and more variable under contiguous HL. The interpretation of these metrics in [50] lends support to the conclusion that the observed changes in temporal variability are also associated with changes in the stability of the community in a dynamical systems sense<sup>13</sup>.

Figure 3.19 shows linear fits to the ecosystem level synchrony for the two HL scenarios. In the

<sup>13</sup> More on this, and link to next chapter. Also mention that minimum invariability is dominated by least abundant species.

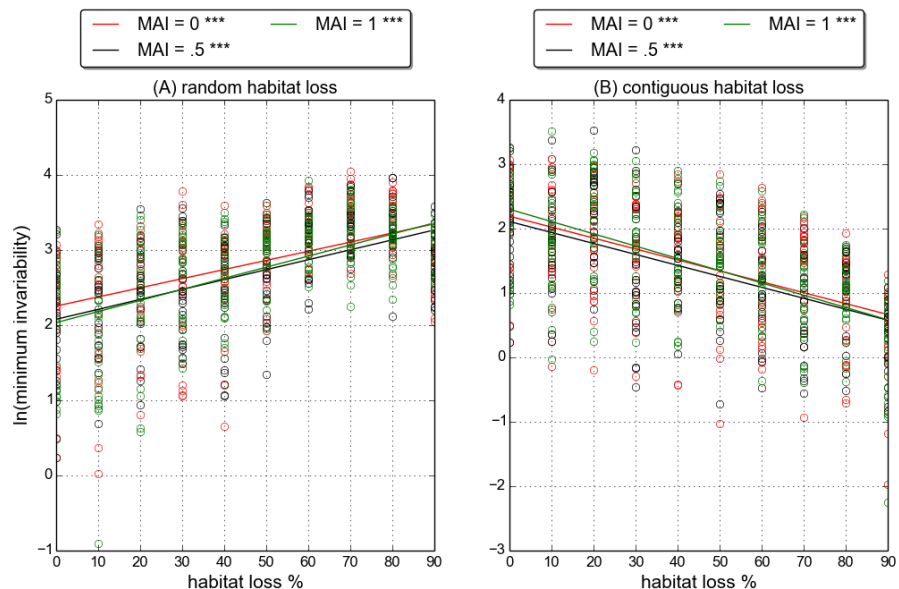


Figure 3.18: **Minimum invariability** as defined in section 2.4.2. Linear fits and p-value markers as in previous plots (see caption of figure 3.6).

### 3.3. RESULTS

---

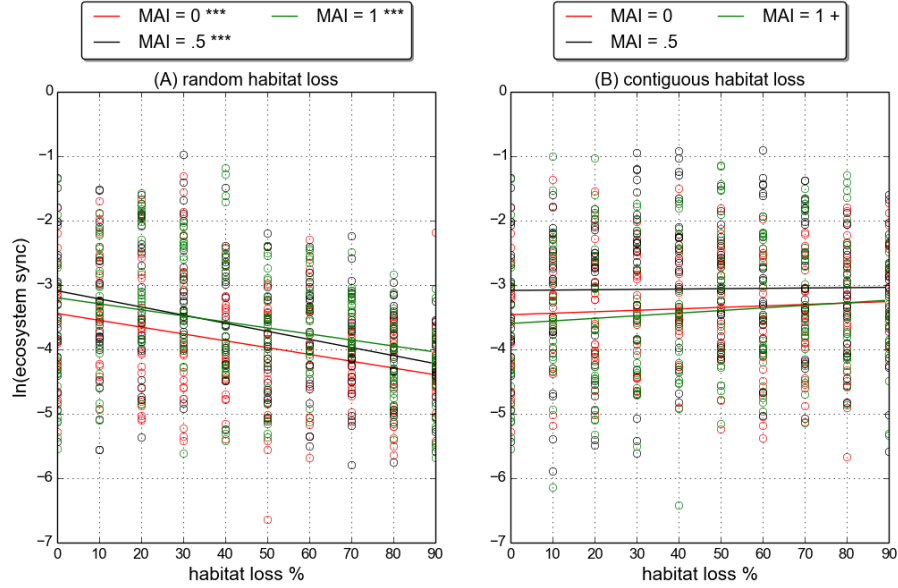


Figure 3.19: **Ecosystem synchrony** as defined in section 2.4.2. Linear fits and p-value markers as in previous plots (see caption of figure 3.6).

random case there is a significant decrease in synchrony, whereas in the contiguous case there is no significant change. Also in all cases the synchrony is relatively low. Perfectly synchronised dynamics for all species would give a log-synchrony value of 0. Therefore all communities are well below perfect synchrony. This is expected from trophic dynamics, since it is well known that predator-prey dynamics leads to a phase lag between the population of predator and prey. However it is important to note that trophic dynamics should also lead to some level of synchrony, as species tend to respond in the same way to fluctuations in a shared resource or predator. Therefore it may be that the change in synchrony under random HL is a signature that the trophic component of the population dynamics is reduced. This would agree with the observed reduction in interaction strengths shown in figure 3.15.

### 3.3.5 Synthesis

Here we summarise the results presented so far, and attempt to synthesise them by explaining the main mechanisms driving the observed community responses to HL. Under contiguous HL communities displayed fewer changes than under random HL. *In the contiguous scenario* we saw that the number of individuals, the frequency of interactions, and to a lesser extent, the number of links, all decreased with HL. However the mean interaction strength and temporal variability increased, representing a reduction in dynamic stability. There were no robust trends in network properties, diversity, evenness, relative abundance by functional group or spatial aggregation, under contiguous HL. *In the random scenario*, as in the contiguous, the number of individuals, the frequency of interactions, and the number of links, all decreased. Unlike the contiguous case, the mean interaction strength and temporal variability decreased, representing an increase in dynamic stability. Under random HL communities became more diverse and more even; displayed a shift in relative abundance towards basal species; and became less aggregated in space. There was also an increase in quantitative vulnerability; a decrease in quantitative generality; and an increase in the interaction diversity of the mutualistic sub-network.

In section 3.2.4 we demonstrated that there is a significant correlation between mean interaction strength and temporal variability. Theoretical population dynamics, in general, suggests that strong inter-specific interactions are destabilising in antagonistic systems [11, 37, 44, 46, 53], and there have been some empirical observations of this effect [54]. In a simple predator-prey model, such as the Lotka-Volterra model, it can be shown that increasing the strength of the coupling between species leads to larger amplitude oscillations and may, in certain models may lead to the extinction of species due to over-predation. This effect is intuitive - the stronger the coupling, or interaction, between species, the greater the effect that one has on the other. In 1972 May showed [44] that for large assemblages of species, with random interactions, the probability of stability is reduced by strong interactions. Together the body of work cited represents a general consensus that antagonistic dynamics are destabilised by strong interactions. Less is known about the dynamics of mutualistic systems, especially when they are embedded in a larger trophic system [42, 66]. However, in some studies mutualisms have been found to play a destabilising role [11, 45]. Again this result is intuitive, since an interaction which provides mutual benefaction to both parties can easily lead to a destabilising positive-feedback. In the IBM we model mutualisms as trophic interactions. The animal mutualist consumes resource from its plant partner in addition to providing the reproduction service. Therefore it is not clear whether the net result of mutualistic interactions on the plant population as a whole is positive or negative. However in either case it can be argued that stronger mutualistic interactions will be destabilising. *Therefore we conclude that the observed changes in interaction strengths are driving the changes in temporal variability under HL* (figure 3.15).

In section 3.3.2 we argued that *changes in the distribution of species abundances can explain how the quantitative network properties respond* under the two HL scenarios. We explained how

### 3.3. RESULTS

---

the evenness of species abundances affects interaction frequencies. Since evenness changes in the random but not in the contiguous scenario, this is able to explain why quantitative network properties are observed to respond to one type of HL but not the other. However we have yet to explain the differential response of species relative abundances under the two scenarios. Therefore we are left with two main questions: what is driving the change in the distribution of species abundances? And, what is driving the change in interaction strengths? In what follows we show that the two are closely related.

We first address the questions of interaction strengths. In both HL scenarios the total number of individuals and the total number of interactions decreases. However in the random and contiguous scenarios mean interaction strengths decrease and increase respectively. Figures 3.20 and 3.21 show that these changes in mean interaction strength are due to the entire distribution of IS3 shifting in opposite directions. Distributions are plotted for MAI= 0.0 and MAI= 1.0, showing the same shifts in both cases. We focus on the MAI= 0.0 case because the pattern is clearer (panel A in these two figures). Under random habitat loss the distribution of IS3 shifts left, towards weaker interactions. The spread also decreases slightly, suggesting less variance in interaction strengths. Under contiguous habitat loss the distribution shifts towards higher interaction strengths, and also becomes much flatter, such that there is a greater spread in interaction strengths. Importantly we see that conclusions based on the mean value of IS3 were not misleading, for example due to a highly skewed distribution. In fact the majority of interactions in a contiguous landscape are stronger than the the majority of interactions in a randomly destroyed landscape, for a given level of HL. However we know, from figure 3.1, that the total number of individuals is similar in either landscape. Since IS3 is calculated by dividing the interaction frequency by the abundance of the two interacting species, it must be the case that interaction frequency is lower for a given number of individuals in a randomly destroyed landscape than a contiguous one. Indeed we saw evidence in figure 3.9 that species interact less frequently in the random scenario than the contiguous, despite comparable total numbers of individuals.

Why would species with the same abundance interact more frequently in a contiguous landscape compared to a landscape with random HL? The answer is simply that randomly destroyed cells present a barrier to the motion of individuals. To demonstrate this we conduct a series of simulation experiments, using the following procedure. We place a single individual randomly in a  $200 \times 200$  landscape. The individual moves according to the same rules that the animal individuals follow in the IBM (defined in section 2.2), but without the bioenergetic constraints. We record what fraction of the available (i.e. not destroyed) landscape cells the individual visits during 5000 time steps. The experiment is repeated 100 times for each level of HL, and for both HL scenarios, to obtain the expected range of motion of an individual in each type of landscape. The results are shown in figure 3.22. Panel A shows an example trajectory of an individual over 5000 iterations in a pristine landscape. Panel B shows the same, but for a

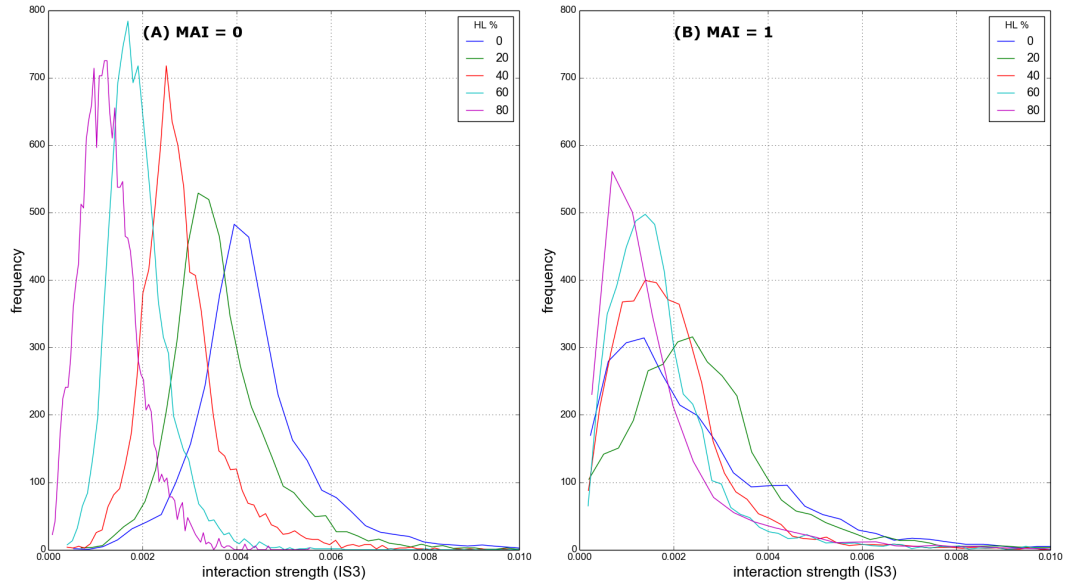


Figure 3.20: **Interaction strength distributions (IS3) under random HL.** Panel A: MAI= 0.0. Panel B: MAI= 1.0. IS3 values for all interactions in each of 25 replicate simulations at the given MAI and HL value, frequency in 100 bins of equal width.

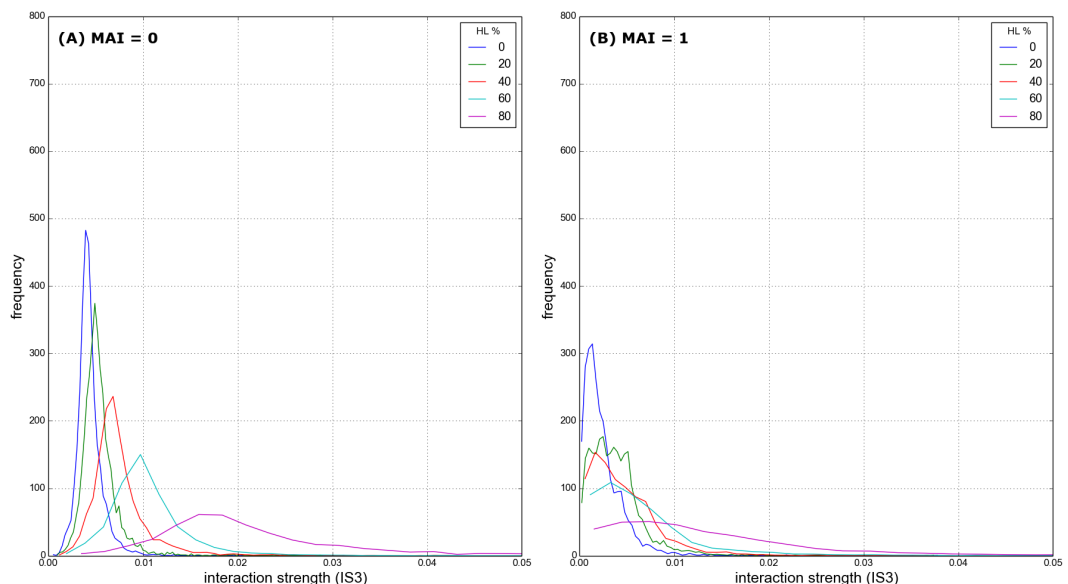


Figure 3.21: Similar to figure 3.20, but for **contiguous HL**.

### 3.3. RESULTS

---

landscape at 40% random HL. It is clear that the range of motion is severely restricted by the destroyed cells. Panel C shows that an individual does not experience such barriers to motion in a contiguous landscape, except at the edges of the available habitat. The result is that the percentage of available landscape that an individual can explore during 5000 iterations increases under contiguous HL, but decreases under random HL. This explains the observed changes in interaction strength. If an individual is less mobile it is harder for it to find interaction partners, even if the potential partners are present in the landscape at the same abundance. The converse is true for individuals with increased mobility.

Another consequence of the reduced mobility of individuals is that, *ceteris paribus*, it decreases the probability of intra-specific interactions. These interactions are required for the sexual reproduction of non-basal species - individuals must encounter a member of the same species in space in order to create offspring. Intra-specific interactions are not recorded during the simulations, but the total number of births and total number of immigrants for each species is recorded. In figure 3.23 we plot the proportion of total births during a simulation that are due to immigration. Here total births includes all new individuals that are created due to immigration, sexual reproduction, mutualistic reproduction, and wind dispersal of plants. From the figure it is clear that immigration is the main source of new individuals - contributing over 50% of new individuals in almost all simulations. We also see that the relative contribution of immigration is roughly constant under contiguous HL, whereas immigration becomes more important under random HL. We can attribute the differing contribution of immigration, in part, to the changes in mobility illustrated in figure 3.22. In the random scenario it becomes harder for individuals to find a mate and therefore reproduce, shifting the balance in favour of immigration. In the contiguous case we may expect the opposite - a reduced contribution from immigration due to individual's increased ability to find a mate. However such an effect is not present - the contribution of immigration is constant under contiguous HL. It must be that any increase in sexual reproduction due to increased mobility is offset by some other mechanism. One possibility is that the offset is due to increased predator mobility, such that prey species are more likely to be consumed before they can find a mate. This effect may be compounded by the high relative abundance of predator species in the contiguous scenario, even at high levels of HL. The relative abundance and mobility of predators here suggests a strong predation pressure, which is supported by the high inter-specific interaction strengths.

This leads us to the second question, regarding the distribution of species abundances. We propose that the increased contribution of immigration in the random scenario, but not in the contiguous scenario, explains the observed changes in species relative-abundance and spatial distributions. The immigration mechanism is a *levelling influence* on the communities, both spatially and between species. All species are equally likely to immigrate, with no dependence on their abundance or distribution in the landscape. Also all empty cells are equally likely to receive an immigrant at each iteration. Therefore, although there is no spatial preference built into the

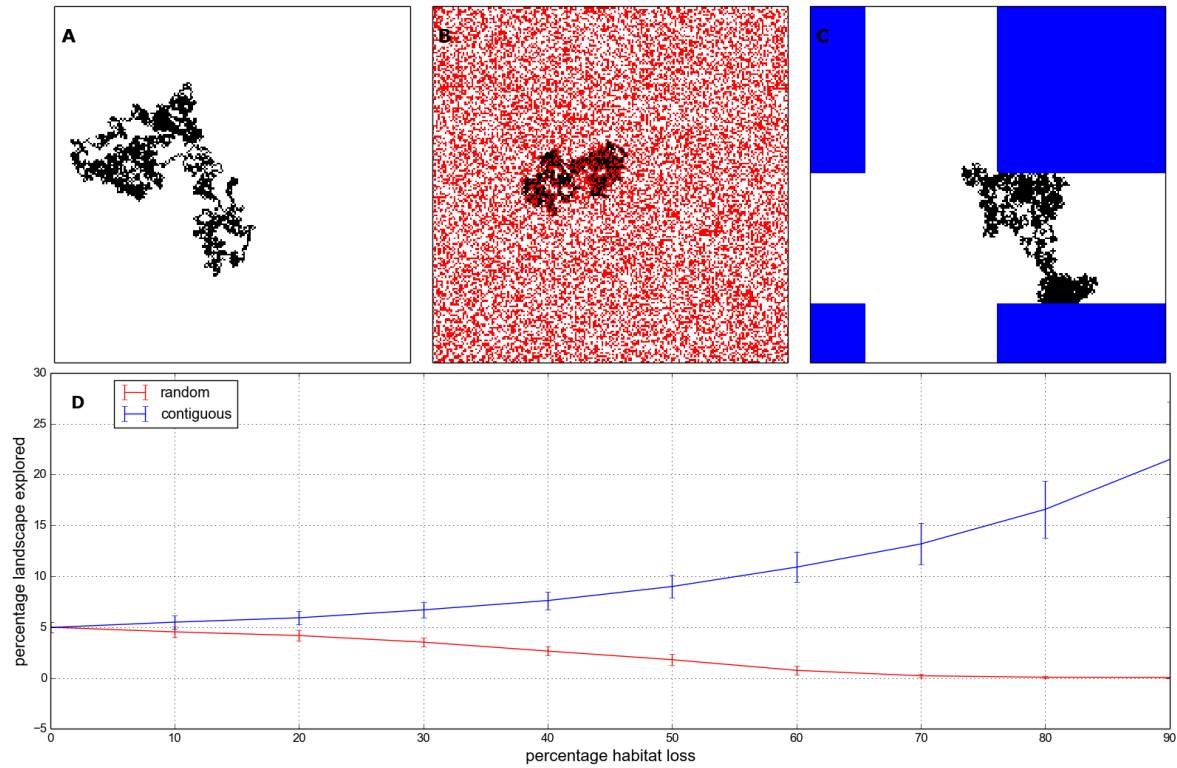


Figure 3.22: **An individual's range of motion** in different habitat conditions. Top row: example trajectory for a single individual over 5000 iterations in (A) pristine landscape; (B) 40% random HL; (C) 40% contiguous HL. Pristine landscape cells shown in white, destroyed cells in red and blue for random and contiguous destruction respectively. Bottom row (D): Percentage of the pristine landscape cells explored by an individual during 5000 iterations. Solid lines indicate mean over 100 repeat runs; errorbars indicate  $\pm 1$  standard deviation.

immigration mechanism, areas of space with a high density of individuals will be locally less likely to receive immigrants than those areas with a low density, simply due to the number of available cells. Therefore immigration, in isolation, acts to make the distribution of individuals more even between species and throughout space. These are both changes that we observe in the random scenario and not the contiguous, and therefore we attribute them, at least in part, to the increased dependence on immigration to supply new individuals.

Another important change, observed in the random but not the contiguous scenario, is the shift in relative abundances of the functional groups. The greatest changes are the increase and decrease in relative abundance of basal and top-predator species respectively. However there is also a decrease in the relative abundance of species in the second trophic level (herbivores and mutualistic-animals). Only omnivore species display no change in relative abundance. *All of these changes in relative abundance can be explained by the change in mobility and its knock on effect on interaction strengths, reproduction and dependence on immigration.*

As previously discussed, the reduction in mobility makes it harder to find prey and therefore

### 3.3. RESULTS

---

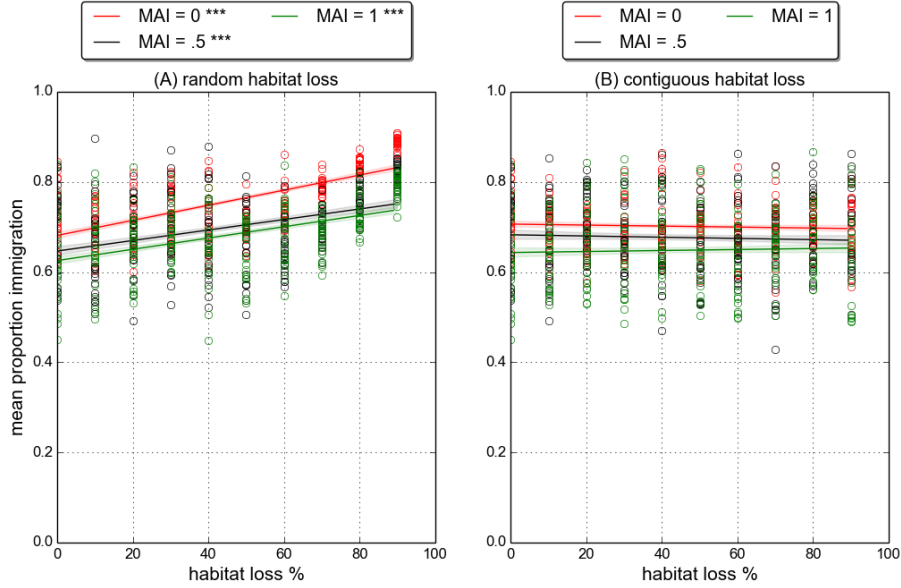


Figure 3.23: **Number of immigrants** as a fraction of the total number of new individuals created over the course of a simulation. Linear fits and p-value markers as in previous plots (see caption of figure 3.6).

reduces interaction strengths. The result is an overall decrease in predation. So species lower in the food chains benefit from reduced predation pressure, whilst species higher in the food chains suffer because less energy is being transferred up the trophic pathway. In addition reduced mobility makes it harder for animal species to find partners with which to reproduce. This negatively affects all animal species and mutualistic plants. However mutualistic plants, although they may be reproducing less frequently, receive the incidental benefit of losing less energy to their mutualistic partners. Therefore we see a shift in relative abundance towards basal species, which benefit from reduced consumption whilst all other species suffer from a reduced ability to find food and reproduction partners. Animal species in the lower trophic levels receive a compensatory benefit of lower predation pressure, which partly explains why species in the second trophic level are hit less hard than top predators. The fact that the relative abundance of omnivore species does not change must be a combination of reduced predation pressure, and a slight quirk of the modelling framework. Due to the way the networks are constructed (see section 2.2.1), there are significantly more omnivore species than any other functional group (this is one problem with the niche model). Since immigrant individuals are drawn uniformly at random from all species, immigrants are most likely to be omnivores. As we have seen (figure 3.22) random HL increases the community dependence on immigration, therefore benefiting omnivores disproportionately. Conversely the functional group with fewest species is the top-predators. Therefore this group receives fewest immigrants, compounding the other effects detailed above.

Therefore it appears that mobility, along with immigration, accounts for all observed changes in species relative abundances.

It is also worth reiterating the point about ecosystem synchrony made in section 3.3.4, where we attributed the reduced synchrony under random HL to a reduction in the trophic component of the dynamics. In this section we have shown that random HL increases the contribution of immigration to the overall number of births (figure 3.23). The creation of individuals due to immigration is a random processes. Births due to reproduction, although stochastic, are dependent on trophic and non-trophic interactions. Therefore the increased contribution of immigration represents a reduction in trophic dynamics and an increase in randomness. We argue that it is indeed this shift driving the decrease in synchrony. We will return to the issue to deterministic versus random dynamics in chapter ??.

### 3.4 Discussion (or conclusion?)

A key feature of these results is that the community response to HL is dependent on the spatial pattern of the perturbation. This has been reported previously in numerous studies [REFS]. In general our findings are in alignment with a common theme amongst the theoretical studies, that is well summarised by Ovaskinen [56]: *This is not a real quote! Damn.*

Here we have studied the difference between two HL scenarios in more detail, and without focus on extinctions. We have also shown that the main difference between the two scenarios is due to differences in mobility through the landscape, changes in interaction strengths, and differential dependence on immigration from an external source.

In what follows we will focus on contiguous HL loss. In part this is to simplify the investigation. By only running simulations and presenting results for a single scenario we are able to study the chosen scenario in more detail. The choice of contiguous over random destruction is also justified by realism. In nature habitat tends to be destroyed in a spatially-autocorrelated manner - for example urban development, agriculture and logging all occur in concentrations rather than being distributed totally at random throughout space. Therefore the result of human activity is often a patchy and fragmented landscape [REFS]. The study of our simulated communities under contiguous HL represents the study of communities in single such fragment, with immigration from an external source. In reality we know that such fragments support a lower richness of species, beyond a certain size. In this chapter we saw that a high immigration rate prevented a loss of species richness. In the next chapter we begin to look at how communities respond to changes in the immigration rate.

Also to discuss:

- Role of interactions and immigration in maintaining biodiversity and community structure under perturbations.
- Importance of interaction strengths throughout the thesis: return explicitly in final chapter.
- Departures from our results in natural communities: what might be different?
- Implications for structure-stability debate
- More explicit discussion of Tylianakis. No loss of species!! Make this a theme..
- Why does IS3 change more or less depending on MAI ratio? (referenced to here in text.) - must be due to abundances...In other words, the change in the diversity of interactions is due to changes in species relative abundances.



CHAPTER



## PERSISTENCE AND STATIONARITY

### 4.1 Introduction

In the previous chapter we analysed in detail how simulated communities responded to two habitat loss scenarios. These simulations used the *default parameter values* for the IBM model, as published in [42]. An important feature of these simulations was that they exhibited almost no species extinctions, even up to 90% habitat loss (HL). This was achieved by a high immigration rate (IR), and was desirable because it allowed us to study underlying structural changes that were not associated with the loss of species [19? ]. Therefore we also intend to use the model to investigate the regime where habitat loss causes extinctions. The obvious way to do this is to reduce the IR. Because this represents a departure from the default parameters and the way in which the model has been used previously, it requires a careful and systematic approach. Therefore in this chapter we ‘stress test’ the model to analyse how it copes with changing IR. This is in preparation for chapter 5 where we will use this analysis as a foundation to study, from a more ecological perspective, how changing IR affects the response of communities to HL. In the first part of this chapter (section 4.2) we look at *closed communities* - what happens when there is no immigration? In the second part (section 4.3) we address an issue that we discover arises from reduced IR, namely increased variability. In particular we focus on the concern that simulations may become dominated by stochastic effects, leading to unreliable results and loss of ecological meaning.

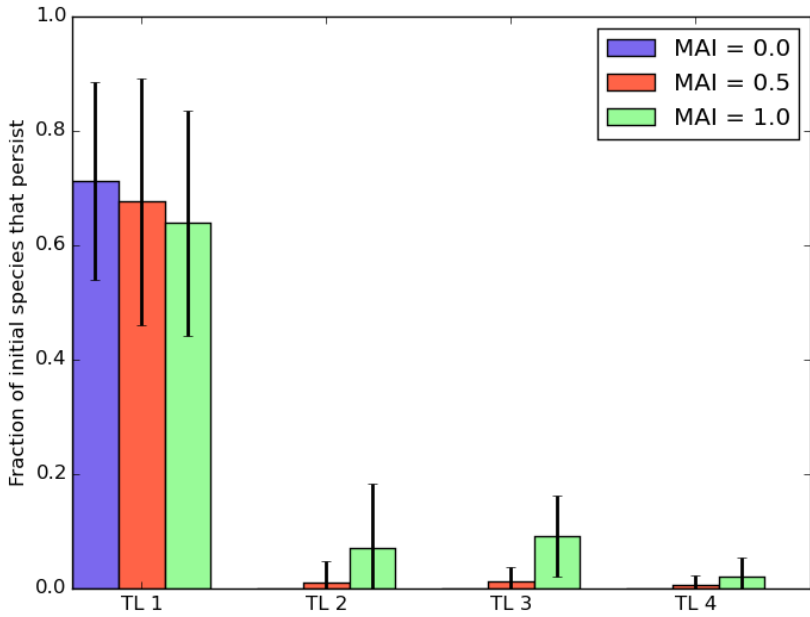


Figure 4.1: **Fractional persistence** by trophic level for three different MAI ratios, with **zero immigration** ( $IR=0$ ). All other parameters set to default values. Fractional persistence measured by the fraction of species initially belonging to a trophic level which have not gone extinct by the end of a simulation (5000 iterations). Solid bars give the mean value over 22 repeat simulations. Error bars show  $\pm$  one standard deviation.

## 4.2 Persistence in closed communities

We define a *closed-community* as one in which there is no inflow of individuals from an external source. In the model this is achieved by setting the immigration rate to zero ( $IR=0$ ). Here we study such communities in a pristine landscape - that is without habitat loss ( $HL=0$ ). The simulation procedure is the same as in the previous chapter. All parameters, except the  $IR$ , take default values unless otherwise stated, and each simulation uses a distinct network topology generated using the method outlined in chapter 2. A species is said to *persist* if there is at least one individual belonging to that species present in the landscape on the final iteration of the simulation. Therefore *fractional persistence* is defined as the fraction of the initial pool of species (or subset of that pool) that persist. We also use the *number of persistent species*, where absolute values are desirable. All abundance measurements given are calculated from the number of individuals belonging to each species on the final (5000th) iteration of the simulation. To reduce the number of figures we sometimes present results for only one or two MAI ratios only (MAI=0.0 or 0.5). In these cases the analysis was performed for all MAI ratios and results were not found to differ qualitatively.

An initial set of simulations with zero IR shows that species persistence is low (Figure 5.1). We see that for an antagonistic community ( $MAI = 0$ ) all non-basal species go extinct, as do around 30% of basal species. Introducing mutualism into the communities slightly improves fractional persistence in the higher trophic levels - we see some persistence of non-basal species, but no more than 10% of the initial pool on average. Therefore, even in the best cases, we expect around 90% of non-basal species to go extinct. It is clear that, given the default parameters, immigration is a requirement for the maintenance of species richness. This is a troubling feature of the model. In nature a true closed-community may not exist, but there are systems which come close (for example remote island ecosystems). It is desirable for our model to be able to describe such systems, and for us to investigate the effects of habitat loss in this extreme case. It may also be informative to discover which factors in our model contribute to the persistence of closed-communities. Here we conduct a systematic review of certain model parameters and their impact on persistence. Due to the large parameter space of the model we study these parameters individually (with other parameter values held constant), and restrict the analysis to four parameters, namely: MAI ratio (section 4.2.1); reproduction rate (section 4.2.2); landscape size (section 4.2.3); number of initial species (section 4.2.4). In addition we look at the effect of the interaction network structure (section 4.2.5).

### 4.2.1 Mutualistic to antagonistic interaction (MAI) ratio

Mutualistic interactions are so named because they confer some benefit to both parties. One novel aspect of our modelling approach is the inclusion of mutualistic interactions into a spatial simulation of trophic dynamics, in a way that avoids Robert May's 'orgy of mutual benefaction' [45] (see chapter ??). In [42] it was shown that increasing the levels of mutualism (MAI ratio) in the community can have a stabilising effect. However in the previous chapter we saw that this stability did not translate into a greater robustness of mutualistic communities to habitat loss. From figure 5.1 we see that mutualism has a small but positive effect on fractional persistence at zero IR. An interesting feature of this effect is that it *cascades* to higher trophic levels - it benefits species other than mutualists. Here we explore the effect of mutualism on persistence in more detail.

Figure 4.2 shows the average abundance dynamics, by functional group (FG), for four different MAI ratios. In panel A we see that the abundance of producers rises to fill the whole landscape ( $200 \times 200 = 40,000$ ), whilst the abundance of all other FGs is at or near zero. From the other panels (B-D) we see that increasing the MAI ratio particularly benefits the mutualistic species (both producers and animals) as expected, and speaks to also confer some small benefit to omnivores and top-predators (their abundances are small but non-zero). Ecologically this makes sense. If mutualism strongly benefits mutualistic species, it will also benefit those species that feed on them. However the benefit may only be transient. The abundance of producers in panel D is still rising, on average, at the end of the simulations.

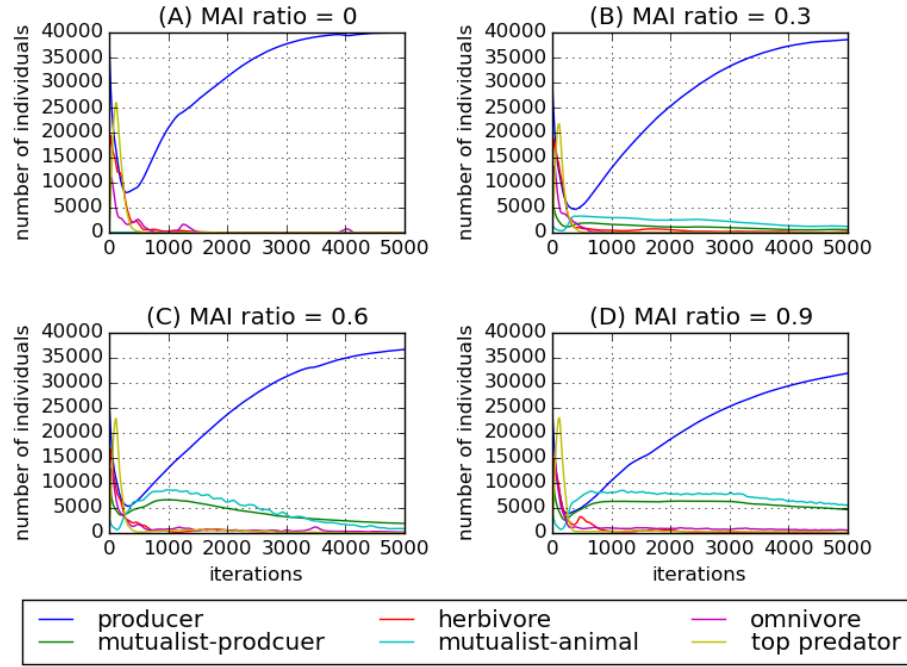


Figure 4.2: **Mean dynamics by functional group** for four different MAI ratios (A-D), without immigration. Lines given by number of individuals belonging to a functional group, averaged over 22 simulations. Colours indicate functional group (see legend).

Figure 4.3 shows the number of persistent species by trophic level for a range of MAI ratios. We see that increasing MAI ratio in fact has very little effect on the absolute number of persistent species in each trophic level. For example at MAI= 1.0 only two persistent species are expected in the second trophic level. Therefore the increase in abundance seen from figure 4.2 must be due to a couple of dominant species. We conclude that mutualism has a negligible effect of overall persistence.

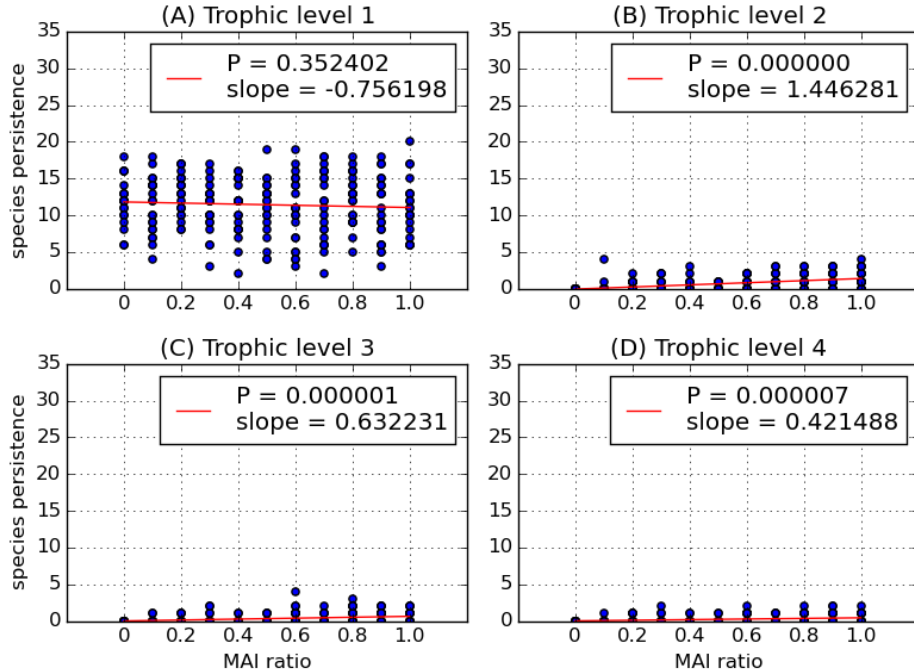


Figure 4.3: **Number of persistent species** plotted against MAI ratio, for each trophic level (A-D). Blue circles give number of persistent species, for a single simulation, on 5000th iteration. 22 repeat simulations at each MAI ratio. Red lines show linear regression fits, with slope and p-value of fit given.

#### 4.2.2 Reproduction rate (RR)

The initial transience in the abundance dynamics (figure 4.2) is characterised by a sharp decline in plant abundance (mutualist and non-mutualist), which reaches a minimum and then rises again. It was hypothesised that this overconsumption of producers, and therefore limited availability of plant individuals, causes many of the extinctions. Indeed in these simulations  $\sim 85\%$  of the extinctions occur during the first 500 iterations. Therefore we look at the possibility of improving persistence by increasing the reproduction rate (RR). The RR parameter defines that rate at which non-mutualist producers reproduce (via the ‘wind-dispersal’ mechanism, see chapter ??). Therefore increasing this mechanism should improve the availability of plant biomass in the system, with potentially cascading effects. The RR parameter does not affect mutualist-producers, which only reproduce via their interactions with mutualist-animals and not via wind-dispersal. Here we vary the RR between 0.01 (default value) and 0.2 and look at the effect on persistence.

Increasing the RR improves the fractional persistence of all trophic levels, as shown in figure 4.4. This effect is greatest for the two lowest trophic levels, but has a small cascading effect on the upper two trophic levels. However, as we saw with MAI ratio, the improvement in persistence is small and even for high RRs we still expect many species to go extinct. Looking at the abundance

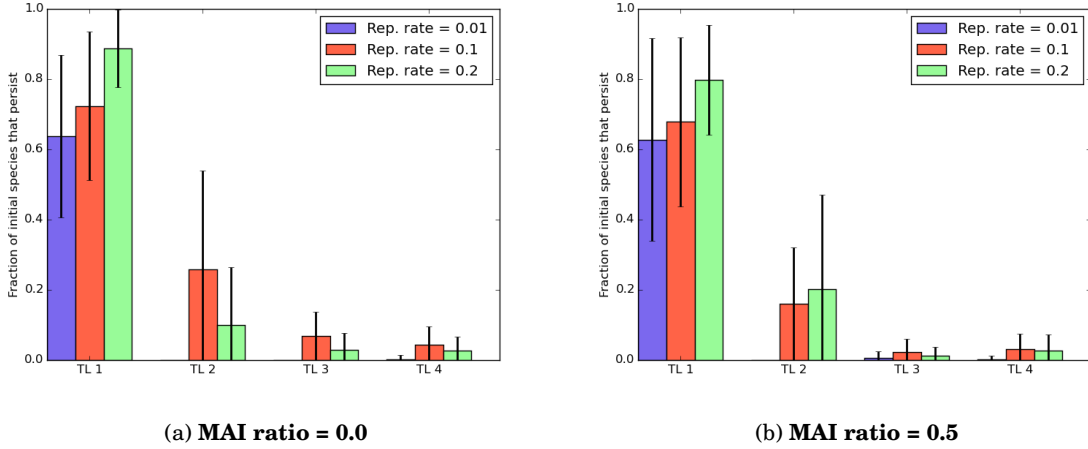


Figure 4.4: **Fractional persistence** by trophic level for three different reproduction rates (RR), at two MAI ratios (A-B). Fractional persistence measured by the fraction of species initially belonging to a trophic level which have not gone extinct by the end of a simulation (5000 iterations). Solid bars give mean value over 22 repeat simulations. Error bars show  $\pm$  one standard deviation.

dynamics in figures 4.5 and 4.6 we see that the extent of the sharp decline in plant abundance during transience is reduced. The resulting increase in the availability of plants does benefit all trophic levels by increasing the number of individuals present. However, because of the low fractional persistence, it must again be the case that these communities are dominated by just a couple of species in each trophic level, with all other species going extinct. The results for MAI= 1.0 (not shown) are qualitatively similar since these communities contain fewer plants that reproduce via ‘wind-dispersal’. In the remaining simulations for this section we choose to use RR= 0.1 . This is because of the resulting improvement in abundances across trophic levels. It was decided that this, combined with changes in other parameters, may lead to greater changes in persistence<sup>1</sup>.

<sup>1</sup>However it does affect the trade-off between mutualism/non-mutualism for plants

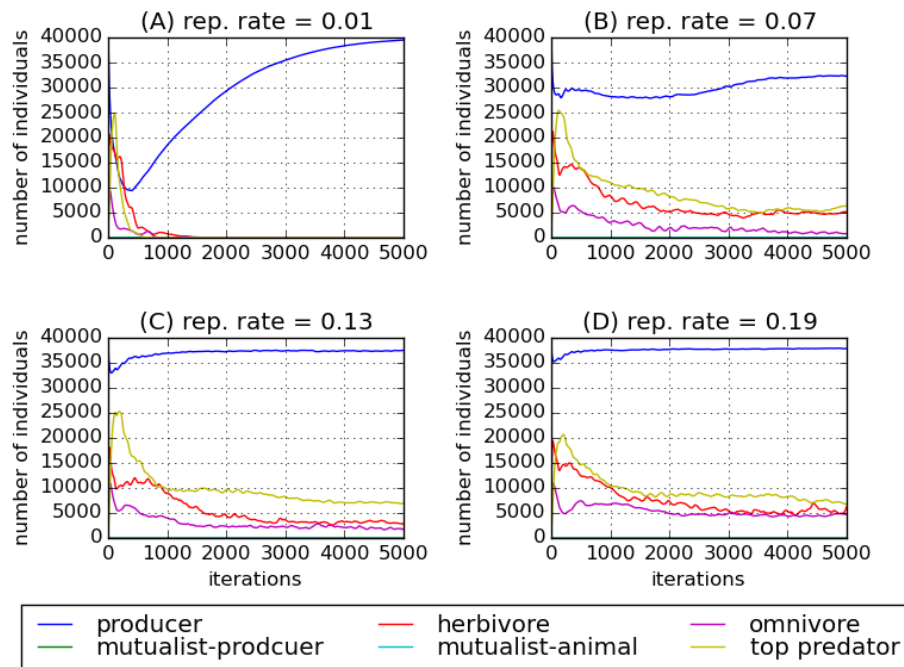


Figure 4.5: **Mean dynamics by functional group** for four different reproduction rates (A-D), at **MAI=0**. Lines given by number of individuals belonging to a functional group, averaged over 22 simulations. Colours indicate functional group (see legend).

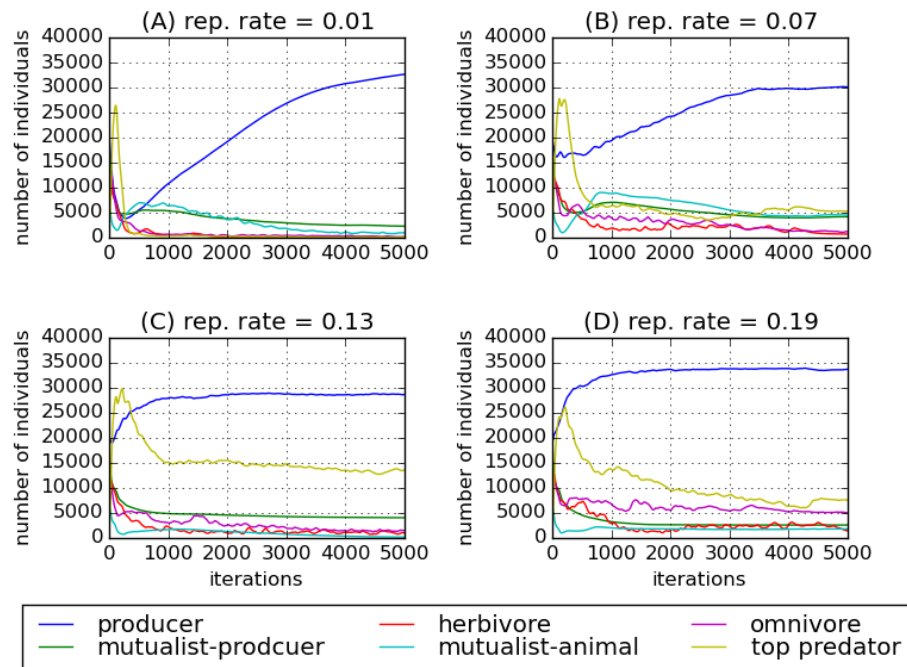


Figure 4.6: **Mean dynamics by functional group** for four different reproduction rates (A-D), at **MAI=0.5**. Lines given by number of individuals belonging to a functional group, averaged over 22 simulations. Colours indicate functional group (see legend).

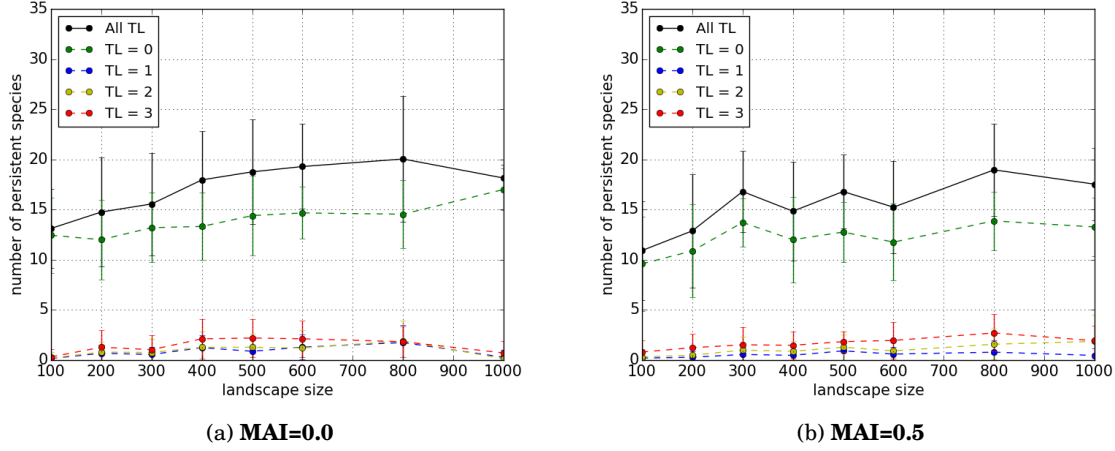


Figure 4.7: **Landscape size** against species persistence (on 5000th iteration), for two MAI ratios (A,B). Total persistence, and persistence by trophic level. Points show mean value over 25 replicates. Error bars show  $\pm$  one standard deviation.

#### 4.2.3 Landscape size

We hypothesised that competition for space may be causing species extinctions, and that therefore increasing the size of the landscape may improve persistence. We varied the width of the landscape between 100 and 1000 cells, running 25 repeat simulations at each width. These simulations were run for  $MAI = 0.0$  and  $0.5$ , and used the increased reproduction rate  $RR = 0.1$ . Figure 4.7 shows how the number of persistent species changes in response to landscape size. For both AMI ratios there is an overall increase in species persistence up to a landscape width of 800. This increase in persistence is driven by small increases in the species richness of each trophic level. Beyond a width 800 cells persistence appears to decline, but we do not explore this result further. Even with a landscape of  $800 \times 800$  we do not expect more than 20 persistent species - this represent the extinction of around two thirds of the initial species pool. Therefore we conclude that landscape size does not resolve the problem of extinctions. Further simulations are run using the default landscape width of 200.

#### 4.2.4 Number of initial species

All previous simulations have been run with an interaction network consisting of 60 species. We consider the possibility that beginning the simulation with a larger network may result in a greater number of persistent species. In this way we may hope to evolve a stable network structure as extinctions kill off species that are not viable. Here we vary the number of species in the network between 30 and 240, and look at the effect this has on persistence. As in the previous section, 25 repeat simulations are run for each number of species, both MAI= 0.0 and 0.5.

Using a network of more than around 70 species causes a problem with our network generation procedure. As described in chapter ?? we use the niche model to create interaction networks, but reject those which do not satisfy our trophic constraints. With a large number of species the probability of the niche model generating a network that meets our trophic constraints becomes vanishingly low. In particular, as discussed previously, the niche model overestimates the number of omnivore species, and underestimates the number of herbivores. To overcome this problem we here construct networks in two different ways: 1) we use the standard niche model with no trophic constraints; and 2) we ‘rewire’ networks generated using the niche model via the following procedure. A species is selected uniformly at random from trophic levels which contain more than the desired number of species. This species is then moved to a trophic level which contains too few species, and is linked to other species which are selected at random from a pool of possible candidates. Possible candidates are defined by the new trophic level of the species that has been moved e.g. a herbivore can only eat plants, and only be eaten by species in higher levels. The number of new links created is chosen to preserve the degree of the moved species (in/out degree cannot necessarily be preserved because of the change in trophic level). The procedure is repeated, moving randomly selected species until all trophic constraints are satisfied. Mutualistic links are then introduced using the standard method. Here we use the same constraints as were applied in the original network generation procedure. That is the fraction of species belonging to trophic levels one, two and four must be at least 0.25, 0.25 and 0.05 respectively. We refer to the networks generated using procedures 1 and 2 as *niche* and *rewired*, respectively. Simulations are run for both types of network.

Figures 4.8 and 4.9 show how the number of persistent species responds to the number of species in the initial network. For the niche model networks we see that there is little change in species persistence. Whereas for the rewired networks we see a large increase in total persistence. However this increase is mainly due to plant species, with only a small change in persistence for trophic levels two, three and four. The difference between the results niche and rewired networks is due to the fact that large niche model networks are dominated by omnivores. It appears that the omnivores species out-compete each other and therefore we do not see a large change in persistence. Conversely, for the rewired networks the number of species in each trophic level grows proportionally with the total number of species. The only significant benefit is to plant species, to seem to be able to coexist in larger numbers. We conclude that increasing the number

#### 4.2. PERSISTENCE IN CLOSED COMMUNITIES

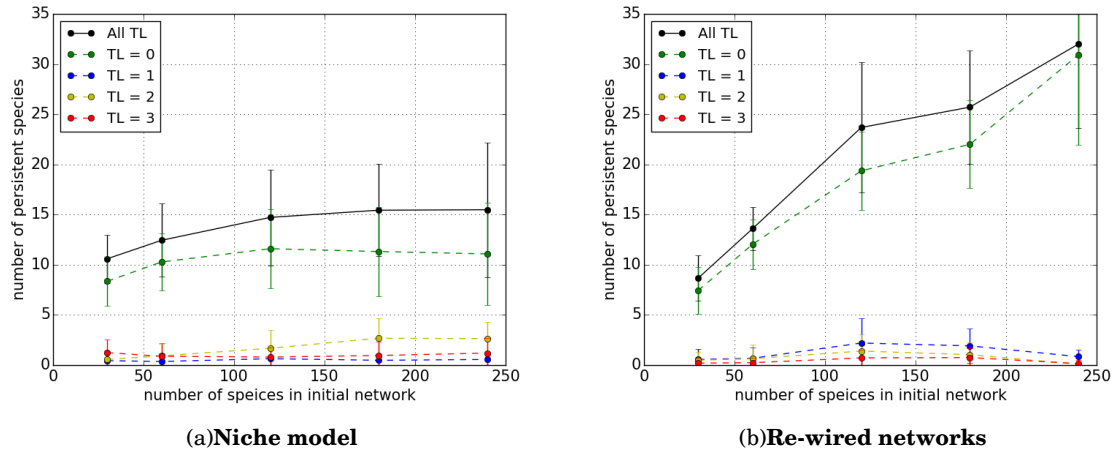


Figure 4.8: **Number of initial species** against species persistence at **MAI=0**, for two types of initial network: (A) Interaction network generated using standard niche model, and (B) generated using re-rewired niche model topology (see text). Total persistence, and persistence by trophic level. Points show mean value over 25 replicates. Error bars show  $\pm$  one standard deviation.

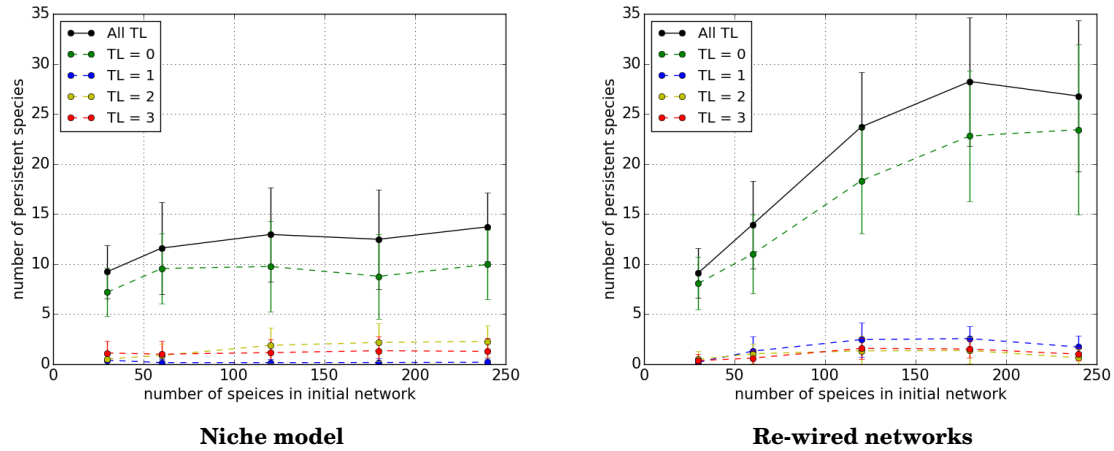


Figure 4.9: Similar to figure 4.8, but with **MAI=0.5**.

of initial species is not able to generate the diverse communities that we had hoped for. However the rewiring algorithm developed for this analysis represents a novel modification to the niche model, which may be useful for the generation of realistic interaction networks.

#### 4.2.5 Network structure

In the results presented above one feature stands out - there is significant variation in persistence between replicate simulations. Presumably some of this variation is due to random noise. However some of this variation may be due to the structure of the interaction network used. For example community ecologists have often associated modularity with stability in antagonistic communities, and nestedness with stability in mutualistic networks [66]<sup>2</sup>. Here we look for systematic differences in persistence that are due to network structure. To do this we choose one ‘good’ and one ‘bad’ networks from the simulations used in the section 4.2.4. From the 25 repeat simulations using a *rewired* network of 120 species we select the communities that display the best and worst persistence profiles. The best case, giving the ‘good’ network, had persistent species in all trophic levels and two persistent species in each of trophic levels three and four. In contrast the worst case, giving the ‘bad’ network , had no species persistence in any trophic level above one. With each of these two networks we run 100 repeat simulations (MAI= 0.0) to test if the classification is reliable.

Panel A in figures 4.10 and 4.11 shows the structure of 120 species network, for the good and bad cases respectively. Visually there is little to distinguish the two networks. However we find that they have very different persistence properties. Panel C of these figures shows the average number of persistent species in each trophic level. It is clear that the good network performs better on average, in terms of persistence, than the bad network. We do not analyse the network structures here, however this could be an interesting avenue of further work. We simply conclude that the network structure is an important determinant of community dynamics in our simulation, with an effect on persistence that is repeatable.

#### 4.2.6 Discussion

Here we discuss the results from the first part of the chapter, main points to include:

- Immigration seems to be a requirement in our model for strong persistence and diversity.  
This may also be true in nature..Island bio-geography theory.
- Strong evidence that competition is causing extinctions - dominance of higher trophic levels by one of two species. But this does not appear to be competition for space, except maybe in the case of plants (see landscape size results)
- Principle of competitive exclusion in action - number of niches, and limiting resources.  
Discuss this in detail with references. Our species do not have differential traits.
- Results imply that network structure is important. Many possible topologies to explore!  
Again may references here to include. Interesting topic.

---

<sup>2</sup>Although the debate is open on this one..

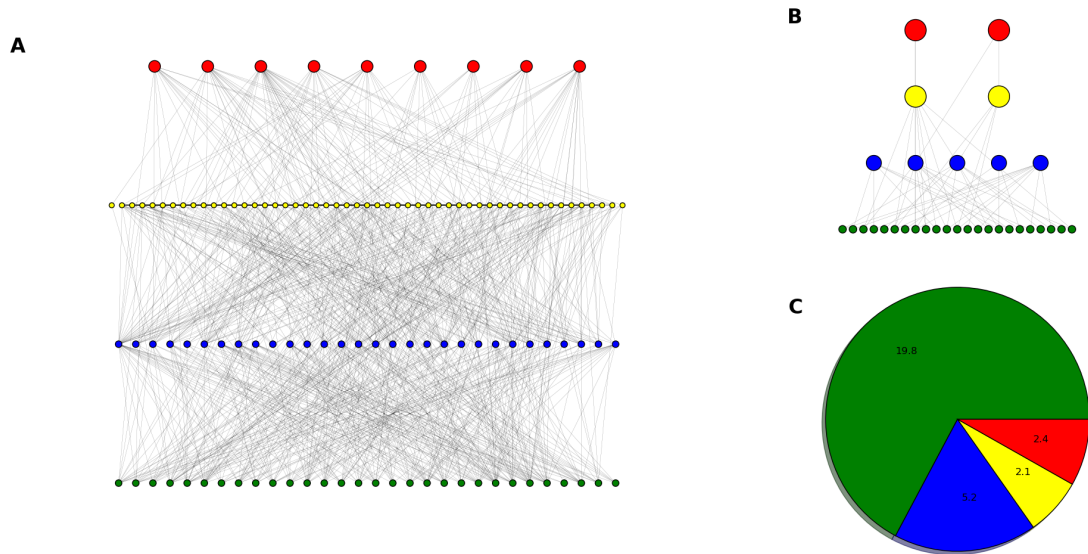


Figure 4.10: Example of a ‘**good network structure**’. Colours represent trophic level. (A) Antagonistic network of 120 species, rewired from the niche model (see text), used as input for simulations. (B) Example of ‘pruned’ network consisting of the species that persist after 5000 iterations. (C) Mean number of species belonging to each trophic level in the pruned network, averaged over 100 replicate simulations (all using A as the initial network).

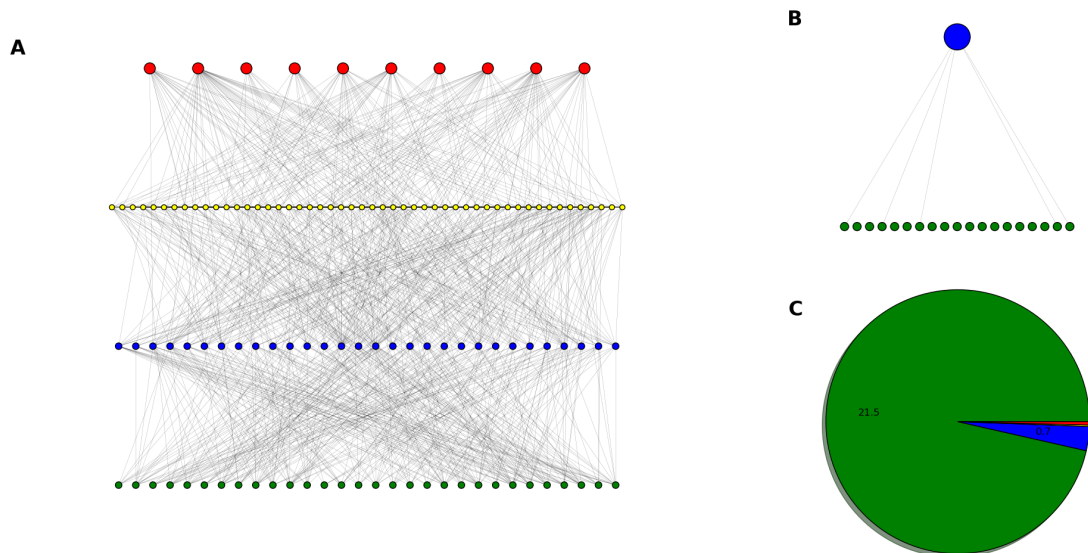


Figure 4.11: Example of a ‘**bad network structure**’. Similar to figure 4.10, but with a different initial network of 120 species used as input for the simulations.

- Novel algorithm for rewiring niche model networks that overcomes well documented issues.
- There may be a region of parameters space or network structure for which there is stable coexistence - but we cannot find it!
- Noticed some cascading effects - nice bit of ecology.
- Main point for follow on: we have now seen a high immigration scenario (no extinctions) and a zero immigration scenario (many extinctions). What happens in between?

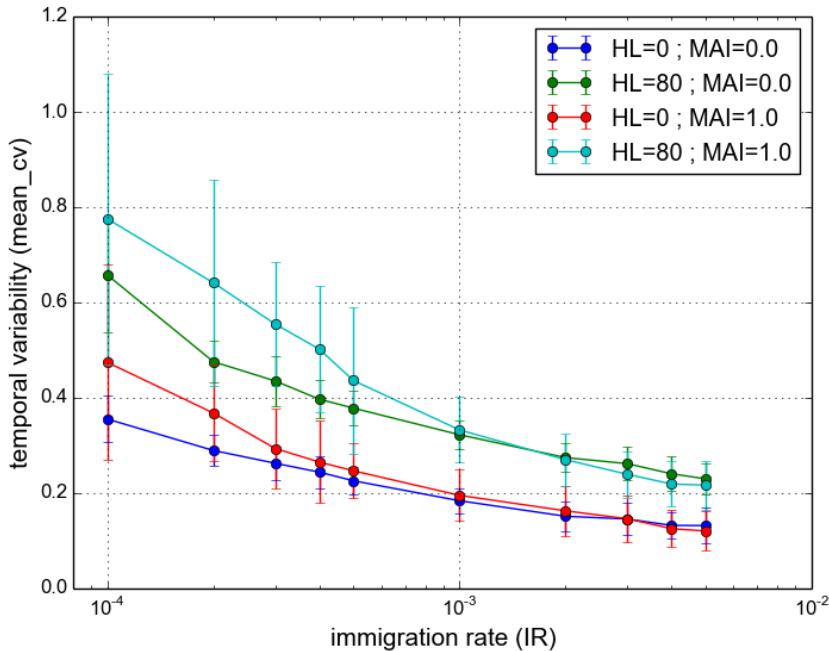


Figure 4.12: **Temporal variability** against immigration rate (IR). Points show mean value over 50 repeat simulations. Error bars show  $\pm$  one standard deviation.  $HL = 0$ , all other parameters take *default values*.

### 4.3 Problems with temporal variability

From the section 4.2 we concluded that immigration is required for our model to produce persistent communities. Therefore, in order to study communities that exhibit extinctions due to habitat loss, we must investigate the region between zero immigration and high immigration rate ( $IR \sim 0.005$ ). As we began to investigate this region we found a robust feature of the model - reducing immigration rates *increases the temporal variability* of the dynamics. Here temporal variability is measured using the same metric described in chapter 3 i.e. the coefficient of variation in species population dynamics, averaged over all species in the community. In the previous chapter *contiguous* habitat loss was shown to increase temporal variability, up to a average value of  $\sim 0.3$  for  $HL = 90\%$ <sup>3</sup>. Figure 4.12 illustrates that reducing the immigration rate can push the temporal variability well above this level, even in pristine landscape.

This increased variability may bring into question the validity of results derived from the simulation output. Implicit in our analysis so far is the assumption that *stationarity* (see section 4.3.1) is reached by the end of the simulation. The results presented in the previous chapter (and in [42]) are either calculated from a ‘snapshot’ of the simulation state on the final (5000th) iteration or, in the case of the network and variability metrics, are calculated from samples

<sup>3</sup>Reference figure in previous chapter?

aggregated over the final 200 iterations. For results obtained in this way to be reliable the simulation must reach a sufficiently steady state after 5000 iterations. In the high immigration regime (HIR) it may be reasonable to assume that this is the case. From inspection, the HIR simulations contain transient dynamics within the first 1000 iterations, followed by a period of relatively constant abundance (see for example figure 4.15). This latter period was assumed, in chapter 3 and in [42], to be the simulation's steady-state. However the high level of variability illustrated in figure 4.12 now motivates us to question this steady-state assumption.

In section 4.3.1 we conduct a detailed analysis of the *stationarity* of population dynamics generated by the IBM model. We then address the concern that the simulations with high variability may become dominated by randomness. In section 4.3.2, use *recurrence quantification analysis* to look for signatures of determinism in the simulation output. Finally we close the chapter (section 4.3.3) by looking at how the accuracy and reliability of our numerical results are affected by increased variability.

### 4.3.1 Second-order stationarity

We introduce here three tests for second-order (or ‘weak’) stationarity in time series. Second-order stationarity may be defined as the time invariance of the first and second moments of the data. Specifically Hsu [30] states that a random process  $X(t), t \in \mathbf{Z}^+$  is second-order stationary if:

$$(4.1) \quad \mathbf{E}[X(t)] = \mu \text{ (constant)},$$

$$(4.2) \quad R_X(t,s) = \mathbf{E}[X(t)X(s)] = R_X(|s-t|),$$

where  $R_X(t,s)$  is the *autocorrelation* function of the process. Conceptually these conditions state that a second-order stationary time series has constant mean, and an autocorrelation dependent only on time separation. From now on we refer to a time series satisfying 4.1 and 4.2 as *stationary*. If the conditions are not met we call the time series *non-stationary*. Non-stationary time series cannot be fit to a constant distribution. Non-stationarity may be due, for example, to a trend in the data or a change in the parameters of the data generator.

In our case the data generator is the IBM model and there are several possible causes of non-stationarity. It may be that there is no steady-state equilibrium in the model. For example the number of individuals may undergo a random-walk. From previous analysis this situation seems unlikely, since we have observed what appear to be deterministic population cycles. However randomness has not been explicitly tested for. Another possibility is that a steady-state equilibrium exists, but that a long transience means it is not reached during the time frame of our simulations.

### 4.3.1.1 Tests for stationarity

We compare three different tests of stationarity: the Kwiatkowski-Phillips-Schmidt-Shin (KPSS) [40]; the Augmented Dickey-Fuller (ADF) [65]; and the the Priestley-Subba Rao (PSR) [60] tests. These tests were chosen for their popularity in the time series literature. All three are implemented in the programming language *R* [62] - the former two in the package *tseries*, and the latter in the package *fractal*.

The ADF test has a null hypothesis that the time series is non-stationary. The test models the data as an auto-regressive process (see section 4.3.4), and the null hypothesis is that this process has a *unit root*. The test produces a statistic that is negative. The greater the magnitude of the test statistic the more evidence there is to reject the null hypothesis in favour of stationarity.

The KPSS test complements the ADF test in that the null hypothesis is stationarity. The data is modelled as the sum of a random-walk and an error component, and tests the hypothesis that the variance of the random walk is zero. The test statistic is always positive, and the greater its magnitude the more evidence there is to reject the null hypothesis in favour of non-stationarity.

The null hypothesis of the PSR test is also that the series is stationary. The test is based on the idea that non-stationary processes have power spectra that change over time [60]. These are called *evolutionary spectra*. The test, as implemented in *R*, returns several statistics. We quote the ‘p-value for T’ which can be thought of as the confidence that the estimated spectral density functions are constant in time.

### 4.3.1.2 Characterising the tests

To understand the performance of the stationarity tests (section 4.3.1.1) we apply them to three example time series, which we refer to as HI, RW and NS. The first series, HI, is taken from a single IBM simulation run with high immigration rate (IR= 0.001), zero mutualism (MAI= 0.0) and otherwise default parameters (table ??). The series represents the total number of individuals of all species at each iteration. The simulation was run for 50,000 iterations, compared with the 5000 used in previous chapters. The increased length allows more time for the simulation to reach steady-state, and allows comparison of tests applied to different sections of the series. The first 1000 iterations were discarded, since these contain clearly transient dynamics (see figure 4.15B), leaving a time series of 49,000 points. A high immigration rate was chosen because it reduces the temporal variability of the dynamics, as was discussed in chapter 5. Therefore the HI series is more likely to be stationary than the output of a simulation with a lower IR (section 4.3.1.3).

The series RW and NS are chosen as a negative and a positive control respectively. Both have the same length as HI. RW is a non-stationary series generated by a one-dimensional *random-walk*, defined as:

$$(4.3) \quad x(t) = \sum_{i=1}^{t-1} Z_i,$$

where  $Z_i$  are independent random variables that may take a value of either  $-10$  or  $+10$ , both with probability half. An ensemble of such random walks was generated and a single instance was chosen with mean and variance closest to the HI series. RW has mean and standard deviation of 15525.2 and 1549.8 respectively, compared to 15915.8 and 1545.6 for HI. For comparison, NS is a stationary series generated by drawing each value independently from a normal distribution with mean and variance equal to that of HI. The three series are plotted in figure 4.13.

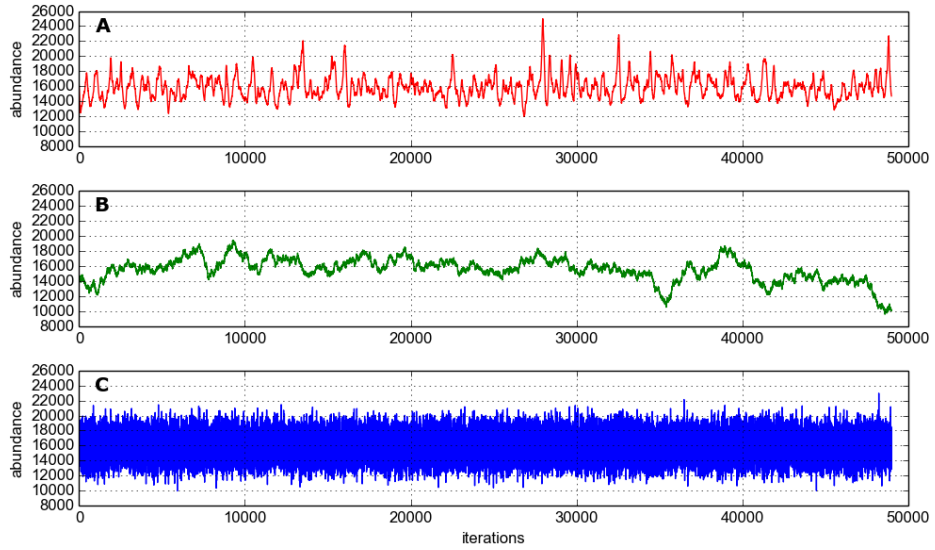


Figure 4.13: The three time series used to characterise the performance of the stationarity tests (see text for details of how they are generated). The initial 1000 points removed such that all are 49,000 points long. (A) HI: total abundance dynamics of a simulation with high immigration rate; (B) RW: a random walk without drift; and (C) NS: a series generated by independent sampling from a normal distribution.

	A.D.F.		P.S.R.		K.P.S.S.	
	stat	p-value	stat	p-value	stat	p-value
HI	-15.401	<0.01	-	0.0004782808	0.5395	0.03277
RW	-4.0386	<0.01	-	0.9929773	18.7453	<0.01
NS	-37.5348	<0.01	-	0.811097	0.0466	>0.1

Table 4.1: Results of applying the three stationarity tests to the three time series shown in figure 4.13. P-values that indicate evidence for stationarity at 95% confidence are highlighted in green. The test statistics are also given for the ADF and KPSS tests.

Initially we apply the three stationarity tests to the entire length of the time series. The results are shown in table 4.3.1.2. ADF finds significant evidence that all three series are

stationary, at 99% confidence. We may be suspicious of this result since we know that RW is generated by a non-stationary process. However RW is a particular instance of a random walk, chosen from several thousand to closely match the mean and variance of HI. Therefore it may not be unreasonable that it can pass as stationary. The test statistic for ADF indicates that there is most evidence for NS to be stationary, followed by HI, then RW. The KPSS test ranks the series in the same order, based on the magnitude of the test statistic. According to this test NS is clearly stationary (accept  $h_0$ ), and RW is clearly non-stationary (reject  $h_0$  at 99% confidence), whilst HI is borderline. For HI we would accept the null-hypothesis of stationarity at 95% confidence, but reject it at 99%.

The PSR test gives unexpected results. It concludes that RW and NS are both stationary, whilst HI is non-stationary with a high degree of confidence ( $p\text{-value} < 0.001$ ). In fact, according to PSR, RW is more likely to be stationary than NS. This result contradicts what we know about the series. Therefore we do not use this test in the analysis that follows. However the apparently erroneous result may contain interesting information about the HI series and the process that generated it (see the discussion in section 4.3.4).

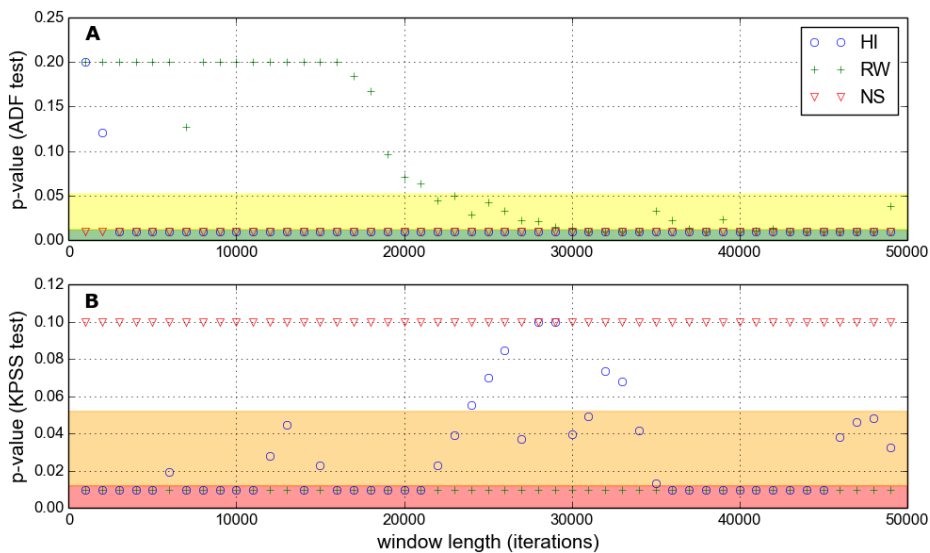


Figure 4.14: Two tests for stationarity applied to samples of varying size (window length). Samples are taken from the three time series (HI,RW,NS) shown in figure 4.13. All three time series contain 49,000 points. Sample windows begin at the first point and increase in length from 1000 to 49,000 points. Minimum p-value plotted is 0.01, actual values may be lower. (A) ADF test, with p-values capped at 0.20. The 95th and 99th percentile shaded yellow and green respectively, indicate significant evidence for stationarity. (B) KPSS test, with p-values capped at 0.1. The 95th and 99th percentile shaded orange and red respectively, indicate significant evidence for non-stationarity.

Having discarded the PSR test, we now apply ADF and KPSS to samples of varying sizes, taken from the three series (HI,RW,NS). Sampling begins at the first point of the series and takes

consecutive points up to the desired length of samples. Sample lengths range from 1000 to 49,000 data points. Again, as we saw in table 4.3.1.2, the two tests perform differently. The KPSS test correctly identifies RW and NS as non-stationary and stationary respectively, for all sample sizes. This is shown in figure 4.14B. The ADF test (figure 4.14A) correctly identifies NS as stationary for all sample sizes. For short sample sizes it also correctly identifies RW as non-stationary. However, for sample sizes much above 20,000, ADF finds significant evidence that RW is stationary at 95% confidence. This is an interesting result. Although RW is generated by a non-stationary process, it appears to fool the ADF test by staying ‘stationary enough’ over many time points.

There is mixed evidence for the stationarity of HI, as shown in figure 4.14. ADF, for all sample sizes above 2000, finds significant evidence that HI is stationary. Whereas KPSS, on the whole, gives significant evidence that HI is non-stationary - There are only seven cases where there is insufficient evidence to reject the null hypothesis that the HI series is stationary, and these occur at sample sizes between 24,000 and 34,000. From these results it appears that the KPSS test is a stricter test of stationarity, and is less sensitive to the size of the sample. Although it appears that the ADF test is biased in favour of stationarity, it does order the series correctly in the above examples and is a useful complement to KPSS. Also it may be that the sensitivity of ADF to sample length is useful, since processes may appear stationary/non-stationary at different scales.

We consider the possibility that the method of sampling from the time series affects the results of the stationarity tests. For example samples taken near the beginning of an IBM simulation run may be more likely to give the non-stationary series because of transient dynamics. Alternatively a non-stationary data generator may produce sections of time series that appear stationary purely by chance. This sensitivity to sampling is investigated by *reversing* the time series and repeating the above analysis (results not shown). For HI, RW and NS we see no qualitative change in the results presented above. We also scan sampling windows of fixed length along the series to look for time dependence in the test results. The time at which samples are taken appears to make no qualitative difference, and there is no systematic change in the results that would suggest the simulation becomes more stationary the longer it is run<sup>4</sup>.

**HI simulation.** We now focus on the simulation data used to generate HI and look in more depth at whether this dataset can be considered stationary. We use the same two tests, ADF and KPSS, for the stationarity of univariate time series. Since our abundance vector is 60-dimensional ( $N = 60$  species), it is necessary to perform some manipulation to get a time series we can test. Previously we used the total number of individuals as our time series. However simply summing over species (l1-norm) is not necessarily the most informative metric to use. One possible issue is that the phase differences between species oscillations that we would expect due to trophic interactions (see chapter ??) may mean that temporal variability is cancelled out

---

<sup>4</sup>Note that for certain LI simulations there was some small change in stationarity results over the course of the time series. However they did not tend towards increased stationarity, rather there seemed to be some parts of the time series which, by chance, appeared more or less stationary than others.

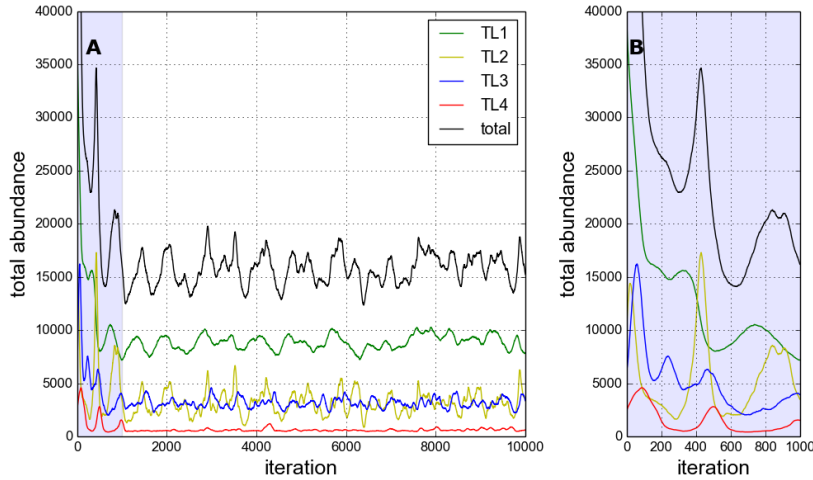


Figure 4.15: Population dynamics of a simulation from the HI ensemble: total number of individuals, and by trophic level. (A) First 10,000 iterations of simulation run (total = 50,000 iterations). (B) Enlargement of first 1000 iterations, showing transience.

when aggregating abundances in this way. It is possible that simulations which appear stationary according to some aggregate metric (e.g. total number of species) may have non-stationary underlying dynamics. This suggests that it is most informative to consider stationarity at the species level. We also consider the stationarity of abundances by trophic level, as an alternative aggregate metric.

The dynamics of the HI simulation are aggregated by trophic level to create four new time series TL1–4. These *trophic dynamics* are plotted in figure 4.15. The initial period of transience is expanded in panel B. As in the previous analysis this part of the time series (first 1000 iterations) is removed. The ADF and KPSS tests are applied to the four trophic series separately and the results are shown in figure 4.16. According to ADF all trophic levels are stationary for samples sizes greater than 4000. TL1 appears to be least stationary according to ADF, requiring a sample size of at least 4000 to reject the null hypothesis at 95% confidence. According to KPSS TL1 is non-stationary for all sample sizes, whilst TL2 and 3 are stationary for samples sizes above 6000 and 1000 respectively. KPSS gives mixed results for TL4, with no clear dependence on sample size. It is hard to reconcile these results with an observation of the dynamics in figure 4.15, indicating the usefulness of the statistical tests. It may be informative to consider if there are general trends in the stationarity of trophic levels.

The dynamics of all the species belonging to each trophic level are plotted in figure 4.17. It is clear here that the community is dominated by a few abundant species, mainly in the lower trophic levels, with a large number of relatively scarce species. This agrees with the rank abundance plots from chapters ??, and with the long tailed distributions seen in real world communities. It also appears from this figure that the more abundant species exhibit large

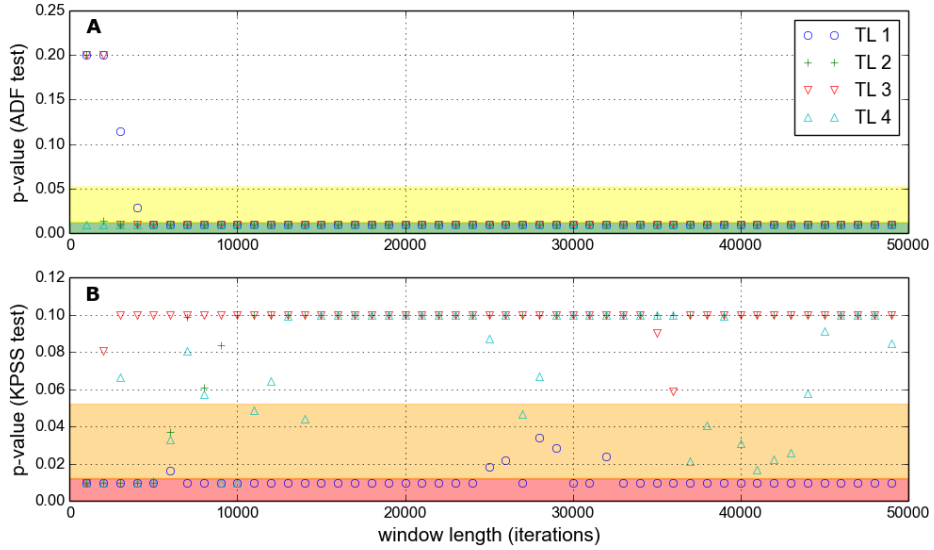


Figure 4.16: Similar to figure 4.14, but here the tests are applied separately to each trophic level of the HI simulation shown in figure 4.15.

amplitude oscillations in their dynamics. This leads us to hypothesise that the most abundant species may be non-stationary, whereas the least abundant species may be stationary. We test this hypothesis by applying the ADF and KPSS tests to the three most abundant and three least abundant species in the HI simulation. Species are selected based on their average abundances over the whole simulation (minus the initial transience).

We see from figure 4.18 that all six species are stationary according to ADF, given sufficiently large sample size. However the sample size for all three of the abundant species to be stationary is greater (panel A:  $\geq 9,000$  points) than for the three least abundant species (panel C:  $\geq 2,000$  points). This suggests that the most abundant species are indeed ‘less stationary’ than the least abundant species. The KPSS test supports this conclusion. KPSS finds that the three least abundant species are stationary above samples sizes of  $\sim 18,000$ , whereas two of the most abundant species are non-stationary for almost all sample sizes. Inspecting the dynamics in figure 4.17 we see that these non-stationary species are those with largest amplitude fluctuations in their abundances.

In general we conclude that the choice of metric used to generate the time series does affect the conclusions about stationarity. Overall we cannot be confident that the HI simulation is stationary, based on the results presented above for species, trophic and total abundances. This is largely due to the apparent strictness of the KPSS test. Considering species dynamics individually is the most informative. It allows for the possibility that some species abundances may be more variable than others, and information is not lost by aggregating. In the following analysis we propose that stationarity tests should be applied to species dynamics, and then the number of

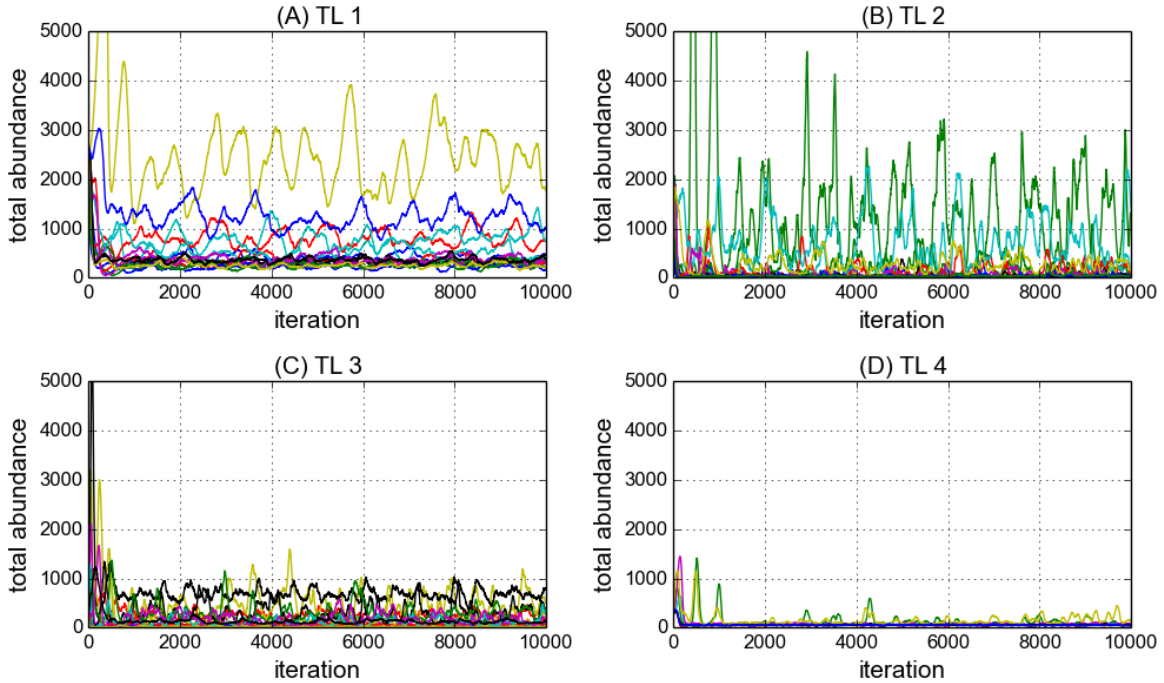


Figure 4.17: Dynamics of all species in the first 10,000 iterations of the HI simulation shown in figure 4.15. Each colour represents of different species, each panel (A-D) shows a different trophic level (TL1 – 4).

stationary species (NSSP) used as an aggregate statistic. If NSSP equals the total number of species, then the community dynamics is fully stationary (according to the test used).

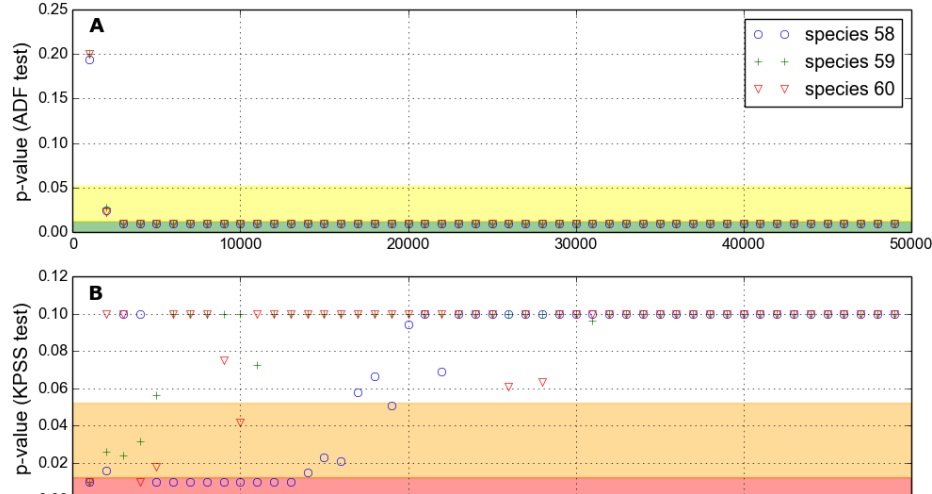
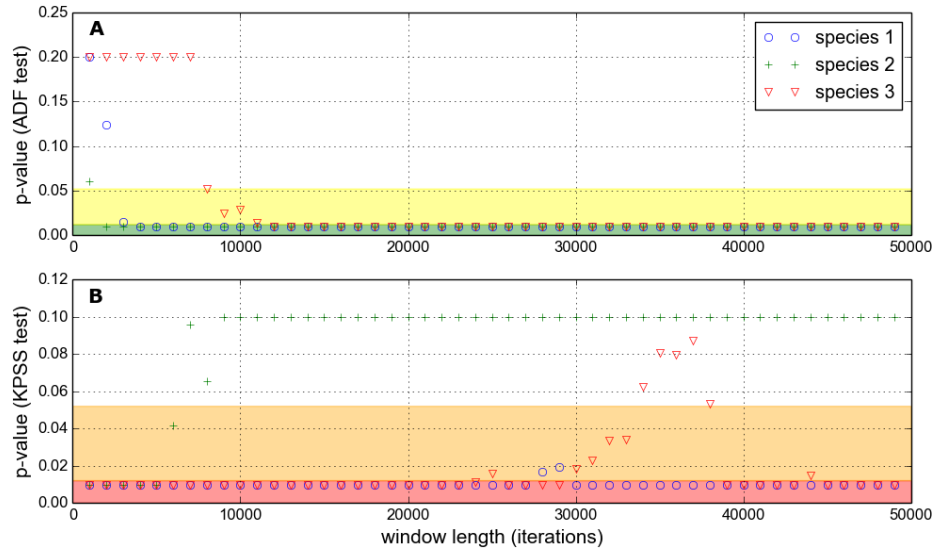


Figure 4.18: Similar to figure 4.14, but here the tests are applied separately to individual species from the HI simulation shown in figure 4.15. (A) The three species with highest long-term average abundance. (B) The three species with lowest long-term average abundance.

### 4.3.1.3 Stationarity results

We now pursue a general investigation of the stationarity of communities simulated with the IBM model. First we test the stationarity of three ensembles of new simulation runs (figure 4.19). The new simulations use default parameters, unless otherwise specified, and are run for 50,000 iterations. Two ensembles of 100 simulations each are run for high ( $IR=0.001$ ) and low ( $IR=0.0001$ ) immigration rates, which we refer to here as the HI and LI ensembles respectively. A third ensemble of 50 shorter simulations (10,000 iterations) is run, at high immigration rate, using a fixed interaction network, which we call the NM1 ensemble. All networks are generated using the niche model as described in section ??, with zero mutualism ( $MAI=0.0$ ). Each simulation uses a uniquely generated network, except for those of the NM1 ensemble. Stationarity testing is done using the ADF and KPSS tests characterised in section 4.3.1.2 above. As standard the initial 1000 iterations are discarded in an attempt to remove transience. The tests are then applied to a sample taken from the abundance time series of each species. The results presented in this section give the number of stationary species (NSSP) in the community, at the 95% confidence level.

As the length of the samples taken from the abundance time series increases, the average NSSP also increases. This is true of both tests and for all three ensembles, as we can see from figure 4.19A. According to ADF all species are stationary, on average, for sufficiently large sample length. The required length of sample is larger for the LI ensemble than for HI. For KPSS, although the NSSP does increase with sample length, it is not clear that it will asymptotically approach 60 species in the limit of many iterations. The average NSSP at 49,000 sample points is just under 40 and just over 20 for HI and LI ensembles respectively.

To check the time dependence of stationarity (i.e. are species more likely to be stationary after many iteration of a simulation?) samples of length 3000 were taken from different points along the time series. From figure 4.19B we can see that there is no clear trend in stationarity over 49,000 iterations. The average NSSP is almost the same whether the sample is taken from iterations 1000-3000 or 46,000-49,000. This result also holds for windows of different length, which are not plotted here.

On average we see that the LI ensemble is less stationary than the HI ensemble. This we expected from the results of chapter ?. However we cannot be confident that either ensemble contains communities with stationary species distributions. This may be problematic for the interpretation of our results, and we discuss this further below. Interestingly the NM1 ensemble gives very similar results to the HI ensemble. This may be because we have accidentally chosen NM1 to closely resemble the average of this ensemble (see both panels of figure 4.19). Alternatively it may be that stationarity of the simulation output is not dependent on the interaction network structure.

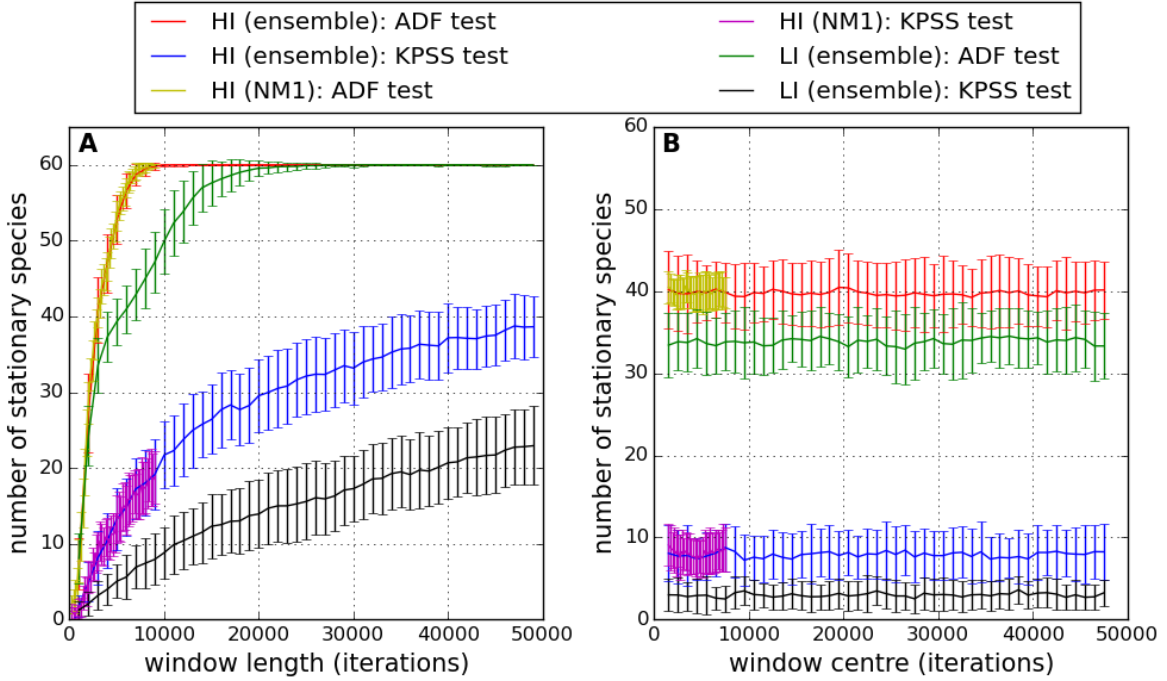


Figure 4.19: The number of stationary species (NSSP) according to the two stationarity tests (ADF and KPSS) at the 95% confidence level. Results averaged over three different ensembles of simulations: HI; NM1 (high immigration) and LI as described in the text. The first two are high immigration ensembles, whilst the latter is low immigration. Solid lines indicate mean results for the ensemble. Error bars indicate  $\pm 1$  standard deviation. (A) Each species abundance time series is sampled with a window of increasing length, as in figure 4.18. (B) Each species time series is sampled with a window of length 3000 iterations, which is scanned along the series to check for changes in stationarity over time.

In chapter ?? we will <sup>5</sup> explore a slice of parameter space by varying immigration rate and habitat loss. Here we study the stationarity of the simulations that we will use in that chapter. All simulations are 5000 iterations long. The initial 1000 iterations are discarded and the ADF and KPSS tests applied, species by species, to the remaining 4000. Figure 4.20 shows the average NSSP across the region of parameter space investigated, for three MAI ratios (MAI= 0.0, 0.5, 1.0). The results are qualitatively the same for both tests, although NSSP is higher for ADF than for KPSS as expected. On average reducing IR reduces the NSSP. A weaker effect, but still visible is that increasing HL reduces the NSSP. Most striking is the effect of MAI ratio on stationarity - the average NSSP is greater across the whole parameter region at MAI= 0.0 than at MAI= 1.0, with MAI=0.5 in between the two. Increasing mutualism also appears to reduce the dependence of NSSP on IR. Figure 4.21 summarises these trends using cross sections taken from the heat maps in figure 4.20, with error bars added. It is clear that there is high variability across replicate

<sup>5</sup>These results could be moved to the start of the next chapter.

simulations, and this variability appears to be greatest for high mutualism (MAI=1.0).

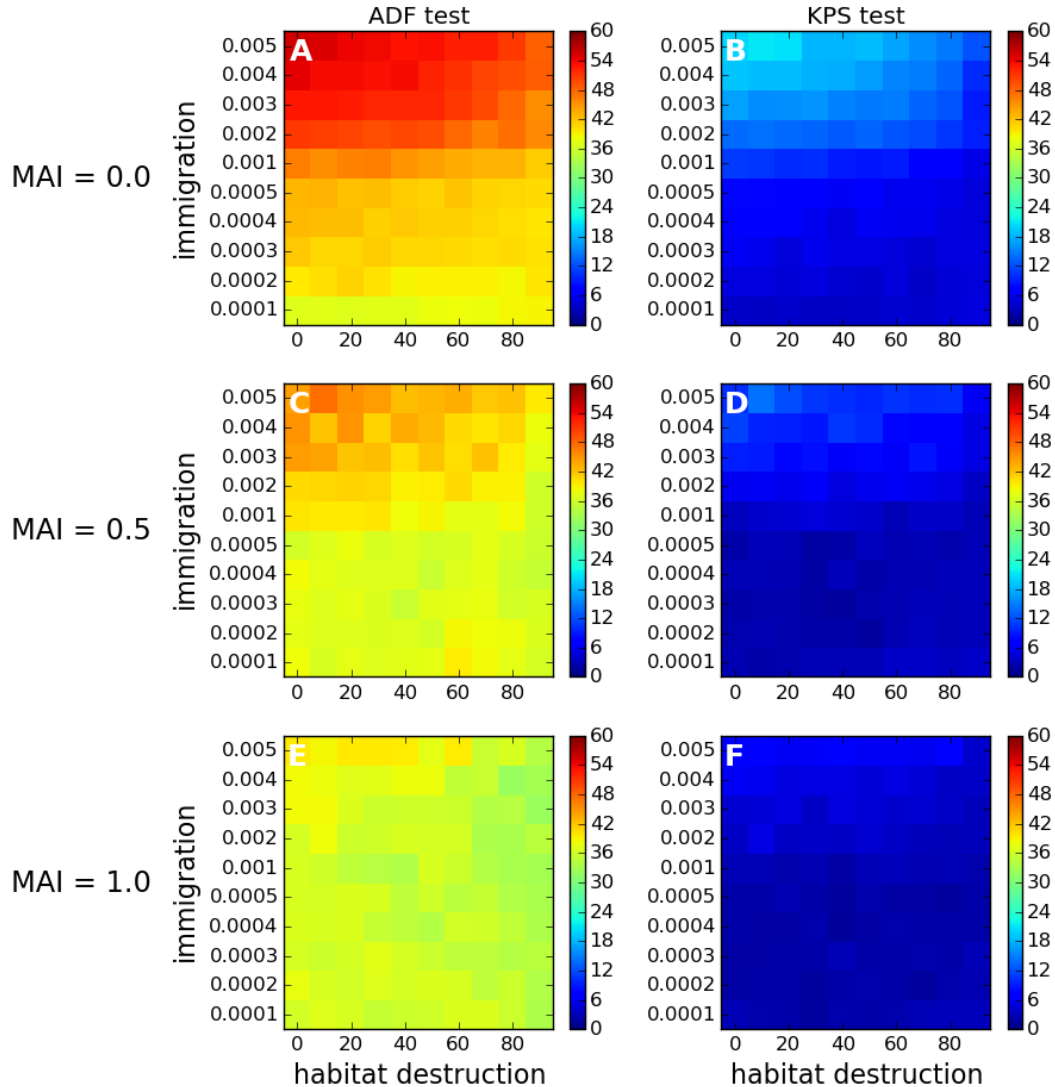


Figure 4.20: The average number of stationary species (NSSP) according to the two stationarity tests (ADF and KPSS) at the 95% confidence level. Each cell on the grid represents the mean value over 50 repeat simulations. All simulations are 5000 iterations with default parameter values. Tests are applied to the final 4000 iterations of each species abundance time series. These correspond to the simulations presented in chapter ??.

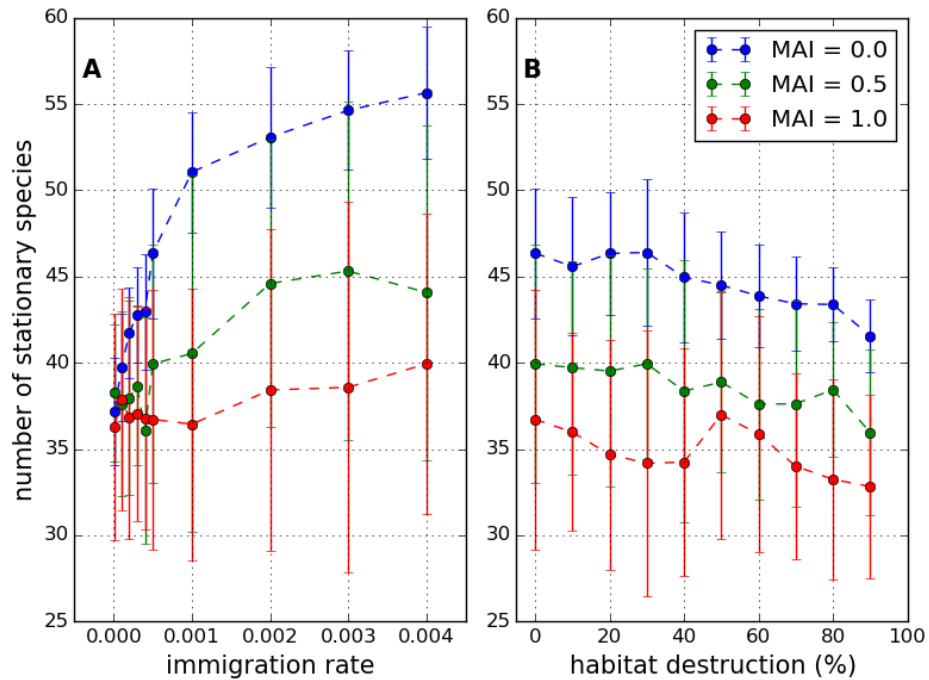


Figure 4.21: The number of stationary species (NSSP) according to the ADF test at the 95% confidence level. Points show mean value over 50 replicates. Error bars show  $\pm$  one standard deviation. Tests are performed on the same simulations depicted in figure 4.20. (A) Plotted against immigration rate (IR), with zero habitat destruction. (B) Plotted against habitat destruction, with IR= 0.001 (high immigration regime).

### 4.3.2 Determinism tests

We have seen that population dynamics becomes highly variable, especially at low IR, and indeed may not be stationary. From inspection of the population dynamics it appears that there is a strong stochastic component, even in the case of high immigration (for example Figure 4.17). This leads us to speculate that in some instances the simulation output may become dominated by randomness. This randomness is an interesting feature of the model, and indeed is likely to play an important role in real ecosystems (see discussion 6.6). However much of our analysis (chapters 3 and 5) involves interpreting the simulation results in terms of the ecological mechanisms built into the model, in particular the patterns and structures generated by species interactions. If the model output lacks determinism it does not seem meaningful to conduct such analyses. Therefore we present here a test for determinism based on *recurrence quantification analysis* (section 4.3.2.1), which we then apply to our model output (section 4.3.2.2).

#### 4.3.2.1 Recurrence quantification analysis

Recurrence quantification analysis (RQA) maybe be used to detect signatures of determinism [4, 29, 43]. The analysis is based on the idea of *recurrence* - deterministic dynamical systems tend to return to similar regions of phase space. Moreover, when they do, their trajectories tend to remain close in phase space for some amount of time. In the case of chaotic systems the trajectories will diverge, at a rate which is broadly determined by the maximal Lyapunov exponent [29]. However, even for chaotic systems, there is some tendency for neighbouring trajectories to remain close. RQA aims to detect the presence of this feature in the dynamics. The analysis is often used with univariate time series (such as in [29]), in which case time-delay embedding must be used to increase the dimensionality of the phase space. However, since we have a time series for each of the 60 species, our phase space is already high dimensional. Therefore our first step is to construct a recurrence matrix (RM). The RM is a binary matrix whose elements, for a system  $x(t) \in \mathbb{R}^N$ , are given by the function:

$$(4.4) \quad d_{ij} = \begin{cases} 1 & \text{if } \|x(i) - x(j)\| < r \\ 0 & \text{if } \|x(i) - x(j)\| \geq r \end{cases},$$

where  $r$  is a threshold distance that defines the measure of ‘closeness’ in phase space. Various methods have been proposed to choose the value of  $r$ . These methods are discussed in [4], but we use the method which they employ throughout their paper:  $r$  is chosen such that  $\sim 10\%$  of the elements of the RM are equal to one.

Having constructed the RM it can be visualised as a *recurrence plot* (Figure 4.22). Such plots can be visually striking (search recurrence plots for examples), but are difficult to interpret without experience. An important feature, in the search for determinism, are *diagonal lines* - lines parallel to the leading diagonal. Such lines indicate that trajectories which find themselves

'close' in phase space remain close, for a period of time given by the length of the line. Visual inspection can detect the presence of diagonal lines but it is better to use a quantitative pattern detection method. A common metric that quantifies the relative abundance of diagonal lines is the *percentage of determinism* (%DET) [4, 43], and is given by:

$$(4.5) \quad \%DET = \frac{NPD}{NREC} \times 100,$$

where NREC is the number of entries in the RM equal to one; and NPD is the total number of points found on diagonal lines of length greater than or equal to two. The %DET allows quantitative comparison of the level of determinism between different RMs. In [4] they develop three statistical tests, based on %DET and two similar metrics, for the null hypothesis of pure randomness in the time series. However in the current analysis we make do with a comparison of the value of %DET between different test cases.

#### 4.3.2.2 Results

We test for determinism in the simulation ensembles HI and LI used in section 4.3.1 (see for example Figure 4.19). Each ensemble consists of 100 repeat simulations with different network structures. These simulations are used because one ensemble is from the high immigration regime (HI: IR= 0.001) and one is from the low immigration regime (LI: IR= 0.0001). Therefore the temporal variability is higher on average in the LI ensemble than the HI ensemble. The simulations in these ensembles are also longer than other simulations - being run for 50,000 iterations they allow for more chance of recurrent dynamics and therefore provide more information from which to detect a signature of determinism. In both ensemble the communities are antagonistic (MAI= 0) and the landscape is pristine (HL= 0). Therefore we do not cover the full range of parameters explored in other analyses, but we at least consider one highly variable and one less variable scenario.

For comparison of the values %DET we construct randomised data in two different ways. In [4] they state a random process would generate a RM with NREC points distributed uniformly at random<sup>6</sup>. We construct such matrices by randomly permuting the elements of another RM, to obtain a randomised RM with the same number (NREC) of points. In addition we also construct RMs by randomising the time series of each species. This preserves the mean and variance of the population dynamics, but removes any determinism. The randomised time series are then used to construct an RM<sup>7</sup>.

Figure 4.22 shows four example recurrence plots. Panels A and B show the RMs of single simulations from ensembles HI and LI respectively. Panels C and D show randomised versions of panel B generated by randomising the matrix, and by randomising the time series respectively.

<sup>6</sup>They actually say arbitrarily at random, but 'uniformly' is better?

<sup>7</sup>This description needs improving

Panels A and B clearly have some structure, whilst the structure is lost in panel C as expected. Panel D retains some structure. In particular it contains the leading diagonal, since even the randomised time series is identically equal to itself. It also contains horizontal and vertical bands, created by points in the time close that are unusually distant (or close) to a large number of other points in the phase space. A subtle but detectable feature of panels A and B is the presence of diagonal lines (parallel to the leading diagonal) suggesting determinism. This feature is lost in panel D, as we would expect from the randomised time series. Interestingly panel A looks very similar to figure 1(c) in [4]: an RM generated from the dynamics of a noisy chaotic Hénon attractor (see discussion 6.6).

We calculate the %DET for each simulation in the HI and LI ensemble. In each case, for comparison, we also calculate the %DET for the dynamics of the ten most and ten least abundant species<sup>8</sup>, and for the two randomised versions of the data. These results are shown in figure 4.23. The randomised data shows little variation, with a %DET $\sim= 10$  in all cases. The %DET for the least abundant species is slightly greater than for random data, suggesting some evidence of determinism but also a strong stochastic component. In both the HI and LI ensembles there is good evidence for determinism at the whole community level, with %DET consistently  $> 30$  and  $> 40$  respectively. It is interesting that there is more evidence of determinism in the LI ensemble than in the HI ensemble, as we previously conservatively assumed that the high temporal variability of the LI dynamics could mean that it lacked determinism. It is also clear for these results that the deterministic component of the dynamics is dominated by the most abundant species. This, together with the results from previous sections tells us a lot about the dynamics of the model (see discussion below). We conclude here that the analysis so far suggests that non-stationarity may be largely due to deterministic population dynamics/oscillations of the most abundant species, while the dynamics of the less abundant species are more random and more stationary although they appear to have a deterministic component.

### 4.3.3 Accuracy and repeatability

In chapter 3 we used ‘snapshots’ of the simulation state to calculate species abundances. Clearly this sampling method yields different results depending on when the measurement is taken. The snapshot method was justified by the assumption that simulations reached stationarity and therefore we were sampling from a steady-state distribution (with suitably low variance). However, as we saw in section 4.3, stationarity cannot be guaranteed. The results of section 4.3.2 suggest that this lack of stationarity is due to deterministic population dynamics, especially those of the most abundant species. Irrespective of the cause, here we look at how temporal variability affects the *accuracy* of our results. In particular we focus on measurements of species abundance and how these depend on the length of sample taken from the dynamics. To do this we make

---

<sup>8</sup>Justify this, above?

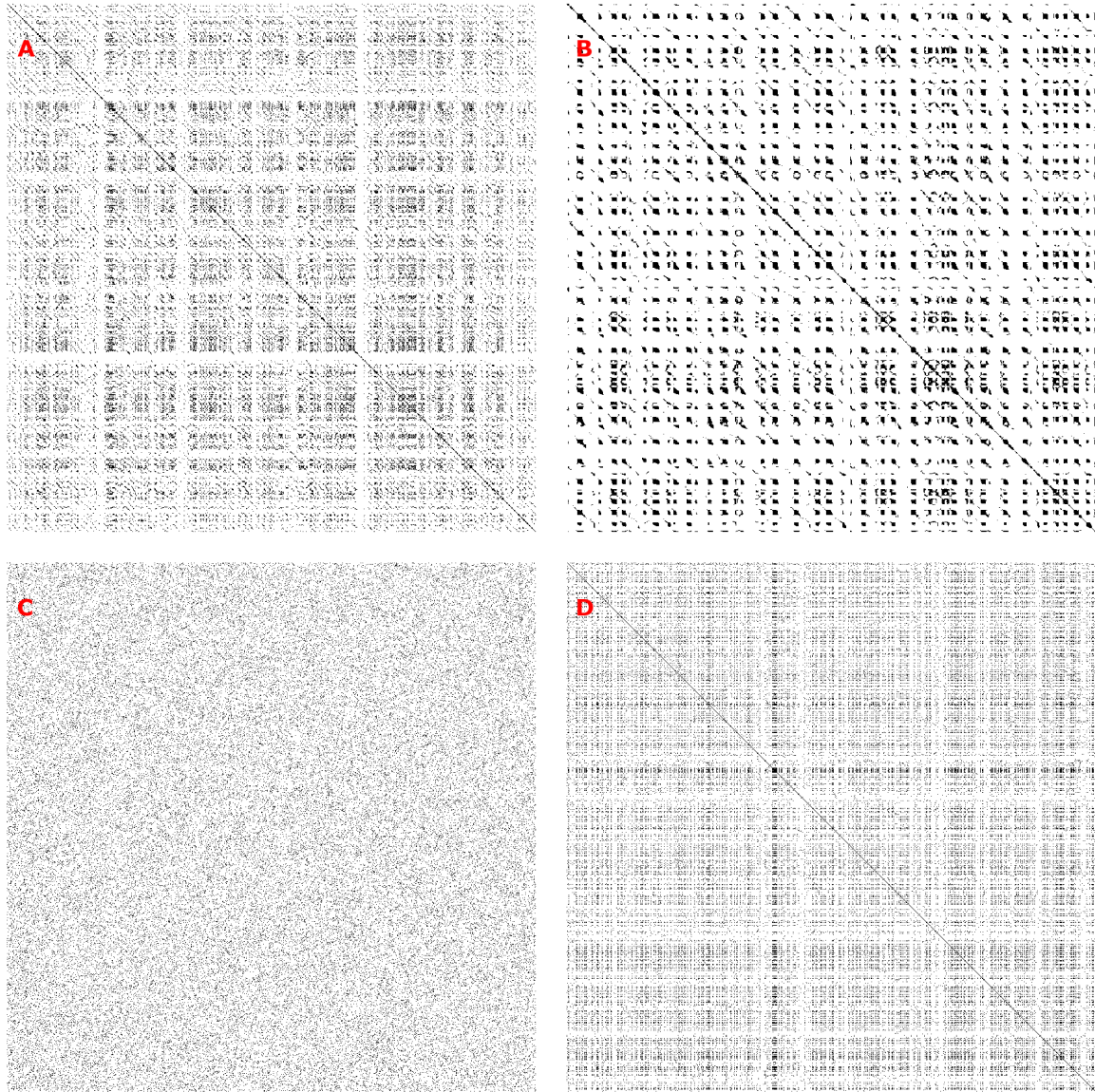


**Figure 4.22: Recurrence plots** defined by equation 4.4. (A) High immigration simulation ( $IR=0.001$ ). (B) Low immigration simulation ( $IR=0.0001$ ). (C) Randomised recurrence matrix (permutation of the elements of the matrix in B). (D) Randomised time series (permutation of species population time series from B, such that mean and variance for each species are preserved). In simulations for both A and B:  $HL=0$  and  $MAI=0.0$ ; number of iterations = 50,000; sampled every 50 iterations to construct plots.

the assumption that the *long term average* abundance is what we want to measure<sup>9</sup>. We also look at the *repeatability* of our results by running replicate simulations with the same network structure.

---

<sup>9</sup>Justify this, especially in light of stationarity results. Existence of stable equilibrium? What if chaotic?

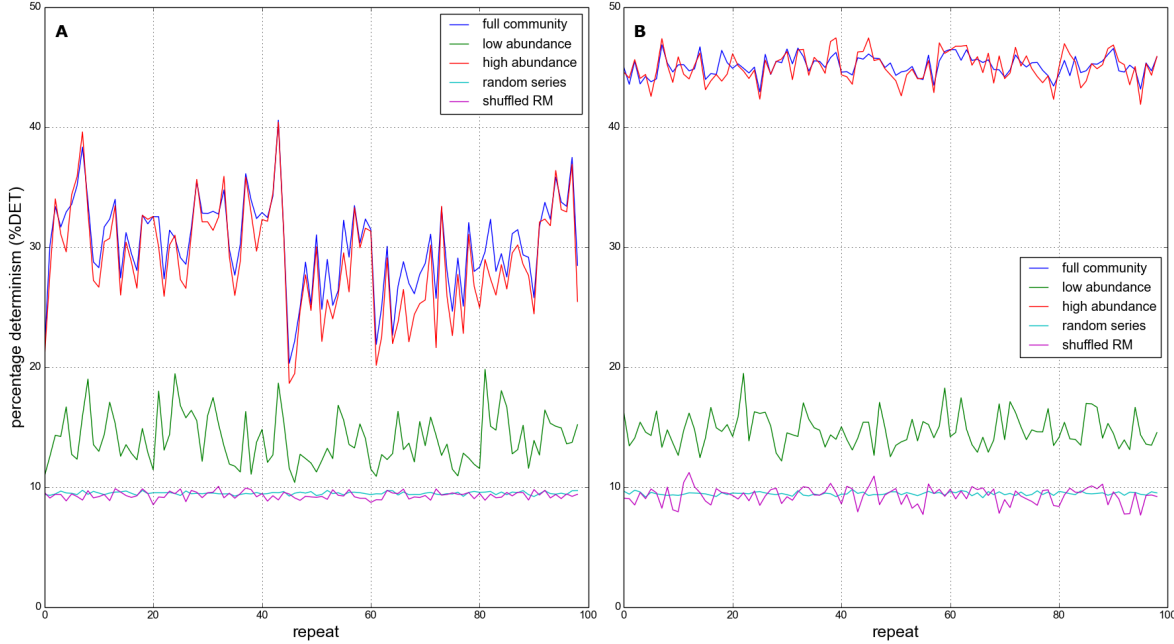


Figure 4.23: **Percentage determinism (%DET)** defined by equation 4.5. Value calculated for whole community, ten least and ten most abundant species, and for two randomised versions of the data (see text). For 100 repeat simulations at: (A) High immigration rate ( $IR=0.001$ ); and (B) Low immigration rate ( $IR=0.001$ ). In simulations for both A and B:  $HL=0$  and  $MAI=0.0$

#### 4.3.3.1 Accuracy

- Define mean relative error MRE metric
- Explain how linear regression is to asses accuracy
- Define the estimators we test: snapshot, and averages over increasing sample length.
- Figure 4.24 can be use to justify using the long term average.
- Figure 4.25 shows how estimator regression works
- Figure 4.26 shows that the snapshot estimator is way off long term average measurement of abundance. And that quality of the estimator improves with sample length. How much error can we tolerate? Averaging over 2000 iterations is pretty good based on  $R^2$  values.

#### 4.3.3.2 Repeatability

- Repeat simulations with same network structure - NM1 from above
- Introduce rank abundance spectra - what does it tell us about repeatability?

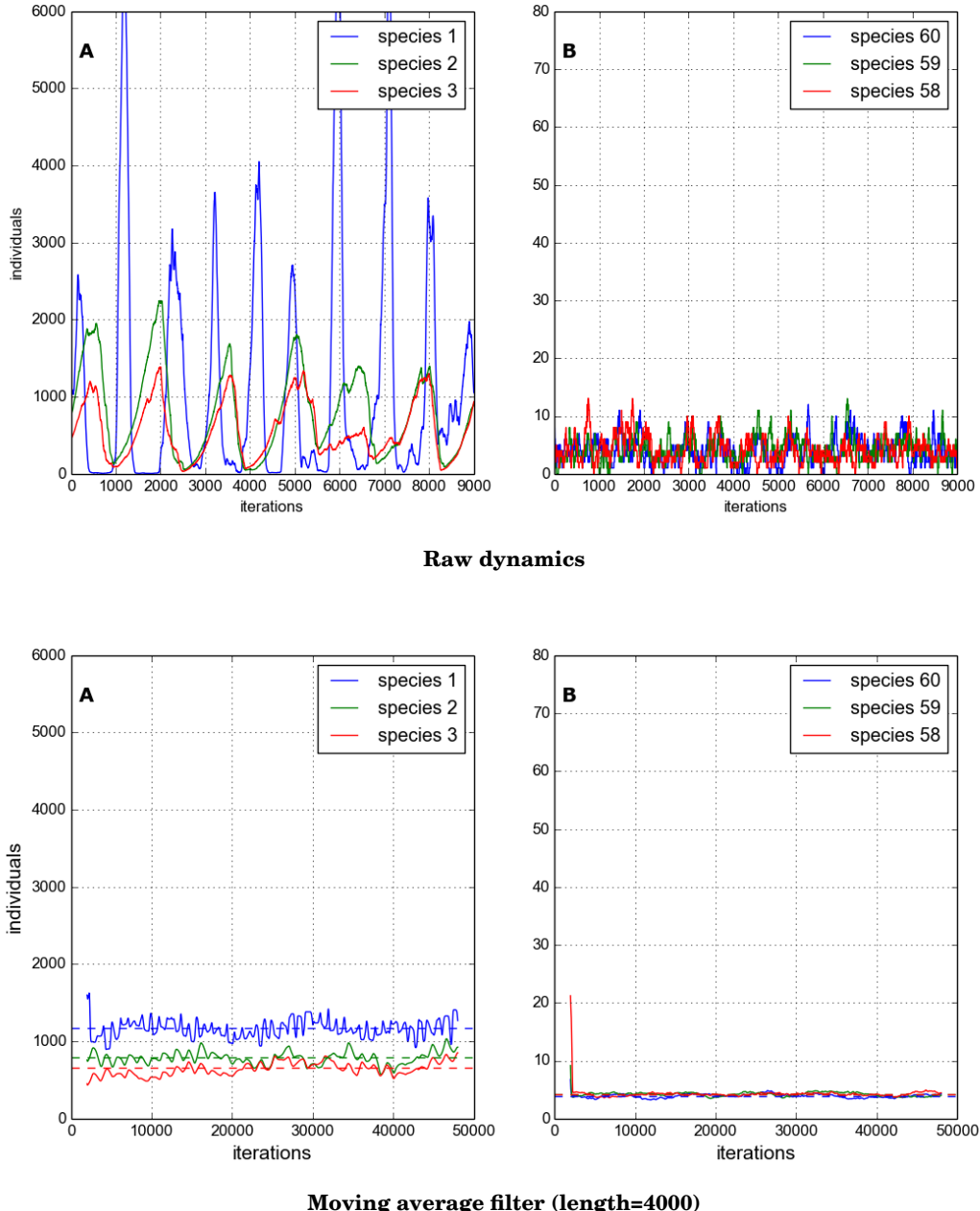


Figure 4.24: Example dynamics of (A) the most abundant and (B) the least abundant species, taken from a single simulation in the LI ensemble. Top: Raw dynamics (without averaging). Bottom: Moving average filter of length 4000 iterations. Dashed lines indicate the long term average throughout the whole simulation.

- Figure 4.27 shows us that simulation results (of abundance at least) are pretty repeatable across replicates.

#### 4.3.4 Discussion

Here we discuss the results from the sections on stationarity, determinism and accuracy. Main points to include:

- Main conclusion: not all species in communities are guaranteed to be stationary, even in high immigration regime. Therefore steady-state assumption not valid. Two questions: how does this affect our results? Second most important question: why are they not stationary? Hypothesis: deterministic chaos? Alternative hypothesis: stochastic fluctuations about a stable equilibrium (but is this deterministic? and why would this not appear stationary?)
- How do the stationarity results relate to real-world ecosystems? Concepts of stability etc. (many references).
- Mention other possible tests for stationarity, and wavelet analysis.
- Simulations do no get more or less stationary with time. (i.e. 5000 iterations is probably enough) This means we do not need to throw away all previous results. But may need to reconsider how to calculate them.
- Most abundant species are the least stationary.
- Low immigration simulations are less stationary than high immigration
- But! - low immigration simulations are more deterministic! Therefore the lack of stationary must be due to increased amplitude of deterministic dynamics? This is confirmed by visual inspection of dynamics, and what we know from theory.
- Ok, good, so our simulation results are not completely random (except maybe the least abundant species?) But what about accuracy of our results?
- In the case of low immigration very long sample windows are required for abundance estimates to approach the long term average. We may have to accept some error in our results..
- Simulation results appear to be repeatable, according to rank abundance spectra, which is good! (Also according to results in first half of the chapter looking at how network structure affects persistence).

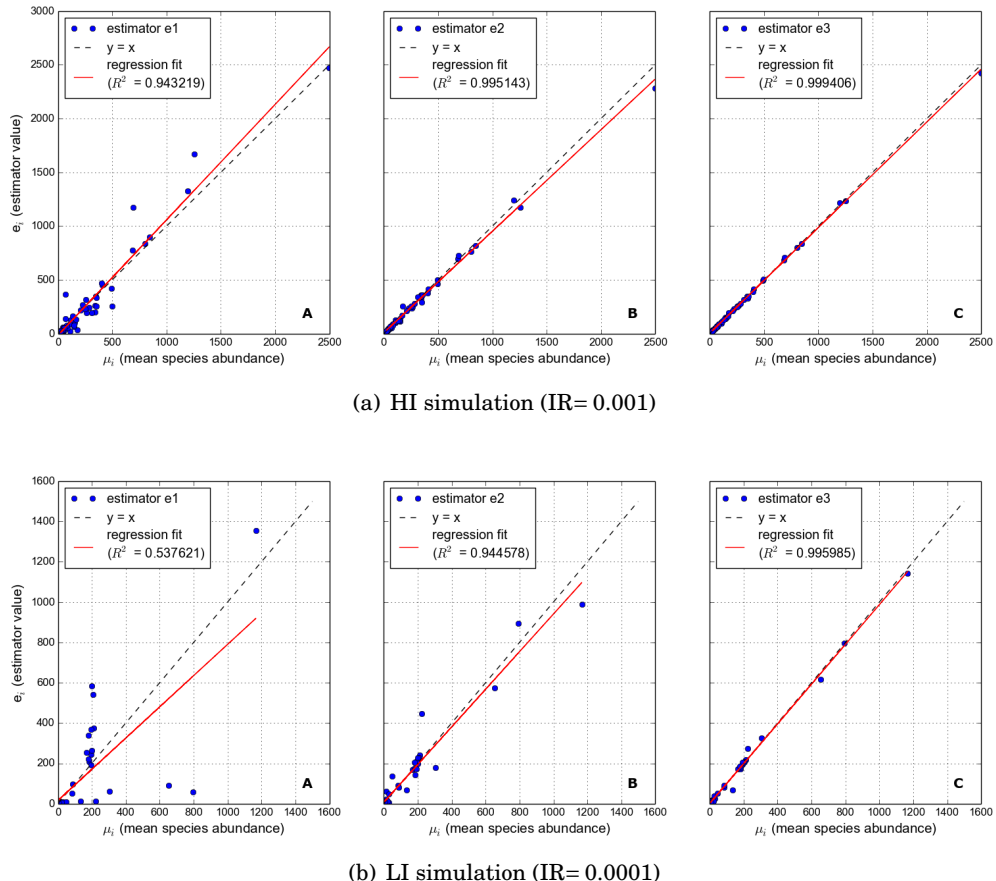


Figure 4.25: Performance of three different estimators of species abundance, applied to (A) a single HI simulation and (B) a single LI simulation. Estimator ‘e1’ is a snapshot of abundance on 5000th iteration; ‘e2’ is an average over 4000 iterations; and ‘e3’ is an average over 29,000 iterations. Points are the long-term mean abundance of a species, plotted against the estimator value for that species. Red lines show linear regression fits for the estimator, and how close the estimator is to modelling the ‘true value’ of species abundances (dashed blue line).

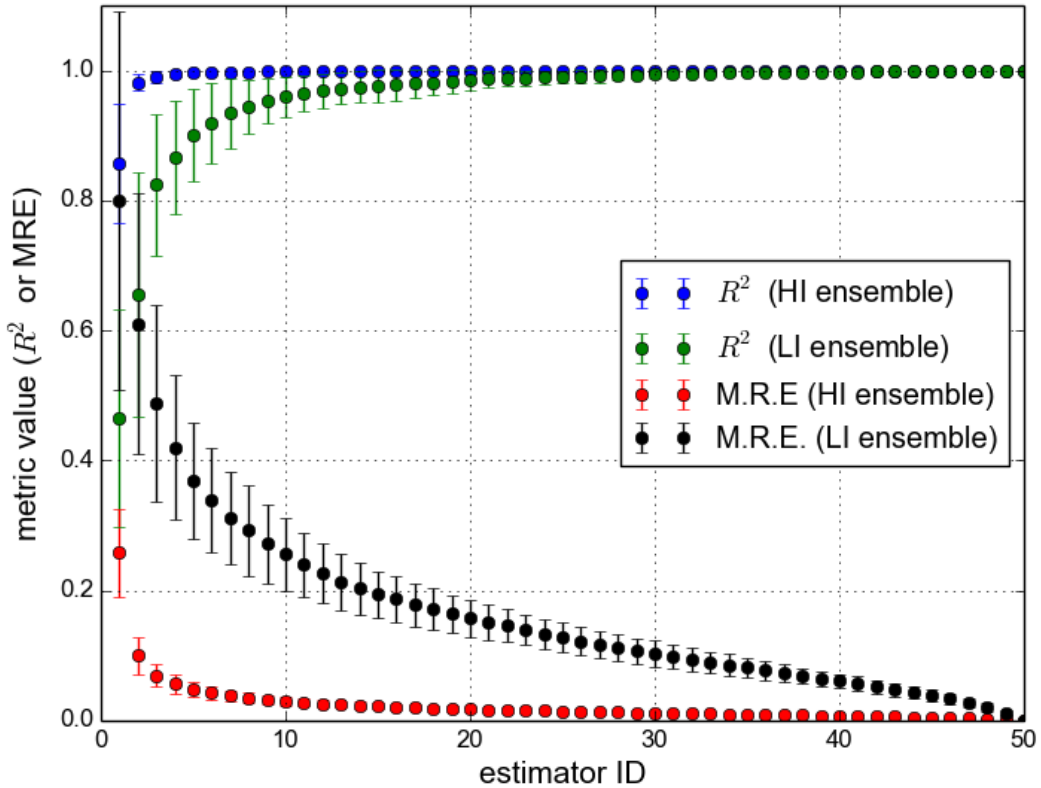
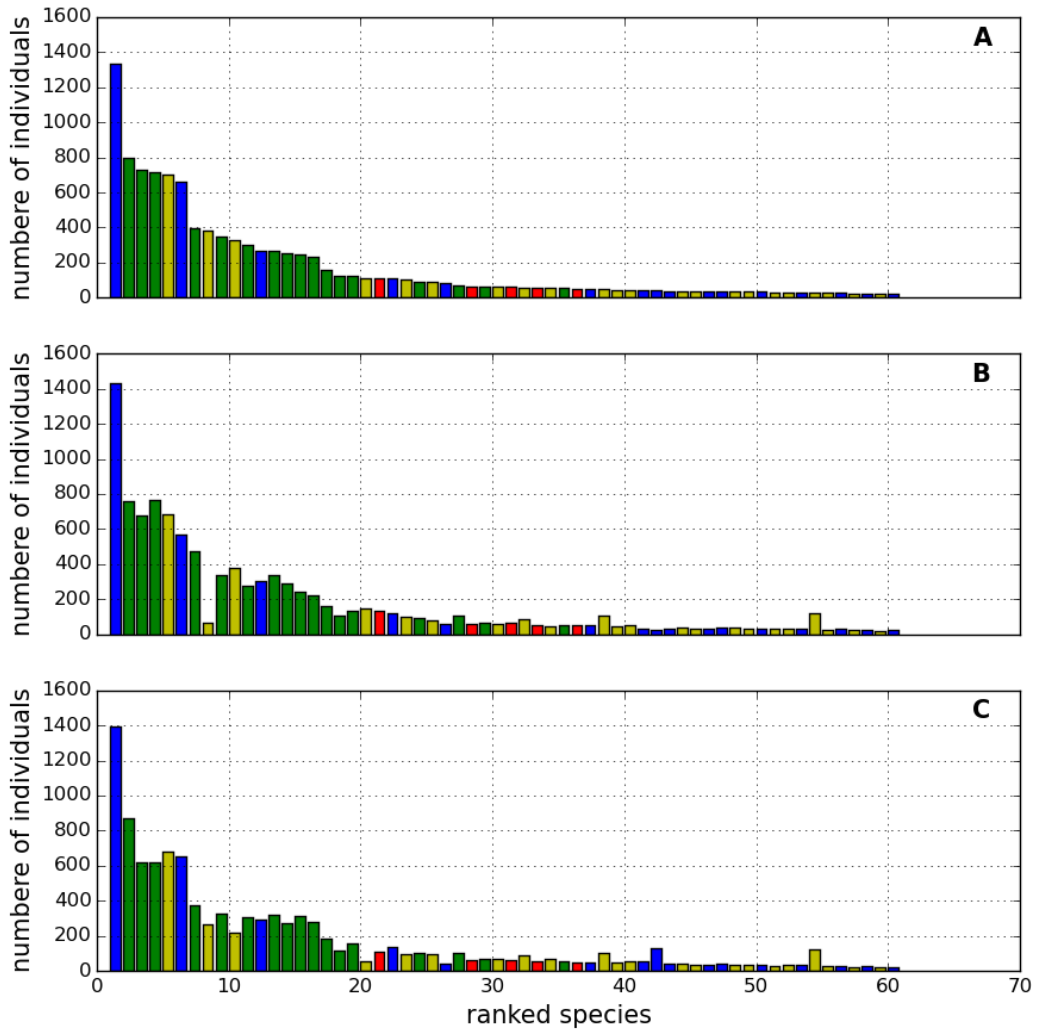


Figure 4.26: Performance of 50 different estimators for species abundance, measured by  $R^2$  value and mean relative error MRE (see text for definitions). The first estimator (estimator ID=1) is uses ‘snapshot’ of simulation state at 5000th iteration (as used in previous chapter), the remaining estimators (IDs= 2,..,50) use average abundances over sample windows ranging from length 1000 to 50,000 in steps of 1000. Points indicate mean value of metric over ensemble of simulations. Error bars indicate  $\pm$  one standard deviation.



**Figure 4.27: Rank abundance spectra (RAS)** for three simulations from the NM1 ensemble (see text). Species abundances measured as long term average (over iterations 1000-9,000). Species are ranked according to their abundances in the first simulation (panel (A)). Ranking is retained in panels (B) and (C), which show abundances from two different simulations. Colouring of species by trophic level is consistent with previous figures.

## 4.4 Conclusion

Main conclusions of chapter:

- Immigration required for persistence
- Strong competition in our model
- Network structure is important
- Communities are not stationary
- But are deterministic!<sup>10</sup> (At least partly)
- Simulations are repeatable
- But accuracy of results affected by sampling intensity: THIS NEEDS CAREFUL CONSIDERATION. WHAT TYPE OF SAMPLING WILL WE USE IN THE NEXT CHAPTER?

---

<sup>10</sup>Possibly chaotic but not really relevant



## VARYING IMMIGRATION RATE

This chapter explores the interactions between immigration rate, habitat loss and MAI ratios - choose a better title.

TODO: link up these section references. (and add recent papers into .bib file)

TODO: finish discussion of results. But first redo analysis with averaging? TODO: look at "effective immigration" rates..? (inversely proportional to total biomass) TODO: show some results here for 0 HL TODO: look at longer runs (steady-state) TODO: look at over-abundance of top trophic level (re-run results) TODO: averaging of RADS (and others..) WAIT FOR STEADY STATE. TODO: either end each section with ecological context and implications, or have in separate section after results. TODO: finds out about Kevin McCann on omnivory (biomass pyramids?)

### 5.1 New predictions (Temp)

New predictions and questions following on from previous chapters, which are now basically complete. Need to make this chapter follow on nicely, and demonstrate improved understanding of the model!

- At lower IR we should start to see more extinctions along the HL gradient
- Contiguous HL did not change community structure (RA, diversity, evenness, network metrics). Only interaction strengths and variability changed (not synchrony). However we expect that, along the IR gradient these properties will change, due to less input from immigration which as we saw is a levelling influence. Therefore we expect communities to become less even, and perhaps more aggregated in space (although we cannot test the latter..we could maybe..)

- Following from above: can we find an IR where we see interesting behaviour along the HL gradient, either extinctions or changes in community structure (not just changes in variability). Is there a critical threshold for IR beyond which this occurs?
- We know from previous chapter that dynamics becomes more variable, but also more deterministic, with reduced IR. Is this associated with increased interaction strengths? How does this carry across along the HL gradient? What does synchrony tell us (or determinism tests?)
- From previous chapter we know that need long term averages. Problem: network metrics still only calculated over 200 iterations. Do a comparison of some results 200 vs 4000 iterations?
- 50 REPLICATES, NOT 100 AS STATED IN TEXT BELOW!

## 5.2 Assumptions of what has gone before

- Discussion of what we will now refer to as "default parameter values" (see table ??)
- Conclusion that the default immigration rate is high and this is an open system. This represents a restricted scenario where the regional species pool is constant and high (60 species), all species are equally likely to immigrate and dispersal from outside our 'world' is not heavily constrained. In this chapter we look at varying immigration rates, habitat loss and MAI.
- A discussion of the "rescue effect" due to immigration. Probability of species spawning. Effective immigration, although currently that concept is first mentioned in this chapter.
- Context of 'viable species' as opposed to those that only remain due to immigration 'bubbling' along close to zero. (note that this is quite realistic)
- Snapshots of system versus averaging of metrics over a number of iterations (seems a bit late in the thesis to realise that this is a problem in chapter 4!) - averaging over replicates can justify this to some extent (25 in previous chapters, 100 here).
- Discussion of the functional groups and their names. These assumed below.
- It may be that this model is well approximated by GLV. If so it would make sense to discuss the results with reference to that? Should try to fit?

[64]

### 5.3 Literature review for immigration

Possibly include here a summary of recent work on immigration, including IBT and meta-community theory. (Alternative is that this goes in introductory chapter.)

IBT -> species area relationship (SAR), does high immigration reduce this effect. [76] - Search for immigration.

[35] Many studies of dispersal/immigration take a metacommunity approach. In general higher dispersal between communities is found to promote better species richness, and lower variation between communities. However we are interested in...

[41] shows, using a metapopulation model, that competitive plant communities benefit from high immigration. In these communities competition for space would lead to the extinction of all but one species. Therefore some immigration is required for diversity to exist. (Similar to our case of zero IR. Is there evidence for spatial competition in our simulations?) Some metrics change with IR some do not (check which ones, do they agree with their experiment, and ours?) They have species specific immigration rates, and an intensity parameter (otherwise same as ours with effective rate proportional to number of vacant sites...nice). Our simple case is simpler than their simple case 1 (IBT -size of regional pool and degree of isolation). They call the immigration a 'propagule rain'.

Their model displays classical competitive exclusion: "This result is different from that usually found in metapopulation competition models (Levins and Culver 1971; Horn and MacArthur 1972; Slatkin 1974; Hastings 1980; Nee and May 1992; Tilman 1994). These models implicitly or explicitly allow interference competition between species within sites, and coexistence is obtained when there is a trade-off between competitive superiority and colonization ability. Because we do not consider interference, there is no possibility for such a trade-off in our model and, hence, coexistence in a closed community is impossible. As mentioned earlier, we deliberately ignore trade-offs associated with interference competition because we wish to explore the effects of immigration from an external source on their own."

They never get stochastic extinctions because their model is continuous, therefore use an extinction threshold.

"Thus, there is always stable coexistence in a community with a propagule rain." (Interesting discussion at end : where does the propagule rain come from?)

As immigration goes to zero they find that most species have a density close to zero (therefore likely extinct) and that dominance is determined by basic reproductive rate ( $r = c/m$ ). Also space is more fully occupied as IR increases. (Figure 1 nice plot of expected number of species versus immigration intensity). Interesting change in dominance relationships (relative abundances) with IR.

Experimental results by Mouquet and Loreau [52] suggest that immigration has a positive impact on plant community diversity. (Manipulation of seed rain.) However it also shows that certain community-level properties do not depend on IR e.g. total biomass (check others). Also local competition effects.<sup>1</sup>

[23] importance of the propagule pool in determining local diversity, and shifting limitations hypothesis (SLH) [9] dispersal as a community structuring mechanism, immigration increasing local diversity, effect differs between plants and animals, intermediate dispersal rates best?

[80] Importance of dispersal in maintaining diversity in fragmented habitat patches (small tropical forest fragments). Dispersal limitation versus edges effects. Must be other REFS for this as well?

[10] Obviously proponents of neutral theory, but suggests the importance of immigration, and measures immigration rate close to ours..

[14] mathematical treatment of 3D prediction model, effect of immigration rates.

[61] "Although previous studies as far as we are aware did not investigate the effects of landscape context on immigration rates, immigration has consistently been shown to increase population size in patches both in field studies and simulation models [44], [47]." Importance of landscape context.

[38] Changes in demographic rates due to Hfrag, in addition to population sizes and extinctions.

[26] 70 per cent of remaining forest within 1km of forest edges. Fragmentation effects. Smallest and most isolated patches most vulnerable. Reduce biodiversity by 13 to 75 per cent (metrics?) and reduce biomass, affecting ecosystem functions.

[71] Testing different HL scenarios on neutral and non-neutral communities. Habitat alteration reduces average level of specialisation - 'functional homogenisation'.

[1] Communities are more repeatable (similar between repeats) for high immigration rates. Use IBM model. Immigration from regional species pool. Zero sum natural theory dynamics.

[28] SAR updated to account for habitat fragmentation i.e. habitat loss that is not contiguous. Very relevant for discussion somewhere.

[24] spatial competition.

[17] food web plasticity, stabilising and predictable.

---

<sup>1</sup>Nice structure here - theoretical results, followed up a few years later by experimental study. Talk about this somewhere.

## 5.4 Motivation

In chapter ?? we saw that no species go extinct, even at extreme levels of habitat destruction ( $HL = 90\%$ ), when using the default parameter set (see table ??). Motivated by [74], this allowed us to explore community responses to habitat loss that are not associated with, or may precede, the loss of species. The lack of extinctions produced by the model were shown to be due to a rescue effect from immigration. Even species which go locally extinct from the landscape may be replaced by this immigration.

The simulations presented so far represent *open* communities with a strong influx of individuals belonging to all species.

the default immigration rate (IR), as given in the default parameter values is relatively high, corresponding to an open community. In particular, at the IR, we expect no extinction of species

This behaviour (control for species richness). However for such a heavily impacted community to not exhibit local extinctions would be unusual in nature [REF]. This may be considered an edge case - an open ecosystem with a strong influx of individuals from all species. Although the local habitat may be very close to total destruction the community is sustained by strong immigration from surrounding habitats. In reality such a strong and uniform rescue effect from immigration is unlikely due to spatial auto-correlation, differential dispersal rates and other effects (see discussion in section ??[references - York pollinator study]).

- propagule rain
- Require a uniform species pool to be maintained (trad IBT  $\rightarrow$  continent), or heterogeneity at landscape level [REF]

In this chapter we further investigate the impacts of habitat loss (HL) on multi-species communities with different proportions of mutualistic and antagonistic interactions (MAI ratios). We now consider other realistic scenarios by varying the immigration rate parameter. At one extreme we have the above scenario of high immigration, where extinction is prevented. At the other extreme we have closed communities with zero immigration. In this case there is no rescue effect from surrounding habitats, and we may expect to see extinctions in response to habitat loss. Although a totally closed system does not exist in nature certain systems may come close to this ideal. For example an island community that is a sufficiently distant from other land (see discussion on Island bio-geography theory in section ??) will have very low immigration rates, and systems that are effectively closed may be artificially achieved in controlled situations (e.g. laboratory mesocosm). Although extremely open and extremely closed systems are possible, most real-world communities lie within these two extremes. By changing immigration rates, the approach followed here

allow us to explore the entire range of possible responses<sup>2</sup> of biological communities to habitat loss.

For the default parameter values (see table ??) zero IR results in the inevitable extinction of all non-plant species, in our simulated communities. We will refer to this scenario as *community collapse*. Even for pristine habitats (0% HL) we do not see stable and persistent communities without some non-zero IR (some increase in persistence with MAI ratio - see chapter ??). This result is demonstrated in chapter ??, where we explore factors contributing to stability. For now we accept the general result that, with the default parameters, zero IR results in community collapse<sup>3</sup>. In this chapter we are interested in the regime between these two extremes of zero IR, where we see many extinctions even at 0%HL, and high IR where we see no extinctions even at 90%HL. We are particularly interested in finding IRs for which communities are stable at low levels of HL, but where collapse is initiated as HL is increased. This is a scenario that we see in real-world communities. We are also interested in how community composition and stability vary with HL and IR, and how this is mediated by MAI ratio. (And interaction strength distributions.)

---

<sup>2</sup>Not sure about this..

<sup>3</sup>weaken this statement, parameter dependent, or at least refer forwards again to next chapter

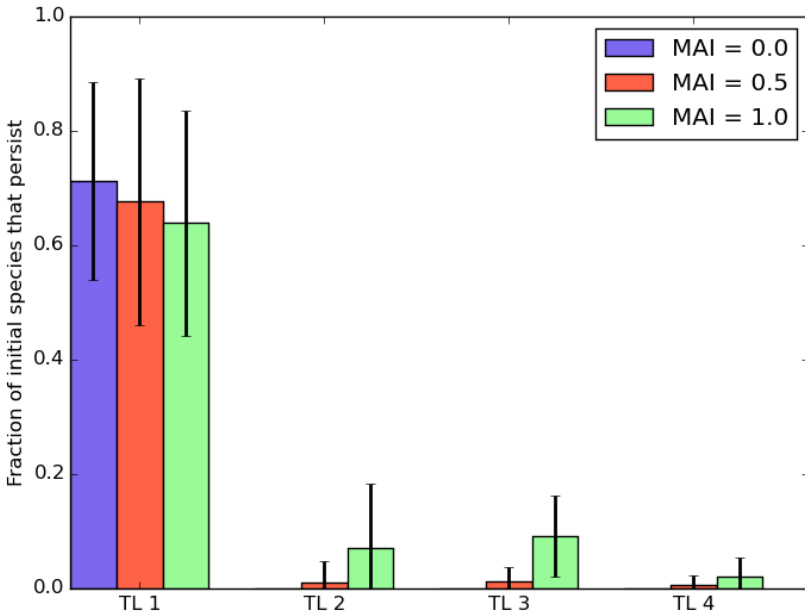


Figure 5.1: Fractional persistence by trophic level for three different MAI ratios. Fractional persistence is measured by the fraction of species initially belonging to a trophic level which have not gone extinct by the end of a simulation (5000 iterations). The solid bars give the mean value, taken from 22 repeat simulations. Error bars show  $\pm$  one standard deviation. (Simulations from chapter ??)

## 5.5 Exploration of parameter space: habitat loss and immigration

Motivated by the above we explore a two dimensional slice of parameter space. The immigration rate (IR) and the level of habitat destruction (HL) are varied and one hundred repeat simulations are conducted at each pair value. Therefore we are able to estimate how the simulated communities are expected to behave across this region of parameter space, by averaging over the repeats. These simulations are run for three different MAI ratios: 0.0, 0.5 and 1.0. As in previous simulations each repeat uses a different interaction network topology, generated with the procedure described in section ???. All other parameters are held constant at their default values (table ??), including the number of iterations which remains at 5000.

In order to speed up the simulations certain metrics used in the previous analysis (chapter ??) are not calculated. Particularly the spatial stability metrics are computationally expensive. Only two pieces of information are saved as output from these simulations: the underlying network structure and the abundance time-series for each species. The abun-

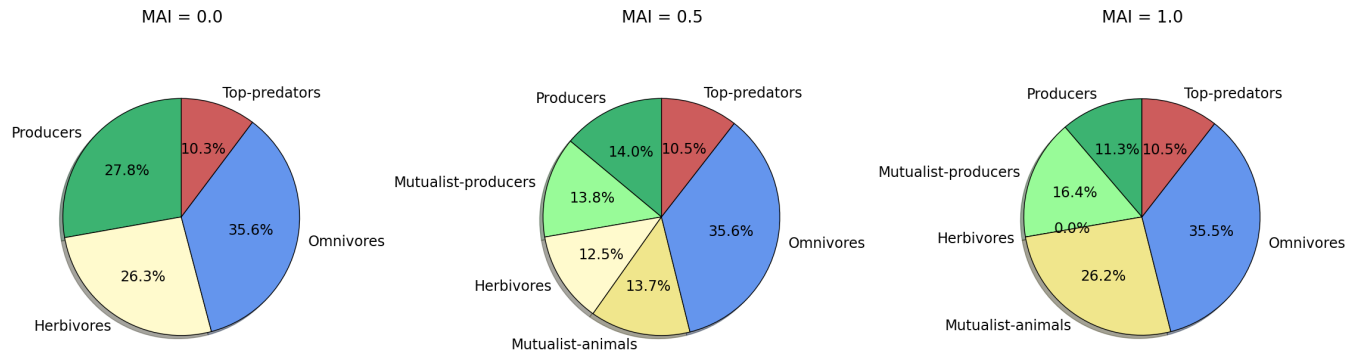


Figure 5.2: Mean number of species belonging to each functional group for the three MAI ratios in consideration (0.0, 0.5, 1.0). The results are averaged over one thousand simulations with the given MAI ratio, selected from the total ensemble of simulations that were run for this chapter (and used to generate e.g. fig 5.11). The species numbers depicted are independent of all simulation parameters, other than those that define the interaction network. That is the average number of species in each function group depends on the niche model parameters (connection and number of species), the MAI ratio, and the trophic constraints that we impose.

dance time-series is simply a record of the abundance of each species at every simulation iteration. (What do we calculate from these and why..) By limiting the simulation output the scope for analysis is restricted but the parameter space can be explored in more detail (higher resolution, greater number of repeats)<sup>4</sup>. This ‘first pass’ scan of the parameter space allows us to construct a general picture of how the model behaves in this region. It may also be used to identify subsets of the region of parameter space on which to focus further computational effort for e.g. spatial analysis.

The entire range of habitat destruction is explored from pristine landscape (0%HL) to near total destruction (90%HL) in steps of 10%. In the current chapter all habitat is destroyed using the contiguous algorithm since it was decided that this is more realistic (see discussion in section ??). Ranges for the IR were chosen based on previous simulations. Since  $IR = 0.005$  is sufficiently high to prevent any extinctions, this was taken as the maximum of the range. Simulations using  $IR = 0$  have already determined that this leads to community collapse, therefore these were not repeated. A value of  $IR = 0.0001$  was heuristically selected as the lower bound, at which some non-zero extinction is expected in pristine habitat for all MAI ratios<sup>5</sup>.

<sup>4</sup>The changes to the model output reduced run times by up to a factor of 10. This required changes in how the interaction network is represented and therefore previously used network metrics could not be calculated. However it would be easy to modify the code to save some information on interaction frequencies and spatial states, which could be used in later analysis. This has not been done yet -ON THE WAY.

<sup>5</sup>Dani thinks we should maybe look at lower IR values.

## 5.5. EXPLORATION OF PARAMETER SPACE: HABITAT LOSS AND IMMIGRATION

---

The choice of MAI ratios allows us to compare purely antagonistic ( $MAI = 0.0$ ), mixed ( $MAI = 0.5$ ) and purely mutualistic ( $MAI = 1.0$ ) communities. Figure 5.2 shows the expected fraction of species belonging to each of the six functional groups in the interaction networks for these communities. The constraints we place upon the niche model are that at least 25%, 25% and 5% belong to the first, second and fourth trophic levels respectively. In particular it is known that the unconstrained niche model struggles to generate realistic number of species in the second trophic level [REF]. The figure shows that the interaction networks meet these constraints and that, as expected, the largest number of species is found in the third trophic level<sup>6</sup> i.e. the functional group labelled *omnivores*. Antagonistic communities are missing the two mutualist functional groups from the first two trophic levels, whereas the mixed communities have a roughly 50 : 50 split between mutualists and non-mutualists as expected (this split is not exact because it is links that are switched no species). Importantly although the purely mutualistic communities contain no herbivores (as all their links to plants have been switched), they do contain non-mutualist plants. These plants are those that share no interactions with the first trophic level<sup>7</sup>, therefore the link replacement procedure does not give them any mutualist partners. These plants remain wind dispersed and are predated upon by animals from trophic levels three and four<sup>8</sup>.

---

<sup>6</sup>Perhaps these constraints should be changed in future simulations - discuss with Daniel. - he thinks OK. Suggests look at RADS with colouring by TL. REQUIRES LOOKING AT SINGLE NETWORK.

<sup>7</sup>Is this realistic - Daniel? - RESTSAE QUESTION: REALISTIC THAT PLANTS ARE NOT EATEN BY FIRST TROPHIC LEVEL..

<sup>8</sup>Should there be a constraint that top predators do not consume plants? Not in original niche model. (Dani says no. Re-run. Does it make a difference?)

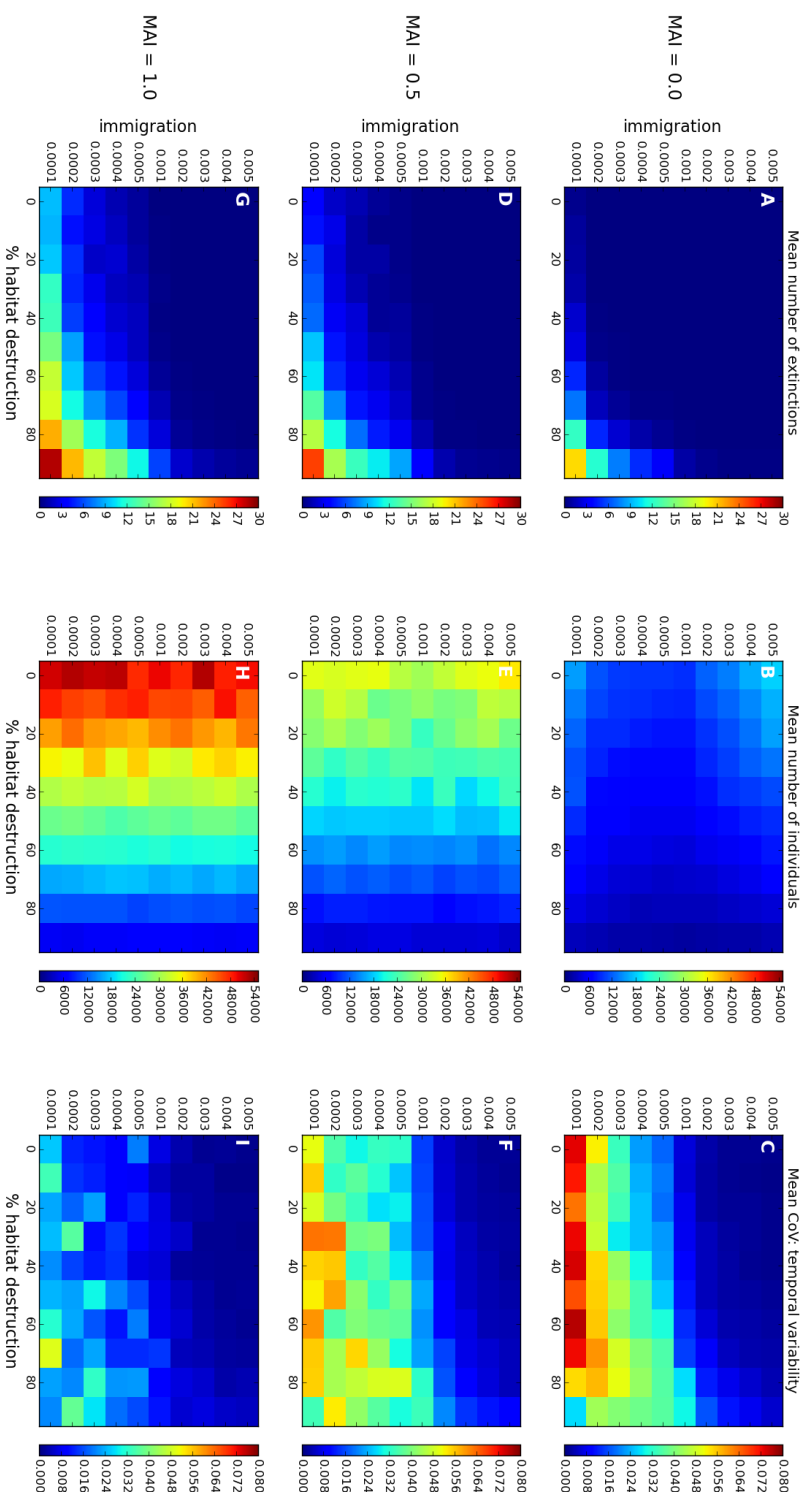


**Figure 5.3: Summary heat maps:** Each heat map shows the value of a certain response metric across a 2-dimensional slice of parameter space. The parameters varied are immigration rate  $IR$  (y-axis) and percentage habitat destruction  $HL$  (x-axis). Each row of plots corresponds to a different MAI ratio as labelled. To construct the heatmaps one hundred repeat simulations were run for each combination of parameter values, with each simulation using a different underlying network. The mean value of the response metrics is taken over the hundred repeats. Therefore each pixel shows an estimate of the expectation value of the metric at those parameter values. The left column shows the expected number of species that are extinct at the end of a simulation; the central column shows the expected biomass (total number of individuals) at the end of a simulation; and the right column shows the expected temporal variability (coefficient of variation of total biomass) of the dynamics during the final thousand iterations of a simulation. The latter is used as a proxy for stability (see text).

### 5.5.1 Summary heat-maps

The results of these simulations can be concisely represented as heat maps over the region of parameter space explored. Figure 5.11 shows how the expected value of three summary metrics varies across this space: the number of extinct species, community biomass (total number of individuals) and temporal variability in community biomass. The response of each of these metrics is discussed individually below. The latter is used as a proxy for stability and is measured by the coefficient of variation (CoV) of the community biomass about its mean during the final thousand iterations of a simulation. (later..) This metric is often used to assess dynamic stability, but should not be confused with rigorous mathematical metrics relating to the stability of the equilibrium state of the system [REF]. It should be noted that the other two metrics, and all abundance measures in the following analysis, are calculated from a snapshot of the system state on the final iteration of a simulation. (Dani points out that average over replicates.., compare with averaged analysis, and discuss in context of steady state.)

#### Extinctions

No species extinctions are expected for sufficiently high levels of IR, across the whole range of HL values and for all MAI ratios. This results is visible in the left column of figure 5.11 and was already discussed in section ???. It is found that reducing the IR leads to an increasing number of extinctions. At low IR extinctions are possible, even in pristine landscape. This fits the previous observation that zero IR always leads to community collapse.

Increasing HL generally increases the number of expected extinctions. However nowhere in the parameter space do we see community collapse. In the most extreme case of low IR and high HL ( $MAI = 1.0, HL = 90, IR = 0.0001$ ) an average of close to thirty extinctions may be expected. Although this expected loss of half of the species is fairly catastrophic, it does not guarantee total collapse of the community. The trophic constraints imposed in the food-web generation procedure ensure that at least 25% of species belong in the first (basal) trophic level (figure 5.2). In practice this very rarely (quantify) reaches above 30%. Therefore a loss of thirty species suggests that at least 40% of the remaining species are non-basal<sup>9</sup>. In other words, despite significant loss of species, there is some persistence in higher trophic levels.

For all three MAI ratios there exists an IR where the expected number of extinctions is zero in pristine landscape, but increases with HL. So although the immigration rescue effect prevents total community collapse, we do have a situation where HL can initiate species

---

<sup>9</sup>If all thirty species lost are non-basal we are left with 3/5 basal species to 2/5 non-basal. IN NATURE HIGHER TROPHIC LEVELS USUALLY MORE VULNERABLE [REF]. IS THIS THE CASE. OOO, COMMUNITY COLLAPSE.

extinctions. The IR at which extinctions are initiated is increased by increasing the MAI ratio. This effect of MAI ratio on extinctions is general. On average we expect a greater number of extinctions for high MAI (1.0) than for low MAI ratio (0.0), all else being equal. At the lowest IR and with pristine habitat we may expect about one extinction with a MAI ratio of 0.0, compared to about ten extinctions with a MAI ratio of 1.0. This can possibly be explained by looking at the second column in figure 5.11. On average a higher MAI ratio lead to a greater total number of individuals at the end of a simulation<sup>10</sup>. This means that there are fewer empty landscape cells into which an individual may immigrate at random. This reduces the *effective immigration rate* and so weakens the rescue effect. Any very rare species, only made viable by immigration, will be the ones hit by this and are likely to go extinct<sup>11</sup>.

### Community biomass

There are strong trends in expected community biomass. Increasing HL has a negative effect on community biomass. This is intuitive and has been seen before. Also previously discussed (chapter ??) is the result that, on average, communities with higher MAI ratio can support a greater biomass. However this effect is striking in these results, especially at low levels of HL. In a pristine habitat with an IR of 0.005, the expected number of individuals for a community with  $MAI = 0.0$  is around 20,000, compared to around 50,000 for a community with  $MAI = 1.0$ . In fact, across the parameter space, purely mutualistic communities have around twice the biomass of purely antagonistic ones. Therefore in some sense mutualism appears to be ‘better’ for the community. (Dani: although having more individuals means rescue effect less likely, and perhaps increase competition for space) In section ?? we discuss whether it is better for the community as a whole, or only for those species that engage in mutualistic interactions.

For antagonistic communities ( $MAI = 0.0$ ) the biomass is dependent on IR. Both very high and very low IRs support high biomass, whereas intermediate IRs support less (central panel, top row, figure 5.11). The effect of high IR is intuitive - births due to high immigration supplement births due to reproduction in the local community. This supplementary effect is greater at higer IR. However the increase in biomass at very low IR is harder to explain. We know that at zero IR all non-plant species go extinct [REF CHPAT/SEC]. So we may expect

---

<sup>10</sup>Mechanism behind this? - From the Theoretical Ecology paper: "communities with larger MAI ratios hosted a larger number of individuals ( $F(1273) = 98.69, p < 0.001$ ) (Fig. 4). In spite of a decline in the abundance of non-mutualistic primary producers and herbivores with increasing MAI ratios (as expected due to a larger fraction of mutualistic species), the increase in mutualistic plants and animals overcompensated for this loss, causing an overall increase in abundance. This overcompensation was due to mutualistic plants becoming more abundant than non-mutualistic ones since mutualistic consumers do not consume as much resources from them and are, additionally, beneficial for their reproduction.

<sup>11</sup>To determine if this is what is happening need to look at total abundances?

that in the region of low IR non-plant species become increasingly rare<sup>12</sup>. In an antagonistic community this means a reduction in the number of herbivores and omnivores, which will benefit plant species. Therefore we may propose that the increase in the biomass at low IR is accounted for by an increased abundance of plants<sup>13</sup>. This reasoning suggests that we should expect a difference in composition between the abundant antagonistic communities seen at low and high IR (see section ?? - ABUNDANCE DISTS.).

Mutualism removes the dependence of community biomass on IR. Although the total biomass does not vary with IR for these communities ( $MAI = 0.5, 1.0$ ) there may be changes in community composition. For example it is still reasonable to suspect that non-plant species become increasingly rare at low IR. However in a mutualistic community this has a different effect. It will benefit those plants that still have antagonistic interactions, but it will be detrimental to mutualist plants since they will be less likely to interact with a partner and therefore less likely to reproduce. So we may expect a shift in the relative abundances of the two functional groups of plants in favour of the antagonists at low IR (see section 5.5.3).

### Temporal variation

In general increasing HL increases the temporal variability of the dynamics. That is, communities are less stable in damaged landscapes. This result is only seen in the case of contiguous habitat destruction, as opposed to random destruction, and is discussed in more detail in section ?? where it was shown to be associated with changes in the distribution of interaction strengths. Also communities are less stable at lower IR. This fits with previous results. It has been shown that communities are very stable and resistant to HL at high IR (section ??). It has also been shown that they are unstable at zero IR, exhibiting community collapse (section ??). This suggests that the model has a stable and an unstable regime, and that there must be a transition between the two when moving from high to low IR. The right-hand column of figure 5.11 shows a signature of this. Interestingly the loss of dynamic stability is greatest for antagonistic communities and weakest for purely mutualistic communities. This suggests that mutualism has a stabilising effect on community dynamics. It appears to confer better dynamic stability in the face of HL and changing IR (but there are also more extinctions as discussed..).

Another interesting feature of the CoV plots is that the trends described above appear to be broken at very low IR and high HL, where an increase in stability is visible. One potential mechanism is that this is an averaging effect. If some communities are totally collapsing in this region they would exhibit stable dominance of plant species, which would

---

<sup>12</sup>This can be checked later.

<sup>13</sup>This proposed mechanism may be working in reverse in the  $MAI=1.0$  communities.

contribute positively to average community stability. However it may be that this effect is due to another mechanism.

As mentioned previously the loss of dynamic stability is troubling since it calls into question the way that we calculate abundance metrics. Therefore the conclusions drawn in the following discussion may not be general and may not hold if the metrics were averaged over a number of iterations.(Dani: don't stress this here, put in limitations section.)

### 5.5.2 Example dynamics

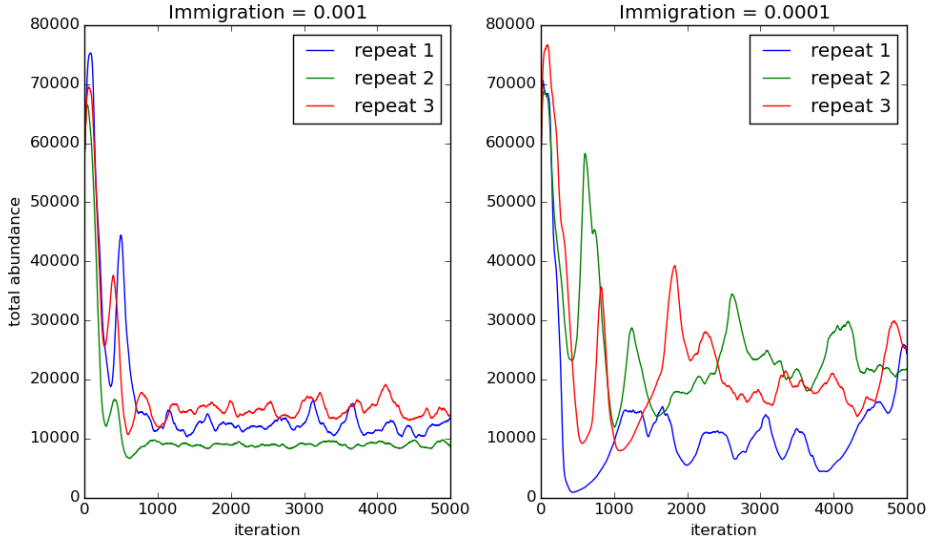


Figure 5.4: Temporal dynamics of the total biomass of communities over the course of six simulations. Each panels shows the dynamics for three distinct simulations, each in a different colour. The left panels shows communities with a high immigration rate, and the right panel for a low immigration rate. In all cases there is no habitat destruction  $HL = 0$ .

Figure 5.4 illustrates the loss of stability in passing from a high to a low IR regime. This transition was proposed in section ???. The dynamics of three example antagonistic communities are depicted for each regime. These communities were selected at random from the one hundred repeat simulations at these parameter values. Antagonistic communities are shown because the increase in temporal variability is greater for these than for those with mutualism (see figure 5.11).

In the high IR regime, shown in the left-hand panel of figure 5.4, we see that the total biomass of each community undergoes an initial transience followed by a period of relative stability. It appears that, during this second period, the system is undergoing stochastic fluctuations about its stable equilibrium<sup>14</sup>. In the low IR regime, shown in the right-hand panel, we see that the community biomass exhibits large scale fluctuations throughout the course of the simulations. It is not clear from inspection that the system is being perturbed about a stable equilibrium.<sup>15</sup> It may be that the reduction in IR increases the length of the initial transience, and that the communities illustrated are yet to reach steady-state after 5000 iterations. Or it may be that these communities reach their steady-state, but that the

<sup>14</sup>Test for this?

<sup>15</sup>I would rephrase this. For example: there are different explanations for this pattern: (i) Explanation 1, (ii) Explanation 2.

stochastic fluctuations are amplified because the equilibria are less stable<sup>16</sup>.

Figure 5.5 shows example dynamics by trophic level of four antagonistic communities in the high and low IR regimes. The left-hand panels depict two communities in the high IR regime. Again the initial transience is followed by a period of relative stability, which is consistent across trophic levels. It is clear from these two plots that the positions of the system's equilibria and the size of the fluctuations about it vary between simulations.

The right-hand panel of figure 5.5 depicts two communities in the high IR regime. It is clear from inspection that the mean and the variance of the biomasses varies between trophic level, and between simulation. The lower plot shows dynamics dominated by species from the first trophic level, with large scale but decreasing amplitude fluctuations in the second trophic level. The upper plot shows perhaps even less stable dynamics with increasing amplitude fluctuations in the first and fourth trophic levels, and very low abundances in the intermediate trophic levels. In both simulations there are several instances where the biomass of an entire trophic level comes close to zero. However, as figure 5.11 shows, we should only expect around one extinct species at the end of a simulation at this IR. It must be that that immigration is preventing stochastic extinctions here<sup>17</sup>, by providing some buffering to populations at the low end of their biomass fluctuations and by rescuing those species that do go extinct<sup>18</sup>.

The breakdown of dynamics by trophic level demonstrates that the timing of measurement will affect the calculation of relative abundance metrics, and not just that of the aggregate community biomass. If the fluctuation in trophic biomass were more synchronous between levels, the timing of the measurement would be less significant. However the figure shows that even the ordering of trophic levels by abundance is dependent on time<sup>19</sup>. Therefore further analysis should attempt to remove this time dependence by averaging biomasses over a number of iterations. The plots suggest that the increase in community biomass at low IR (discussed in section ??) may be a genuine effect. However it is hard to determine the contribution of the increased fluctuations without averaging the abundances over time.

(There may be other points in parameter space where it would be informative to plot the dynamics...e.g. high mutualism region, temporally stable) (Could plot biomass dynamics, averaged over replicates?)

---

<sup>16</sup>Further mathematical analysis to try and determine this? - Final chapter on model fitting?

<sup>17</sup>At this IR we would expect on average four immigrations per iteration, if the landscape were empty.

<sup>18</sup>It would be interesting to look at the breakdown of these trophic dynamics by species - e.g. how synchronous are the different species in the same trophic level with each other.

<sup>19</sup>This is beginning to look make the results seem invalid.

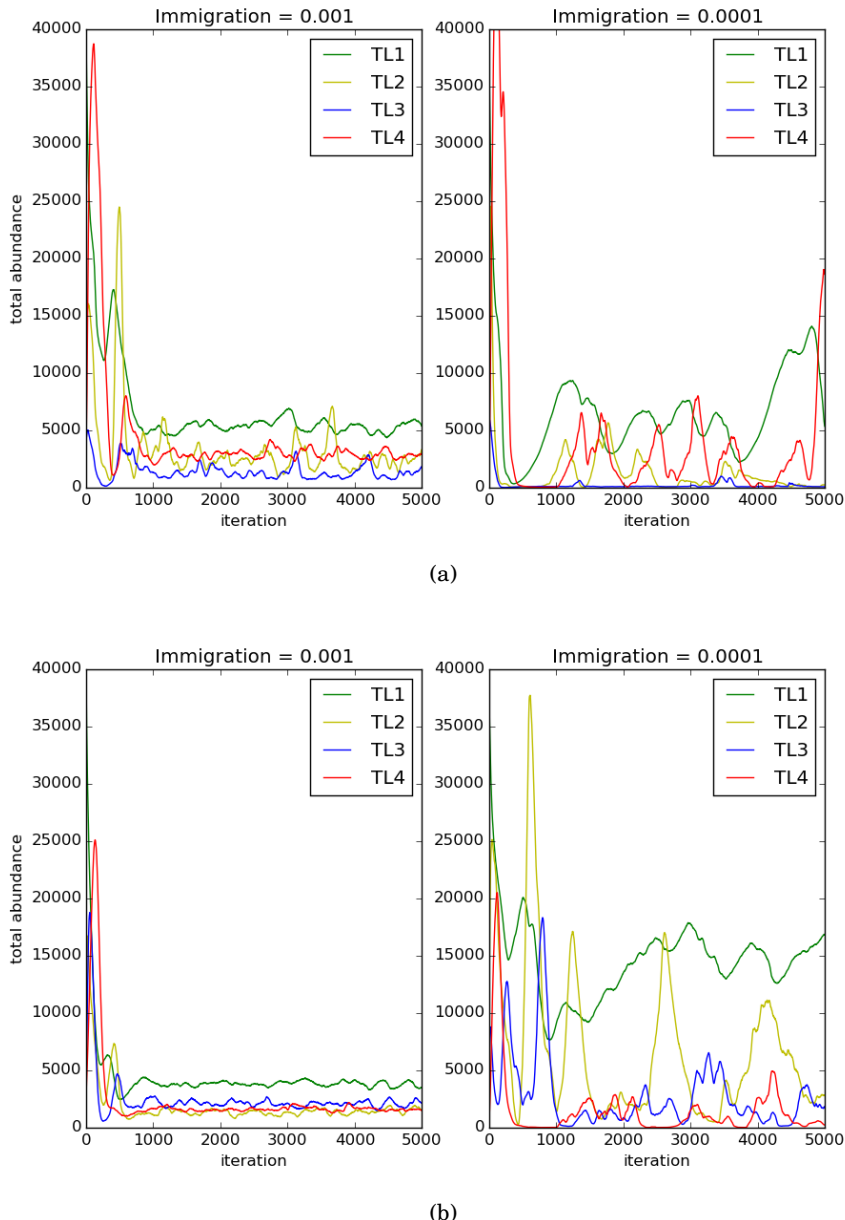


Figure 5.5: Dynamics from four individual simulation runs, with biomasses aggregated by trophic level. Each panel represents the dynamics of a single simulation run. In all cases the MAI ratio is 0.0, and there is **no habitat destruction** ( $HL = 0$ ). The coloured lines represent the temporal dynamics of the biomass of each trophic level, as indicated in the legends. Two immigration scenarios are presented. **Left column: high immigration. Right column: low immigration.**

### 5.5.3 Relative abundances and abundance distributions

Contextualise - begin this section with the points made above that suggest useful to look at RADS.

Figure 5.6 shows the mean relative abundance of each trophic level for antagonistic and mutualistic communities, across the parameter space. For purely antagonistic communities the proportion of individuals in each trophic level varies strongly with IR and weakly with HL. At low IR antagonistic communities become dominated by plant species. This is in agreement with the mechanism proposed in section ??, whereby plants benefit from a scarcity of animal consumers at low IR. At high IR the distribution of biomass is much more even across trophic levels. In this region of parameter space the biomass of trophic levels one and four are roughly equal at around 30%, with the remaining 40% of the biomass split fairly evenly between trophic levels two and three. This biomass distribution is not necessarily unrealistic for a community in nature, however it does not conform to the classic *biomass pyramid* (see discussion in section ??). In fact the distribution at low IR is much closer to the standard pyramid.

Mutualistic communities ( $MAI=1.0$ ) show much less variation in their trophic composition across the parameter space. The first two trophic levels are most abundant, with slightly more biomass in the first trophic level than the second. The third and the fourth trophic levels are much less abundant with around 20 – 30% of the biomass split fairly evenly between them. This distribution is remarkably constant over the parameter space. Only at extreme levels of disturbance ( $IR = 0.0001, HL \geq 70\%$ ) do the communities begin to be dominated by plants.

Figure 5.7 shows the mean relative abundance of each functional group for mutualistic communities with  $MAI = 0.5$  and  $MAI = 1.0$ . As expected purely mutualistic communities are dominated by functional groups two and four (mutualistic producer and animals) across the whole region of parameter space. Functional groups five and six do relatively better at high IR and low HL. Whereas at low IR and high HL the relative abundance functional group 1 increases significantly. This is an indication of the shift in favour of antagonists, suggested in section ??, due to the low biomass making it hard for mutualists to reproduce and less likely that plants will be eaten. The same patterns are seen in the case of  $MAI = 0.5$ , however the trends appear stronger since the relative abundances are less robust to changes in IR and HL.

### 5.5.4 Rank abundance distributions

These results, as with the other should be recalculated using averaged metrics.

Figure 5.9 shows the mean rank abundance distributions for a range of IR and HL values. Communities with all three MAI ratios are shown in different colours. Across the parame-

ter space mutualistic communities (blue) have less even distributions than antagonistic communities. This difference is more pronounced at low IR and high HL.

An interesting feature of the RADs is that some of them display an apparent discontinuity in the distribution. This is perhaps most pronounced in the bottom left panel of figure 5.9 ( $IM = 0.0001, HL = 0, MAI = 1.0$ ). A sigmoidal shape is a feature of log-normal abundance distributions and is often observed in natural communities [REF]. However this extreme case does not appear to fit. What is driving this distribution? The ‘flat’ section of low abundance species could be those species whose presence is sustained only by continuous immigration and which are therefore present in roughly equal abundances?

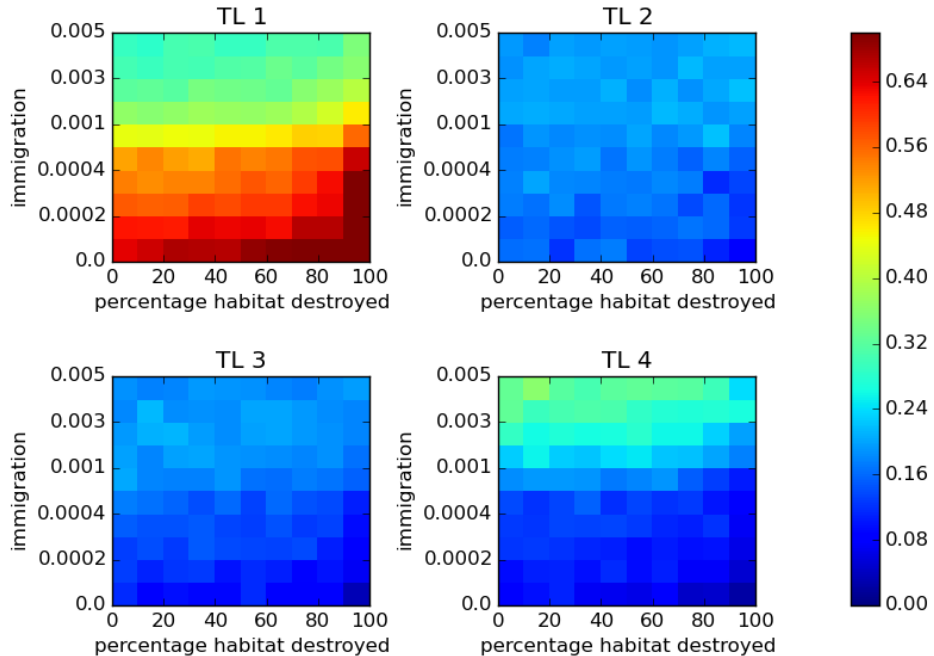
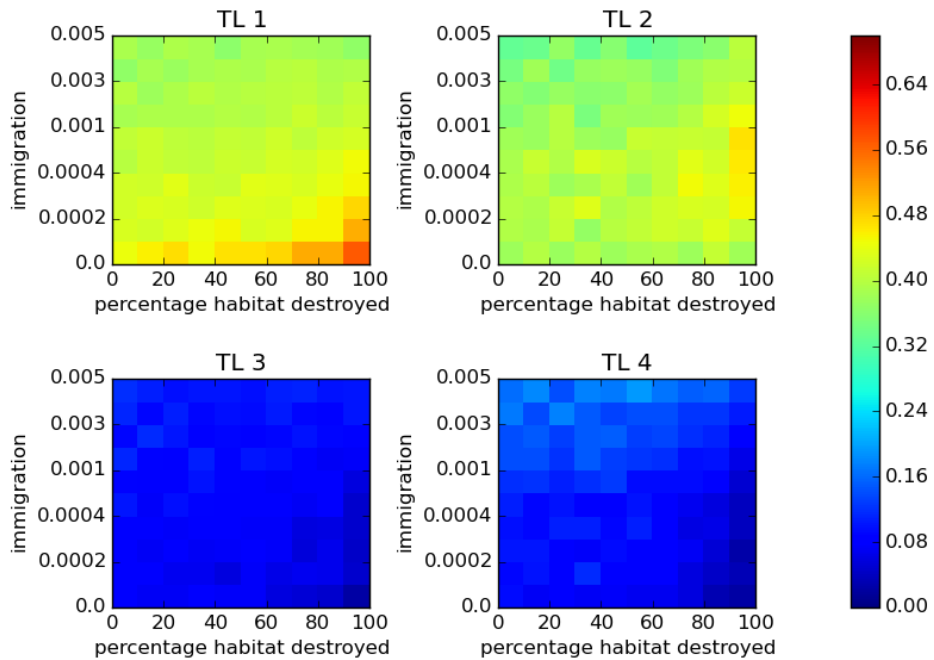
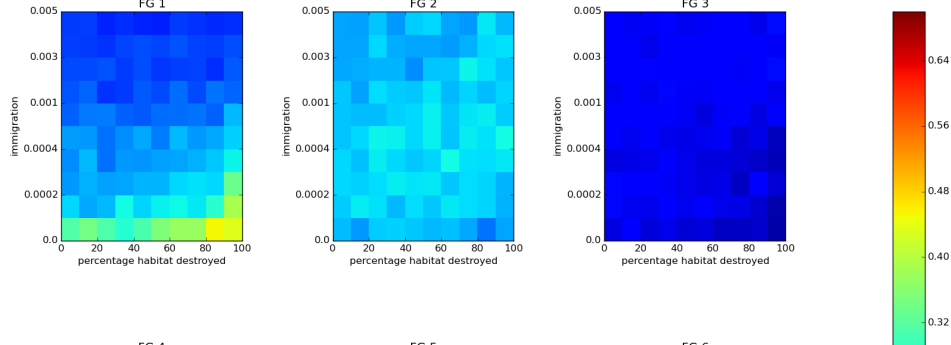
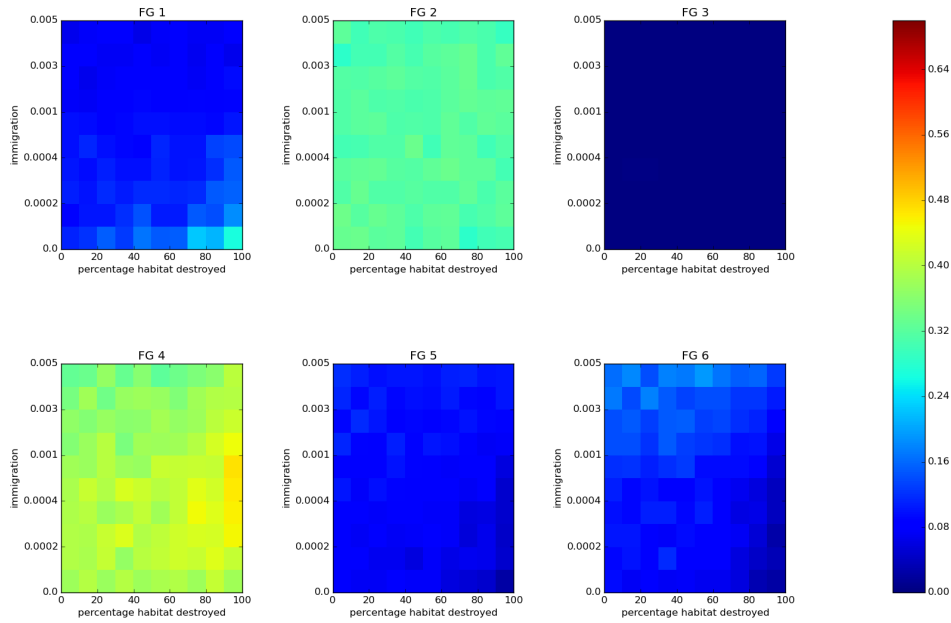

 (a)  $MAI = 0.0$ 

 (b)  $MAI = 1.0$ 

Figure 5.6: The relative abundance of species belonging to each of the four trophic levels. Above:  $MAI = 0.0$ . Below:  $MAI = 1.0$ . Each pixel on the heat maps corresponds to an average over one hundred repeat simulations at those parameter values. The abundances are measured at the end of each simulation.

## 5.5. EXPLORATION OF PARAMETER SPACE: HABITAT LOSS AND IMMIGRATION



(a)  $MAI = 0.5$



(b)  $MAI = 1.0$

Figure 5.7: The relative abundance of species belonging to each of the six functional groups. Above:  $MAI = 0.5$ . Below:  $MAI = 1.0$ . Each pixel on the heat maps corresponds to an average over one hundred repeat simulations at those parameter values. The abundances are measured at the end of each simulation.

## 5.6 Points for discussion (Rough Notes)

A comparison of the relative merits of being a mutualist versus a non-mutualist is worthwhile. Importantly it must be remembered that mutualistic interactions are also trophic interactions. In our case, energy is transferred from producer to animal. In nature for example the bee receives energy from the nectar, but also carries pollen to fertilise other flowers. So there is some loss/detriment to the producer as well as the benefit of reproduction (These mechanisms are in place in the model through the bioenergetic parameters. Traditionally, simulating mutualistic communities has failed because the simulations ended in an 'orgy of mutual benefaction'). It is an interesting strategy from an evolutionary perspective...discuss this (with relation to link switching)?

In the model species become mutualistic by having at least one of their links, in the antagonistic interaction network, switched for a mutualistic link. Table ?? shows the default parameter values used for most simulations. Lets consider the potential benefit of switching a single herbivorous link for a mutualistic link, for either party. If the plant is a non-mutualist it must impart 20% of its energy to the offspring when reproducing (this happens with a probability of 0.01 on each iteration). It is also subject to lose 70% when it is encountered by this herbivore. If it were to switch this herbivorous link for a mutualistic link it would only lose 25% of its energy in the interaction, and it would pass on a seed that is almost guaranteed<sup>20</sup> to generate an offspring. Therefore the cost of reproducing is slightly increased for a mutualist, but the cost of interacting with an individual from the trophic level above is dramatically reduced. There is an additional benefit that the mutualistic reproduction can occur over a greater distance. The net gain loss of this change depends on the probability/rate of interactions. We should investigate this, however the results suggest that being a mutualist is of significant benefit to plants. (These mechanisms are in place in the model through the bioenergetic parameters. Traditionally, simulating mutualistic communities has failed because the simulations ended in an 'orgy of mutual benefaction')

Question: in the above analysis are mutualistic plants are relatively more abundant than non-mutualistic ones, except in the case of high habitat loss or low immigration (when there are few enough mutualistic partners that interactions become infrequent?)

For animals there is no cost to carrying and spawning the seed of their mutualistic partners. The only change in the switching of mutualistic links is the amount of energy that they receive from the interaction. During a herbivorous interaction, the herbivore takes 70% of the plant's energy, and assimilates it with an efficiency of 80%. Therefore it obtains 60% of the plant's energy. During a mutualistic interaction the animal-mutualist takes and

---

<sup>20</sup>Really? We could look at how many mutualistic interactions lead to a new individual. It would only not occur in very crowded situations.

assimilates 25% of the plants energy. Therefore on an interaction by interaction basis there is a negative trade off for an animal in switching its link to mutualistic. However there may be an emergent benefit in that this type of interaction is much better for plants, therefore increasing the plant biomass and therefore indirectly benefiting animal (mutualists and non-mutualists?) due to the increased frequency of interactions (density of plants).

Mutualism in general stabilises dynamics, and leads to communities with more realistic biomass pyramids - i.e. dominated by the first two trophic levels, with fewer individuals in TL2/3.

It could be argued that the RADS are realistic, and the some immigration is a requirement to prevent stochastic extinction of the very rare species, which are found in nature. This begs the question as to what mechanism prevents their extinction in nature? And are they the most vulnerable to extinction?

## 5.7 Habitat loss with low immigration

## 5.8 Questions for Alan or Daniel

- Worried about general flow and structure of discussion. Feels like trying to present too much information all at once. How to not turn into a list of facts, where the relevance gets lost?
- Since the dynamics do not necessarily reach steady state should I re-do analysis with average over a time window? (We need a discussion section where the results are discussed in the context of current literature in the field, real-world communities, etc. Also, contextualizing (see a previous comment) is important so the reader does not feel like we include all these metrics because we can. For doing this it is always helpful to write down the main findings as bullet points and develop them; also, the limitations of the model should be presented here as well as the ways forward)
- Can I use "we"??
- Tense?
- Figure 1.1 summary heatmaps: too much information in one figure? (feels that way from discussion).
- OK to use plant, basal and producer interchangeably?
- The ability of the top predator to survive almost entirely on plant matter is troubling.
- Is it in fact OK to use biomass and number of individuals interchangeably? (We need a discussion section where the results are discussed in the context of current literature in the field, real-world communities, etc. Also, contextualizing (see a previous comment)

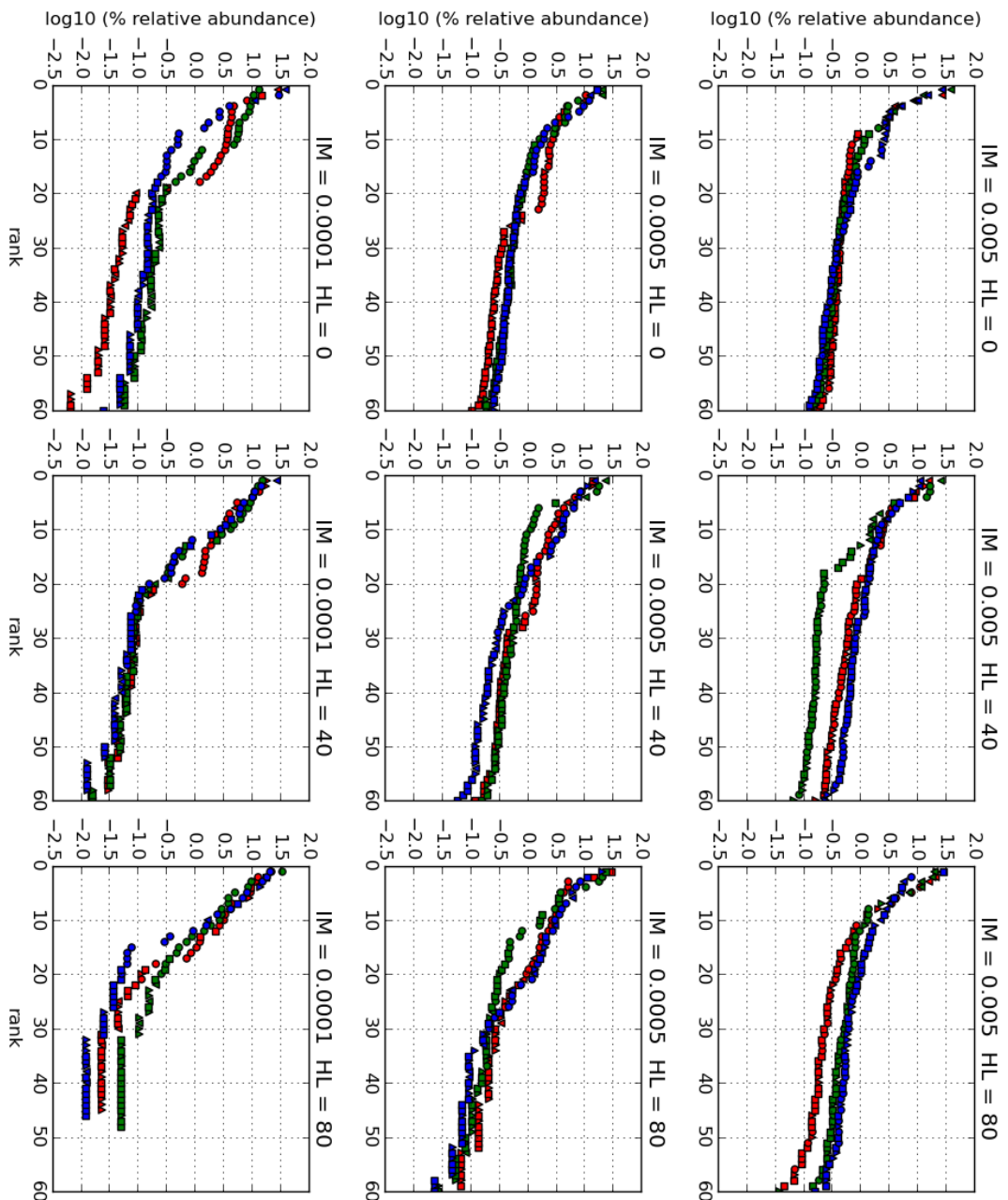


**Figure 5: Rank abundance distributions** for individual simulation runs, for nine different pair values of immigration rate and habitat destruction. Each distribution is for a single community at the end of an individual simulation run. The different colours correspond to different MAI ratios: red = 0.0; green = 0.5; blue = 1.0. And the different symbols correspond to different trophic levels: circle = 0; upwards triangle = 1; square = 2; downwards triangle = 3.

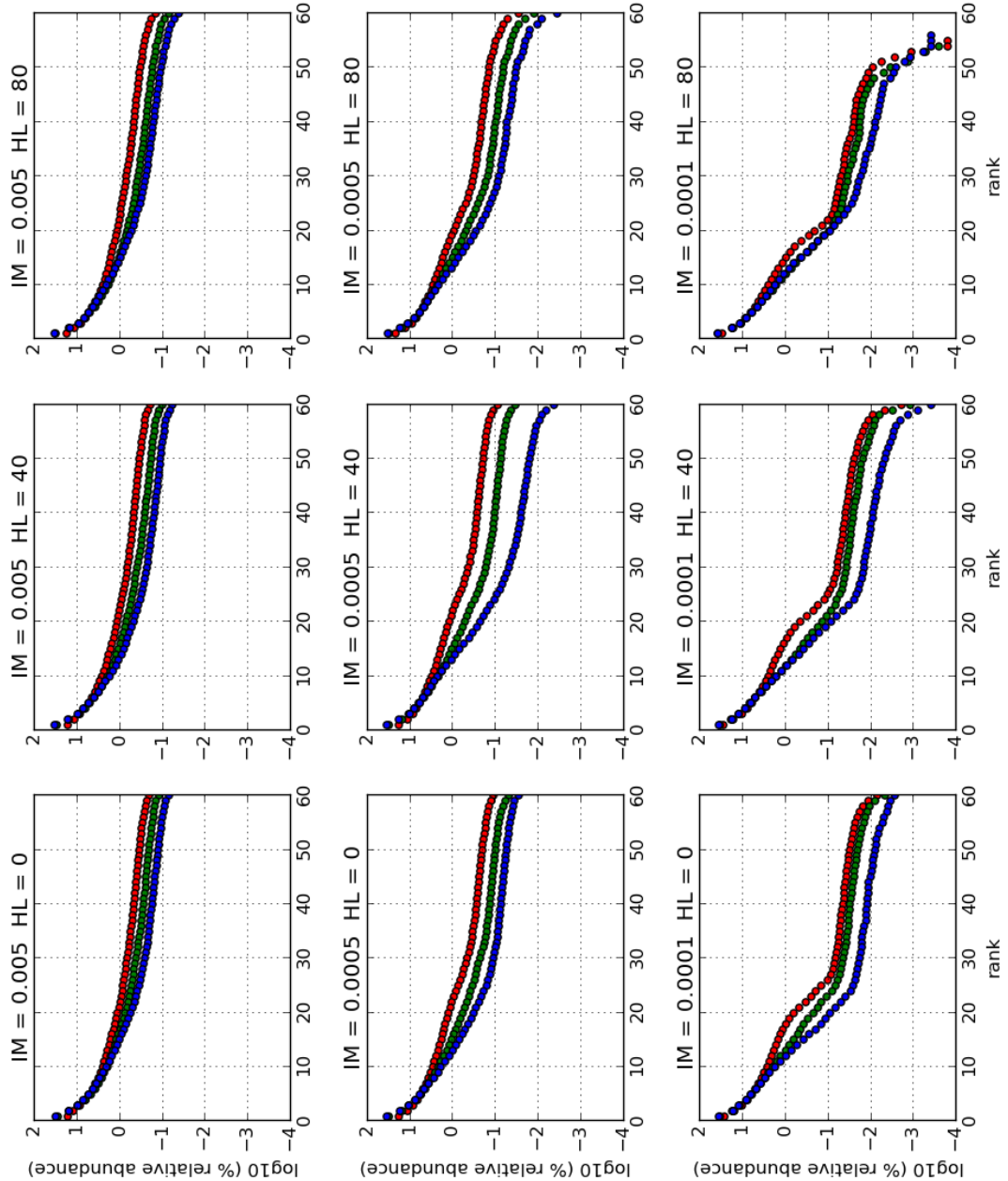


Figure 5.9: **Average rank abundance distributions** over one hundred simulation runs, for nine different pair values of immigration rate and habitat destruction. Each distribution is calculated using the mean relative abundance of the ranked species, averaged over the final abundances of one hundred repeat simulations. The different colours correspond to different MAI ratios: red = 0.0; green = 0.5; blue = 1.0.

is important so the reader does not feel like we include all these metrics because we can. For doing this it is always helpful to write down the main findings as bullet points and develop them; also, the limitations of the model should be presented here as well as the ways forward)

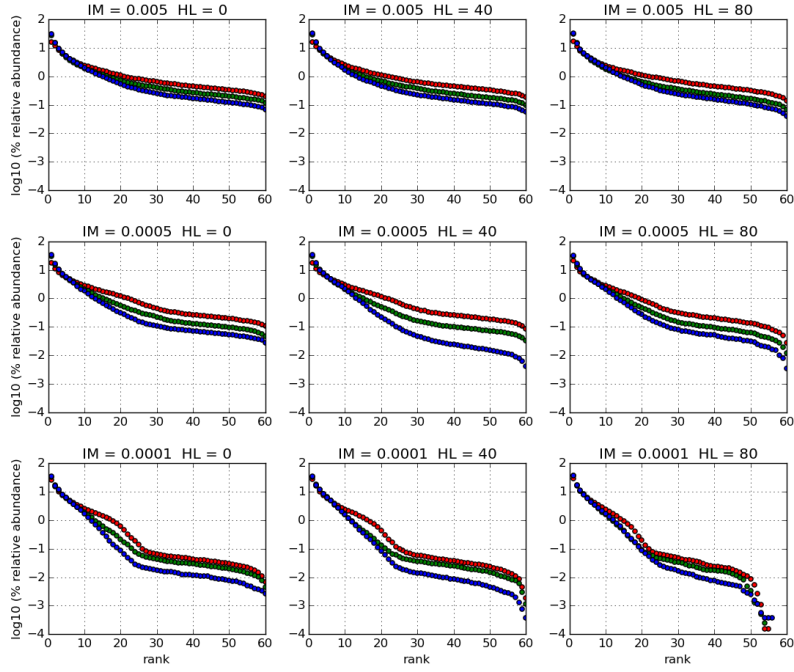
- Theme for discussion seems to be developing: point out a feature of the results, explain what could be causing it (in the model), relate this to other results. (should add to this - comment on how this may relate to the real world??) (Agree. The discussion section to summarize and explain, contextualize the results is needed.)

RADS: Good. As the main changes are observed for different IR it is good to include plots of abundance vs rank with the lines representing different IRs. Also, it could be nice to see if they deviate from a classical lognormal or lognormal family type distribution (which is usually found in nature)

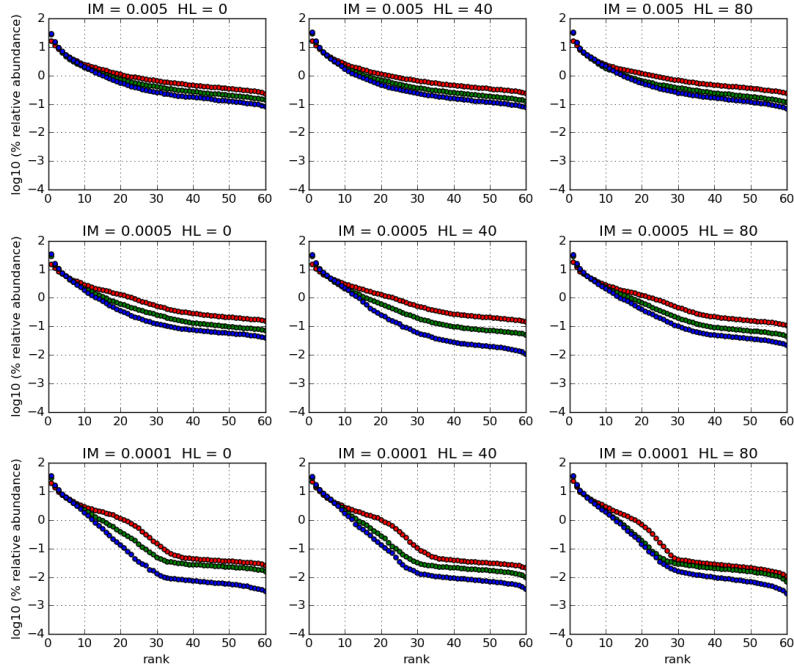
Are the legends correct? The plots next to this note are similar. I think they have different IR, right?

## 5.9 RADS with averaging

Here we show the difference between rank abundance distributions calculated using two different samplings from the simulations..



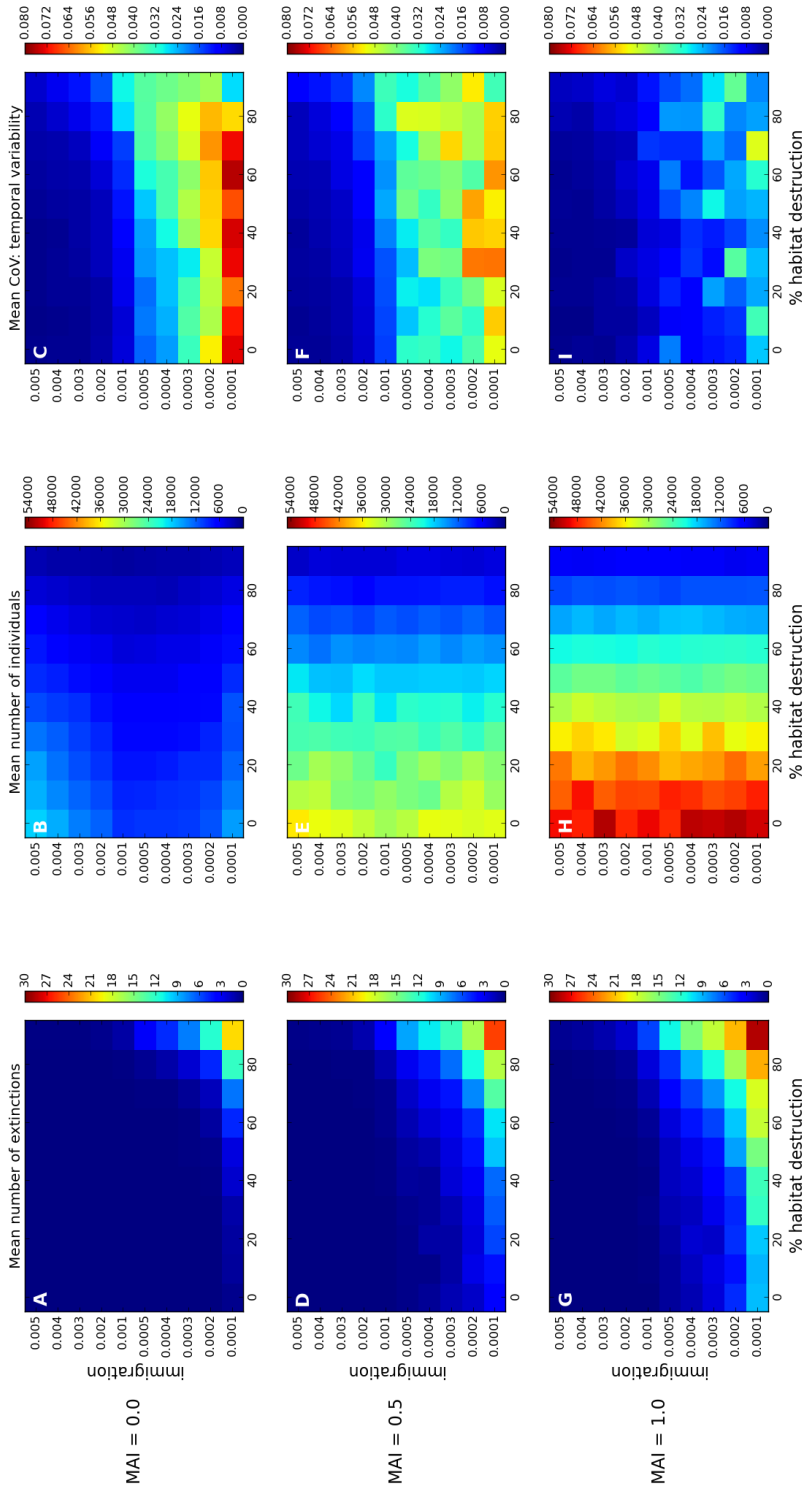
(a) From snapshot of final simulation state



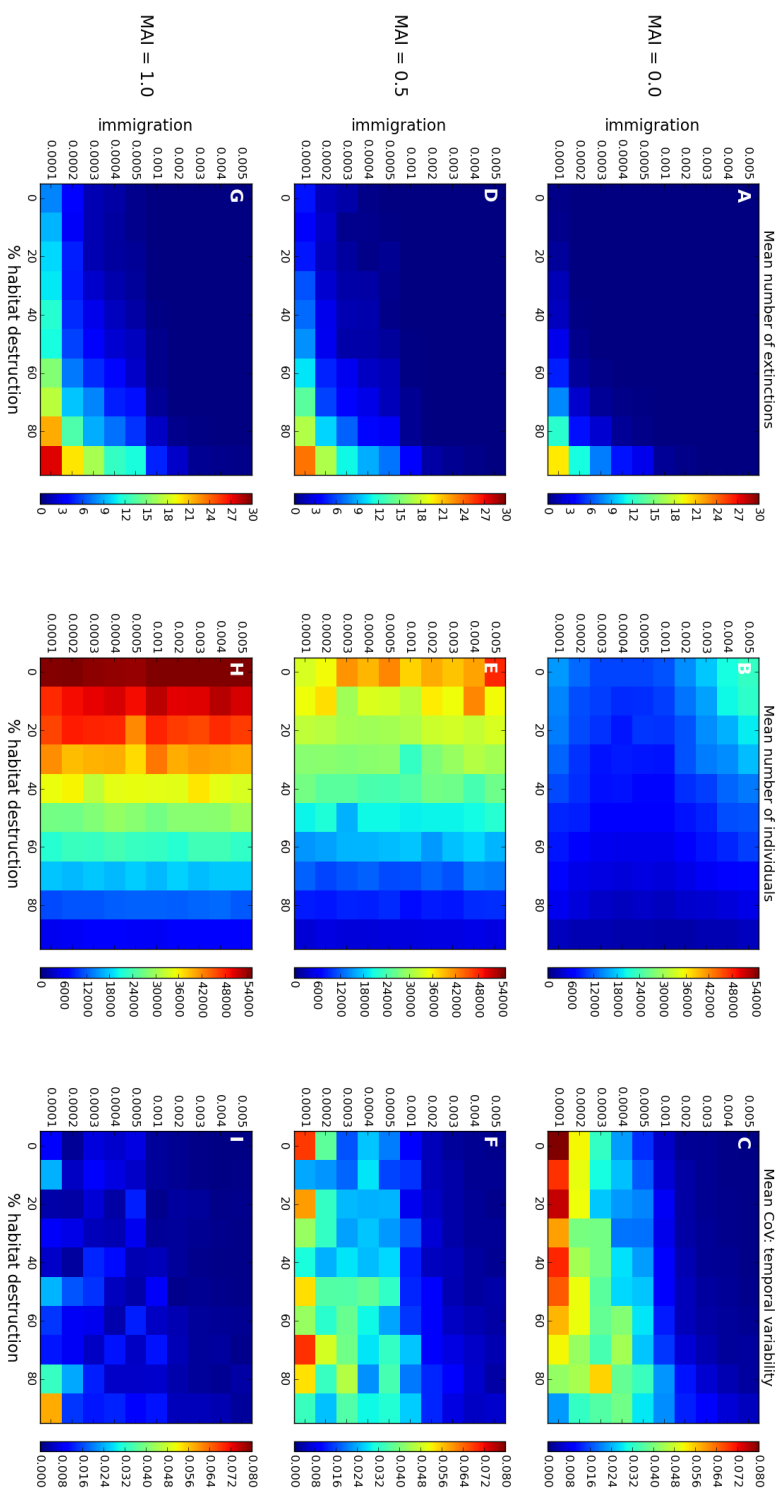
(b) Abundances averaged over final 1000 iterations

Figure 5.10: **Average rank abundance distributions** over one hundred simulation runs, for nine different pair values of  $\text{immigration rate}$  and  $\text{habitat destruction}$ . Each distribution is calculated using the mean relative abundance of the ranked species. The different colours correspond to different MAI ratios: red = 0.0; green = 0.5; blue = 1.0.

### **5.10 New results: without vegetarian predators**



**Figure 5.11: VEGETARIAN PREDATORS. Summary heat maps:** Each heat map shows the value of a certain response metric across a 2-dimensional slice of parameter space. The parameters varied are immigration rate  $IR$  (y-axis) and percentage habitat destruction  $HL$  (x-axis). Each row of plots corresponds to a different MAI ratio as labelled. To construct the heatmaps one hundred repeat simulations were run for each combination of parameter values, with each simulation using a different underlying network. The mean value of the response metrics is taken over the hundred repeats. Therefore each pixel shows an estimate of the expectation value of the metric at those parameter values. The left column shows the expected number of species that are extinct at the end of a simulation; the central column shows the expected biomass (total number of individuals) at the end of a simulation; and the right column shows the expected temporal variability (coefficient of variation of total biomass) of the dynamics during the final thousand iterations of a simulation. The latter is used as a proxy for stability (see text).



**Figure 5.12: NO VEGETARIAN PREDATORS. Summary heat maps:** Each heat map shows the value of a certain response metric across a 2-dimensional slice of parameter space. The parameters varied are immigration rate  $IR$  (y-axis) and percentage habitat destruction  $HL$  (x-axis). Each row of plots corresponds to a different MAI ratio as labelled. To construct the heatmaps one hundred repeat simulations were run for each combination of parameter values, with each simulation using a different underlying network. The mean value of the response metrics is taken over the hundred repeats. Therefore each pixel shows an estimate of the expectation value of the metric at those parameter values. The left column shows the expected number of species that are extinct at the end of a simulation; the central column shows the expected biomass (total number of individuals) at the end of a simulation; and the right column shows the expected temporal variability (coefficient of variation of total biomass) of the dynamics during the final thousand iterations of a simulation. The latter is used as a proxy for stability (see text).

CHAPTER



## INFERRING SPECIES INTERACTIONS

### 6.1 Motivation

In this chapter we investigate the possibility of quantifying species interaction strengths from observed population dynamics. This was discussed at length in the introduction (section ??), however we now reiterate some of the important points here and to motivate our approach to the problem.

- metrics for interaction strength (choice of IM metric)
- hare-lynx dataset (ongoing debate!)
- Availability of time-series data. Plankton system (complications! e.g. seasonality)
- Motivate simulation approach (known interactions)
- Timme approach to fit GLV (use of GLV in general - constant interaction strengths)
- Simplify the problem (two species predator prey, but see extension)

We implement and test a novel method for quantifying species interactions from population dynamics. Initially we test this method using two distinct ODE simulation models to generate the population dynamics. These two models are referred to as the *linear* and *holling* models. The GLV can fit the *linear* model exactly. Therefore the results presented in section 6.3.1 serve as a test of our numerical method. We characterise the robustness of the method to the addition of noise, and under sparsity of sampling. The *holling* model cannot be fitted exactly by the GLV because it uses a different form of *functional response*. Therefore applying our method to population dynamics simulated using the *holling* model provides a test of its ability to give approximate

estimates of interaction strength, when underlying structure of the system is not of GLV type. This is also tested in the presence noise and under sparse sampling, and the results are presented in section 6.3.2. In section 6.3.3 we provide a preliminary look at how the method could be used to determine the type of functional response present, by observing the dynamics. Having characterised the performance of our method using ODE models, we then apply it, in section 6.5, to dynamics generated using the IBM model of previous chapters. This represents a first step towards applying the method to empirical data, since it involves a spatial system and a larger number of species. We conclude the chapter with a discussion of how the method could be developed further towards empirical application.

## 6.2 Methodology

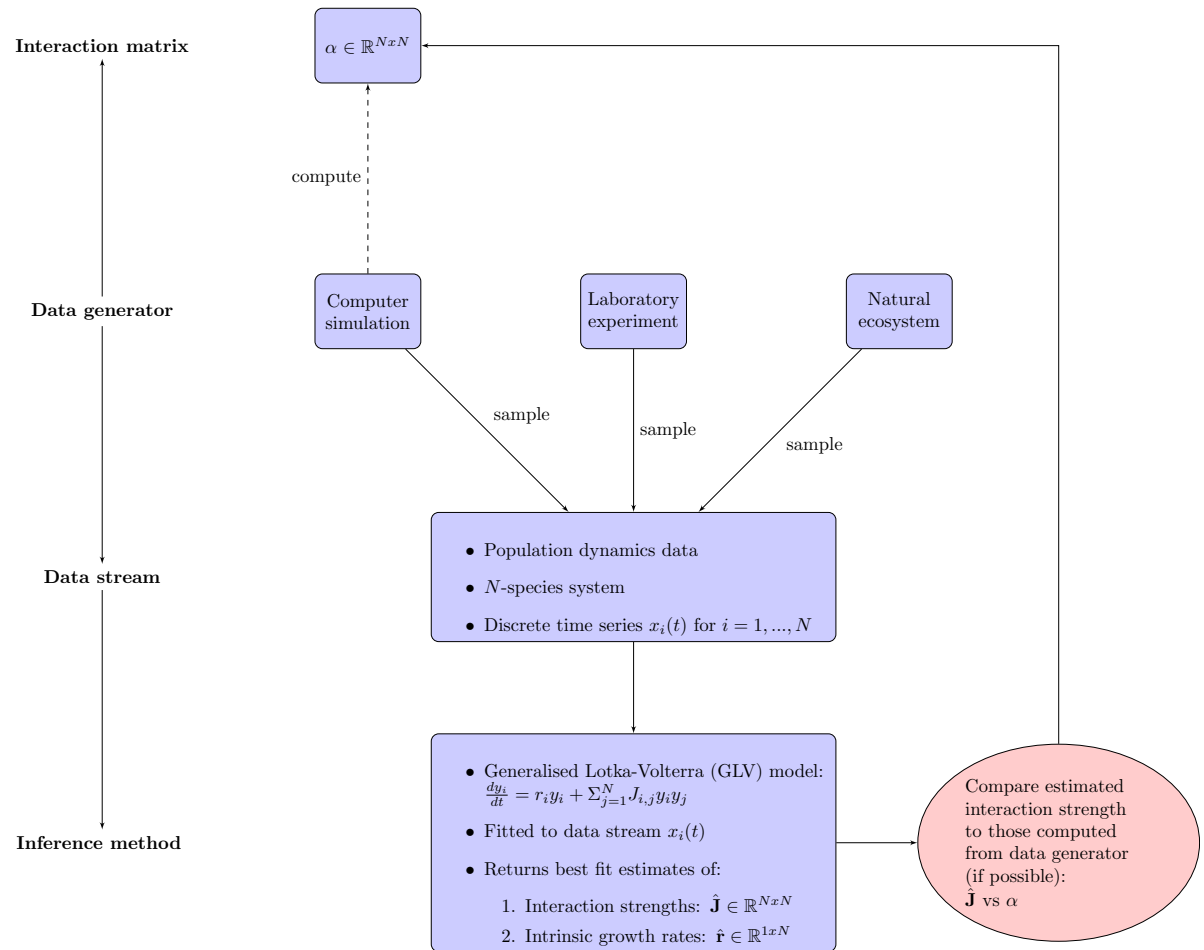


Figure 6.1: This is what we do.

To summarise our methodology, we simulate population dynamics then sample these dynamics and fit a *generalised Lotka-Volterra* (GLV) model. The fitted GLV parameters give us estimates

of the species interaction strengths (and other parameters), which we then compare to those used in the original simulation. The details of all the stages are given below. In section 6.2.1 the *interaction matrix* (IM) is introduced. The IM is the metric used to quantify the strength of species interactions and is key to this chapter. We also introduce the *generalised Lotka-Volterra* (GLV) model, and show that this model has constant interaction strengths, given by the coupling matrix  $J$ . In section 6.2.2 we give a general framework for ODE predator-prey modelling, and derive the two models that we use to simulate population dynamics. We then discuss, in section 6.2.3 the details of how these models are simulated *in silico*, including the selection of model parameters. Section 6.2.4 gives the details of the numerical method we use for fitting the GLV model to sampled population dynamics. In section 6.2.5 we give an example of the full methodology in action.

### 6.2.1 Interaction strength

The metric used for species interaction strength is key to this chapter. As discussed in section 6.1 there are several metrics available [REF]. However there is one that is a natural choice, given our methodology. This metric allows us to calculate the interaction strengths from our simulation models, and to directly compare them to the estimates obtained by fitting the GLV model. The metric is called the *interaction matrix* (IM). The elements of the IM,  $\alpha_{ij}$ , quantify the effect of a small change in the population density of species  $j$  on the per capita growth rate of species  $i$  [REF]. Therefore the IM elements are given by:

$$(6.1) \quad \alpha_{ij} = \frac{\partial}{\partial x_j} \left( \frac{1}{x_i} \frac{dx_i}{dt} \right),$$

where  $x_i$  and  $x_j$  are the population densities of species  $i$  and  $j$  respectively. In the case of our two species systems the IM is a  $2 \times 2$  matrix, but trivially extends to quantify all  $N^2$  pair-wise interactions between species in a  $N$ -species system (including self-interactions).

Using the IM we are able to calculate the interaction strengths exactly from the models that we use for simulation. This is because they are ODE models with explicit expressions for  $dx_i/dt$ , so we can evaluate the partial derivative in equation 6.1 to obtain analytic forms for all the IM elements ( $\alpha_{00}, \alpha_{01}, \alpha_{10}, \alpha_{11}$ ). Depending on the model used the IM elements are either constants, or are functions of prey density. The interaction strengths for our simulation models are given at the end of section 6.2.2, and are illustrated in figure 6.2.

**Generalised Lotka-Volterra.** The GLV model is the extension of the Lotka-Volterra equations to  $N$  species. We use this model to fit to simulated population dynamics and obtain estimates of the underlying interaction strengths. The GLV model is given by:

$$(6.2) \quad \frac{dx_i}{dt} = r_i x_i + \sum_{j=1}^N J_{ij} x_i x_j,$$

where  $x_i$  is the population density of species  $i$ ;  $r_i$  is the intrinsic growth rate;  $N$  is the number of species and  $J_{ij}$  is the coupling between species  $i$  and  $j$ . Applying equation 6.1 to equation 6.2 we see that  $\alpha_{ij} = J_{ij}$ , such that the IM for the GLV model is equal to the coupling matrix. Therefore, by fitting the GLV model to population dynamics, the fitted parameters  $J_{ij}$  give us numeric estimates of interaction strength. To perform the fit we use the method detailed in section 6.2.4.

### 6.2.2 Population models

We use ordinary differential equation (ODE) models to simulate two species predator-prey dynamics. Therefore the mathematics presented in this section focuses on this case. However the framework may be easily extended to include other interaction types (competition and mutualism), and to model larger systems in a similar way. For a two species system the dynamics are governed by two coupled equations, one for each species. Importantly it is possible, using the IM introduced in section 6.2.1, to calculate the species interaction strengths from the model. The model equations take the general form:

$$(6.3) \quad \begin{aligned} \frac{dx_0}{dt} &= G_0(x_0) + \alpha_{01}x_1 H(x_0, x_1), \\ \frac{dx_1}{dt} &= G_1(x_1) + \alpha_{10}x_0 H(x_0, x_1) \end{aligned}$$

where species  $x_0$  and  $x_1$  are the population densities of the prey and the predator species respectively; the  $G_i(x_i)$  are the intrinsic growth functions of each species; the  $\alpha_{ij}$  are constant coefficients and  $H(x_0, x_1)$  is the functional response (FR) of the predator. This form is standard in the literature [REFS] and many models may be expressed in this way by choosing different functional forms for  $G$  and  $H$ . The coefficients  $\alpha_{01}$  and  $\alpha_{10}$  are negative and positive respectively, such that the prey losses biomass, and the predator gains biomass as a result of the interaction. These coefficients may be used to introduce asymmetry into the interaction terms. For example it is common to choose  $|\alpha_{01}| > |\alpha_{10}|$ , to model the inefficiency of the predator in the conversion of biomass from the prey. For the intrinsic growth functions we use the functional forms:

$$(6.4) \quad G_0(x_0) = r_0 x_0 \left(1 - \frac{x_0}{K_c}\right)$$

$$(6.5) \quad G_1(x_1) = -r_1 x_1,$$

where  $r_i \in \mathbb{R}^+$  is the intrinsic growth rate of species  $i$ , and  $K_c$  is the carrying capacity of the prey species. Therefore the predator has an exponential intrinsic mortality, whereas the prey species has logistic intrinsic growth. These use of these functional forms in predator-prey modelling was made popular by Rosenzweig and MacArthur [REF]. They are now widely used [REFS].

The FR defines the per-predator rate of consumption of prey. We focus on the forms proposed by Holling in the 1950s [REFs], which are also widely used [REFS]. However it is worth noting that various other forms have been proposed and there is an ongoing debate about which to use [REFS] (see discussion in section 6.6). There are three types of Holling FR, referred to as types I, II, and III. These can be expressed as:

$$(6.6) \quad H_I(x_0, x_1) = x_0,$$

$$(6.7) \quad H_{II}(x_0, x_1) = \frac{x_0}{x_0 + K_s},$$

$$(6.8) \quad H_{III}(x_0, x_1) = \frac{x_0^2}{x_0^2 + K_s^2},$$

where  $x_0$  is the prey density, and  $K_s$  is the saturation constant for the predator, giving the prey density at which the per-predator consumption rate reaches half-maximum. We choose to narrow our investigation by focusing here on the first two forms: Holling type I and type II. Therefore we have two distinct simulation models, which we refer to as the *linear* and *holling* models.

**Linear model.** This model uses the type I FR. As is clear from equation 6.6, type I is the simplest of the Holling functions: the per-predator predation rate increases linearly as the abundance of available prey increases. The slope of this linear relationship given by the  $a_{ij}$  parameters in equations 6.5. The linear FR is the same as is used in the famous Lotka-Volterra equations [REF], meaning that our linear model may be expressed in GLV form (equation 6.2). We may rescale the equations of the linear model in order to reduce the number of parameters. This makes the local stability analysis simpler, and reduces the dimension of the search space when probing the equations numerically via simulation. The re-scaled equations are given by:

$$(6.9) \quad \frac{d\chi_0}{dt} = A\chi_0(1 - \chi_0) - B\chi_0\chi_1$$

$$(6.10) \quad \frac{d\chi_1}{dt} = -\chi_1 + C\chi_0\chi_1,$$

where  $\chi_0$  and  $\chi_1$  are the re-scaled prey and predator population densities respectively; the parameters  $A, B, C \in \mathbb{R}^+$ . The equilibrium population densities are given by:

$$(6.11) \quad \chi_0^* = \frac{1}{C}$$

$$(6.12) \quad \chi_1^* = \frac{A}{B} \left(1 - \frac{1}{C}\right),$$

Therefore  $\chi_0^*$  is always positive, and  $\chi_1^*$  is positive if  $c > 0$ . This is a requirement for physical realism, since it is not possible to have negative populations of species. In most applications it

is also required that this equilibrium is stable, to allow for the coexistence of species. We use these conditions on the equilibrium for parameter selection, which is discussed in section 6.2.3. By applying equation 6.1 to equations 6.9 and 6.10 we can evaluate the elements of the IM for the linear model. This gives:

$$(6.13) \quad \alpha_{linear} = \begin{bmatrix} -A & -B \\ C & 0 \end{bmatrix},$$

such that all the interaction strengths are constants, which is illustrated in figure 6.3.

**Holling model.** This model uses the type II FR, which is a non-linear function of prey density. As we can see from equation 6.7 and figure 6.2, this FR models predator saturation - individuals take a certain amount of time to process and digest prey - such that the response curve flattens out at high prey densities. The difference between the type I and II functions is illustrated in figure 6.2. We may perform a similar rescaling as we did with the linear model to reduce the number of parameters. The resulting equations for the holling model are given by:

$$(6.14) \quad \frac{d\chi_0}{dt} = A\chi_0(1-\chi_0) - \frac{B\chi_0\chi_1}{\chi_0+D}$$

$$(6.15) \quad \frac{d\chi_1}{dt} = -\chi_1 + \frac{C\chi_0\chi_1}{\chi_0+D},$$

where the saturation constant  $D \in \mathbb{R}^+$ , and the other symbols are the same as in equations 6.9 and 6.10. The equilibrium populations for this model are given by:

$$(6.16) \quad \chi_0^* = \frac{D}{C-1}$$

$$(6.17) \quad \chi_1^* = \frac{ACD(C-1-D)}{B(C-1)^2},$$

Therefore  $\chi_0^*$  is positive if  $C > 1$ ,  $\chi_1^*$  is positive if  $C - D > 1$ . Again we use these conditions, and the requirement of stability, to constrain our choice of parameters (6.2.3). As we did for the linear model, we can evaluate the IM for the holling model, giving:

$$(6.18) \quad \alpha_{holling} = \begin{bmatrix} -A + \frac{B\chi_1}{(\chi_0+D)^2} & \frac{-B}{\chi_0+D} \\ \frac{CD}{(\chi_0+D)^2} & 0 \end{bmatrix},$$

such that the three non-zero elements of the IM are functions of prey density  $\chi_0$ , instead of constants. The shape of these interaction functions is shown in figure 6.2, and we will return to them in section 6.2.5.

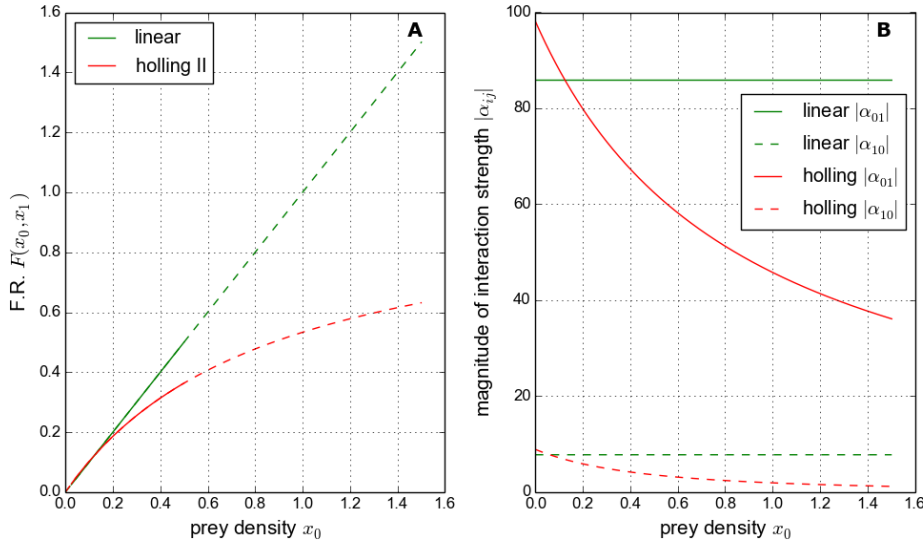


Figure 6.2: Example of (A) the functional response curve, and (B) the corresponding inter-specific interaction strengths for one parameter set of the *linear* model, and one of the *holling* model.

	A	B	C	D
linear	0.1 - 100	0.1 - 100	1 - 100	N/A
holling	0.1 - 100	0.1 - 100	1.1 - 100	0.1-99

Table 6.1: Ranges from which parameters were selected uniformly at random for the two ODE simulation models. The parameters are all allowed to vary over at least three orders of magnitude, to ensure that our investigation covers a large region of parameter space. The restrictions on parameters C and D ensure that it is always possible to achieve an equilibrium population of both species that is strictly positive (see equations 6.11, 6.12, 6.16, 6.17)

### 6.2.3 Simulation procedure

We apply a strict recipe when running simulations in order to ensure consistency and to allow comparison of our numerical results. Key to this is the control of certain variables across simulations, and also our method for parameter selection, both of which are discussed below. All simulations are run using the first-order forward Euler approximation to the ODE model. We use additive Gaussian noise to simulate *process error*. Therefore we implement the stochastic difference equation :

$$(6.19) \quad \chi_{i,t+1} = \chi_{i,t} + \Delta t \Delta \chi_{i,t} + \xi_{i,t},$$

where  $\Delta t$  is the integration time step,  $\Delta \chi_i$  is given by the right hand side of ODE model being simulated (e.g. equations 6.9, 6.10 for the linear model); and the additive noise term

$\xi_{i,t} \sim \mathcal{N}(0, \sigma_{noise} \chi_{i,t} \Delta t)$ . The value of  $\sigma_{noise}$  is quoted as *noise intensity* in what follows. In the event of stochastic extinction of either species, both population densities are reset to their initial conditions. The case where  $\sigma_{noise} = 0$  is referred to as the *deterministic* model. In all the results presented the simulations were run with a time step  $\Delta t = 10^{-4}$ . All code was implemented in the language *Python*, and large computations were performed on the UoB HPC cluster *Blue Crystal* [REF].

The goal of fitting the GLV model to simulated population dynamics requires that the dynamics contain enough information to perform the fit - it is not possible to fit the a model if species populations are sitting at equilibrium. Therefore we follow the precedent set in [REF], such that all simulated dynamics of the *deterministic models* exhibit two ‘large amplitude’ oscillations about a stable equilibrium (see condition 2 below). Every simulation is run with the initial population densities set to half of their equilibrium value. This ensures that all systems start consistently away from equilibrium.

**Parameter selection.** We select an ensemble of 100 parameter sets for both simulation models (*linear* and *holling*). Parameters are selected uniformly at random from predefined ranges, which are given in table 6.1. This range ensures that a positive equilibrium population is possible (see equations 6.11, 6.12, 6.16, 6.17), but also allows for parameters to vary over at least three orders of magnitude so that our investigation covers a large region of parameter space. The selected parameters are then accepted if they meet the following conditions:

1. The equilibrium population is positive, and is locally a stable spiral (eigenvalues of the Jacobian have negative real part and complex conjugate imaginary part).
2. The deterministic dynamics exhibit at least two full rotations in the phase plane before relaxing to within 5% of the equilibrium (Euclidean distance in the phase plane).
3. The population densities do not differ by more than an order of magnitude, in the deterministic case.

The two parameter sets generated by the above procedure are used for the simulation results presented in section 6.3. All simulations , including those with  $\sigma_{noise} \neq 0$ , are run for the length of time  $T_{2P}$  required to achieve two full oscillations in the deterministic case, for that parameter set.

#### 6.2.4 Numerical estimation method

To estimate the inter-specific interaction strengths we use a numerical method, adapted from [67], to fit the GLV model to the population dynamics. The method gives ‘best fit’ estimates of the GLV parameters, which include constant coefficients for the interaction strengths as we saw in section 6.2.1. We include here a derivation of the method, slightly adapted and simplified for

our purposes. Say the dynamics of the population density of a species  $x_i$  is governed by coupled differential equations of the form:

$$(6.20) \quad \dot{x}_i = r_i f_i(x_i) + \sum_{j=1}^N J_{i,j} g_{ij}(x_i, x_j),$$

where  $\dot{x}_i = \frac{d}{dt}x_i$ ;  $N$  is the number of species in the system and  $i, j$  index the species. The  $r_i, J_{i,j} \in \mathbb{R}^+$  are constants, and the functions  $f_i$  and  $g_{ij}$  are known. This form looks familiar, indeed all of the ODE models discussed so far may be expressed in this form - there is an intrinsic growth term, and a linear sum of interaction terms. To express the GLV model (equation 6.2) in this form, we have:

$$(6.21) \quad f_i(x_i) = x_i$$

$$(6.22) \quad g_{ij}(x_i, x_j) = x_i x_j,$$

It would be possible to use this method to fit models other than the GLV, so long as the functions  $f_i$  and  $g_{ij}$  are *known and parametrised*. Since the functions  $f_i$  and  $g_{ij}$  are known there are  $N+1$  unknowns in equation 6.20:  $r_i$  and  $J_{i,j}$  for  $j = 1, \dots, N$ . Therefore, if we knew the exact values of  $\dot{x}_i, x_i$  and the  $x_j$ 's, at  $N+1$  time points, then we could solve the equation for  $r_i$  and the  $J_{i,j}$ 's. However in any practical application our knowledge of the system is not *exact*; the system is subject to noise; and the model may be an imperfect description of the dynamics. So the equation cannot be solved exactly. We must look for an approximate solution. To do this the full state of the system is sampled at  $M+1$  time points  $t_m$  for  $m \in 1, \dots, M, M+1$ . These samples are used to construct estimates for the states  $x_i$  and their time-derivatives  $\dot{x}_i$  at  $M$  intermediate time points, for every species  $i$ .

The simplest way to estimate the time-derivatives is to take the finite difference between observations at two consecutive time points, giving estimates:

$$(6.23) \quad \hat{x}_i(\tau_m) := \frac{x_i(t_m) - x_i(t_{m-1})}{t_m - t_{m-1}},$$

where  $\tau_m \in \mathbb{R}, m \in \{1, \dots, M\}$  is the midpoint of the two time-points:

$$(6.24) \quad \tau_m := \frac{t_{m-1} + t_m}{2}.$$

To evaluate the functions  $f_i, g_{ij}$  at these new time-points we must estimate the states  $x_i(\tau_m)$  from our observations. We use the linear interpolation:

$$(6.25) \quad \hat{x}_i(\tau_m) := \frac{x_i(t_{m-1}) + x_i(t_m)}{2}.$$

So from equation 6.20 we can now construct  $M$  equations using our  $M + 1$  samples:

$$(6.26) \quad \hat{x}_i(\tau_m) = r_i f_i(\hat{x}_i(\tau_m)) + \sum_{j=1}^N J_{i,j} g_{ij}(\hat{x}_i(\tau_m), \hat{x}_j(\tau_m)).$$

We now simplify the notation such that equation 6.26 may be written

$$(6.27) \quad \hat{x}_{i,m} = r_i f_{i,m} + \sum_{j=1}^N J_{i,j} g_{ij,m},$$

where the subscripts  $i, j$  indicate the species, and  $m$  indicates the time-point  $\tau_m$  for which the equation holds. This system of  $M$  equations can be expressed in matrix form:

$$(6.28) \quad X_i = J_i G_i,$$

where we have

$$(6.29) \quad X_i = \begin{pmatrix} \hat{x}_{i,1} & \hat{x}_{i,2} & \cdots & \hat{x}_{i,M} \end{pmatrix} \in \mathbb{R}^{1 \times M},$$

$$(6.30) \quad J_i = \begin{pmatrix} r_i & J_{i,1} & J_{i,2} & \cdots & J_{i,N} \end{pmatrix} \in \mathbb{R}^{1 \times (N+1)},$$

$$(6.31) \quad G_i = \begin{pmatrix} f_{i,1} & f_{i,2} & \cdots & f_{i,M} \\ g_{i,1,1} & g_{i,1,2} & \cdots & g_{i,1,M} \\ g_{i,2,1} & g_{i,2,2} & \cdots & g_{i,2,M} \\ \vdots & \vdots & \ddots & \vdots \\ g_{i,N,1} & g_{i,N,2} & \cdots & g_{i,N,M} \end{pmatrix} \in \mathbb{R}^{(N+1) \times M}.$$

The system 6.28 has  $N + 1$  unknowns ( $J_{i,k}$  for  $k = 1, \dots, N + 1$ ) and  $M$  equations. In the case when  $M > N + 1$  the system is over constrained and there is no exact solution in general. We look for an approximate solution  $\hat{J}_i$  that minimises the error between the LHS and RHS of equation 6.28. We take the error function:

$$(6.32) \quad E_i(\hat{J}_i) = \sum_{m=1}^M (X_{i,m} - \sum_{k=1}^{N+1} \hat{J}_{i,k} G_{i,k,m})^2,$$

which we want to minimise with respect to the matrix elements  $\hat{J}_{i,k}$ . That is

$$(6.33) \quad \frac{\partial}{\partial \hat{J}_{i,k}} E_i(\hat{J}_i) \stackrel{!}{=} 0.$$

By taking the derivative of the RHS of equation 6.32 we have that:

$$\begin{aligned}\frac{\partial}{\partial \hat{J}_{i,k'}} E_i(\hat{J}_i) &= \frac{\partial}{\partial \hat{J}_{i,k'}} [\sum_{m=1}^M (X_{i,m} - \sum_{k=1}^N \hat{J}_{i,k} G_{i,k,m})^2] \\ &= -2 \sum_{m=1}^M [(X_{i,m} - \sum_{k=1}^N \hat{J}_{i,k} G_{i,k,m}) G_{i,k',m}]\end{aligned}$$

To find the minimum of the error function we equate this to zero, giving:

$$\begin{aligned}0 &= \sum_{m=1}^M (-X_{i,m} G_{i,k',m} + G_{i,k',m} \sum_{k=1}^N \hat{J}_{i,k} G_{i,k,m}) \\ &= (-X_i G_i^T)_{k'} + \sum_{m=1}^M G_{i,k',m} (\hat{J}_i G_i)_m \\ &= (-X_i G_i^T)_{k'} + \sum_{m=1}^M (\hat{J}_i G_i)_m G_{i,m,k'}^T \\ (6.34) \quad &= -X_i G_i^T + \hat{J}_i G_i G_i^T\end{aligned}$$

Therefore we conclude that:

$$(6.35) \quad \hat{J}_i = X_i G_i^T (G_i G_i^T)^{-1},$$

which, in our case, is the analytic form for the best estimate of the row corresponding to species  $i$  in parameter matrix of the GLV model. For a two species system, by applying equation 6.35 to each species, we can obtain the full set of GLV parameter estimates:

$$(6.36) \quad \hat{J} = \begin{pmatrix} \hat{J}_{0,0} & \hat{J}_{0,1} \\ \hat{J}_{1,0} & \hat{J}_{1,1} \end{pmatrix},$$

and

$$(6.37) \quad \hat{r} = \begin{pmatrix} \hat{r}_0 & \hat{r}_1 \end{pmatrix}.$$

We perform the computation by constructing the matrices  $X_i$  and  $G_i$  for both species, and do the matrix multiplication using the *Python* package *numpy*[REF]. The fact that the error minimisation has an analytic solution makes it very computationally efficient, allowing us to perform many replicate calculations. However the performance of the method may be lower than other, more computationally expensive, model fitting algorithms (see discussion section 6.6). It is possible to assess the goodness of fit achieved by evaluating the error function (equation 6.32).

### 6.2.5 Examples

Here we show examples of the dynamics of both models, both with and without noise..For the holling model we also show the variability in interaction strengths during the simulations..We also present a table with the results of the GLV, comparing them to the simulation interaction strengths..

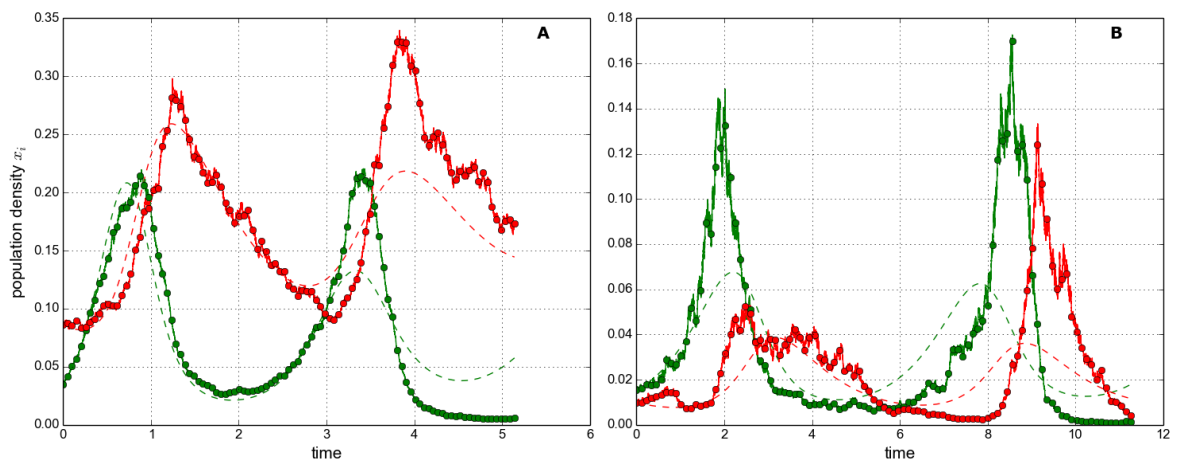


Figure 6.3: Example linear dynamics. 100 sampels. Two different parameter sets. A: noise=20. B:noise=50.

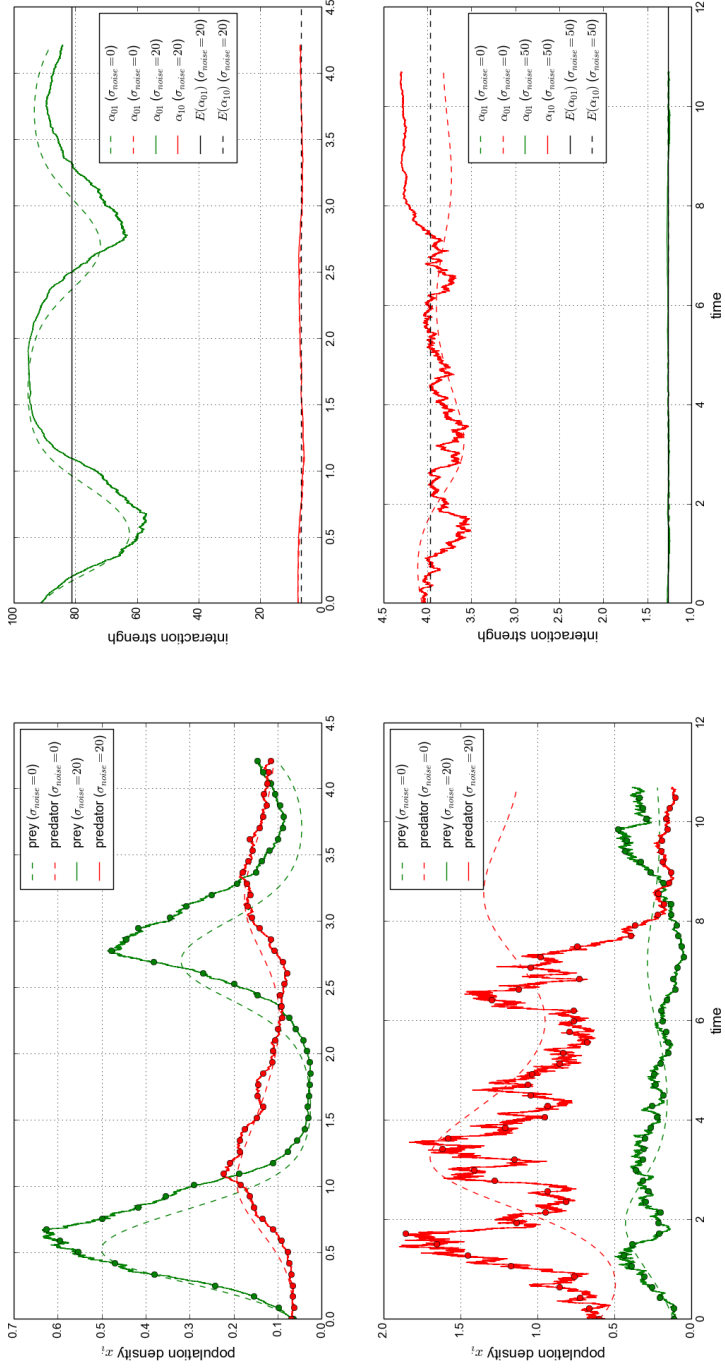


Figure 6.4: Example Holling II dynamics.

## 6.3 Results

In this sections we characterise the numerical performance of the method, described in section 6.2.4, for estimating the strength of interactions between species. The method is tested on the dynamics of two different ODE systems: a Lotka-Volterra (LV) and a Holling type II (HII) system. In the first case it is simply a test of a model fitting procedure. This is because the method works by fitting a generalised Lotka-Volterra (GLV) model to the dynamics, and the LV systems can be expressed as a GLV systems. Therefore we are simply simulating using one model, and then testing a method of estimating the model parameters from the simulated dynamics. We test the effects of noise and sampling frequency. In the second case, the HII system cannot be expressed as a GLV system. Therefore the GLV model that we fit can only approximate the dynamics and we cannot make a direct comparison between the parameters of the simulation model and the GLV model used for estimation. In this case we compare to the mean interaction strengths (see section 6.3.2).

### 6.3.1 Linear model

Initially we run repeated simulations of the LV model using a single parameter set. We investigate how the numerical estimates of the model parameters respond to two variables: the level of noise in the simulations; and the number of samples used for estimation. Other variables are held constant using the simulation procedure described in section 6.2.3. We then generalise these results by looking at the relative error in the estimates, for repeated simulations using an ensemble of 100 selected parameter sets (as described in section 6.2.3).

**Single parameter set.** Here we can make direct comparison between model parameters. The GLV model for two species has six parameters:  $r_0, r_1, J_{00}, J_{01}, J_{10}, J_{11}$ . These correspond respectively to the following constant values of the LV system used for simulations:  $A, -1, -A, -B, C, 0$  (see equation ??). In general we find that the numerical estimates perform well at low noise intensities and poorly at high noise intensities. This is illustrated in figures 6.5 and 6.6. We also find that the estimates improve with the number of samples used, up to a point. Beyond this point the use of more samples does little to improve the estimates, and in some cases makes them worse. This behaviour is illustrated in figures 6.7 and 6.8. These patterns were found to hold across all parameter sets investigated, but are only shown using a single parameter set here for clarity.

In panel **A** of figures 6.5 and 6.6 we see that the mean value of the estimates approaches the true value for low noise and, in panel **B** that the variance in the estimates approaches zero. This tells us that the method consistently gives a good fit of the GLV to the dynamics of the LV system, even when only 100 sample points are used (figure 6.5). As the noise intensity is increased the mean values of the estimates deviate from the true values, and the standard deviation in the estimates increases. Comparing the two figures we see that the response to noise is very similar

whether 100 or 10,000 samples are used. A notable exception to this is a spike in the variance in panel **B** of figure. However this appears to be a single statistically anomalous result and not part of the trend. Panel **C** of both figures shows that the error function, which is minimised by the estimation method, increases with noise for both species. This cannot be directly compared between the two plots because of the different number of samples used. However it indicates that in both cases (100 and 10,000 samples) the quality of the fit is high in the deterministic case, and decreases with noise.

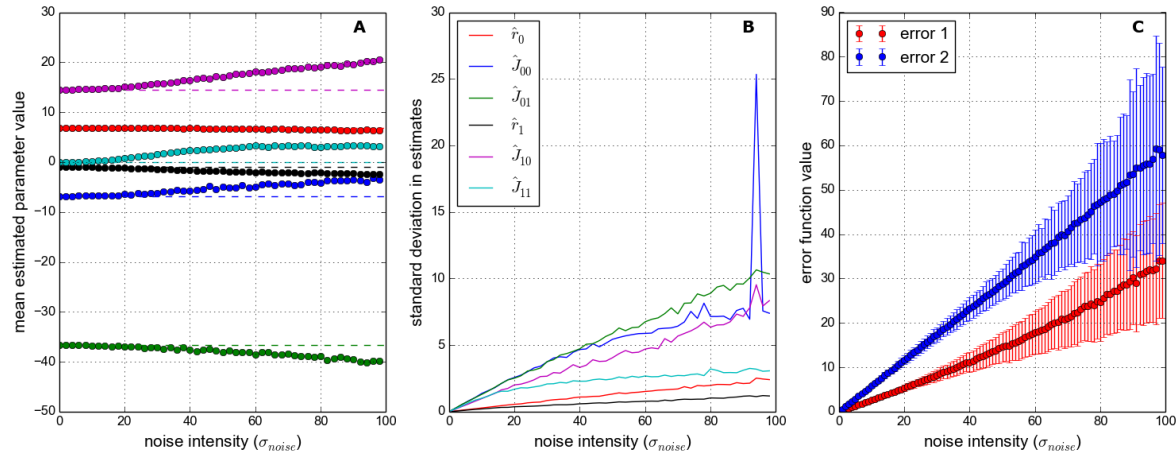


Figure 6.5: Effect of noise on numerical estimates. Here the method uses 100 samples from simulated dynamics. All simulations run using the LV model with a single parameter set. The noise intensity varies between 0 (deterministic) and 100. See section 6.2.5 for an intuition of how noisy this is. 1000 repeat simulations run at each noise level. **Panel A:** Mean estimated parameter values (each dot representing mean over 1000 repeats). The ‘true’ parameter values of the simulation model are shown by dashed lines. **Panel B:** Standard deviation in estimates. **Panel C:** Value of the error functions used in the estimation method, one for each species. The dots show the mean error, and the bars show  $\pm$  one standard deviation.

We now look at how the estimates respond to the number of samples used, in the cases of low and high noise intensity. Figure 6.7 shows the low noise case, with  $\sigma_{noise} = 10$ . In panel **A** we see that the mean value of the estimates quickly converges to close to the true parameter values, as the number of samples increases. Panel **B** shows that the standard deviation in the estimates quickly becomes small, but non-zero. Above about 32 samples there is no visible improvement in the estimates, as measured by the mean or standard deviation. In figure 6.8 we see the effect of a higher noise intensity. Here we have  $\sigma_{noise} = 50$ . Panel **A** shows that the estimates do not converge on the true parameter values, even for large numbers of samples. Also the standard deviation in the estimates, shown in panel **B**, is higher than in the low noise case. Again we find that there is little, if any, improvement in the estimates beyond about 32 samples.

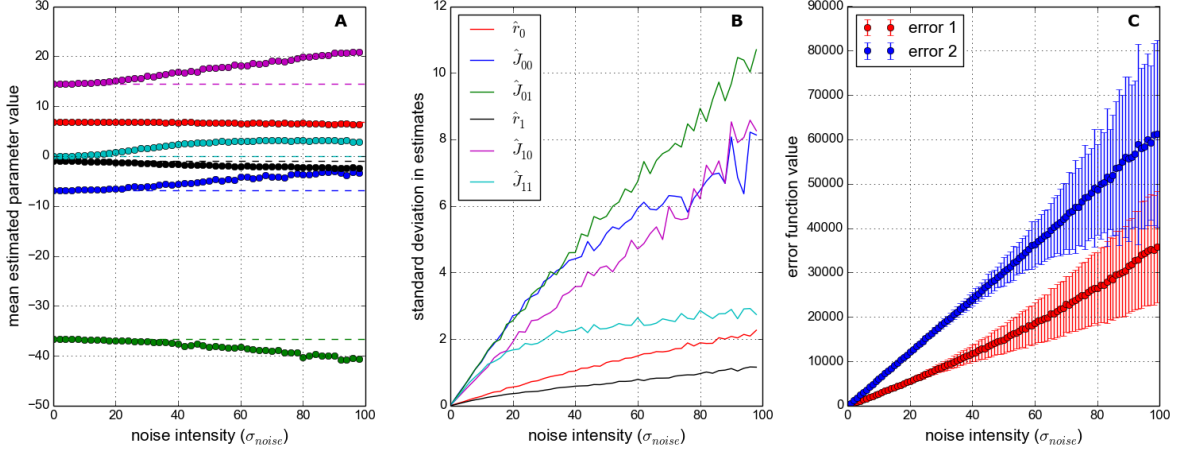


Figure 6.6: Exactly as in figure 6.5 but using 10,000 samples from the simulated dynamics.

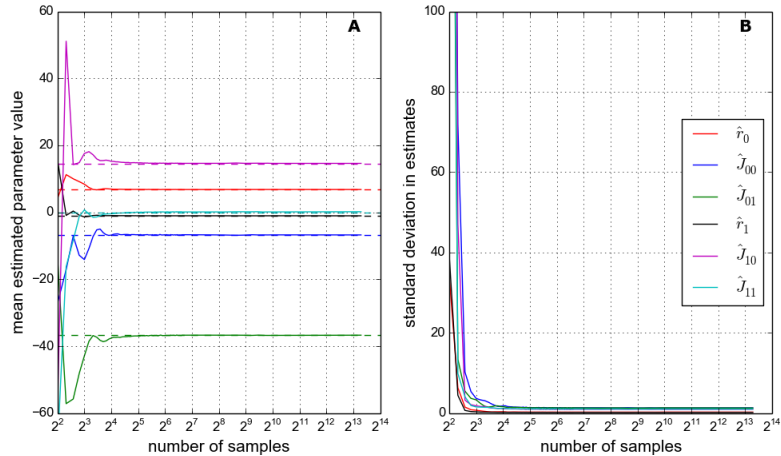


Figure 6.7: Effect of the number of samples on numerical estimates. All simulations run using the LV model with a single parameter set. The noise intensity  $\sigma_{noise} = 10$ . Number of samples ranges from 4 to 10,000. Samples drawn from simulated dynamics at equal intervals. 1000 repeat simulations for each number of samples. **Panel A:** Solid lines show mean estimated parameter values. Dashed lines show the ‘true’ parameter values of the simulation model. **Panel B:** Standard deviation in estimates.

**Ensemble of parameter sets.** Run 10 repeats for each of 100 parameter sets. In general the trends described above hold across the ensemble..

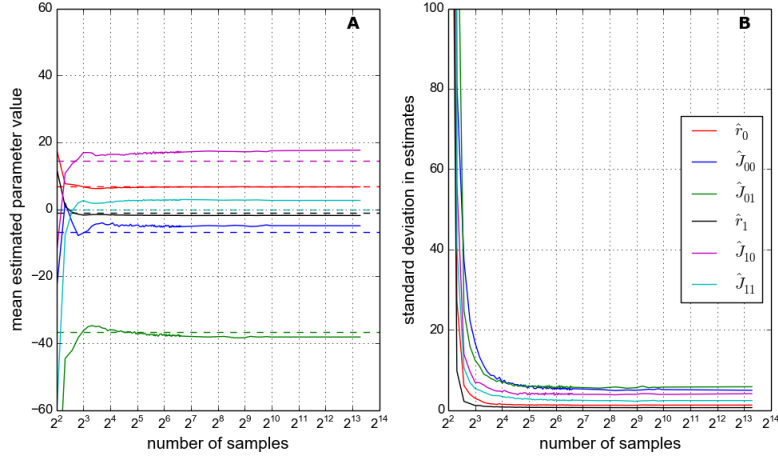


Figure 6.8: Exactly as in figure 6.7 but with noise intensity  $\sigma_{noise} = 50$ .

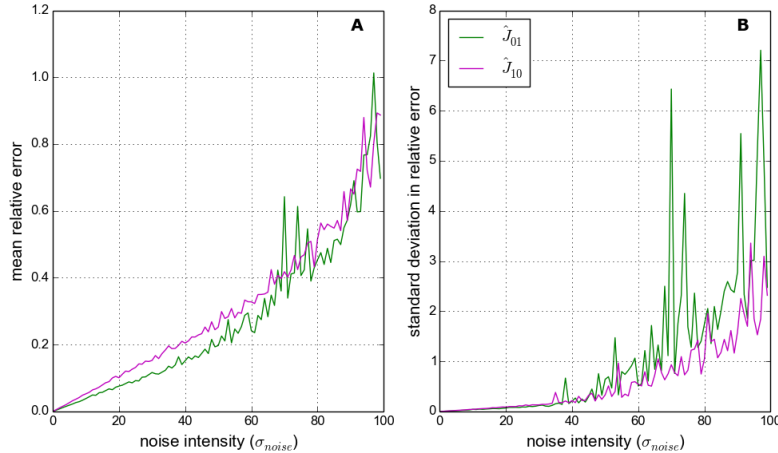


Figure 6.9: Nonsense. 1000 samples used.

### 6.3.2 Holling model

### 6.3.3 Range sampling

## 6.4 TEMP : other results

This section shows some plots which I was not planning to put into the thesis but are worth discussing..

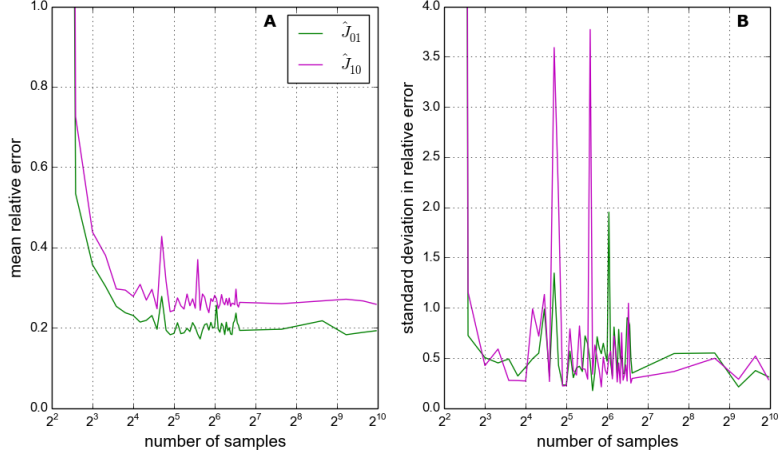


Figure 6.10: Nonsense. Noise is 50.

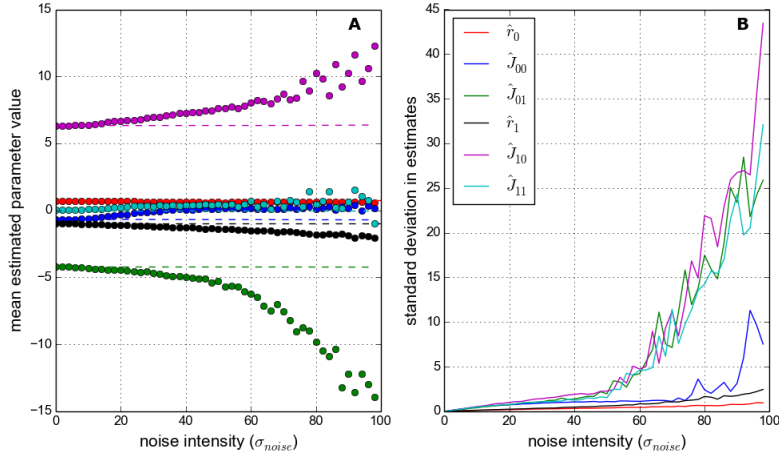


Figure 6.11: Nsamples is 10,000.

## 6.5 Application to IBM (optional)

In this section we apply the methodology for inferring species interactions to the IBM simulations. In the previous section we have seen that the method works well when fitting the GLV to two species predator-prey dynamics simulated with ODE models. In the case that the dynamics is governed by the Lotkva-Volterra equations, and in the absence of noise, fitting the GLV model produces true estimates of the underlying parameters which include the inter-specific interaction strengths. The estimates require relatively few samples in order to achieve high accuracy, and which converge on the true parameter values as the sampling intensity increases. However as noise is added to the simulations the accuracy of the estimates decreases. In particular we found that, in the presence of noise, the estimates do not converge on the true parameter values -

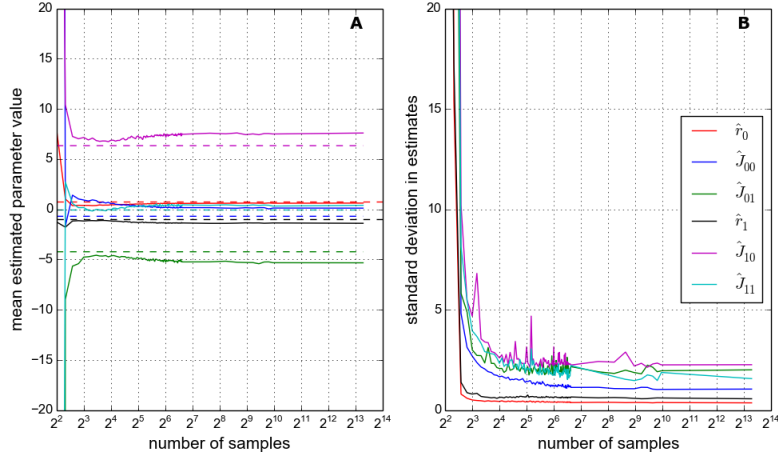


Figure 6.12: Noise is 50.

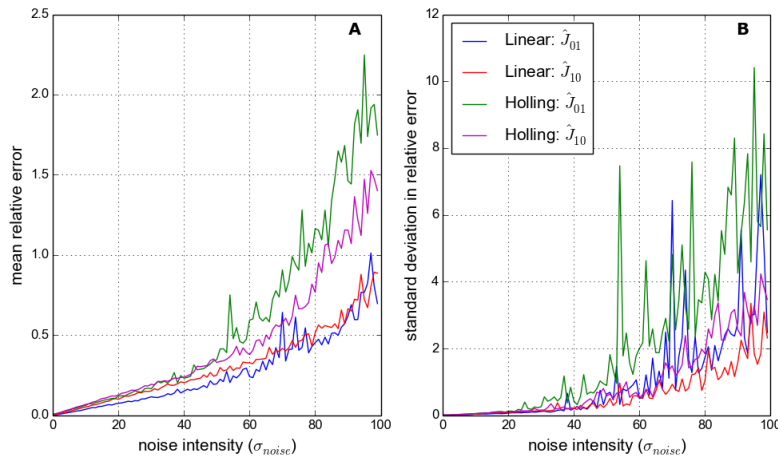


Figure 6.13: Noise is 50.

that is, noise introduces systematic error in to the estimates. In the case that the dynamics are governed by the Holling II model matters are complicated - but in general we find that the GLV can approximately capture the strength of species interactions (and also the dynamics?), provided there is not too much noise, and the FR is not too non-linear<sup>1</sup>.

Can the IBM dynamics by approximated by the GLV model? The hypothesis is that is can. Argue this..and refer to previous mention of LV type dynamics. Refer forward to testing linearity of FR. Exponential growth and decay, linear FR. However there are certain problem/factors that may hinder this approach/represent a departure from GLV dynamics...Noise, spatial effects, bioenergetic model - time delay? Immigration (one component of noise).

The issue of noise is important since, as we have shown in chapter REF, there is a strong

<sup>1</sup>This is all need to be demonstrated - WORK TO DO!

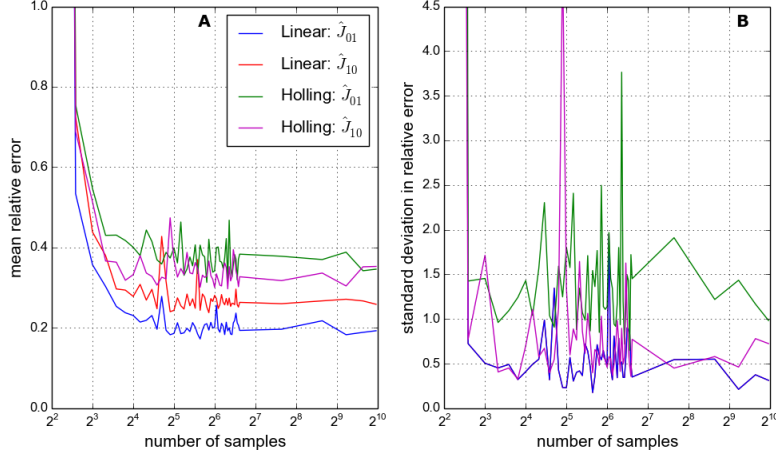


Figure 6.14: Noise is 50.

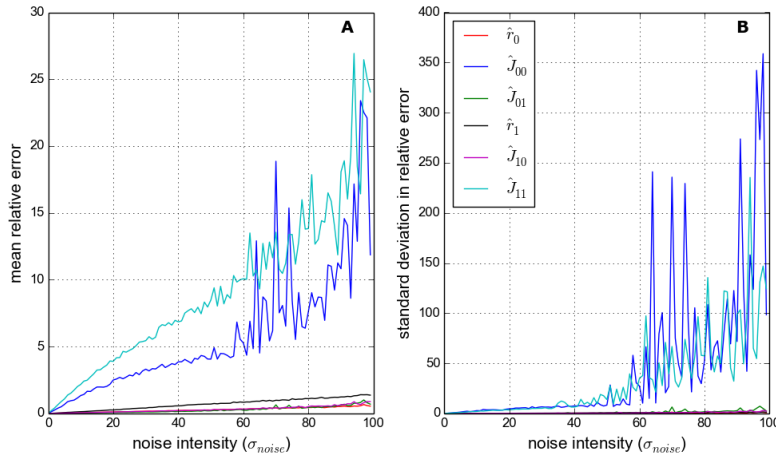


Figure 6.15: Nonsense. 1000 samples used.

stochastic component to the IBM simulations.

Modelling individuals, not biomass or energy. Is this problematic? Set herb-frac to 1. Other issues?

### 6.5.1 Testing functional response (and intrinsic growth functions)

Here we demonstrate the linearity of the predator functional response for animal predators in the second and third trophic levels (using 2sp and 3sp chain) - demonstrate that there is a slight difference. But basically linear. Other issues that may arise - high noise and low abundances create error.

We also conduct an experiment to test the intrinsic growth and death rates of plant and animal species - by setting herb-frac=0.0. Demonstrate they are well approximated by exponential.

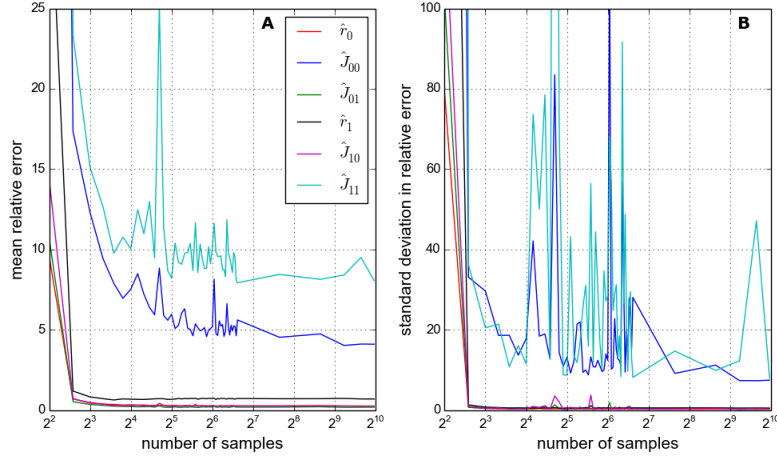


Figure 6.16: Nonsense. Noise is 50.

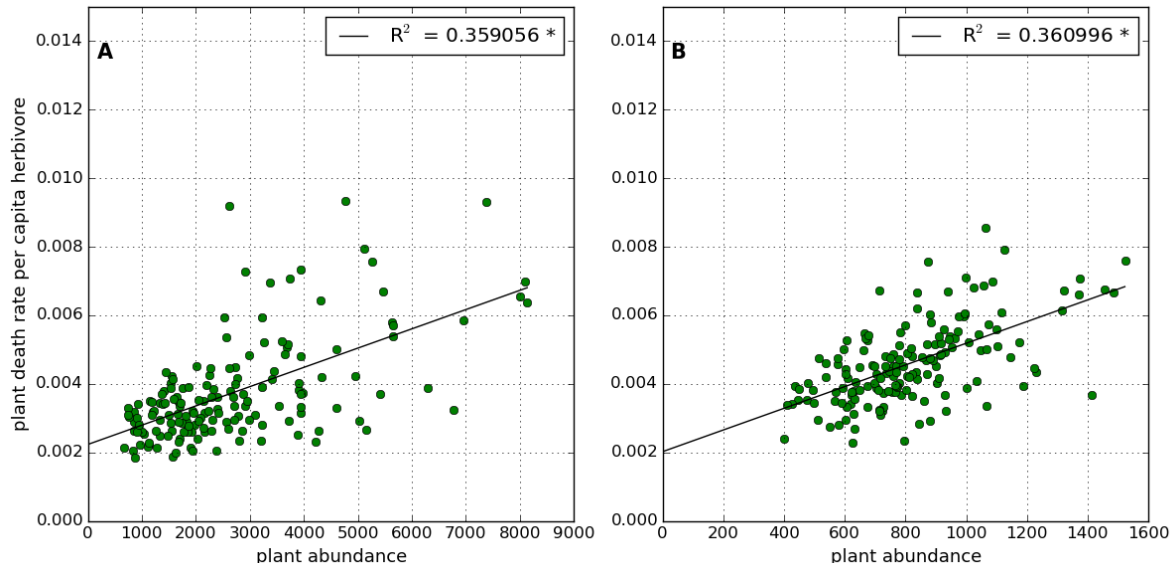


Figure 6.17: Plant functional response

In the absence of immigration.

Carrying capacity: is there evidence for density dependent birth/death? - use this fact in later analysis. Also discuss that the carrying capacity will vary with the number of species, not just a single species thing (non-pairwise interactions in competition for space - argghh!)

### 6.5.2 2 Species IBM model

IMPORTANT: carrying capacity depends on other species...introduce a new term into the model and test it?

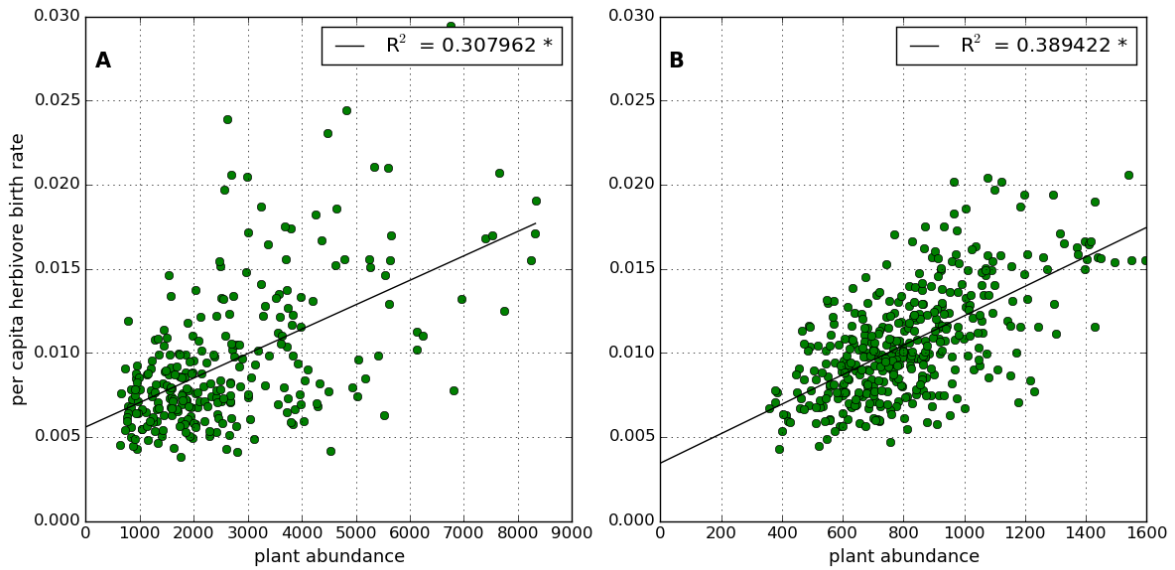


Figure 6.18: Herbivore functional response

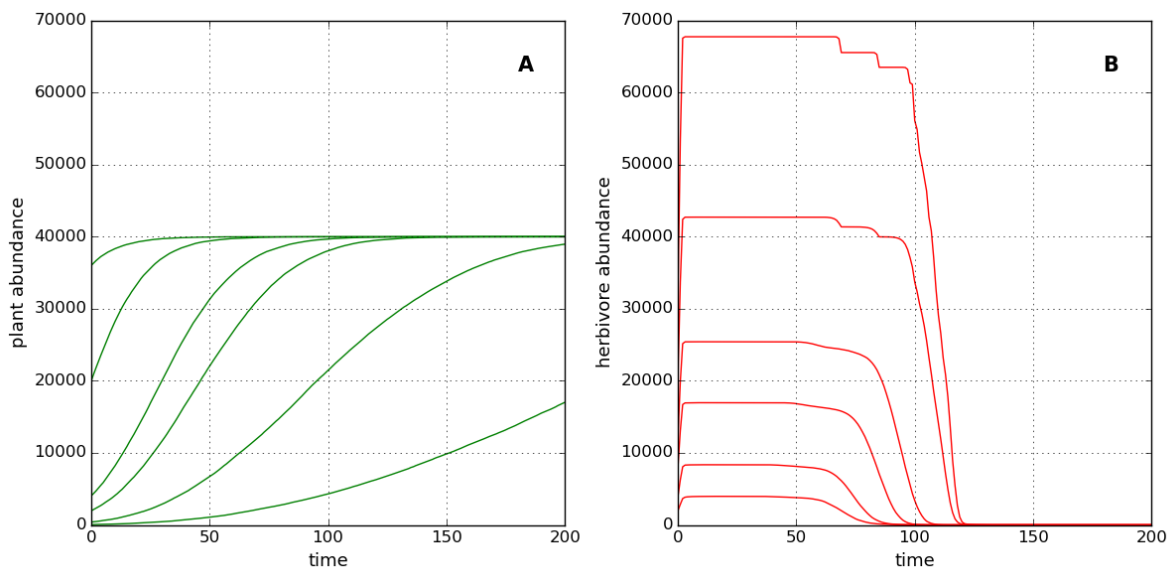


Figure 6.19: Intrinsic growth/mortality.

Define the model and what the inferred parameters represent:

- $J_{01}$ : per-capita rate consumption of the prey
- $J_{10}$ : per-capita rate reproduction of predator, due to consumption of prey. Not as well defined. But only source of predator births? Numerical response! (get REF)
- $J_{00}$ : intra-specific regulation of prey growth - see carrying capacity experiment.
- $J_{11}$ : intra-specific regulation of predator mortality? Check this. Expect zero? Or expect high number of predators means more reproduction because easier to find partner, therefore reduce mortality? Or increase birth rate. Not clear. Again SEE EXPERIMENT.
- $r_0$ : prey intrinsic growth rate. Estimate from exp?
- $r_1$ : predator intrinsic mortality rate. Estimate from exp?

So we know what values to expect, or at least the signs. We can evaluate the model fit by comparing the values of these estimates with birth/death rates from the simulations. Although not totally fair. We can also simulate GLV with the inferred parameters - does it match. Is the equilibrium the same? And check the error function of the fit. We show all this in the results section below.

**Dynamics of the model** we two species is a new thing. Here we show that with the default parameters we get relaxation-type oscillations. This is interesting, we try fitting to these in the two species case. But they become problematic for larger number of species. Argue why. Therefore we increase the reproduction rate (refer to previous chapter), which creates more WORD dynamics. We also fit to these.

PLOT: DYNAMICS UNDER IR, RR AND HL.

Also show dependence on immigration (show that it is low and what happens if it is high), concede that this is a limitation.

### 6.5.3 Extend methodology (3, 4 and 5 species)

MULTI-SPECIES DENSITY DEPENDENCE?!

This does not require much since we presented a general framework previously.

Show 3 species dynamics with the two different RR. Conclude which is better.

### 6.5.4 Results

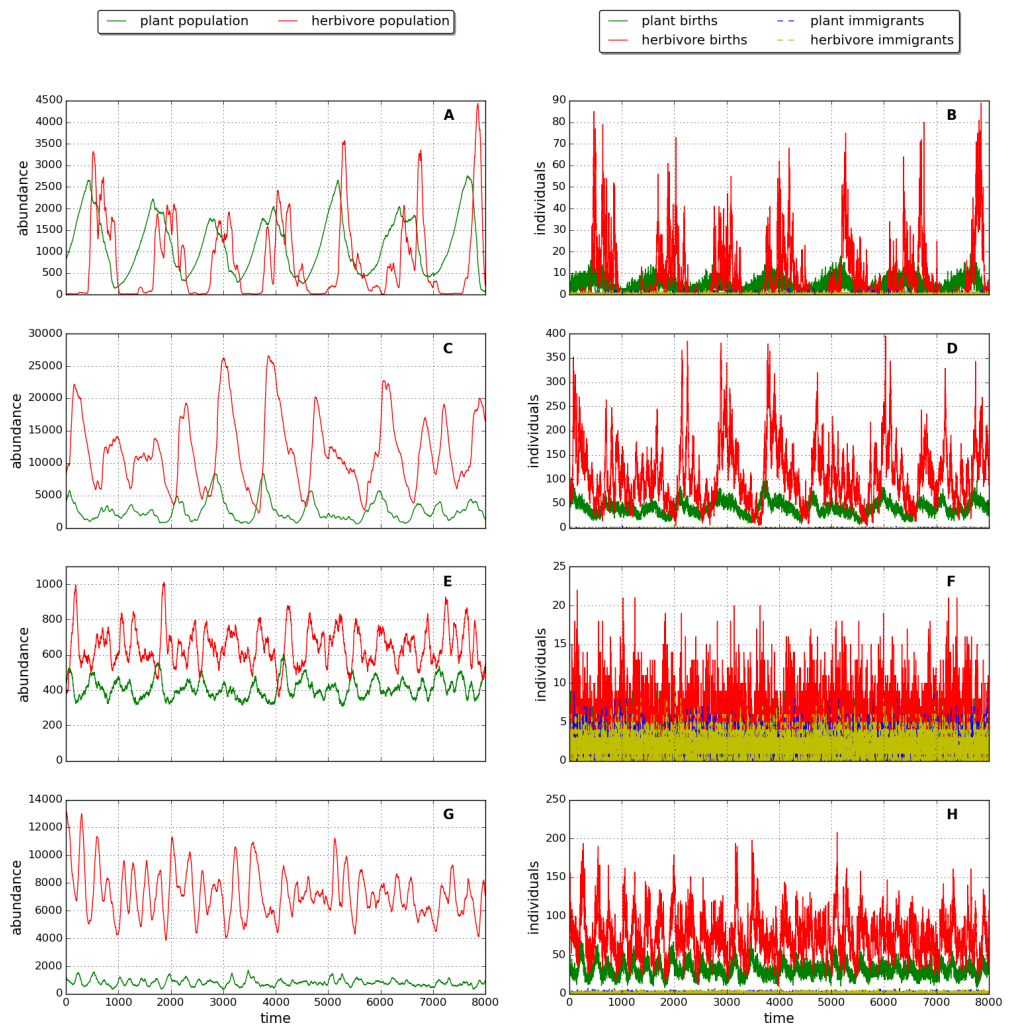


Figure 6.20: 2 species dynamics

### 6.5.5 2 species

Here we compare the results of two species.

For a single IR we look at convergence of all 6 parameters (over the ensemble) - correct signs, correct magnitudes?

Maybe repeat for other IRs and HL.

We then show rate estimates as time series and introduce quality metric for this<sup>2</sup>.

Demonstrate the quality decreases with IR and HL (box plot?). And how estimated parameters respond to the two HL scenarios (refer to previous findings). Hopefully support!

---

<sup>2</sup>Still not sure about this

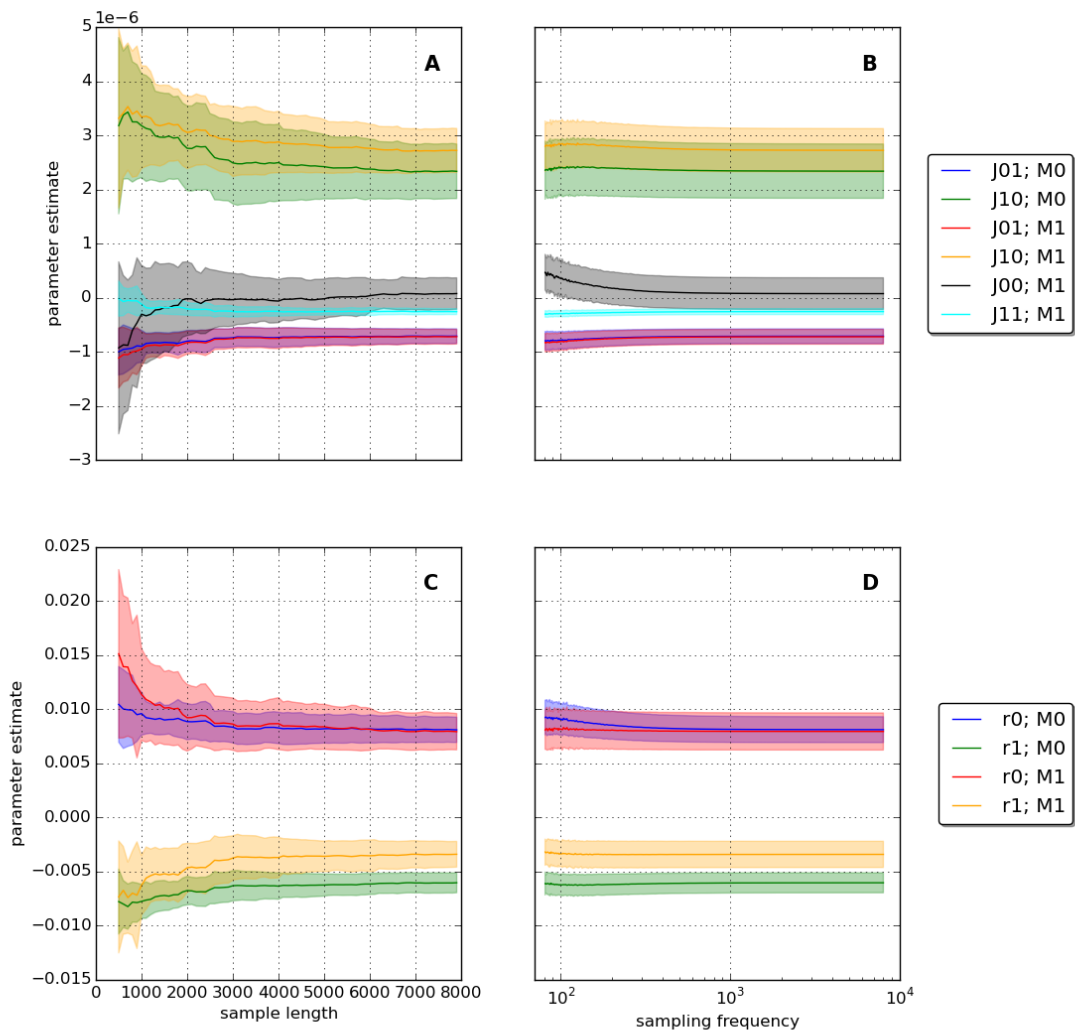


Figure 6.21: Convergence of estimates. 2 species.

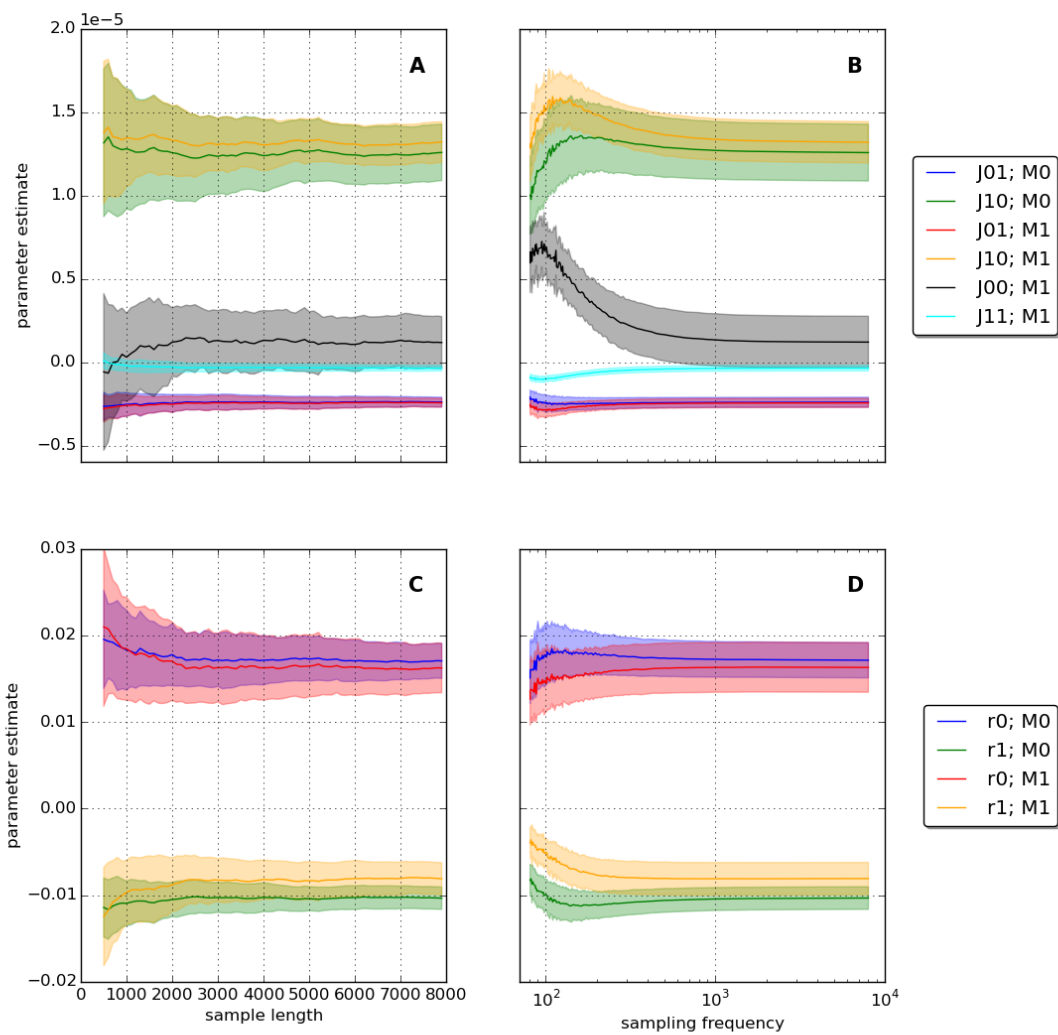


Figure 6.22: Convergence of estimates. 2 species.

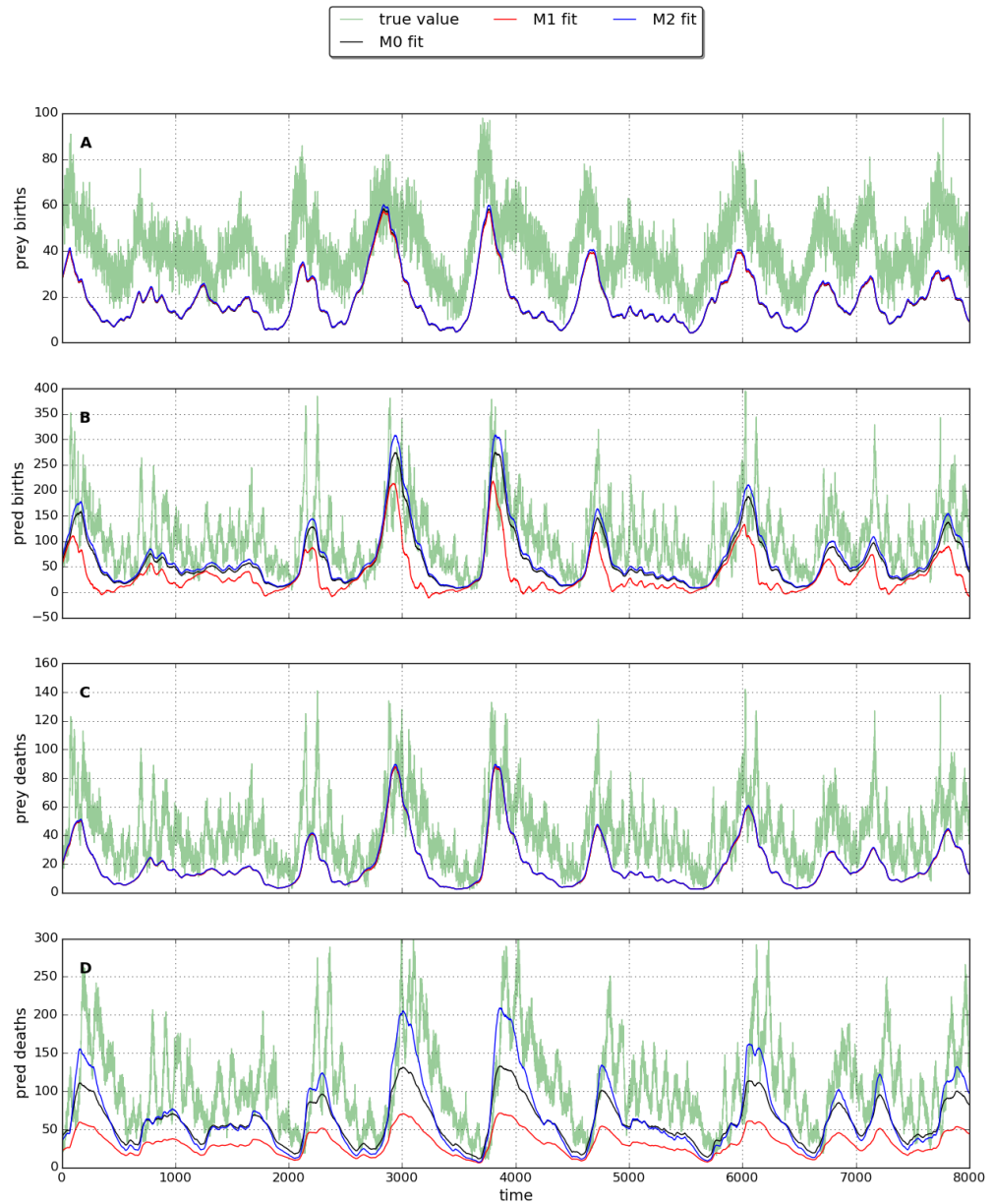


Figure 6.23: Predicted births/deaths. Low IR.

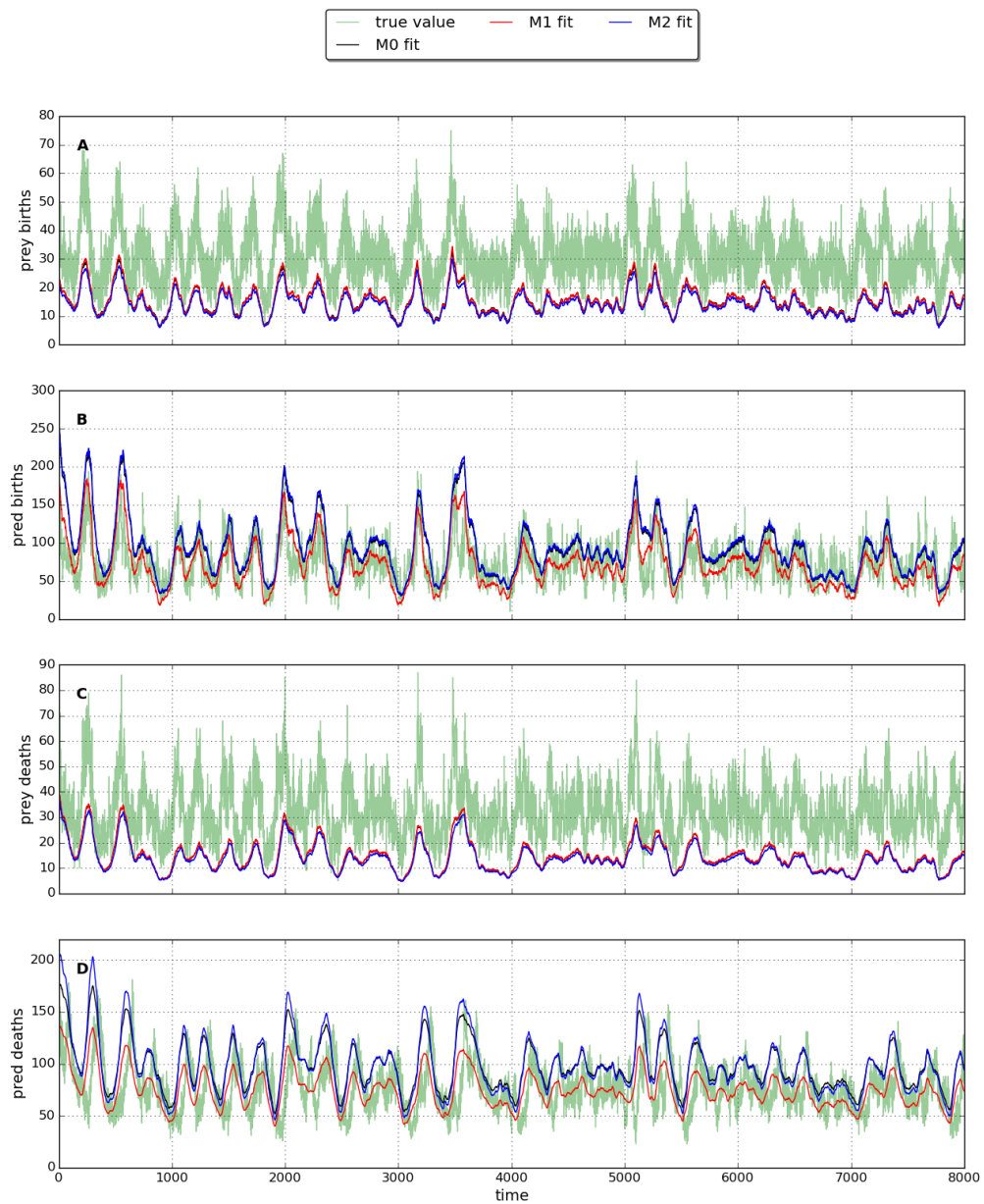


Figure 6.24: Predicted births/deaths. High IR.

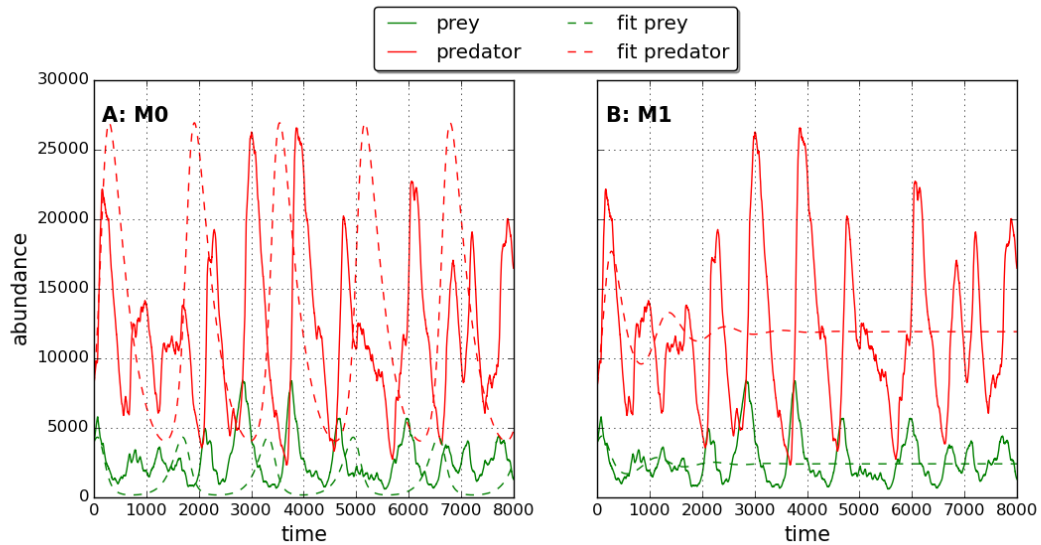


Figure 6.25: Fitted dynamics.

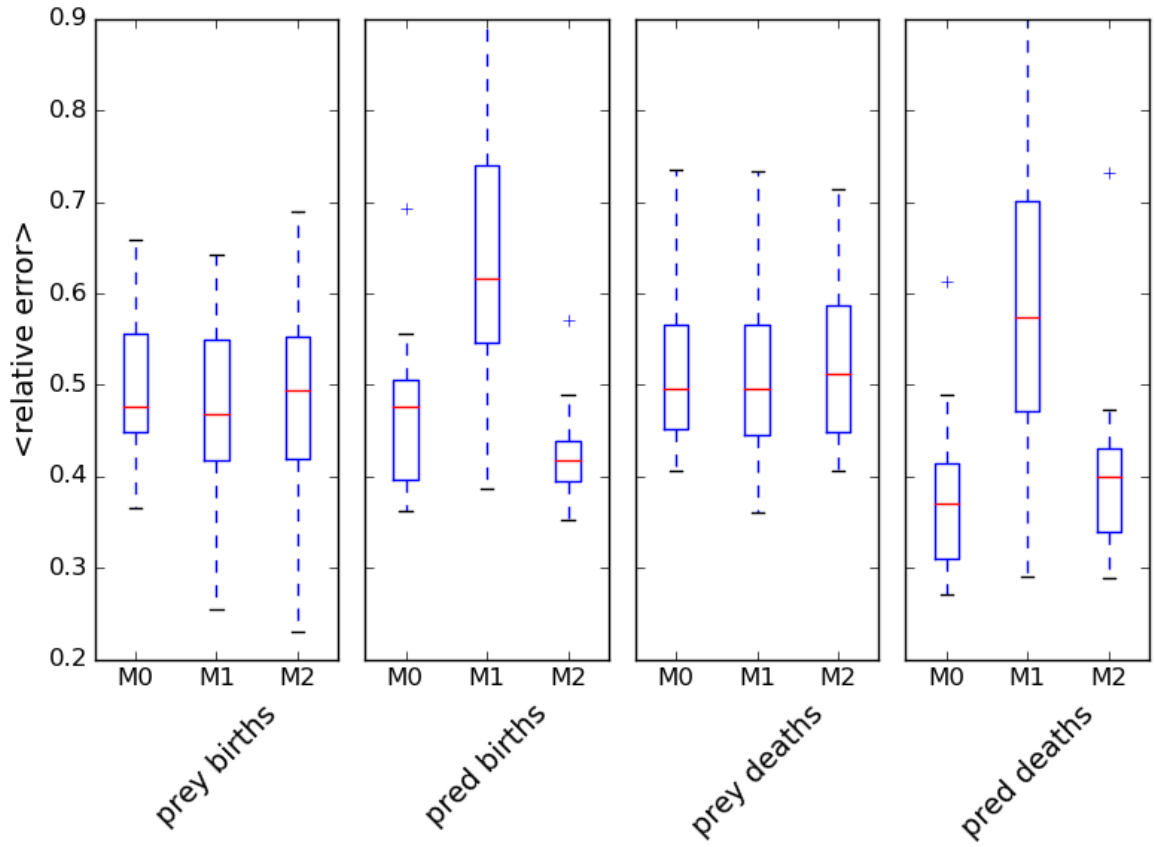


Figure 6.26: Quality. LI.

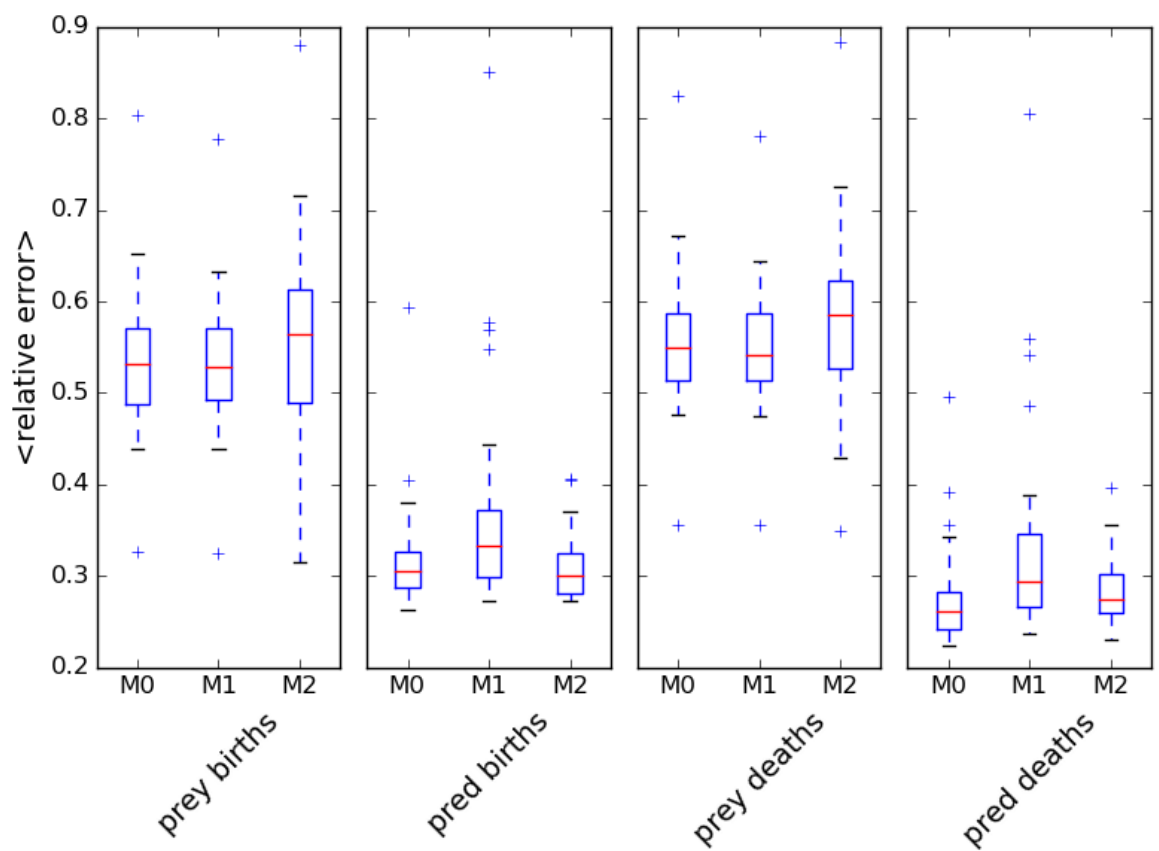


Figure 6.27: Fitted dynamics.

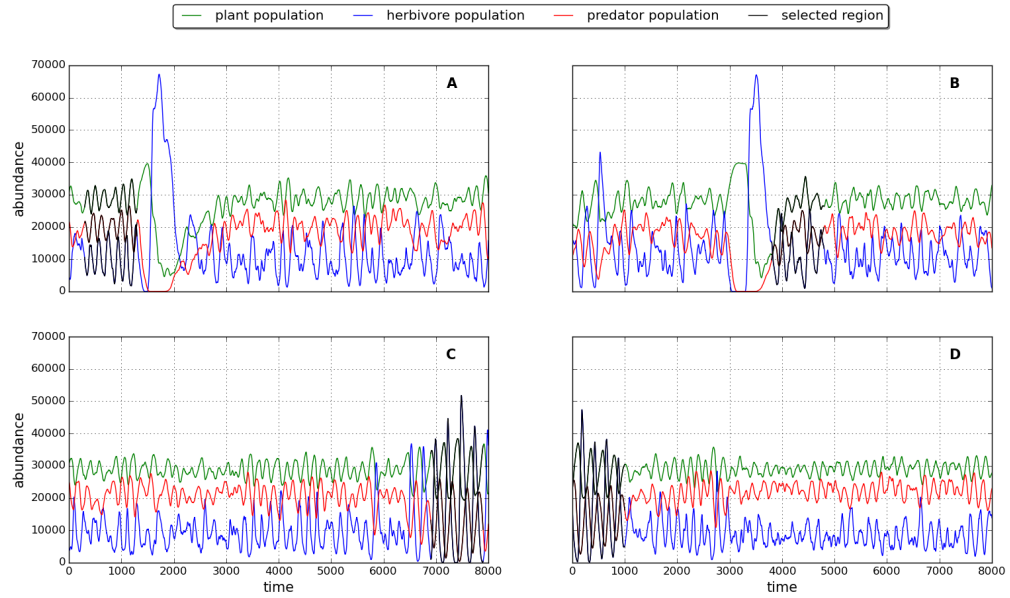


Figure 6.28: 3 species dynamics

### 6.5.6 3 species

The two species results suggest that intra-specific interactions contribute to predator deaths, whereas they contribute to prey births. This is problematic for rate estimation since we are starting from the position of not knowing which species are basal. For the purposes of calculating the rate we pretend that we know...This is in agreement with the Lotka-Volterra formulation.

The alternative convention is that intra-specific interactions are

Extra term does not improve the estimates.

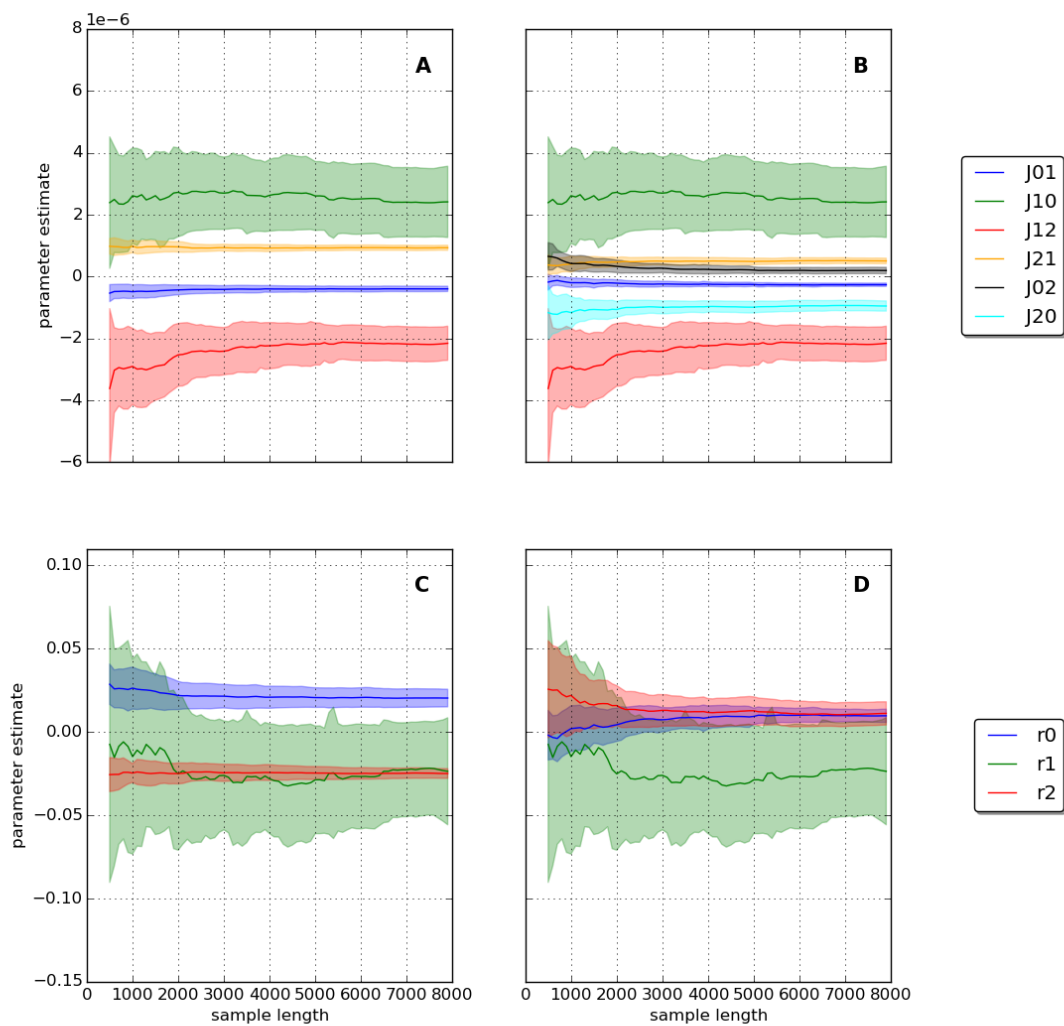


Figure 6.29: Convergence of estimates. 3 species.

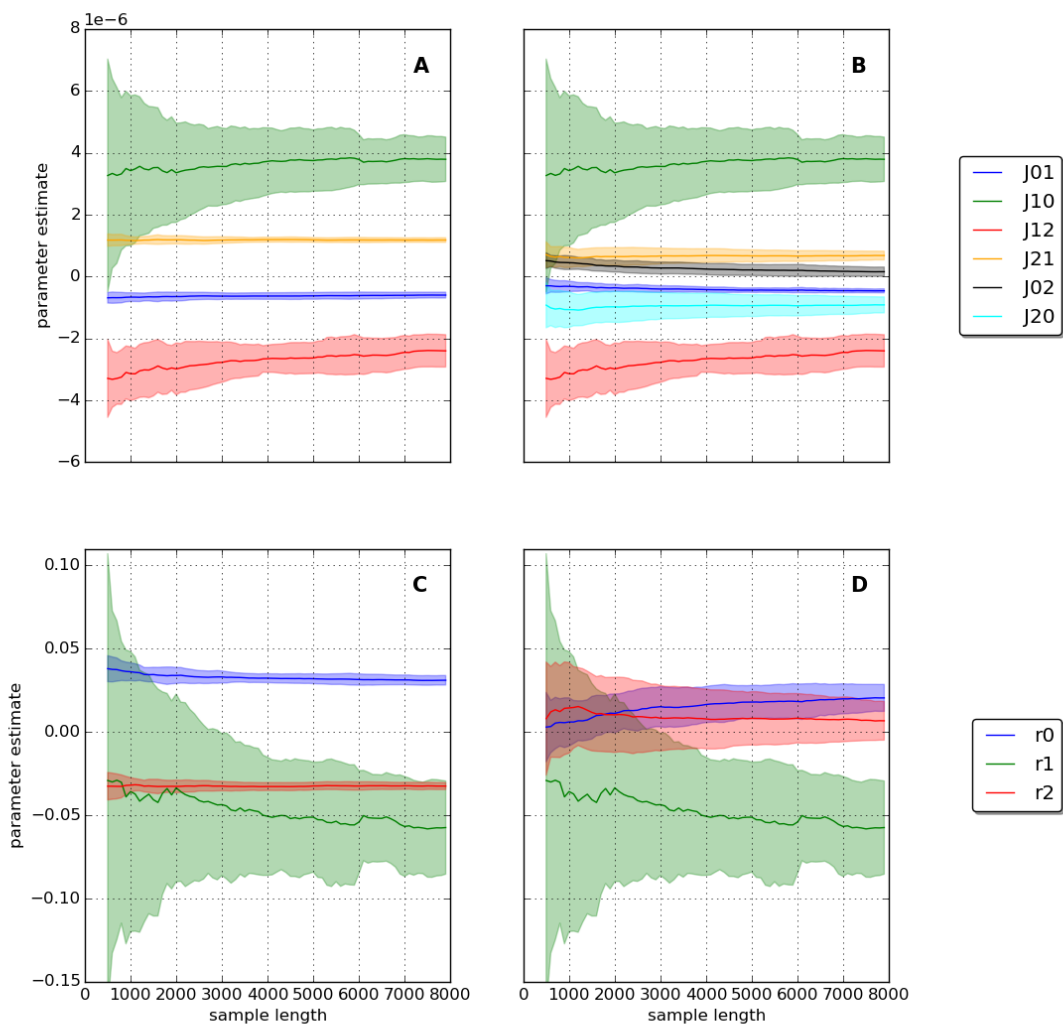


Figure 6.30: Convergence of estimates. 3 species.

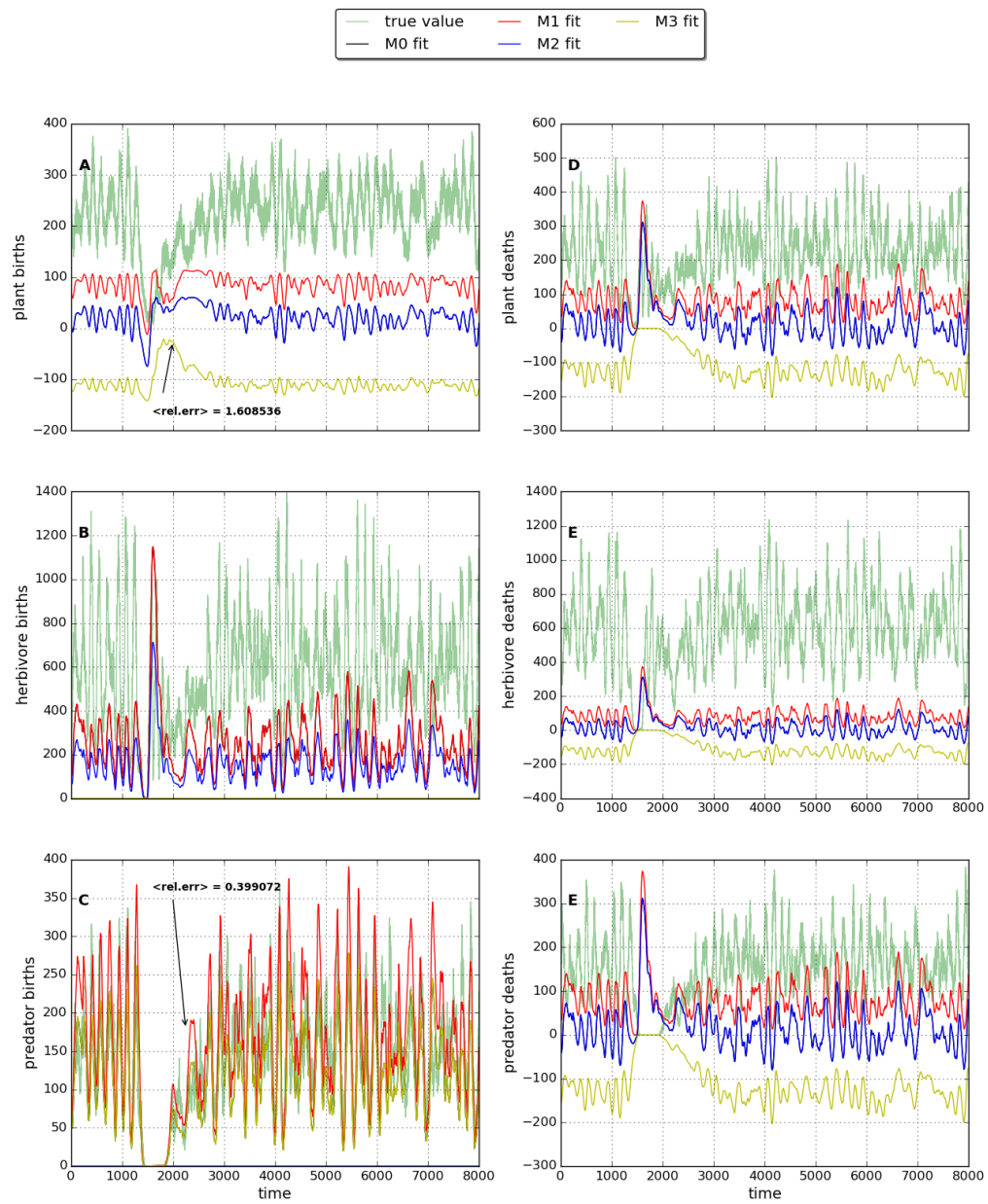


Figure 6.31: Predicted births/deaths. Low IR.

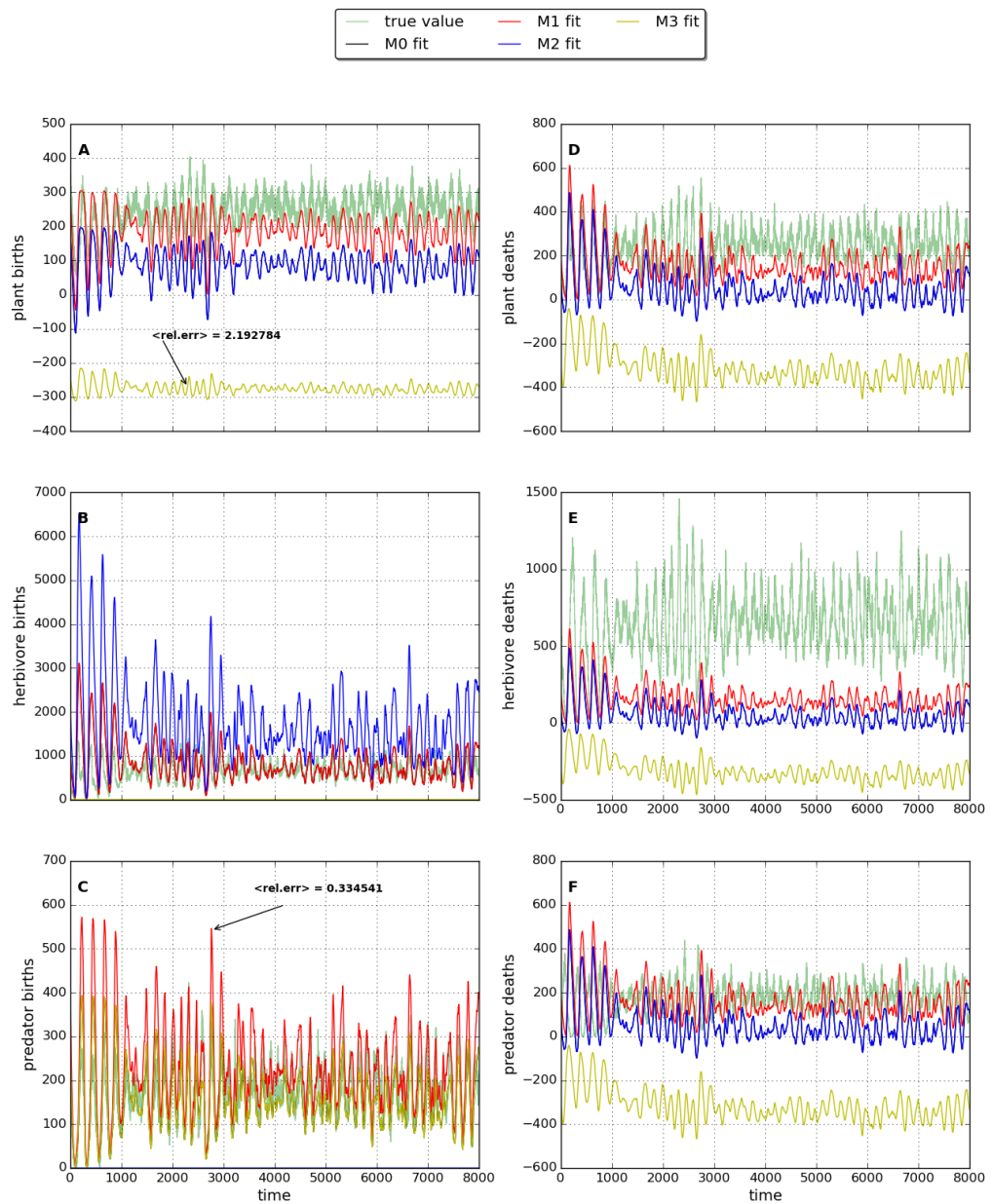


Figure 6.32: Predicted births/deaths. High IR.

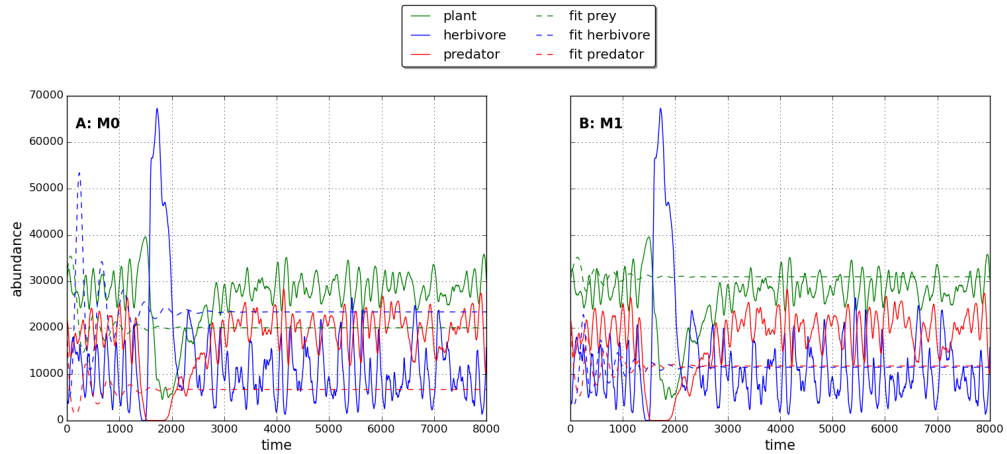


Figure 6.33: Fitted dynamics.

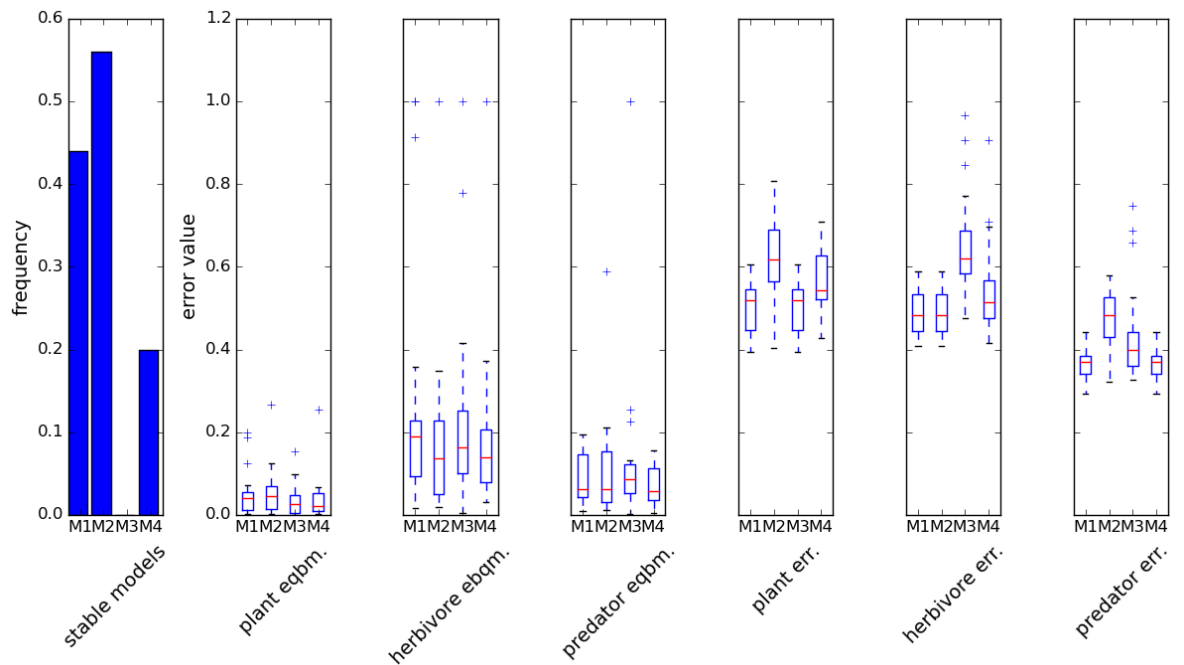


Figure 6.34: Stability and error

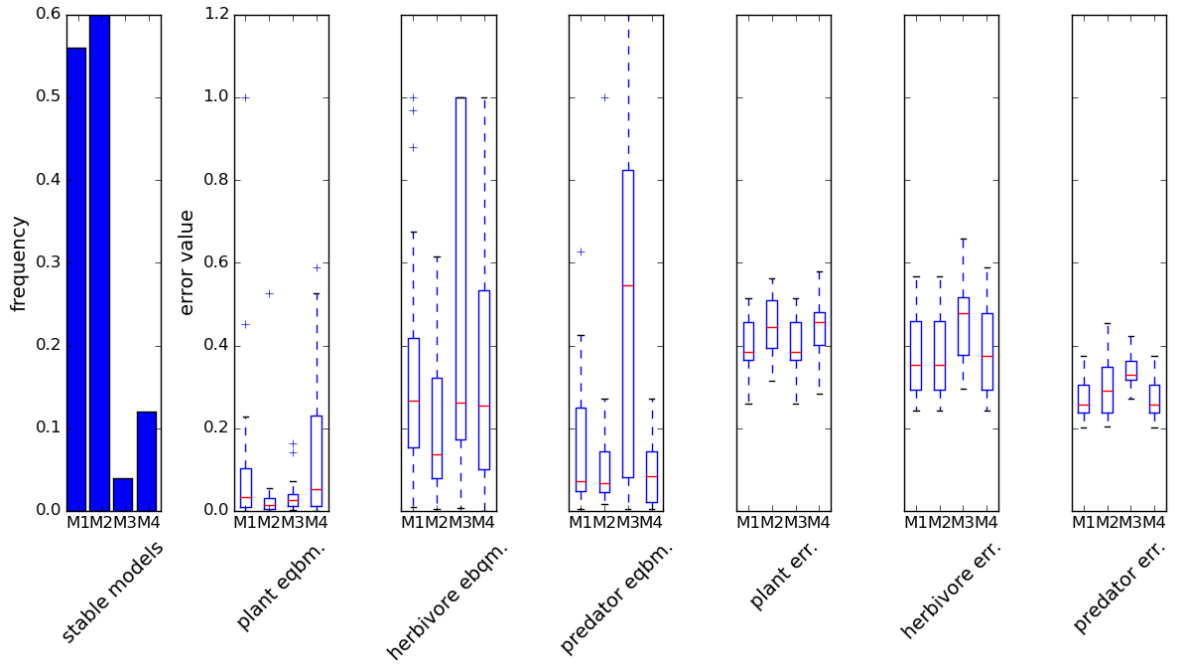


Figure 6.35: Stability and error

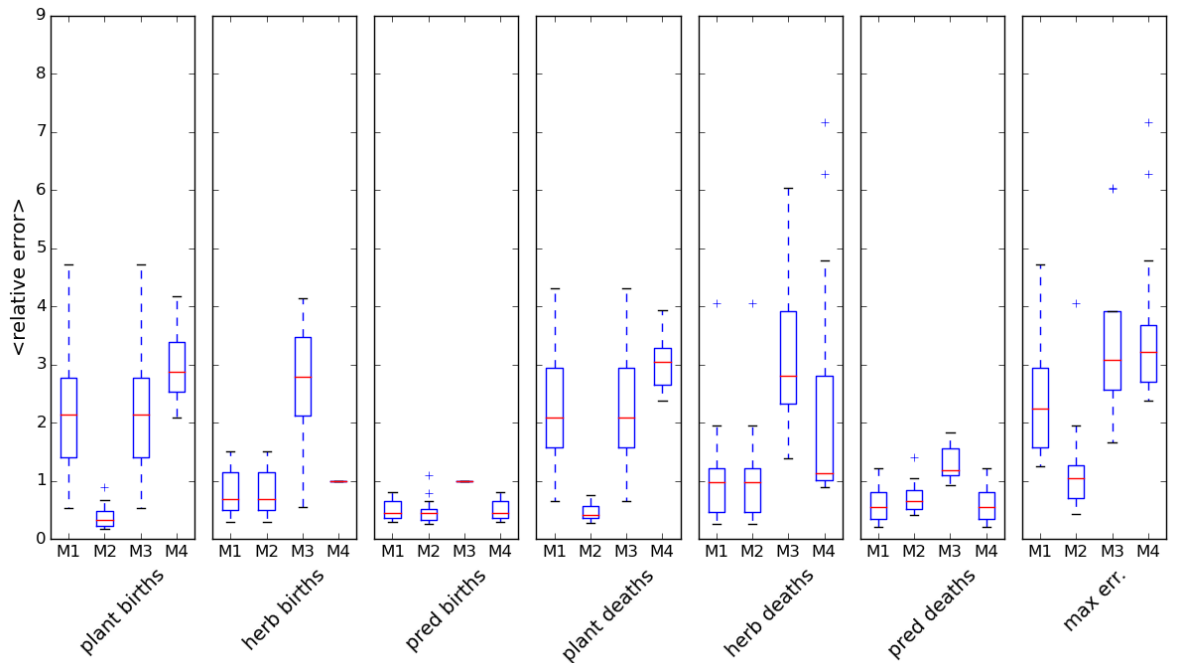


Figure 6.36: Quality 3sp LI

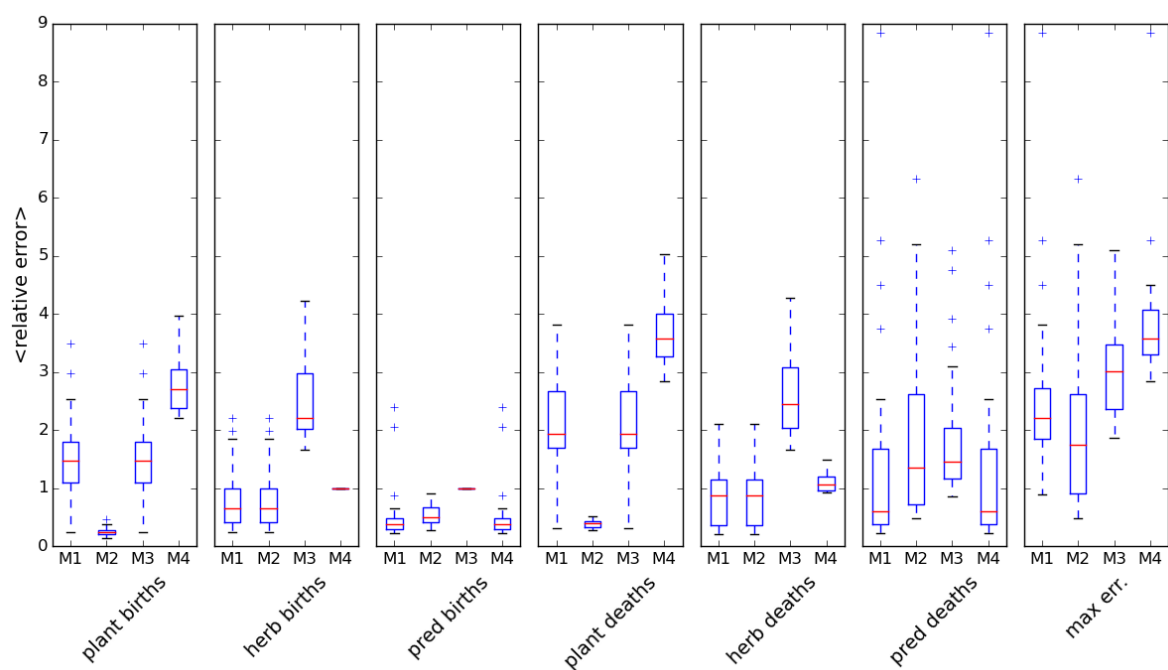


Figure 6.37: Quality 3sp HI

**6.5.7 5 species**

## 6.5. APPLICATION TO IBM (OPTIONAL)

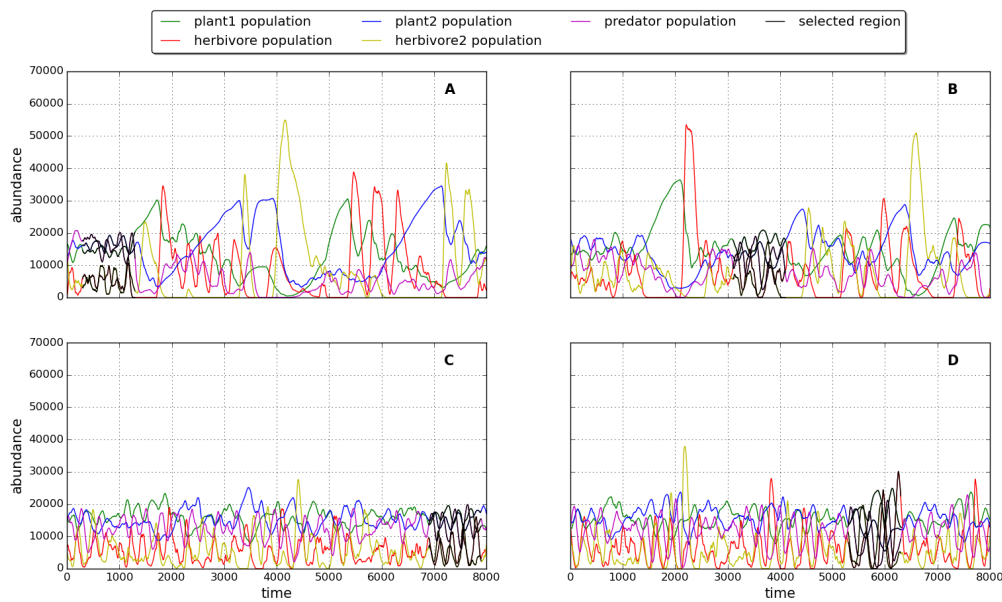


Figure 6.38: 5 species dynamics

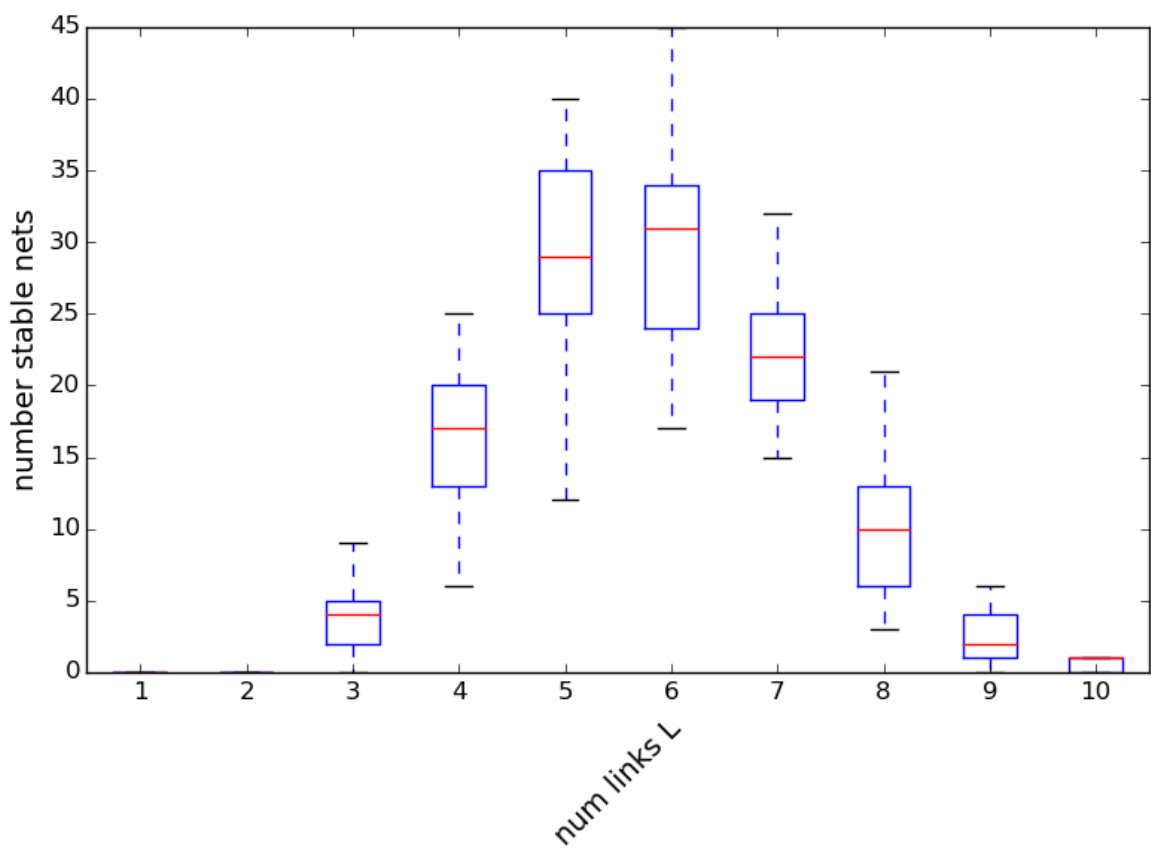


Figure 6.39: 5 species: number of stable models

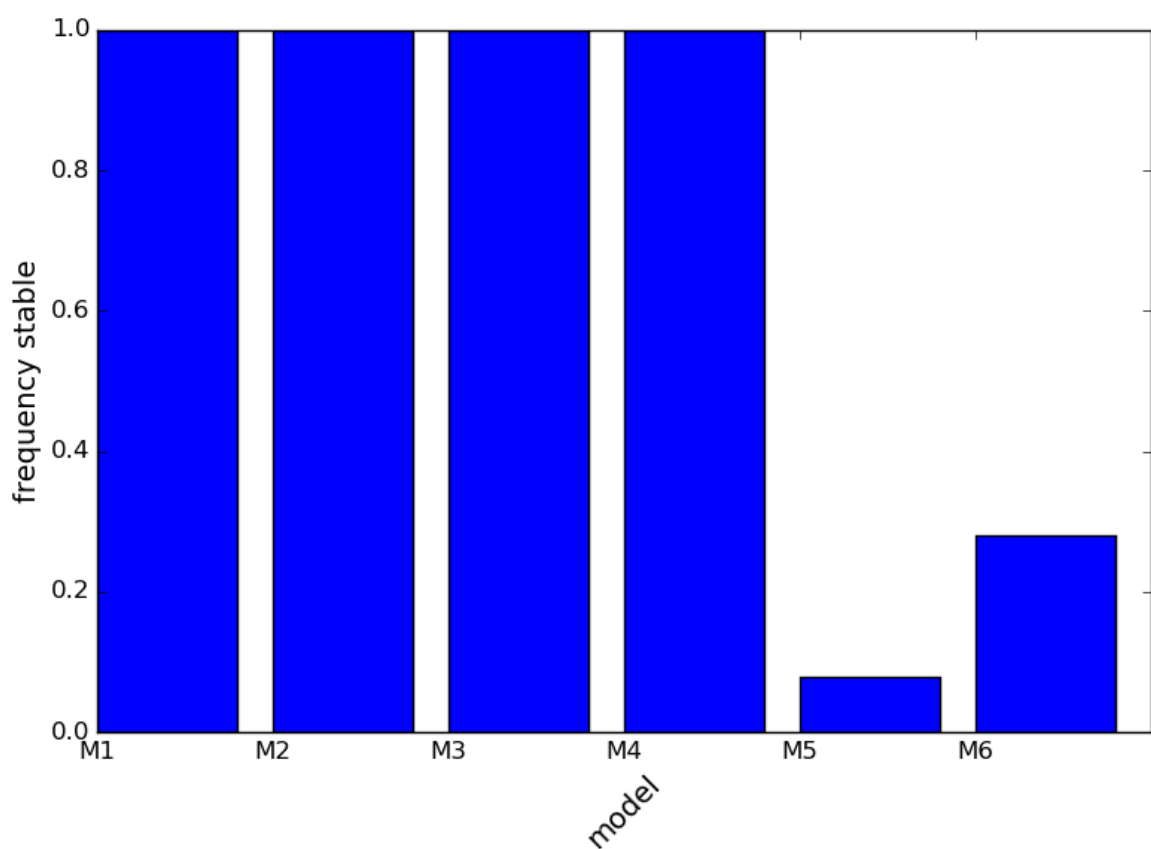


Figure 6.40: 5 species: stability of selected models

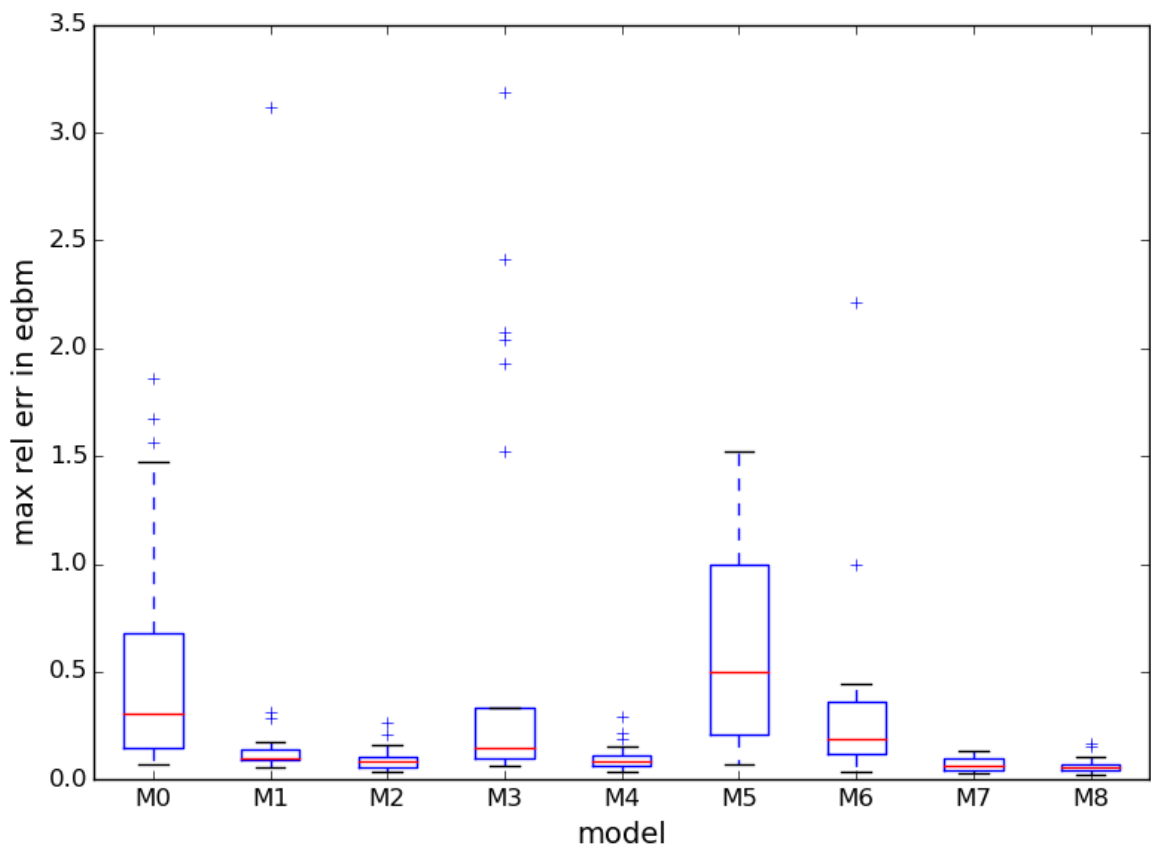


Figure 6.41: 5 species: error in equilibrium

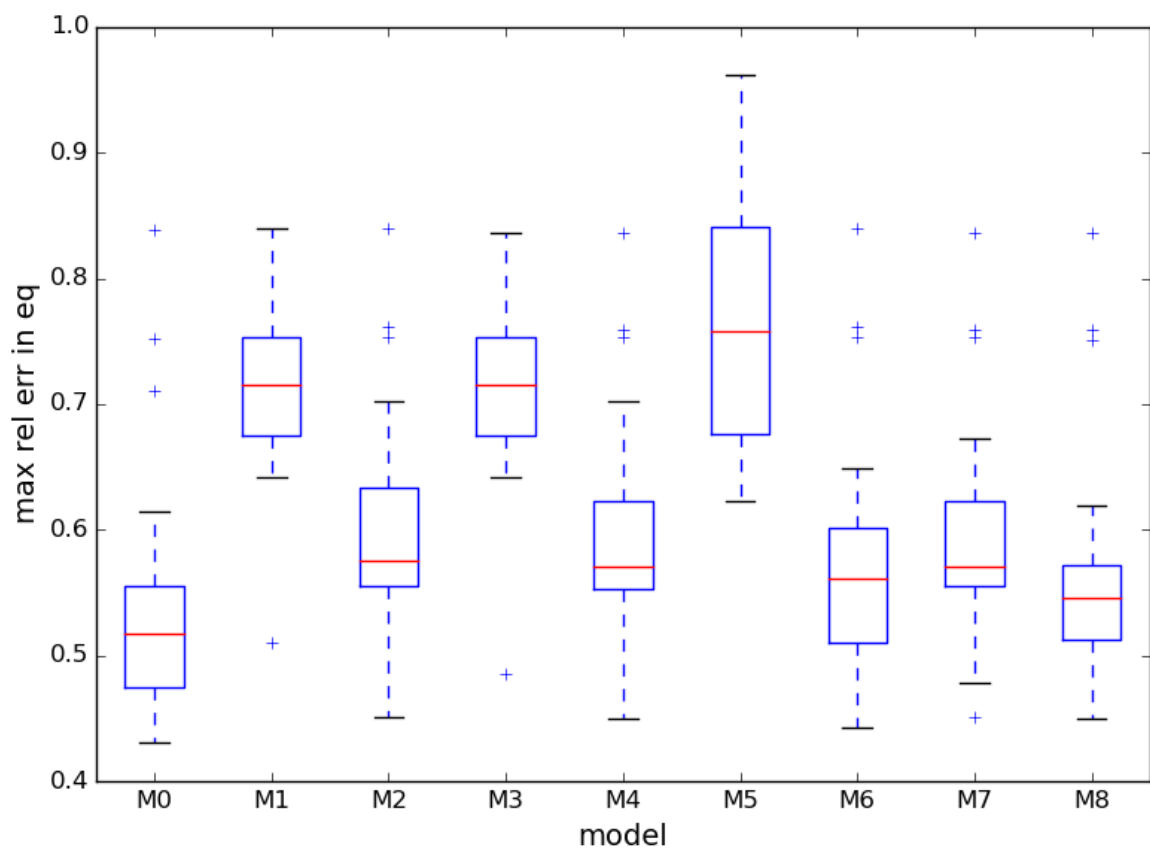


Figure 6.42: 5 species: error in gradient fit function

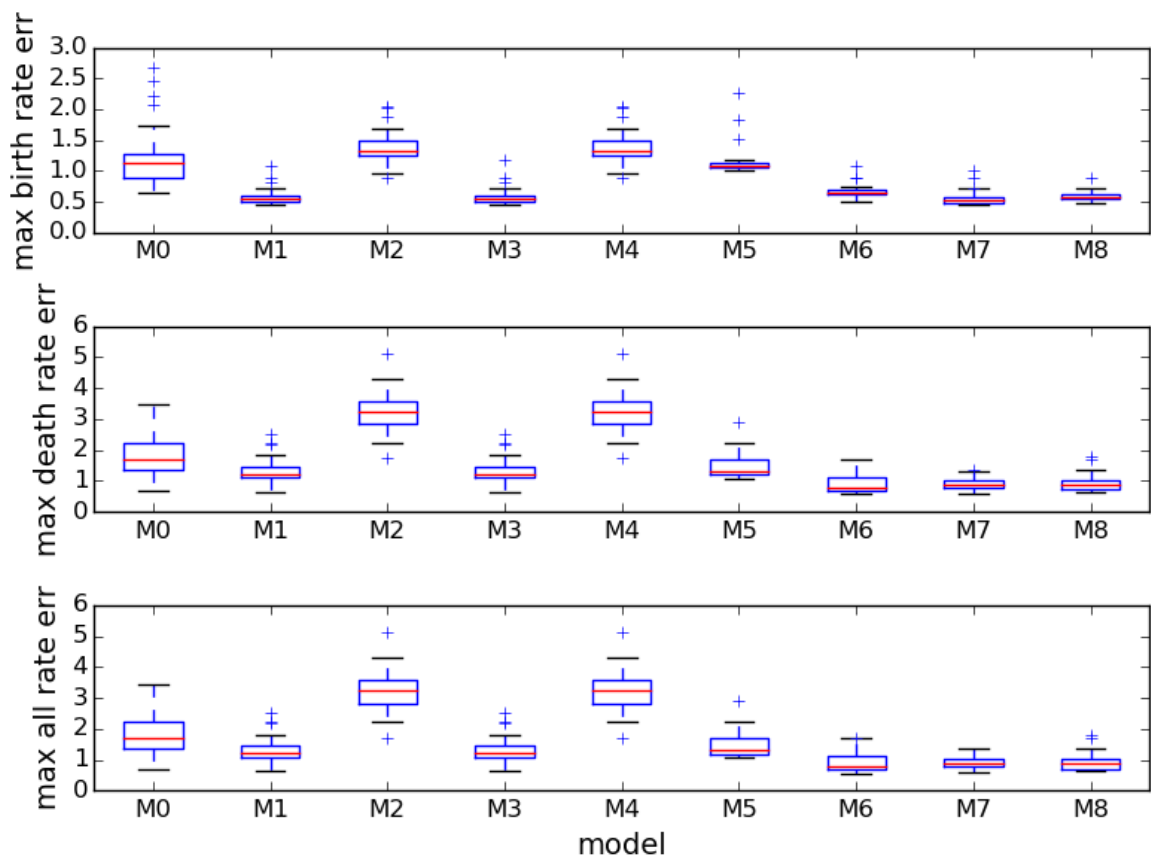


Figure 6.43: 5 species: errors in rate estimates

## 6.5. APPLICATION TO IBM (OPTIONAL)

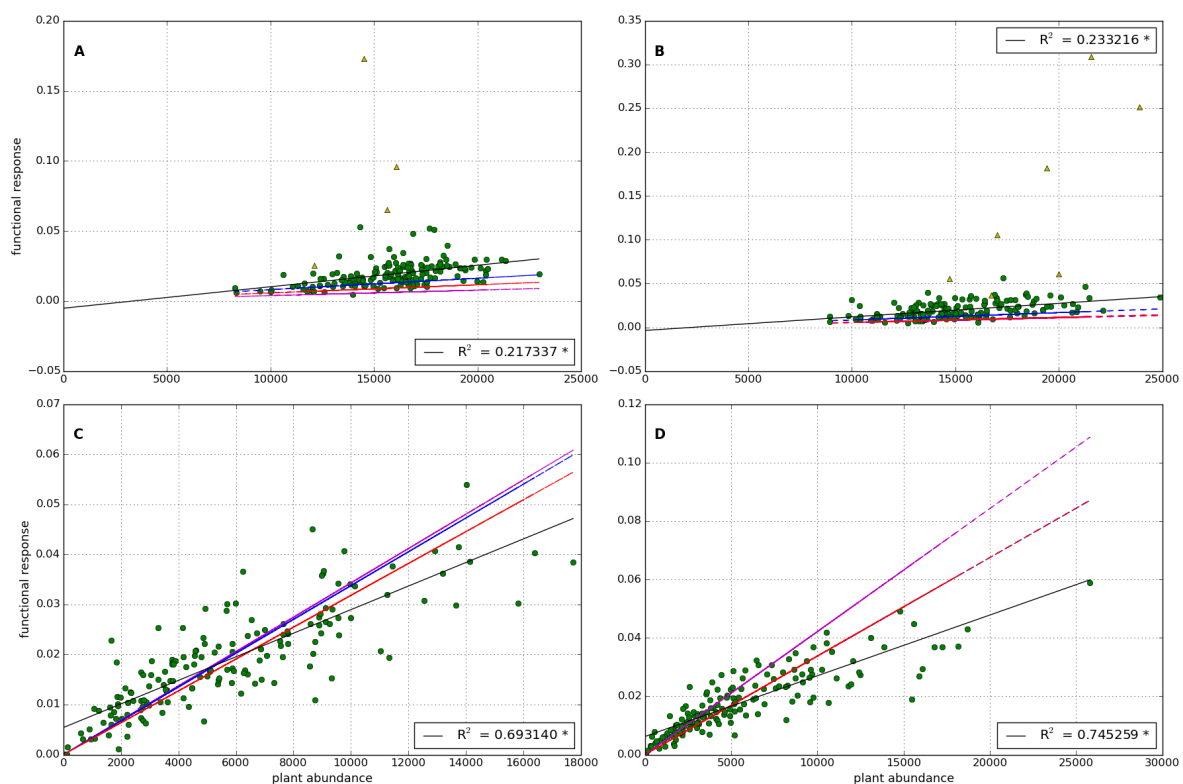


Figure 6.44: 5 species: functional response (High IR)

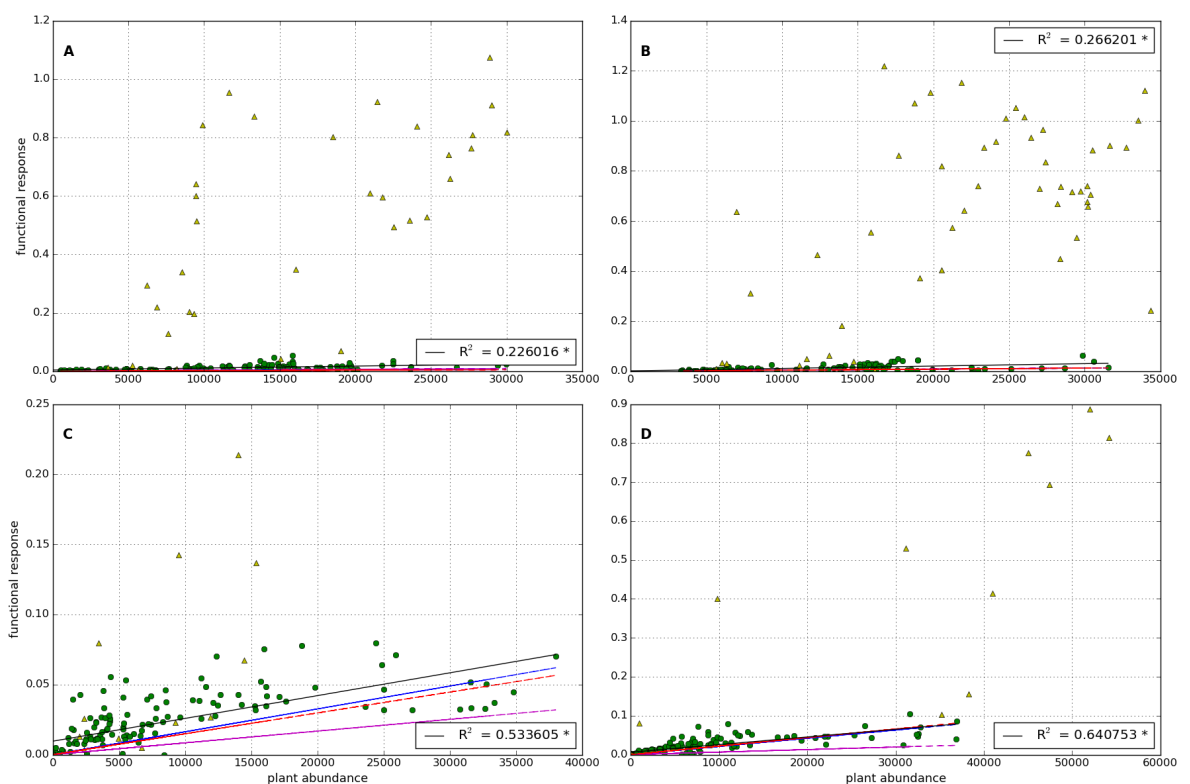


Figure 6.45: 5 species: functional response (Low IR)

## 6.6 Discussion

Points referenced in text above, make sure to discuss them!..

- Discuss how this methodology could be used on empirical data...
- Limitations of ODE models (non-spatial, response to debate on FR)
- Possibility of extending to more than two species systems (if this is actually done then change ref in text above)
- discussion of other forms of FR (not H) - or discussed already in intro?
- good GLV fit to LV even with 100 sample points - realistic?
- how good is the method of model fitting. Discuss more computationally expensive options (mentioned in section on Timme method)
- Spatial heterogeneity - we do not explore this here, but acknowledge that it represents a source of error. Gives example in extremis - 2 species only interacting on boundary. Also we know that there is some level of spatial aggregation, especially at low IR - possibly show one plot of this?
- Could introduce prey handling to IBM to create non-linear FR.
- Our method could be used to pick out coupling to other variables e.g environmental (temperature) if expressed in a certain way.
- In real application would not have luxury of selecting the section of time series with best fit! Would be lucky to have 1000 time points at all!



## BIBLIOGRAPHY

- [1] D. AI, P. DESJARDINS-PROULX, C. CHU, AND G. WANG, *Immigration, local dispersal limitation, and the repeatability of community composition under neutral and niche dynamics*, (2012).
- [2] M. ALBRECHT, P. DUELLI, B. SCHMID, AND C. B. MÜLLER, *Interaction diversity within quantified insect food webs in restored and adjacent intensively managed meadows*, Journal of Animal Ecology, 76 (2007), pp. 1015–1025.
- [3] E. ANDERSON, Z. BAI, C. BISCHOF, S. BLACKFORD, J. DEMMEL, J. DONGARRA, J. DU CROZ, A. GREENBAUM, S. HAMMARLING, A. MCKENNEY, AND D. SORENSEN, *LAPACK Users' Guide*, Society for Industrial and Applied Mathematics, Philadelphia, PA, third ed., 1999.
- [4] T. APARICIO, E. F. POZO, AND D. SAURA, *Detecting determinism using recurrence quantification analysis: Three test procedures*, Journal of Economic Behavior & Organization, 65 (2008), pp. 768–787.
- [5] J. BASCOMPTE AND P. JORDANO, *Plant-animal mutualistic networks: the architecture of biodiversity*, Annual Review of Ecology, Evolution, and Systematics, (2007), pp. 567–593.
- [6] E. L. BERLOW, A.-M. NEUTEL, J. E. COHEN, P. C. DE RUITER, B. EBENMAN, M. EMMERSON, J. W. FOX, V. A. JANSEN, J. IWAN JONES, G. D. KOKKORIS, ET AL., *Interaction strengths in food webs: issues and opportunities*, Journal of animal ecology, 73 (2004), pp. 585–598.
- [7] N. BLÜTHGEN, J. FRÜND, D. P. VÁZQUEZ, AND F. MENZEL, *What do interaction network metrics tell us about specialization and biological traits*, Ecology, 89 (2008), pp. 3387–3399.
- [8] D. BOSSIO, M. S. GIRVAN, L. VERCHOT, J. BULLIMORE, T. BORELLI, A. ALBRECHT, K. SCOW, A. S. BALL, J. PRETTY, AND A. M. OSBORN, *Soil microbial community response to land use change in an agricultural landscape of western kenya*, Microbial ecology, 49 (2005), pp. 50–62.

## BIBLIOGRAPHY

---

- [9] M. W. CADOTTE, *Dispersal and species diversity: A meta-analysis*, The American Naturalist, 167 (2006), pp. 913–924.
- [10] R. CONDIT, R. A. CHISHOLM, AND S. P. HUBBELL, *Thirty years of forest census at barro colorado and the importance of immigration in maintaining diversity*, (2012).
- [11] K. Z. COYTE, J. SCHLUTER, AND K. R. FOSTER, *The ecology of the microbiome: Networks, competition, and stability*, Science, 350 (2015), pp. 663–666.
- [12] C. DARWIN AND W. F. BYNUM, *The origin of species by means of natural selection: or, the preservation of favored races in the struggle for life*, AL Burt, 2009.
- [13] A. DOBSON, D. LODGE, J. ALDER, G. S. CUMMING, J. KEYMER, J. MCGLADE, H. MOONEY, J. A. RUSAK, O. SALA, V. WOLTERS, ET AL., *Habitat loss, trophic collapse, and the decline of ecosystem services*, Ecology, 87 (2006), pp. 1915–1924.
- [14] K. L. DRURY, J. D. SUTER, J. B. RENDALL, A. M. KRAMER, AND J. M. DRAKE, *Immigration can destabilize tri-trophic interactions: implications for conservation of top predators*, Theoretical Ecology, (2015), pp. 1–12.
- [15] J. A. DUNNE, R. J. WILLIAMS, AND N. D. MARTINEZ, *Food-web structure and network theory: the role of connectance and size*, Proceedings of the National Academy of Sciences, 99 (2002), pp. 12917–12922.
- [16] D. M. EVANS, M. J. POCOCK, AND J. MEMMOTT, *The robustness of a network of ecological networks to habitat loss*, Ecology letters, 16 (2013), pp. 844–852.
- [17] E. S. EVELEIGH, K. S. MCCANN, P. C. McCARTHY, S. J. POLLOCK, C. J. LUCAROTTI, B. MORIN, G. A. McDougall, D. B. STRONGMAN, J. T. HUBER, J. UMBANHOWAR, ET AL., *Fluctuations in density of an outbreak species drive diversity cascades in food webs*, Proceedings of the National Academy of Sciences, 104 (2007), pp. 16976–16981.
- [18] R. M. EWERS, R. K. DIDHAM, L. FAHRIG, G. FERRAZ, A. HECTOR, R. D. HOLT, V. KAPOS, G. REYNOLDS, W. SINUN, J. L. SNADDON, ET AL., *A large-scale forest fragmentation experiment: the stability of altered forest ecosystems project*, Philosophical Transactions of the Royal Society of London B: Biological Sciences, 366 (2011), pp. 3292–3302.
- [19] J. A. FOLEY, R. DEFRIES, G. P. ASNER, C. BARFORD, G. BONAN, S. R. CARPENTER, F. S. CHAPIN, M. T. COE, G. C. DAILY, H. K. GIBBS, ET AL., *Global consequences of land use*, science, 309 (2005), pp. 570–574.
- [20] C. FONTAINE, P. R. GUIMARÃES, S. KÉFI, N. LOEUILLE, J. MEMMOTT, W. H. VAN DER PUTTEN, F. J. VAN VEEN, AND E. THÉBAULT, *The ecological and evolutionary*

- implications of merging different types of networks*, Ecology Letters, 14 (2011), pp. 1170–1181.
- [21] M. A. FORTUNA AND J. BASCOMpte, *Habitat loss and the structure of plant-animal mutualistic networks*, Ecology Letters, 9 (2006), pp. 281–286.
- [22] M. A. FORTUNA, A. KRISHNA, AND J. BASCOMpte, *Habitat loss and the disassembly of mutualistic networks*, Oikos, 122 (2013), pp. 938–942.
- [23] B. L. FOSTER, T. L. DICKSON, C. A. MURPHY, I. S. KAREL, AND V. H. SMITH, *Propagule pools mediate community assembly and diversity-ecosystem regulation along a grassland productivity gradient*, Journal of Ecology, 92 (2004), pp. 435–449.
- [24] R. P. FRECKLETON, A. R. WATKINSON, AND M. REES, *Measuring the importance of competition in plant communities*, Journal of ecology, 97 (2009), pp. 379–384.
- [25] A. GONZALEZ, B. RAYFIELD, AND Z. LINDO, *The disentangled bank: how loss of habitat fragments and disassembles ecological networks*, American Journal of Botany, 98 (2011), pp. 503–516.
- [26] N. M. HADDAD, L. A. BRUDVIG, J. CLOBERT, K. F. DAVIES, A. GONZALEZ, R. D. HOLT, T. E. LOVEJOY, J. O. SEXTON, M. P. AUSTIN, C. D. COLLINS, ET AL., *Habitat fragmentation and its lasting impact on earth’s ecosystems*, Science Advances, 1 (2015), p. e1500052.
- [27] M. HAGEN, W. D. KISSLING, C. RASMUSSEN, D. CARSTENSEN, Y. DUPONT, C. KAISER-BUNBURY, E. O’GORMAN, J. OLESEN, M. DE AGUIAR, L. BROWN, ET AL., *Biodiversity, species interactions and ecological networks in a fragmented world*, Advances in Ecological Research, 46 (2012), pp. 89–120.
- [28] I. HANSKI, G. A. ZURITA, M. I. BELLOCQ, AND J. RYBICKI, *Species-fragmented area relationship*, Proceedings of the National Academy of Sciences, 110 (2013), pp. 12715–12720.
- [29] S. HAZLEDINE, *The Analysis and modelling of chaotic calcium oscillations*, PhD thesis, Department for Computational Systems Biology, John Innes Centre, 2009.
- [30] H. P. HSU, *Schaum’s outline of theory and problems of probability, random variables, and random processes*, McGraw-Hill, 1997.
- [31] H. I. JAGER, E. A. CARR, AND R. A. EFROYMSON, *Simulated effects of habitat loss and fragmentation on a solitary mustelid predator*, Ecological Modelling, 191 (2006), pp. 416–430.
- [32] D. H. JANZEN, *The deflowering of central America*, Nat. Hist, 83 (1974), pp. 48–53.

## BIBLIOGRAPHY

---

- [33] R. KAARTINEN AND T. ROSLIN, *Shrinking by numbers: landscape context affects the species composition but not the quantitative structure of local food webs*, Journal of Animal Ecology, 80 (2011), pp. 622–631.
- [34] S. KÉFI, E. L. BERLOW, E. A. WIETERS, S. A. NAVARRETE, O. L. PETCHEY, S. A. WOOD, A. BOIT, L. N. JOPPA, K. D. LAFFERTY, R. J. WILLIAMS, ET AL., *More than a meal, integrating non-feeding interactions into food webs*, Ecology letters, 15 (2012), pp. 291–300.
- [35] C. KLAUSMEIER, *Habitat destruction and extinction in competitive and mutualistic meta-communities*, Ecology Letters, 4 (2001), pp. 57–63.
- [36] T. M. KNIGHT, M. W. MCCOY, J. M. CHASE, K. A. MCCOY, AND R. D. HOLT, *Trophic cascades across ecosystems*, Nature, 437 (2005), pp. 880–883.
- [37] G. KOKKORIS, A. TROUMBIS, AND J. LAWTON, *Patterns of species interaction strength in assembled theoretical competition communities*, Ecology Letters, 2 (1999), pp. 70–74.
- [38] N. M. KORFANTA, W. D. NEWMARK, AND M. J. KAUFFMAN, *Long-term demographic consequences of habitat fragmentation to a tropical understory bird community*, Ecology, 93 (2012), pp. 2548–2559.
- [39] C. KREMEN, N. M. WILLIAMS, M. A. AIZEN, B. GEMMILL-HERREN, G. LEBUHN, R. MINCKLEY, L. PACKER, S. G. POTTS, I. STEFFAN-DEWENTER, D. P. VAZQUEZ, ET AL., *Pollination and other ecosystem services produced by mobile organisms: a conceptual framework for the effects of land-use change*, Ecology Letters, 10 (2007), pp. 299–314.
- [40] D. KWIATKOWSKI, P. C. PHILLIPS, P. SCHMIDT, AND Y. SHIN, *Testing the null hypothesis of stationarity against the alternative of a unit root: How sure are we that economic time series have a unit root?*, Journal of econometrics, 54 (1992), pp. 159–178.
- [41] M. LOREAU AND N. MOUQUET, *Immigration and the maintenance of local species diversity*, The American Naturalist, 154 (1999), pp. 427–440.
- [42] M. LURGI, D. MONTOYA, AND J. M. MONTOYA, *The effects of space and diversity of interaction types on the stability of complex ecological networks*, Theoretical Ecology, (2015), pp. 1–11.
- [43] N. MARWAN, M. C. ROMANO, M. THIEL, AND J. KURTHS, *Recurrence plots for the analysis of complex systems*, Physics reports, 438 (2007), pp. 237–329.
- [44] R. M. MAY, *Will a large complex system be stable?*, Nature, 238 (1972), pp. 413–414.
- [45] ——, *Patterns in multi-species communities*, Theoretical ecology: principles and applications, (1981), pp. 197–227.

- [46] K. MCCANN, A. HASTINGS, AND G. R. HUXEL, *Weak trophic interactions and the balance of nature*, Nature, 395 (1998), pp. 794–798.
- [47] C. J. MELIÁN AND J. BASCOMPTE, *Food web structure and habitat loss*, Ecology Letters, 5 (2002), pp. 37–46.
- [48] J. MEMMOTT, R. GIBSON, L. CARVALHEIRO, K. HENSON, R. HELENO, M. LOPEZARAIZA, S. PEARCE, AND S. PEARCE, *The conservation of ecological interactions*, Insect Conservation Biology. The Royal Entomological Society, London, (2007), pp. 226–44.
- [49] D. MONTOYA, M. YALLOP, AND J. MEMMOTT, *Functional group diversity increases with modularity in complex food webs*, Nature communications, 6 (2015).
- [50] J. MONTOYA, J. ARNOLDI, AND M. LOREUA, *Resilience, invariability, and ecological stability across levels of organization*, WHICH JOURNAL, (in press).
- [51] A. MOUGI AND M. KONDOH, *Diversity of interaction types and ecological community stability*, Science, 337 (2012), pp. 349–351.
- [52] N. MOUQUET, P. LEADLEY, J. MÉRIGUET, AND M. LOREAU, *Immigration and local competition in herbaceous plant communities: a three-year seed-sowing experiment*, Oikos, 104 (2004), pp. 77–90.
- [53] A.-M. NEUTEL, J. A. HEESTERBEEK, AND P. C. DE RUITER, *Stability in real food webs: weak links in long loops*, Science, 296 (2002), pp. 1120–1123.
- [54] E. J. O'GORMAN AND M. C. EMMERSON, *Perturbations to trophic interactions and the stability of complex food webs*, Proceedings of the National Academy of Sciences, 106 (2009), pp. 13393–13398.
- [55] J. OKSANEN, R. KINTT, P. LEGENDRE, B. O'HARA, M. H. H. STEVENS, M. J. OKSANEN, AND M. SUGGESTS, *The vegan package*, Community ecology package, 10 (2007).
- [56] O. OVASKAINEN, K. SATO, J. BASCOMPTE, AND I. HANSKI, *Metapopulation models for extinction threshold in spatially correlated landscapes*, Journal of Theoretical Biology, 215 (2002), pp. 95–108.
- [57] C. PARMESAN, N. RYRHOLM, C. STEFANESCU, J. K. HILL, C. D. THOMAS, H. DESCIMON, B. HUNTLEY, L. KAILA, J. KULLBERG, T. TAMMARU, ET AL., *Poleward shifts in geographical ranges of butterfly species associated with regional warming*, Nature, 399 (1999), pp. 579–583.
- [58] C. PARMESAN AND G. YOHE, *A globally coherent fingerprint of climate change impacts across natural systems*, Nature, 421 (2003), pp. 37–42.

## BIBLIOGRAPHY

---

- [59] M. J. POCOCK, D. M. EVANS, AND J. MEMMOTT, *The robustness and restoration of a network of ecological networks*, Science, 335 (2012), pp. 973–977.
- [60] M. PRIESTLEY AND T. S. RAO, *A test for non-stationarity of time-series*, Journal of the Royal Statistical Society. Series B (Methodological), (1969), pp. 140–149.
- [61] T. PUETTKER, A. A. BUENO, C. DOS SANTOS DE BARROS, S. SOMMER, AND R. PARDINI, *Immigration rates in fragmented landscapes-empirical evidence for the importance of habitat amount for species persistence*, PLoS One, 6 (2011), p. e27963.
- [62] R CORE TEAM, *R: A Language and Environment for Statistical Computing*, R Foundation for Statistical Computing, Vienna, Austria, 2013.
- [63] D. RAFFAELLI, *How extinction patterns affect ecosystems*, Science, 306 (2004), pp. 1141–1142.
- [64] W. J. RIPPLE AND R. L. BESCHTA, *Trophic cascades in yellowstone: The first 15years after wolf reintroduction*, Biological Conservation, 145 (2012), pp. 205–213.
- [65] S. E. SAID AND D. A. DICKEY, *Testing for unit roots in autoregressive-moving average models of unknown order*, Biometrika, 71 (1984), pp. 599–607.
- [66] A. SAUVE, C. FONTAINE, AND E. THÉBAULT, *Structure–stability relationships in networks combining mutualistic and antagonistic interactions*, Oikos, 123 (2014), pp. 378–384.
- [67] S. G. SHANDILYA AND M. TIMME, *Inferring network topology from complex dynamics*, New Journal of Physics, 13 (2011), p. 013004.
- [68] R. V. SOLE AND J. M. MONToya, *Ecological network meltdown from habitat loss and fragmentation*, Ecological Networks: Linking Structure to Dynamics in Food Webs, (2006), pp. 305–323.
- [69] B. J. SPIESMAN AND B. D. INOUYE, *Habitat loss alters the architecture of plant-pollinator interaction networks*, Ecology, 94 (2013), pp. 2688–2696.
- [70] D. STOUFFER, J. CAMACHO, R. GUIMERA, C. NG, AND L. NUNES AMARAL, *Quantitative patterns in the structure of model and empirical food webs*, Ecology, 86 (2005), pp. 1301–1311.
- [71] A. TEYSSÈDRE AND A. ROBERT, *Contrasting effects of habitat reduction, conversion and alteration on neutral and non neutral biological communities*, Oikos, 123 (2014), pp. 857–865.
- [72] E. THÉBAULT AND C. FONTAINE, *Stability of ecological communities and the architecture of mutualistic and trophic networks*, Science, 329 (2010), pp. 853–856.

---

## BIBLIOGRAPHY

- [73] D. TILMAN, R. M. MAY, C. L. LEHMAN, AND M. A. NOWAK, *Habitat destruction and the extinction debt*, (1994).
- [74] J. M. TYLIANAKIS, T. TSCHARNTKE, AND O. T. LEWIS, *Habitat modification alters the structure of tropical host-parasitoid food webs*, Nature, 445 (2007), pp. 202–205.
- [75] A. VALIENTE-BANUET, M. A. AIZEN, J. M. ALCÁNTARA, J. ARROYO, A. COCUCCI, M. GALETTI, M. B. GARCÍA, D. GARCÍA, J. M. GÓMEZ, P. JORDANO, ET AL., *Beyond species loss: the extinction of ecological interactions in a changing world*, Functional Ecology, 29 (2015), pp. 299–307.
- [76] B. H. WARREN, D. SIMBERLOFF, R. E. RICKLEFS, R. AGUILÉE, F. L. CONDAMINE, D. GRAVEL, H. MORLON, N. MOUQUET, J. ROSINDELL, J. CASQUET, ET AL., *Islands as model systems in ecology and evolution: prospects fifty years after macarthur-wilson*, Ecology letters, 18 (2015), pp. 200–217.
- [77] R. H. WHITTAKER, *Dominance and diversity in land plant communities numerical relations of species express the importance of competition in community function and evolution*, Science, 147 (1965), pp. 250–260.
- [78] R. J. WILLIAMS AND N. D. MARTINEZ, *Simple rules yield complex food webs*, Nature, 404 (2000), pp. 180–183.
- [79] J. B. WILSON, *Methods for fitting dominance/diversity curves*, Journal of Vegetation Science, 2 (1991), pp. 35–46.
- [80] C. E. ZARTMAN AND H. E. NASCIMENTO, *Are habitat-tracking metacommunities dispersal limited? inferences from abundance-occupancy patterns of epiphylls in amazonian forest fragments*, Biological Conservation, 127 (2006), pp. 46–54.

